

# Biennial Report

Zweijahresbericht  
2012/2013

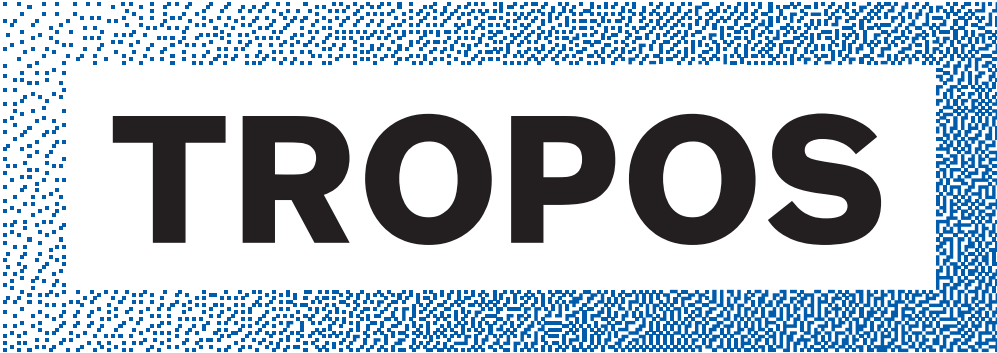
Member of the



**TROPOS**

Leibniz Institute for  
Tropospheric Research





**TROPOS**

Leibniz Institute for  
Tropospheric Research

Member of the



## **Imprint**

Published by

**TROPOS**

Leibniz Institute for Tropospheric Research  
Leibniz-Institut für Troposphärenforschung e.V. Leipzig  
Member of the Leibniz Association ( WGL )

Permoserstraße 15  
04318 Leipzig  
Germany

Phone: ++49 (341) 2717-7060  
Fax: ++49 (341) 2717-99-7060  
Email: [info@tropos.de](mailto:info@tropos.de)  
Internet: <http://www.tropos.de>

Copy Editors  
Katja Schmieder, Konstanze Kunze, Kerstin Müller,  
Heike Scherf, Beate Richter, Tilo Arnhold (Photographer)

Editorial Board  
Andres Macke, Hartmut Herrmann, Ina Tegen,  
Frank Stratmann, Alfred Wiedensohler

Photo and illustration credits © TROPOS / as described  
in the captions / 19 top - background image: original  
photography from NASA

## Table of Contents

- 3    **Introduction / Einleitung**
- 11    **Overview of the individual contributions /  
Übersicht der Einzelbeiträge**

### Articles

- 21    D. van Pinxteren et al.: Overview of field campaigns on multiphase chemistry and aerosol physics
- 30    R. Wolke et al.: Regional Scale Amine Chemistry Dispersion Modelling with COSMO-MUSCAT
- 40    H. Wex et al.: Insights on ice nuclei gained with LACIS
- 48    A. Ansmann et al.: Saharan Dust Long-range Transport and Aerosol-Cloud-Interaction Experiment SALTRACE: Observations and Modelling
- 56    F. Mothes et al.: Lab and field studies on photocatalysis to improve urban air quality
- 59    T. Berndt and T. Jokinen: Mechanistic investigations on the formation of ELVOCs
- 61    J. Schindelka et al.: Formation of organosulfates from sulfate radical reactions in atmospheric aerosols
- 64    T. Schaefer and H. Herrmann.: Oxidation of Glyoxal in the Tropospheric Aqueous Phase
- 67    P. Bräuer et al.: CAPRAM mechanism development and modelling
- 70    R. Schrödner et al.: Cloud Chemistry Modelling with COSMO-MUSCAT: A 2D Sensitivity Study
- 73    S. Barthel et al.: Model study on the temperature dependence of primary marine aerosol emission
- 76    M. Simmel et al.: UDINE: Ice formation in altocumulus clouds over Leipzig: Remote sensing measurements and detailed model simulations
- 79    S. Horn: ASAMgpu nested in WRF – on the way to an operational LES forecast
- 82    K. Schepanski et al.: Evaluation of Saharan dust source activation with regional model simulations and satellite observations
- 85    B. Wehner et al.: Probing the atmospheric boundary layer aerosol using an unmanned aerial vehicle (UAV)
- 88    W. Birmili et al.: On the effectiveness of Low Emission Zones: Decrease in ambient black carbon and particle number concentrations in Leipzig
- 91    A. Wiedensohler et al.: Influence of the traffic on the particle mass concentration of equivalent black carbon and the particle number size distribution in La Paz, Bolivia
- 93    J. Voigtländer et al.: Investigation of nucleation, dynamic growth and surface properties of single ice crystals
- 96    S. Henning et al.: Variability of CCN number concentration and particle activation properties at the central European regional background site Melpitz, Germany
- 98    J. Schmidt et al.: Dual-field-of-view Raman lidar measurements: Investigation of aerosol-cloud interactions
- 101    A. Skupin and A. Ansmann: SÆMS: Long-term monitoring of relativehumidity dependence of ambient particle extinction coefficient in the urban atmosphere
- 104    U. Wandinger et al.: ACTRIS: Aerosols, Clouds, and Trace Gases Research Infrastructure Network
- 107    A. Hünerbein et al.: Combining the perspective of satellite- and ground-based observations to analyze cloud frontal systems
- 110    D. Merk et al.: Investigation of the first indirect aerosol effect: Comparison of the satellite and ground perspective

## **Table of Contents**

### **Appendices**

- 115 Publications
  - 115 Publication statistics
  - 115 Publications
- 127 Overview of Appendices / Überblick der Anhänge
  - 127 Knowledge transfer and public visibility / Wissenstransfer und Außenwirkung
  - 129 Equal opportunities and promotion of young researchers / Chancengleichheit und Nachwuchsförderung
  - 131 Cooperations and networking / Bedeutende Kooperationen und Vernetzung in der Forschung
- 133 University courses
- 135 Academical degrees
  - 135 Completed academic qualifications 2012/2013
  - 139 Summary of completed academic qualifications
- 139 Awards
- 139 Reviews
- 140 Guest scientists
- 143 Visits of TROPOS scientists
- 144 Meetings
- 145 International and national field campaigns
- 148 Memberships
- 151 Cooperations
  - 151 International Cooperations
  - 156 National Cooperations
- 160 Boards
  - 160 Boards of trustees
  - 160 Scientific advisory board
  - 161 Members of the TROPOS Association
- 162 Organigram
- 163 Local map

## Introduction / Einleitung

## Overview / Übersicht





### Introduction

In the “Research Park Leipzig/Permoserstraße” close to the Helmholtz Centre for Environmental Research, the Leibniz-Institute for Surface Modification and other research establishments and related businesses you find the Leibniz Institute for Tropospheric Research (TROPOS). Its name identifies the TROPOS as a member of the Leibniz Association. The institute was founded for the investigation of physical and chemical processes in the polluted troposphere.



Fig. / Abb. 1: TROPOS main building. / TROPOS-Hauptgebäude.

A well-defined and globally unique research profile of TROPOS emerged, with a focus on the physical and chemical relations between atmospheric small airborne (aerosols) and cloud particles. Despite their minute absolute amount, aerosol particles and cloud droplets are essential parts of the atmosphere because they control the budgets of energy, water and trace substances of the Earth System. Human activities can change these highly disperse systems and thus feed back on human beings. This may happen via health effects caused by inhaled particles



Fig. / Abb. 2: TROPOS multi-purpose building. / TROPOS-Mehrzweckgebäude.

### Einleitung

Auf dem Gelände des „Wissenschaftsparks Leipzig/Permoserstraße“ in Nachbarschaft zum Helmholtz-Zentrum für Umweltforschung, zum Leibniz-Institut für Oberflächenmodifizierung sowie weiteren Einrichtungen befindet sich seit 1992 das Leibniz-Institut für Troposphärenforschung e. V. (TROPOS). Sein Name weist es als Mitglied der Wissenschaftsgemeinschaft Gottfried Wilhelm Leibniz aus. Gegründet wurde es zur Erforschung physikalischer und chemischer Prozesse in der belasteten Troposphäre.

Es hat sich ein klares und weltweit einzigartiges Forschungsprofil herausgebildet, in dessen Mittelpunkt die physikalischen und chemischen Beziehungen zwischen atmosphärischen Schwebeteilchen (Aerosolen) und Wolkenpartikeln stehen. Trotz geringster absoluter Mengen sind diese Partikel wesentliche Bestandteile der Atmosphäre, weil sie den Energie-, Wasser- und Spurenstoffhaushalt des Erdsystems beeinflussen. Menschliche Aktivitäten können die Eigenschaften dieser hochdispersen Systeme verändern und direkt sowie indirekt auf den Menschen zurückwirken. Das kann sowohl über die gesundheitlichen Wirkungen eingearmelter Partikel



Fig. / Abb. 3: TROPOS cloud laboratory. / TROPOS-Wolkenlabor.  
(Photo: © Stefan Müller-Naumann)

und Nebeltröpfchen als auch über regionale und globale Klimaänderungen geschehen.

Trotz dieser wichtigen Beziehungen zwischen Mensch auf der einen und Aerosol/Wolken auf der anderen Seite sind die physiko-chemischen Prozesse von Aerosol- und Wolkenbildung und die Wechselwirkungen mit Gesundheit und Klima noch wenig verstanden. Dies liegt vor allem an Schwierigkeiten bei der Analyse der beteiligten kleinsten Stoffmengen und an dem komplexen Verhalten troposphärischer Mehrphasensysteme, deren Einzelprozesse in der Atmosphäre nicht klar getrennt beobachtet werden können. In der gegenwärtigen Klimadiskussion zum globalen

## Introduction / Einleitung



Fig. / Abb. 4: During the HOPE measurement campaign in April and May 2013 the instrument suite of the Leipzig Aerosol and Cloud Remote Observations System (LACROS) of TROPOS were operated in Krauthausen, close to Jülich. / Während der HOPE-Messkampagne im April und Mai 2013 waren die Instrumente des Leipzig Aerosol and Cloud Remote Observations System (LACROS) vom TROPOS in Krauthausen bei Jülich in Betrieb.

and fog droplets and through regional and global climate change.

Despite these strong connections between human beings, aerosols, and clouds, important physico-chemical processes of aerosol and cloud formation and the relationships with climate and health are poorly understood. This limitation is mainly due to difficulties with analyzing the very small samples and with the complex behavior of tropospheric multiphase systems, in which individual processes seldom can clearly be distinguished. In climate research this limitation is reflected in much larger uncertainties in predicted anthropogenic aerosol and cloud effects in comparison to numbers published by the Intergovernmental Panel on Climate Change for additional greenhouse gases.

Rapid advances in our understanding of tropospheric multiphase processes and an application of this process understanding to the prediction of the consequences of human impacts can only be expected from concerted approaches from several directions. Consequently, the Leibniz Institute for Tropospheric Research conducts field studies in several polluted regions parallel to the development of analytical methods for aerosol and cloud research.

These tools are not only applied in field experiments but also in extensive laboratory investigations, which form a second major activity. A third approach consists of the formulation and application of numerical models that reach from process models to regional simulations of the formation, transformation and effects of tropospheric multiphase systems. This approach provides the framework for an overall process understanding of tropospheric multiphase systems.

Wandel spiegelt sich diese Kenntnislage in den sehr viel größeren Unsicherheiten in allen zu Aerosol- und Wolkenwirkung veröffentlichten Zahlen im Verhältnis zu Treibhauseffekten der Gase wider.

Rasche Zuwächse im Verständnis troposphärischer Mehrphasenprozesse und eine Anwendung dieses Prozessverständnisses auf die Vorhersage der Folgen menschlicher Eingriffe lassen sich nur durch ein konzertiertes Vorgehen in mehreren Richtungen erwarten. Das Leibniz-Institut für Troposphärenforschung betreibt daher neben Feldstudien in belasteten Regionen auch die Entwicklung eigener physikalischer und chemisch-analytischer Verfahren zur Untersuchung von Aerosolen und Wolken. Diese Verfahren werden auch in ausgedehnten Laboruntersuchungen eingesetzt, der zweiten Hauptarbeitsrichtung des Instituts. Ein dritter Arbeitsbereich entwickelt und wendet numerische Modelle von der Prozessbeschreibung bis zur Beschreibung der regionalen Bildung, Umwandlung und Wirkung troposphärischer Mehrphasensysteme an und bildet den Rahmen für ein umfassendes Prozessverständnis atmosphärischer Multiphasensysteme.

### Feldexperimente

Die Feldexperimente des Instituts dienen der Aufklärung des atmosphärischen Kreislaufs der Aerosolpartikel und Wolkentropfen und der damit verbundenen Prozesse. Die Komplexität des Systems wird dabei unter anderem dadurch bestimmt, dass in der Atmosphäre Partikel und Tropfen auftreten, deren Größe sich im Nano- und Mikrometerbereich um mehr als sechs Zehnerpotenzen unterscheiden kann, die dementsprechend auch unterschiedlichen Umwandlungsprozessen unterliegen. Außerdem kann man im Aerosol alle kondensationsfähigen Stoffe des



Fig. / Abb. 5: TROPOS research station Melpitz near Leipzig. / TROPOS-Forschungsstation Melpitz bei Leipzig.

### Field experiments

Field experiments elucidate the atmospheric life cycle and related processes of aerosol particles and cloud droplets. This task is vastly more difficult than comparable trace gas studies because particle and droplet diameters in the nano and micrometer size range over more than six orders of magnitude in atmospheric aerosols and clouds, all of which play an important role in certain processes. Furthermore, all atmospheric condensable substances can be found in the aerosol and a large number of them contribute to climate and biospheric effects. Essential properties of aerosol particles and cloud droplets of this multidimensional system are not well established on a global scale yet.

This uncertainty and thus the research efforts of the Leibniz Institute for Tropospheric Research start with particle sources. The combustion of fossil and contemporary fuels is one of the most prominent aerosol sources. However, these sources are still poorly characterized in terms of climate-relevant aerosol parameters. According to long-term urban and rural measurements of the institute emissions of particles and their precursor gases are subject to strong physical and chemical transformations that need to be followed with high-resolution sensors in order to identify the underlying processes.

Not even the largest highly polluted regions in the plumes of North America, Europe, Africa, the Indian subcontinent, Amazonia, and Eastern Asia are sufficiently characterized in terms of aerosol burdens and ensuing climate effects. The institute focuses thus its participation in international field campaigns and dedicated long-term studies in Asia, South America and the marine troposphere over the northern and southern Atlantic. In recent years, the study of



*Fig. / Abb. 6: Pyranometer during the measurement campaign HOPE near Jülich. / Pyranometer während der HOPE-Kampagne (HD(CP)2 Observational Prototype Experiment) bei Jülich.*



*Fig. / Abb. 7: Measuring site at Schmücke, Thüringer Wald, in September/October 2010. / Messstation auf der Schmücke im Thüringer Wald im September/ Oktober 2010.*

Erdsystems finden, von denen eine große Zahl das Klima und die Biosphäre und deren Wirkung beeinflussen. Als Folge dieser Vielfalt und der mengenbedingten analytischen Schwierigkeiten sind wesentliche globale Aerosol- und Wolkeneigenschaften noch wenig bekannt.

Diese Unsicherheit beginnt schon bei den Partikelquellen, die ebenfalls Forschungsgegenstand am Leibniz-Institut für Troposphärenforschung sind. Die Verbrennung fossiler und nachwachsender Brennstoffe zur Energieerzeugung und im Verkehr sind wichtigste Aerosolquellen. Wie sich aus Messungen des Instituts an vielen urbanen Messstellen und kontinentalen Hintergrundstationen ergab, unterliegen die Emissionen von Partikeln und deren Vorläufern enormen physikalischen und chemischen Umwandlungen, die mit hoher zeitlicher Auflösung verfolgt werden müssen, um die beteiligten Prozesse aufzuklären.

Selbst die am höchsten verunreinigten Regionen über Nordamerika, Europa, Afrika, dem indischen Subkontinent, dem Amazonasgebiet und Ostasien sind noch bei weitem nicht hinreichend bezüglich ihrer Aerosolbelastungen und den daraus resultierenden Klimawirkungen charakterisiert. Auf diese Regionen konzentrieren sich daher in internationaler Zusammenarbeit die Feldexperimente des Instituts. Das Institut beteiligt sich deshalb an internationalen Messkampagnen und Langzeitmessungen in Asien, Südamerika und der maritimen Troposphäre über dem südlichen und nördlichen Atlantik. Seit einigen Jahren nehmen Untersuchungen zum Mineralstaub und dessen Wirkung auf den Strahlungshaushalt und Wolkenbildung im Quellgebiet der Sahara, aber auch im Fernfeld über dem Nordatlantik wachsenden Raum ein. Durch Nutzung eines kommerziellen Verkehrsflugzeugs der Lufthansa werden auch Aerosolverteilungen in der belasteten oberen Troposphäre auf

## Introduction / Einleitung

climate-relevant aspects of mineral dust near its most important Saharan source and in the far field over the Atlantic have gained more weight in the institute's research. By means of a commercial aircraft operated by Lufthansa on intercontinental routes, aerosol measurements are conducted even in the polluted upper troposphere.

At TROPOS different ground-based remote sensing methods are coupled in order to reach a synergistic picture of the vertical distribution of clouds and aerosols as well as their processing. The Leipzig Aerosol and Cloud Remote Observation System (LACROS), that has been developed to this end, will be further developed towards a European network prototype instrument.

On smaller scales, investigations concerning new particle formation, the interactions between aerosol particles and clouds, and the influences of turbulent mixing processes on cloud development are carried out with help of the helicopter-borne measurement platform ACTOS. In addition, process studies are conducted at suitable locations such as mountain observatories to study particle nucleation, particle processing through clouds and the influence of anthropogenic aerosols on the optical properties of clouds.

The TROPOS leads several regional, national and European measurements networks to monitor aerosols and cloudiness. The TROPOS hosts the WMO World Calibration Centre for physical in-situ aerosol measurement to assure high quality standards at national and international observatories.

Field campaigns are supported and complemented by the development, provision and analyses of atmospheric parameter from satellite data. In this respect products from the geostationary European



*Fig. / Abb. 9: View from the Campus of Peking University on a heavily polluted day. / Blick vom Gelände der Peking Universität an einem stark verschmutzten Tag.*

regelmäßig beflogenen interkontinentalen Routen vermesssen.

Am TROPOS werden verschiedene bodengebundene Fernerkundungsverfahren gekoppelt, um so zu einem synergistischen Bild der vertikalen Verteilung von Aerosolen und Hydrometeoren sowie deren Prozessierung zu gelangen. Das hierzu entwickelte Leipzig Aerosol and Cloud Remote Observation System (LACROS) wird darüberhinaus zu einem Prototyp-Instrument eines europäischen Messnetzes entwickelt.

Auf kleineren Skalen werden Untersuchungen zur Partikelbildung und Wechselwirkung zwischen Aerosolpartikeln und Wolken und der Einfluss turbulenter Mischungsprozesse auf die Wolkenentwicklung mit Hilfe der hubschraubergetragenen Messplattform ACTOS durchgeführt. Zusätzlich werden Bergstationen zu Prozessstudien genutzt, die sich dem Verständnis von Einzelprozessen, wie der Partikelneubildung, der physiko-chemischen Veränderung des Aerosols beim Wolkendurchgang und dem Einfluss von Aerosolen auf die Entwicklung von Wolken widmen.

Das TROPOS ist maßgeblich an regionalen, nationalen und Europäischen Messnetzen zur Erfassung des Aerosols und der Bewölkung beteiligt. Das Institut betreibt weiterhin das Weltkalibrierzentrum der WMO für physikalische Aerosolmessungen zur Qualitätsicherung von in-situ Messungen an nationalen und internationalen Messstationen.

Feldexperimente werden durch die Entwicklung, Bereitstellung und Analyse von atmosphärischen Parametern aus Satellitendaten unterstützt und ergänzt. So liefern die Produkte des geostationären europäischen Wettersatelliten Meteosat Transportwege und regionale raumzeitliche Felder



*Fig. / Abb. 8: Measurement station "Leipzig-Mitte" of the Saxon State Office for Environment, Agriculture and Geology (LfULG) in Leipzig's city centre. / Messstation Leipzig-Mitte des Sächsischen Landesamtes für Umwelt, Landwirtschaft und Geologie (LfULG), mitgenutzt von TROPOS.*



*Fig. / Abb. 10: Researchers used for the measurement campaign SALTRACE also a cruise of RV METEOR across the Atlantic Ocean. / Für die Messkampagne SALTRACE wurde auch eine Fahrt des DFG-Forschungsschiffes METEOR im tropischen Atlantik genutzt.*

weather satellite Meteosat provide transport paths and regional spatiotemporal fields of aerosol and cloud properties that are also applied to for comparison with results from modelling activities.

### Laboratory experiments

In atmospheric research, there is a continuous development of physico-chemical models for the description of the most relevant process. These models are based on process parameters, which need to be determined in laboratory experiments under controlled environmental conditions.

In the physics section of the institute, laboratory experiments cover the development of a large number of methods to characterize atmospheric particles and droplets. In particular, DMA-based (Differential Mobility Analyzer) size spectrometers and sampling systems for the characterization of cloud droplets and interstitial aerosol particles are designed. Spectroscopic techniques have been developed and applied for the analysis of aerosol particles. Multi-wavelength aerosol LIDAR (Light Detection and Ranging) systems are developed in the field for measuring atmospheric state parameters such as temperature, wind and relative humidity besides aerosol-optical characteristics and aerosol fluxes. Black carbon and mineral, light absorbing aerosol components are quantified with spectroscopic methods in aerosol and cloud samples.

The physics and chemistry departments are jointly carrying out process-oriented laboratory studies. With the large Leipzig Aerosol Cloud Simulator LACIS, the hygroscopic growth of aerosol particles, their activation to cloud droplets and the freezing of cloud droplets are considered. Goals of

von Aerosol- und Wolkeneigenschaften auch zum Vergleich mit entsprechenden Modellierungsergebnissen.

### Laborexperimente

In der Atmosphärenforschung werden kontinuierlich physikalisch-chemische Modelle zur Beschreibung der wesentlichen Prozesse entwickelt. Grundlage derartiger Modelle sind stets Prozessparameter, die in Laborexperimenten unter bekannten Umgebungsbedingungen ermittelt werden.

In der Abteilung Physik werden im Bereich der Laborexperimente zahlreiche Messmethoden entwickelt, die zur Partikelcharakterisierung in boden- und luftgestützten Feldmesskampagnen eingesetzt werden. Im Einzelnen betreffen diese Arbeiten die Weiterentwicklung von DMA-basierenden (Differentieller Mobilitätsanalytator) Größenspektrometern sowie Sammelsysteme zur physikalischen und chemischen Charakterisierung von Wolkentröpfchen und dem interstitiellen Aerosol, also denjenigen Aerosolpartikeln, die innerhalb von Wolken neben den Wolkentröpfchen selbst in der Gasphase suspendiert sind.

Optische Messmethoden werden zur Bestimmung der Extinktion von Partikeln entwickelt und angewendet. Mehrwellenlängenlidare und ein Windlidar werden zur Bestimmung von Aerosoleigenschaften, Aerosolflüssen und meteorologischen Parametern wie Temperatur, Feuchte und Wind im Labor weiterentwickelt und im Feld eingesetzt. Die Anteile „schwarzen Kohlenstoffs“ und mineralischer Aerosolkomponenten in Aerosolproben werden durch spektrale Absorptionsmessungen bestimmt.

Prozessorientierte Laboruntersuchungen werden gemeinsam von den Abteilungen Physik und Chemie durchgeführt. Untersuchungen am Strömungsreaktor

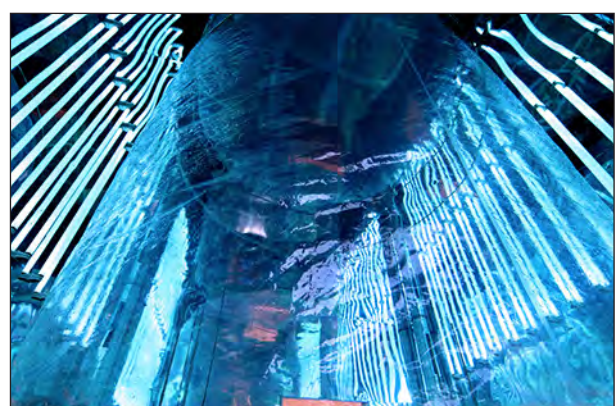


*Fig. / Abb. 11: The TROPOS aerosol chamber (LEAK) with UV lamps. / Die TROPOS-Aerosolkammer (LEAK) mit UV-LAMPEN.*

## Introduction / Einleitung

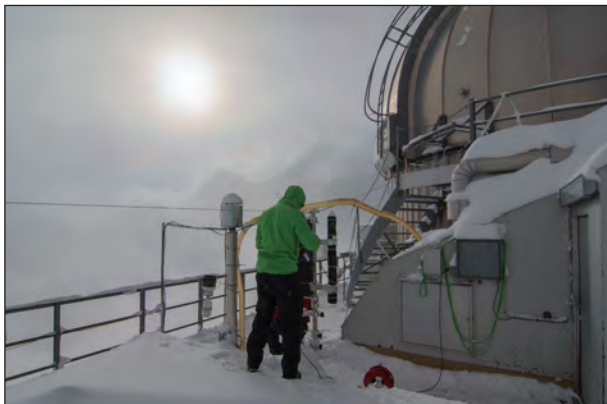


Fig. / Abb. 12: Measurement campaign INUIT-JFJ (Ice Nuclei Research Unit) at the Swiss Jungfraujoch in 3,571 m asl. / Messkampagne INUIT-JFJ (Ice Nuclei Research Unit) auf dem Schweizer Jungfraujoch in 3,571 m ü.M..

these investigations are achieving a better understanding concerning the underlying fundamental processes, the identification of critical and controlling parameters, and the development of parameterizations of cloud and precipitation formation as well as particle aging processes for use in dynamical models.

The chemistry department conducts several process-oriented laboratory studies. Gas phase reactions of various radicals are being investigated in flow reactors. These reactions are important for ozone and particle formation caused by biogenic and anthropogenic emissions of volatile hydrocarbons. These investigations are also done in collaboration with the Physics Department determining hygroscopic growth and cloud droplet activation of the particles formed. The chemical identity of atmospheric particles is being characterized in the Leipzig Aerosol Chamber (LEAK). In a single drop experiment, phase transfer parameters of trace gases and radicals are being determined for different chemical species and surfaces. Experiments with radical reactions in the liquid phase form a core activity of the laboratory experiments, because of their importance for processes in haze particles, fog and cloud droplets as well as in deliquescent aerosol particles. For the understanding of the oxidation of organic trace gases in the tropospheric multi-phase system, a large number of reactions with various radicals are being studied as well as reactions of halogenated oxidants. The latter species are of interest for the emission of reactive halogen compounds from sea salt particles.

Several laboratory experiments are dedicated to the chemical characterization of atmospheric organic aerosol components. Besides the conventional combustion techniques, mass spectroscopic and chromatographic techniques coupled directly to analysis by mass spectrometry or capillary

LACIS betreffen das hygrokopische Wachstum von Aerosolpartikeln unterschiedlichster chemischer Zusammensetzung, deren Aktivierung zu Wolkentröpfchen sowie deren Gefrieren. Ziele dieser Untersuchungen sind die Erlangung eines besseren Prozessverständnisses auf fundamentaler Ebene, die Identifikation kritischer und kontrollierender Parameter und die Entwicklung geeigneter Parametrisierungen zur Beschreibung von Tröpfchen- und Niederschlagsbildung sowie Partikelalterungsprozesse in dynamischen Modellen.

In der Abteilung Chemie werden Gasphasenreaktionen verschiedener Radikale O in Strömungsreaktoren und der Leipziger Aerosolkammer (LEAK) untersucht. Diese Reaktionen sind von Interesse für die Ozon- und Partikelbildung, verursacht durch anthropogene oder biogene flüchtige Kohlenwasserstoffe. Die Untersuchungen laufen auch in Zusammenarbeit mit der Abteilung Physik zur Bestimmung des Feuchtwachstums und der Tropfenaktivierung der erzeugten Partikel.

In einem Einzeltropfenexperiment werden Phasentransferparameter für Spurengase und Radikale untersucht. Die Bestimmung von Phasentransferparametern und reaktiven Aufnahmekoeffizienten wird dabei auf bisher nicht betrachtete chemische Spezies und komplexe Oberflächen ausgeweitet. Im Bereich von Flüssigphasenmechanismen werden Reaktionen von vorwiegend radikalischen Oxidantien mit zeitaufgelösten optischen Nachweistechniken untersucht. Diese Reaktionen laufen in den Tröpfchen von Wolken, Regen und Nebel sowie in wässrigen Aerosolpartikeln ab. Hier werden zum Verständnis der Oxidation organischer Spurengase im troposphärischen Mehrphasensystem eine Vielzahl von



Fig. / Abb. 13: Anne Glover, Chief Scientific Adviser to the President of the European Commission, visits the TROPOS. / Anne Glover, wissenschaftliche Chefberaterin des EU-Kommissionspräsidenten, besucht das TROPOS.

electrophoresis with different sampling and segregation techniques are being developed.

### Modeling

For the description of complex atmospheric processes, model systems of varying dimensions and complexity for micro- and mesoscale problems are developed, tested and applied using data of field experiments and satellite measurements.

One focus of research is the description of cycles, interactions and phase transfer between aerosol particles, gases and clouds. The aim is an improvement in understanding of climate-relevant processes in the troposphere.

Chemistry-transport modeling is realized with the three-dimensional modeling system COSMO-MUSCAT that has been developed at the TROPOS and that is used for simulation of transport of photo oxidants and particles in a mesoscale region.

The model system was successfully tested in international model intercomparison studies and was applied for air quality studies. In several projects the dynamics of primary and secondary particles was simulated and their feedback on the radiative budget was investigated. For further investigations

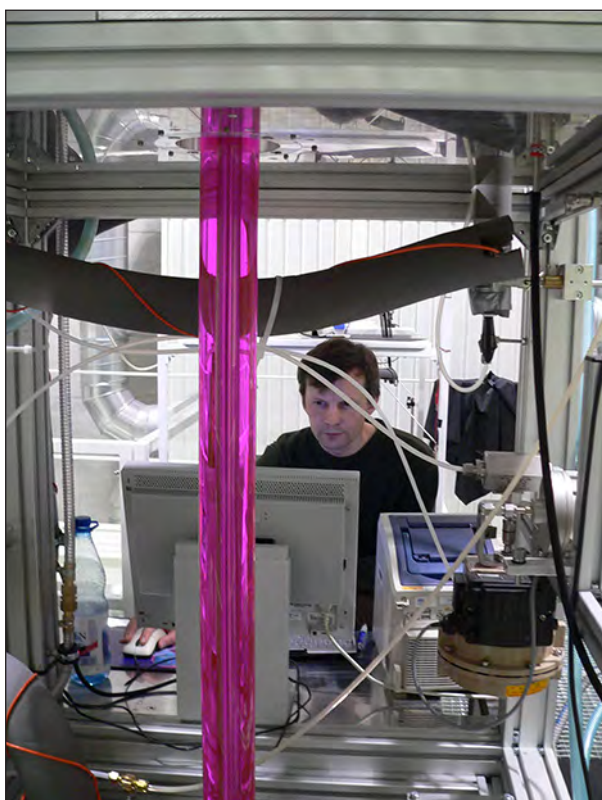


*Fig. / Abb. 14: The "Leipzig Aerosol Cloud Interaction Simulator" (LACIS). / Der Wolkenkanal (LACIS).*

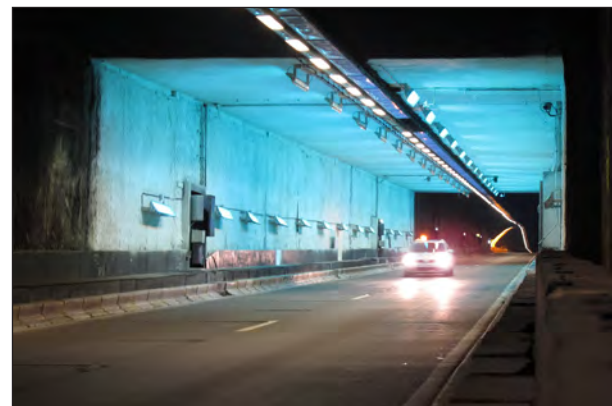


*Fig. / Abb. 15: Experimental test section Leopold II tunnel, Brussels with the applied photocatalytic active coating and additional UV-light sources. / Testabschnitt des Leopold II Tunnels, Brüssel nach Installation der photokatalytisch aktiven Beschichtung und zusätzlichen UV-Lichtquellen. (Photo: PhotoPaq consortium)*

Reaktionen verschiedener Radikale sowie Reaktionen von halogenhaltigen Oxidantien untersucht. Letztere Spezies sind von Interesse bei der Freisetzung von Halogenverbindungen aus maritimen Seesalzpartikeln, der so genannten Halogenaktivierung.

In der analytischen Messtechnik werden in Laborexperimenten Verfahren zur besseren chemischen Charakterisierung der organischen Bestandteile von Aerosolpartikeln entwickelt und getestet. Diese Techniken beruhen zumeist auf massenspektrometrischen Verfahren, die in verschiedenen Kopp lungstechniken eingesetzt werden. Im Bereich der Probenahmetechniken gibt es auch hier eine enge Kooperation mit der Abteilung Physik zur Entwicklung einer gezielten Abscheidung von Partikeln bestimmter Größe und deren chemischer Analyse.

### Modellierung

Zur Beschreibung der komplexen atmosphärischen Vorgänge werden Modellsysteme verschiedener Dimension und Komplexität für die Mikro- bis Mesoskala entwickelt, überprüft und angewendet; auch in Kombination mit Daten aus Feldmessungen und aus satellitengestützten Fernerkundungen.

Ein Forschungsschwerpunkt ist die Beschreibung von Kreisläufen, Wechselwirkungen und Phasenübergängen zwischen Aerosolpartikeln, Gasen und Wolken, um so unser Verständnis klimarelevanter Prozesse in troposphärischen Mehrphasensystemen zu verbessern.

Chemie-Transportmodellierung wird durch das am TROPOS entwickelte 3D-Modellsystem COSMO-MUSCAT realisiert. Seine Brauchbarkeit zur Simulation des Ausbreitungsverhaltens von Partikeln und Gasen auf regionaler Skala wurde in mehreren

## Introduction / Einleitung

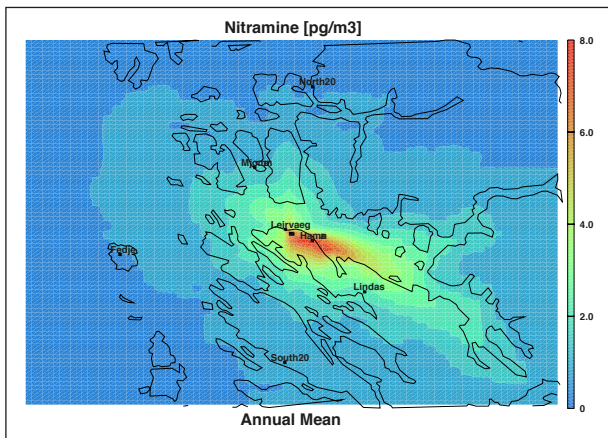


Fig. / Abb. 16: Modelled annual mean concentration of nitramine for the Mongstad region and the basic scenario. / Modellierte mittlere Jahreskonzentration von Nitramine für die Mongstad-Region und das Basis-Szenario.

an “urbanized” version of COSMO-MUSCAT has been developed and can be used with a horizontal grid resolution up to 180x180m. It will be applied for studies of the influence of future climate change on the budget of trace elements.

The model ASAM (All Scale Atmospheric Model) indicates future developments, applicable from the micro to the global scale. It realized cut cells in a Cartesian grid for the description of orography and obstacles. It is currently mainly used for simulations of transport of particles in the microscale domain (urban canyons and urban districts).

One- and two-dimensional process models are also developed and applied. SPECS (SPECtral bin cloud microphysicS) can be used for the investigation of cloud processes with a detailed description of condensation, collision or freezing. SPACCIM (SPectral Aerosol Cloud Chemistry Interaction Model) is a parcel model, which combines detailed microphysics with a complex multiphase chemistry. Both modules can be applied for process modeling as one-dimensional box model version as well as coupled with the mesoscale model COSMO for the investigation of real situations. The process modeling studies are realized in connection with field studies and experiments at LACIS (Leipzig Aerosol Cloud Simulator).

The model simulation of tropospheric multiphase systems is numerically highly demanding. The models need to be sufficiently accurate and numerically efficient to be used productively on existing computer systems. Ongoing developments within the modeling department aim at an increase in the model efficiencies.

internationalen Modellvergleichen und bei der Bearbeitung von Fragen zur Luftqualität im legislativen Bereich gezeigt. In mehreren Projekten wird die Dynamik primärer und sekundärer Aerosolpartikel simuliert und deren Rückkopplungseffekte auf die Strahlung untersucht. Für weitere Anwendungsmöglichkeiten wird zusätzlich eine „urbanisierte“ Version von COSMO-MUSCAT entwickelt, die eine horizontale Gitterauflösung bis hinab zu 180x180 m nutzt. Damit werden auch Untersuchungen zum Einfluss der regionalen Klimavariabilität auf Spurenstoffhaushalte durchgeführt.

Mit ASAM (All Scale Atmospheric Model) steht ein zukunftsweisendes, noch in der Weiterentwicklung befindliches Modell zur Verfügung, dessen dynamischer Kern für Anwendungen vom mikroskaligen bis zum globalen Maßstab eingesetzt werden kann und das in einem kartesischen Gitter mit angeschnittenen Zellen für die Darstellung von Orographie und Hindernissen realisiert wurde. Es wird gegenwärtig vor allem zur Simulation der Ausbreitung von Partikeln im mikroskaligen Bereich (Straßenschluchten, Stadtquartiere) genutzt.

Daneben wurden und werden ein- und zweidimensionale Prozessmodelle entwickelt bzw. weiterentwickelt. SPECS (SPECtral bin cloud microphysicS) dient zur Beschreibung von Wolkenprozessen. Es erlaubt eine explizite und sehr genaue Berechnung der Prozesse Kondensation, Kollision oder Gefrieren. SPACCIM (SPectral Aerosol Cloud Chemistry Interaction Model) ist ein Paketmodell zur gekoppelten größenaufgelösten Beschreibung von Mikrophysik und Mehrphasenchemie. Beide Module können sowohl als Boxmodell zur Prozessmodellierung als

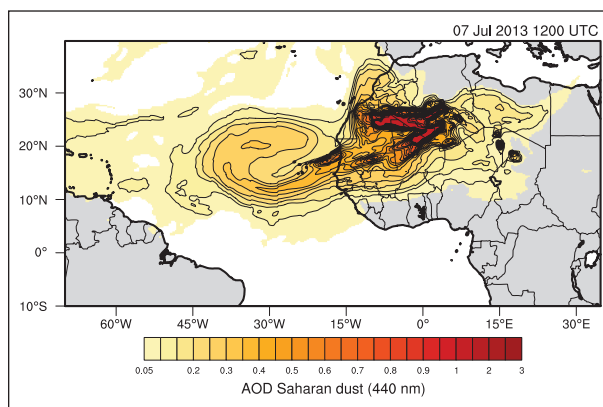
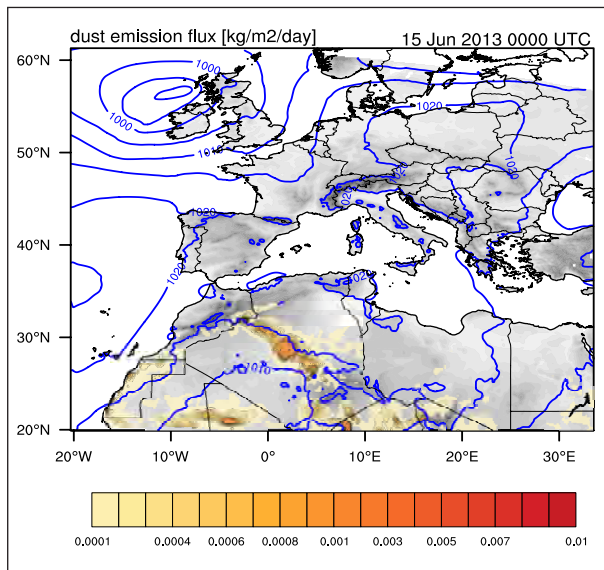


Fig. / Abb. 17: Transport of Saharan dust across the tropical Atlantic Ocean on July 7, 2013: Dust optical thickness as retrieved from COSMO-MUSCAT simulations. / Transport von Saharastaub über den tropischen Atlantik am 7. Juli 2013: Staub optische Dicke berechnet aus COSMO-MUSCAT Simulationen.



*Fig. / Abb. 18: Daily totals of dust emission fluxes [kg/m<sup>2</sup>/day] (shaded colors) simulated by COSMO-MUSCAT for 24-hours prior to 15 June 2013, 00UTC. Blue isobars (contour lines) represent surface pressure [hPa] distribution on 15 June 2013, 00UTC. / Tagessumme des Staubemissionsflusses [kg/m<sup>2</sup>/day] berechnet aus COSMO-MUSCAT Simulationen für den 24-Stunden Zeitraum bis zum 15. Juni 2013, 00UTC. Isobaren in blau spiegeln das Bodendruckfeld [hPa] am 15. Juni 2013, 00UTC wieder.*

auch gekoppelt an das mesoskalige COSMO-Modell zur Untersuchung von realen Situationen verwendet werden. Die Prozessmodellierungen werden im Zusammenhang mit Feldstudien sowie mit den Experimenten am Wolkenkanal LACIS durchgeführt.

Die modelltechnische Behandlung des komplexen atmosphärischen Systems ist numerisch sehr aufwändig. Die zu entwickelnden Modelle müssen hinreichend genau sein und numerisch sehr effizient den jeweils zur Verfügung stehenden Rechnerarchitekturen angepasst werden. Zur Optimierung der verwendeten numerischen Verfahren und Parallelisierungsstrategien liefert die Abteilung Modellierung ebenfalls wesentliche Beiträge.

## Overview of the individual contributions

The biannual report presented here introduces selected work at TROPOS by means of four long and 20 short contributions in the time period 2012 to 2013. The contributions are ordered according to the new department structure

- Chemistry of the atmosphere
- Modelling of atmospheric processes
- Experimental cloud and aerosol microphysics
- Remote sensing of atmospheric processes

with one long and five short contributions from each department, whereby the described work mostly consists of inter-department cooperation.

### Long contributions

#### Chemistry of the atmosphere:

The composition of the atmospheric aerosol results from very heterogeneously distributed and diverse sources, partly trans-continental transport paths as well as complex chemical and physical transformation processes along these paths. For this reason TROPOS has developed a large expertise

## Übersicht der Einzelbeiträge

Der vorliegende Zweijahresbericht stellt in vier längeren und 20 Kurzbeiträgen einige ausgewählte Arbeiten des TROPOS im Zeitraum 2012 bis 2013 vor. Die Beiträge gliedern sich nach der neuen Abteilungsstruktur

- Chemie der Atmosphäre
- Modellierung atmosphärischer Prozesse
- Experimentelle Aerosol- und Wolkenmikrophysik
- Fernerkundung atmosphärischer Prozesse

mit je einem Lang- und fünf Kurzbeiträgen aus jeder Abteilung, wobei die beschriebenen Arbeiten zumeist abteilungsübergreifende Kooperationen sind.

### Langbeiträge

#### Chemie der Atmosphäre:

Die Zusammensetzung des atmosphärischen Aerosols ergibt sich aus sehr heterogen verteilten und verschiedenartigen Quellen, teilweise transkontinentalen Transportwegen, sowie komplexen chemischen und physikalischen Umwandlungsprozessen entlang dieser Wege. Aus diesem Grunde

## Overview / Übersicht

in planning, performing and analysing national and international field campaigns. **Van Pinxteren et al.** summarize four field experiments with respect to the chemical composition of the surface-near aerosol. In the framework of the EU-project PEGASOS (Pan-European Gas-Aerosol-Climate Interaction Study) the formation and transformation of aerosol in a region strongly polluted by industry and farming has been quantified with resolved diurnal cycle. As a contribution to CAREBeijing (Campaigns of Air Quality Research in Beijing and Surrounding Regions) the chemical characterization of the aerosol in the highly polluted metropolitan areas of China provided valuable indications towards local and remote sources. Similar investigations have been carried out in Leipzig and surroundings in regions with different pollution strengths in order to describe the influence of urban sources, especially road traffic, on the aerosol composition. Finally, measurements of the organic compounds in the sea surface film and in marine aerosol particles provide important hints on the particle-wise interaction between ocean and atmosphere.

### Modelling of atmospheric processes:

The decomposition of CO<sub>2</sub> from power plant exhausts by means of amine-based post-combustion CO<sub>2</sub> capture techniques is a "Carbon Capture and Storage" technology to reduce the anthropogenic emission of the green house gas CO<sub>2</sub>. On the other hand the here-applied amines potentially form cancer-inducing particles. **Wolke et al.** coupled the regional transport model developed at TROPOS with a multiphase chemistry mechanism developed for amine-emission. They could proof that in case of typical meteorological conditions the threshold values of the total concentration of carcinogenic particles in the air is not exceeded.

### Experimental cloud and aerosol microphysics:

What kind of aerosol particles with which strength cause the formation of ice is one of the biggest questions in our understanding of the atmospheric water cycle, and a research focus in the cloud laboratory at TROPOS since several years. **Wex et al.** summarize systematic studies on ice activation of various mineral aerosol particles, and arrive at the surprising result that biogenic macromolecules, e.g. from bacteria or pollen, at the surface of "carrier-aerosols" can determine the freezing behaviour of the entire particle. This might explain that laboratory measurements up to now failed to reach the high freezing temperatures reached in nature.

hat TROPOS eine große Expertise in der Planung, Durchführung und Auswertung von nationalen und internationalen Feldkampagnen entwickelt. **Van Pinxteren et al.** fassen gleich vier Experimente zur chemischen Charakterisierung des bodennahen Aerosols zusammen. Im Rahmen des EU-Projektes PEGASOS (Pan-European Gas-Aerosol-Climate Interaction Study) wurde tagesgangauf lösend die Bildung und Transformation des Aerosols in einer von Industrie- und Agrarbetrieben stark belasteten Region quantifiziert. Als Beitrag zu CAREBeijing (Campaigns of Air Quality Research in Peking and Surrounding Regions) lieferte die chemische Charakterisierung des Aerosols in den hochverschmutzten Ballungsregionen Chinas wertvolle Hinweise zu den Beiträgen lokaler und unterschiedlich weit entfernter Quellen. Ähnliche Untersuchungen wurden auch in Leipzig und Umgebung in unterschiedlich stark belasteten Regionen durchgeführt, um den Einfluss urbaner Quellen - insbesondere Straßenverkehr - auf die Aerosolzusammensetzung zu beschreiben. Messungen der organischen Bestandteile im Ozean-Oberflächenfilm und in marinern Aerosolpartikeln geben schließlich wichtige Hinweise auf die partikuläre Wechselwirkung zwischen Ozean und Atmosphäre.

### Modellierung atmosphärischer Prozesse:

Die Abtrennung von CO<sub>2</sub> aus dem Abgas von Kraftwerken durch industrielle Aminwäscheverfahren (*Post-Combustion-Capture*) ist eine „Carbon Capture and Storage“-Technologie, um anthropogene Emissionen des Treibhausgases CO<sub>2</sub> zu verringern. Allerdings können die hierzu verwendeten Amine potentiell krebserzeugende Partikel bilden. **Wolke et al.** koppelten das am TROPOS entwickelte regionalen Ausbreitungsmodell mit einem für die Amin-Emission entwickelten Mehrphasenchemiemechanismus und konnten nachweisen, dass im Falle von Aminwäsche unter typischen meteorologischen Bedingungen die Grenzwerte der Gesamtkonzentrationen karzinogener Partikel in der Luft nicht überschritten werden.

### Experimentelle Aerosol- und Wolkenmikrophysik:

Welche Aerosolpartikel in welchem Maße die Bildung von Eis verursachen ist eine der größten Fragen im Verständnis des atmosphärischen Wasser-kreislaufes und seit einigen Jahren Forschungsschwerpunkt des Wolkenlabors am TROPOS. **Wex et al.** fassen systematische Studien zur Eisaktivität unterschiedlichster mineralischer Partikel zusammen und kommen zu dem überraschenden Ergebnis, dass biogene Makromoleküle z.B aus Bakterien oder Pollen auf der Oberfläche der „Träger-Aerosole“ das

### Remote sensing of atmospheric processes:

Subsequent to the very successful DFG research group SAMUM (Saharan Mineral Dust Experiment) the follow-up research group SALTRACE (Saharan Aerosol Long-range Transport and Aerosol Cloud Interaction Experiment) has been founded in Germany funded from institutes funding. For the first time and as a consequent continuation SALTRACE investigates Saharan dust along its transport path and remote from the sources at the West coast of the American continent. **Ansmann et al.** report on measurements in the framework of SALTRACE that have been performed on Barbados, on the German research vessel METEOR as well as on modelling of the long-range transport of Saharan dust. Thanks to this interplay of remote sensing, in-situ observations and modelling essential indications with respect to the aging, the radiative effects, the cloud indirect effects and the sedimentation of the long-range transported mineral dust have been discovered.

### Short Contributions

#### Chemistry of the Atmosphere:

Besides fine dust and ozone nitrate oxides from fuel burning more and more contributes to the air pollution. By means of field- and laboratory experiments **Mothes et al.** test the potential of photocatalytic active building materials to reduce these nitrate oxides. First results from experiments in a traffic tunnel do not show a significant reduction. However, the analysis of further campaigns is still under way.

Oxidation products of isoprene and terpenes are known to have an important impact on the growth of nanoparticle and on the formation of secondary organic aerosol in general. **Berndt und Jokinen** investigate formation mechanisms of the recently discovered highly oxidized and extremely low-volatility organic compounds (ELVOC), which contribute to particle formation in the atmosphere by means of a formerly unknown mechanism.

Organosulfates are an important fraction of ambient secondary organic aerosol (SOA) and can contribute up to 30% to the organic mass of ambient aerosols. However, their formation mechanisms are not fully understood, yet. By means of liquid phase- and chamber-experiments **Schindelka et al.** explain the formation of these organosulfates.

Essential characteristics for the modelling of chemical reactions are their rate constants. By using an improved laser flash photolysis - long path laser absorption device **Schäfer and Herrmann** yield the highly precise determination of the temperature dependent rate constants for the oxidation of glyoxal by atmospheric relevant radicals. With this, they

Gefrierverhalten des gesamten Partikels bestimmen können. Damit wäre eine Erklärung für die in der Natur gefundenen hohen Gefriertemperaturen gefunden, die bislang im Labor nicht erreicht werden konnten.

#### Fernerkundung atmosphärischer Prozesse:

Im Anschluss an die sehr erfolgreiche DFG-Forschergruppe SAMUM (Saharan Mineral Dust Experiment) hat sich in Deutschland, finanziert aus Institutsmitteln, die Folgegruppe SALTRACE (Saharan Aerosol Long-range Transport and Aerosol Cloud Interaction Experiment) gebildet und in konsequenter Fortsetzung erstmalig den Saharastaub entlang seines Transportweges und fernab der Quellen an der Westküste des amerikanischen Kontinents untersucht. **Ansmann et al.** berichten über die im Rahmen von SALTRACE stattgefunden Messungen auf Barbados, auf dem deutschen Forschungsflugzeug FALCON, auf dem deutschen Forschungsschiff METEOR sowie über die Modellierungen zum Ferntransport des Saharastaubes. Dank dieses Zusammenspiels von Fernerkundung, in-situ Beobachtung und Modellierung wurden entscheidende Hinweise zur Alterung, zur Strahlungswirkung, zur Wolkenbeeinflussung und zur Sedimentation des ferntransportierten Mineralstaubes entdeckt.

### Kurzbeiträge

#### Chemie der Atmosphäre:

Neben Feinstaub und Ozon tragen mehr und mehr Stickoxide aus der Kraftstoffverbrennung zur Luftbelastung bei. **Mothes et al.** prüfen im Feld und im Labor das Potential photokatalytisch aktiver Baumaterialien zur Reduktion dieser Stickoxide. Erste Ergebnisse aus Experimenten in einem Verkehrstunnel weisen keine signifikante Reduktion auf; allerdings stehen Auswertungen weiterer Kampagnen noch aus.

Die Oxidationsprodukte des Isoprens und der Terpene sind bedeutend für das Wachstum von Nanopartikeln und für die Bildung des Sekundären Organischen Aerosols generell. **Berndt und Jokinen** untersuchen Bildungsmechanismen der gerade entdeckten hochoxidierten, organischen Oxidationsprodukte (ELVOCs), die zu einem bislang unbekannten Mechanismus zur Partikelbildung in der Atmosphäre beitragen.

Organosulfate sind ein wesentlicher Bestandteil des sekundären organischen Aerosols (SOA) und können bis zu 30% der organischen Masse des SOA ausmachen. Allerdings ist der Mechanismus ihrer Bildung noch nicht vollständig verstanden.

## Overview / Übersicht

resolved an existing discrepancy concerning the order of magnitudes of this constant and as well as the precise mechanism behind this.

Organic compounds are involved in numerous atmospheric processes and play an important role in the formation of secondary aerosols and in questions concerning air quality. By means of an automatized liquid phase mechanism and its implementation into an expert system **Bräuer et al.** managed to consider more than 7000 reaction schemes, yielding the modelling of unprecedented high resolved scenarios of tropospheric multiphase chemistry.

### Modelling of Atmospheric Processes:

The explicit implementation of the variety of chemical mechanisms in dynamical circulation models is too expensive and requires simplifications and parameterizations. To this end **Schrödner et al.** have combined the coupled chemistry-transport model COSMO-MUSCAT with complex liquid phase chemistry. Comparisons with simplified representations show significant differences in the oxygen-budget, the pH-value of the cloud droplets, and in the formation of organic particle mass.

With 3 to 18 Tg/yr primary maritime aerosol has the largest emission rate of all aerosol types but also the largest uncertainty range in this rate. One reason for that is the inadequate parameterization of emission processes. **Barthel et al.** added to the model a further parameterization of the temperature dependency to the otherwise dominant wind-dependent emission parameterization and with this reached a better agreement between model results and observations.

The continuous ground-based remote sensing at TROPOS enables numerous statistical and exemplarily analysis with respect to the formation of clouds and ice in the atmosphere, especially in comparison to model results. By means of a coupled dynamic-microphyiscs model **Simmel et al.** successfully reproduced observed ice formation processes. They demonstrated, that the assumption on the ice crystal shape in the model has the largest influence on the skill of the model results.

Modelling with the help of Large Eddie Simulations (LES) enables spatial and temporal resolutions comparable to those of ground based active remote sensing. In the framework of a field campaign in Melpitz initiated by TROPOS **Horn** coupled the ASAMgpu LES model to an operational forecast model and with this produced model fields that are directly comparable with observations.

The dynamics of Saharan dust events is qualitatively very impressively detectable from an optimal combination of the radiometer channels of the

**Schindelka et al.** erklären mit Hilfe von Flüssigphasen- und Kammerexperimenten die Bildung dieser Organosulfate.

Wesentliche Kenngrößen für die Modellierung von chemischen Reaktionen sind deren Geschwindigkeitskonstanten. Mittels einer weiterentwickelten Laser-Photolyse-Langweg-Laser-Absorptionsapparatur gelang **Schäfer und Herrmann** die hochgenaue Bestimmung der temperaturabhängigen Geschwindigkeitskonstanten der Oxidation von Glyoxal durch atmosphärisch relevante Radikale und damit die Aufklärung bestehender Diskrepanzen der Größenordnung dieser Konstante sowie des genauen zugrundeliegenden Mechanismus.

Organische Verbindungen sind in zahlreichen atmosphärischen Prozessen involviert und spielen eine wichtige Rolle in der sekundären Aerosolbildung und in Fragen zur Luftqualität. Mittels eines automatisierten Flüssigphasenmechanismus und dessen Implementierung in ein Expertensystem konnten **Bräuer et al.** mehr als 7000 Reaktionsschemata berücksichtigen und so bislang unerreicht hoch aufgelöste Szenarien zur troposphärischen Multiphasenchemie modellieren.

### Modellierung atmosphärischer Prozesse:

Die explizite Umsetzung der Vielfalt von chemischen Mechanismen in dynamischen Zirkulationsmodellen ist zu aufwändig und verlangt nach Vereinfachungen und Parametrisierungen. Hierzu haben **Schrödner et al.** das gekoppelte Chemie-Transportmodell COSMO-MUSCAT mit komplexer Flüssigphasenchemie kombiniert und im Vergleich zu einfachen Repräsentationen signifikante Unterschiede im Sauerstoffhaushalt, im pH-Wert der Wolkentröpfchen und in der Bildung organischer Partikelmasse gefunden.

Mit 3 bis 18 Tg/yr hat primäres maritimes Aerosol die größte Emissionsrate aller Aerosoltypen und auch die größten Unsicherheitsbereiche in den Raten. Ein Grund hierfür liegt in den unzureichenden Parametrisierungen der Emissionsprozesse. **Barthel et al.** fügten im Modell der dominanten Windabhängigkeit-parametrisierung eine zusätzliche Parametrisierung der Temperaturabhängigkeit hinzu und erreichten so eine bessere Übereinstimmung zwischen Modellergebnissen und Messwerten.

Die kontinuierliche bodengebundene Fernerkundung am TROPOS erlaubt zahlreiche statistische und exemplarische Analysen zur Bildung von Wolken und Eis in der Atmosphäre, insbesondere im Vergleich zu Modellergebnissen. **Simmel et al.** konnten mit einem gekoppelten Dynamik-Mikrophysik-Modell für zwei Wolkenfälle beobachtete Eisbildungsprozesse erfolgreich reproduzieren und aufzeigen, dass die Annahme

geostationary satellite Meteosat. In order to arrive at a more quantitative comparison with corresponding model results **Schepanski et al.** simulated the spectral radiances that reach the satellite by means of a radiative transfer model from modelled dust distributions. They could show that it is not the number, but the strength of dust events that determine the atmospheric dust concentration.

### Experimental cloud and aerosol microphysics:

One of the big strategic goals of TROPOS is the coupling of the detailed surface-near aerosol measurements with the remote sensing of the tropospheric column. One path in this direction is the application of miniaturized in-situ measurement devices on board of micro-aircrafts. **Wehner et al.** developed a small and light-weighted aerosol payload that was successfully flown on-board an unmanned airborne vehicle at the measurement field of TROPOS in Melpitz. This laid the cornerstone for future probing of the boundary layer in combination with lidar observations.

During the reporting period the high-precision particle characterization developed at TROPOS has been applied to check the success of the low emission zone with highest regulation level 3 (green tag). By means of trend analysis in 2009 - 2013 **Birmili et al.** proved that the introduction of the low emission zone in Leipzig in 2011 and the corresponding reduction in burning of Diesel fuel lead to a significant reduction in soot mass concentration (black carbon) and in the number of ultrafine particles (diameter range 50-100 nm) in the ambient air near roads. They further showed that the usual application of particle concentration  $PM_{10}$  is inappropriate for the assessment of the air quality.

Las Paz in Bolivia is one of the largest sources of soot that is directly emitted into the free southern hemispheric troposphere. In order to ascertain the total influence of road traffic on the air particle composition the traffic would have to come to a full stop for a sufficiently long time period. During a field campaign in 2012 exactly this situation occurred in Las Paz, which is heavily polluted by truck-traffic, when at the national day of census on the 21st of November, all people had to stay at home. **Wiedensohler et al.** impressively demonstrated the rapid reduction of soot concentrations from the usual  $15 \mu\text{g}/\text{m}^3$  to  $1 \mu\text{g}/\text{m}^3$  due to this occasion.

Formation and growth of ice particles are complex physical processes in the tropospheric multiphase system and lead to a correspondingly large variety of ice particles. A substantial and internationally deeply discussed influence on the scattering behaviour of these particles results from surface roughness. By means of laboratory experiments

der Eispartikelform den stärksten Einfluss auf die Güte der Modellergebnisse hat.

Modellierung mit Hilfe der Large Eddie Simulationen (LES) ermöglicht räumliche und zeitliche Auflösungen, vergleichbar mit denen der bodengebundenen aktiven Fernerkundung. Im Rahmen eines vom TROPOS initiierten Feldexperimentes in Melpitz koppelte **Horn** das ASAMgpu LES-Modell an ein operatives Vorhersagemodell und konnte so Modellfelder erstellen, die mit den Beobachtungen unmittelbar vergleichbar sind.

Die Dynamik von Saharastaubereignissen ist qualitativ sehr beeindruckend aus einer optimalen Kombination der Radiometerkanäle des geostationären Satelliten Meteosat erkennbar. Um zu einer mehr quantitativen Vergleichbarkeit mit entsprechenden Modellergebnissen zu kommen, simulierten **Schepanski et al.** mit Hilfe eines Strahlungstransportmodells aus modellierten Staubverteilungen die am Satelliten ankommende spektrale Strahldichte und konnten so aufzeigen, dass nicht die Anzahl, sondern die Stärke der Staubereignisse die atmosphärische Staubkonzentration bestimmt.

### Experimentelle Aerosol- und Wolkenmikrophysik:

Eines der großen strategischen Ziele des TROPOS ist die Verknüpfung der detaillierten in-situ Messungen des bodennahen Aerosols mit der Fernerkundung der troposphärischen Säule. Ein Weg hierzu ist der Einsatz miniaturisierter in-situ-Messgeräte auf Kleinstfluggeräten. **Wehner et al.** entwickelten eine kleine und leichte Aerosolnutzlast, die erfolgreich an Bord eines unbemannten Fluggerätes auf dem Meßfeld des TROPOS in Melpitz eingesetzt wurde. Hiermit ist der Grundstein für zukünftige Grenzschichterprobungen in Kombination mit den Lidarmessungen des TROPOS gelegt.

Die am TROPOS entwickelte hochgenaue Partikelcharakterisierung wurde im Berichtszeitraum genutzt, um den Erfolg der Umweltzone mit der höchsten Regulierungsstufe 3 (grüne Plakette) zu prüfen. **Birmili et al.** zeigten anhand von Trendanalysen von 2009 - 2013, dass die Einführung der Umweltzone in Leipzig in 2011 und die damit verbundene Reduktion von Dieselsverbrennung zu einer signifikanten Abnahme der Rußmassenkonzentration (black carbon) und der Zahl ultrafeiner Partikel (Durchmesserbereich 50-100 nm) in der Außenluft an Straßen geführt hat und dass die übliche Verwendung der Partikelkonzentration  $PM_{10}$  für die Bewertung der Luftqualität ungeeignet ist.

Für die südliche tropische Hemisphäre ist La Paz, Bolivien, eine der bedeutendsten Quellen von Ruß, das direkt in die freie Troposphäre transportiert

## Overview / Übersicht

**Voigtlander et al.** found that such roughness in general increases during the growth of the particle and decreases again during shrinking in sub-saturated ambient conditions.

One of the most important factors influencing the formation and development of clouds is the availability of cloud condensation nuclei. Thanks to continuous field observations at the research station Melpitz (representative for background aerosol outside of strong local and regional sources) **Henning et al.** could identify (for the first time to our knowledge) a characteristic annual and diurnal cycle of the hygroscopicity of aerosol particles that can be traced back to anthropogenic emission pattern.

### Remote sensing of atmospheric processes:

By means of a new lidar technology the highly developed lidar-based aerosol characterization has been complemented by the characterization of cloud properties like droplet size and droplet number. The synergy of simultaneous aerosol and cloud remote sensing enables the retrieval of aerosol/cloud interactions in real clouds. With the new "duel-field-of-view" Raman lidar technology **Schmidt et al.** found as a first result a strengthened dependency of cloud properties on the aerosol content during dominant updraft situations.

Since 2009 the spectral particle extinction coefficients of unaffected atmospheric particles are continuously measured together with the ambient meteorological conditions like air humidity. From these measurements **Skupin und Ansmann** arrived at a parameterization of the humidity dependency of the particle extinction coefficient from which growth factors of aerosol particles can be calculated. This provides an important bridge between laboratory and field measurements of aerosols.

TROPOS is leading in the European networking of in-situ observations and ground-based remote sensing as it is currently realized in the European research infrastructure project ACTRIS (Aerosol, Clouds, and Trace gases Research InfraStructure network). The goal of ACTRIS is the integration of highly developed ground-based measurement networks for the in-situ and remote measurements of aerosols, clouds, and reactive gases. With ACTRIS a sustainable long-term European research infrastructure shall be established with which quality controlled long-term data with respect to climate change, air quality and transports of pollutants on regional and continental scales shall be obtained. **Wandinger et al.** provide an overview on the activities of TROPOS in ACTRIS.

The observation networks that are building up in ACTRIS open the perspective to permanently

werden kann. Um den vollen Einfluss des Straßenverkehrs in La Paz auf die Rußkonzentration und die Partikelgrößenverteilung in der Luft und somit den Eintrag in die freie Troposphäre zu ermitteln, müsste der Verkehr für einen hinreichend langen Zeitraum komplett zum Stillstand kommen. Genau diese Situation lag während einer Aerosolmesskampagne in 2012 im extrem durch LKW-Verkehr verschmutzten La Paz vor, als am Tag der nationalen Volkszählung am 21. November alle Einwohner zuhause bleiben mussten. **Wiedensohler et al.** demonstrieren eindrucksvoll die hieraus folgende rapide Abnahme der Rußkonzentration von üblichen  $15 \mu\text{g}/\text{m}^3$  auf  $1 \mu\text{g}/\text{m}^3$ .

Bildung und Wachstum von Eispartikeln sind komplexe physikalische Prozesse im troposphärischen Mehrphasensystem und führen zu einer entsprechenden Vielfalt von Eispartikeln. Einen wesentlichen und international viel diskutierten Einfluss auf das Streuverhalten dieser Partikel haben Oberflächenrauigkeiten. **Voigtlander et al.** konnten im Laborexperiment nachweisen, dass derartige Rauigkeiten grundsätzlich beim Wachstum von Eispartikeln zunehmen, und während des Schrumpfens in unterschiedigen Umgebungen wieder abnehmen.

Einer der wichtigsten Einflussfaktoren zur Wolkenbildung- und -entwicklung ist die Verfügbarkeit von Wolkenkondensationskernen. Dank kontinuierlicher Feldmessungen auf der Forschungsstation Melpitz (charakteristisch für das Umgebungsaerosol außerhalb starker lokaler oder regionaler Quellen) konnten **Henning et al.** erstmals einen charakteristischen Jahres- und Tagesgang der Hygroskopizität von Aerosolpartikeln aufweisen, der auf anthropogene Emissionsmuster zurückgeführt werden kann.

### Fernerkundung atmosphärischer Prozesse:

Die hochentwickelte lidar-gestützte Aerosolcharakterisierung am TROPOS wurde mittels einer neuen Lidartechnik um die Charakterisierung der Wolkeneigenschaften wie Tröpfchengröße und Tröpfchenanzahl ergänzt. Die Synergie gleichzeitiger Aerosol- und Wolkenfernerkundung erlaubt die Erfassung von Aerosol/Wolken-Wechselwirkungen in realen Wolken. **Schmidt et al.** konnten mit der neuen „Zweifach-Sichtfeld“ Ramanlidartechnologie als erstes Ergebnis eine verstärkte Abhängigkeit der Wolkeneigenschaften vom Aerosolgehalt während dominanter Aufwindsituationen nachweisen.

Seit 2009 werden am TROPOS kontinuierlich die spektralen Partikelextinktionskoeffizienten der unbeeinflussten atmosphärischen Partikel gemeinsam mit den umgebenden meteorologischen Bedingungen wie Luftfeuchte gemessen. **Skupin und Ansmann** gelangten hieraus zu einer Parametrisierung der Feuchteabhängigkeit

combine atmospheric properties from ground-based remote sensing with aerosol and cloud properties from satellite remote sensing, in order to obtain a more complete picture of the composition and dynamics of the atmosphere as well as characteristic transport paths. **Hünerbein et al.** introduce a such-like combination with an example case of a cold front passage. As an example they managed to relate the ice crystal size at the top of the clouds as measured at the satellite with the instability of the atmosphere obtained from the ground-based measurements.

In a further application of coupling ground-based and satellite-based remote sensing **Merk et al.** investigate the first indirect aerosol effect, which postulates a reduction of particle droplet radius by increasing the number of cloud condensation nuclei. To this end they compare estimates of cloud droplet numbers from ground- and satellite-based remote sensing.

des Partikelextinktionskoeffizienten, aus denen sich die Wachstumsfaktoren von Aerosolpartikeln berechnen lassen. Damit wird eine wichtige Brücke zwischen Labor- und Feldmessungen des Aerosols geschlagen.

TROPOS ist federführend in der europäischen Vernetzung von in-situ Messungen und bodengebundener Fernerkundung, die sich zur Zeit im europäisches Forschungsinfrastrukturprojekt ACTRIS realisiert.

Das Ziel von ACTRIS ist die Integration hochentwickelter, bodengebundener Messnetze für die In-situ- und Fernmessung von Aerosolen, Wolken und reaktiven Gasen. Mit ACTRIS soll eine nachhaltige, langfristige europäische Forschungsinfrastruktur aufgebaut werden, mit der qualitätsgesicherte Langzeitdaten zu Klimaänderungen, Luftqualität und Transport von Schadstoffen auf regionaler und kontinentaler Skala gewonnen werden können.

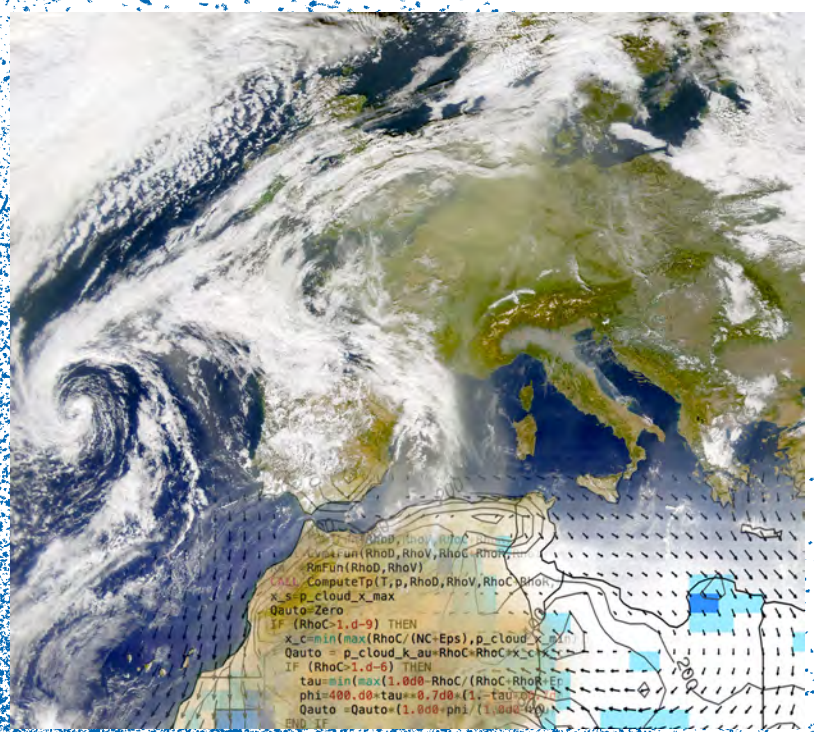
**Wandinger et al.** geben einen Überblick über die Aktivitäten von TROPOS in ACTRIS.

Die in ACTRIS entstandenen Messnetze eröffnen die Perspektive, dauerhaft Atmosphäreneigenschaften aus bodengebundener Fernerkundung mit Aerosol- und Wolkenprodukten der Satellitenfernerkundung zu kombinieren, um so ein vollständigeres Bild der Zusammensetzung und Dynamik der Atmosphäre sowie charakteristischen Transportwege zu erhalten. **Hünerbein et al.** stellen eine derartige Kombination anhand eines Fallbeispiels eines Kaltfrontdurchzugs vor und konnten so z.B. die am Satelliten gemessenen Eiskristallgrößen am Oberrand der Bewölkung mit einer aus den Bodenmessungen erkundeten Instabilität der Atmosphäre in Verbindung bringen.

In einer weiteren Anwendung zur Kopplung von bodengebundener und satellitengetragener Fernerkundung untersuchen **Merk et al.** den ersten indirekten Aerosoleffekt, der eine Verkleinerung der Wolkentröpfchenradien durch Erhöhung der Anzahl der Wolkenkondensationskerne postuliert. Hierzu vergleichen sie Schätzungen der Wolkentröpfchenanzahlen aus bodengebundener Lidar/Radar-Fernerkundung und Satellitenfernerkundung.



## Articles





# Overview of field campaigns on multiphase chemistry and aerosol physics

Dominik van Pinxteren, Yoshiteru Iinuma, Laurent Poulain, Monique Teich, Manuela van Pinxteren, Christian Weller, Gerald Spindler, Konrad Müller, Kanneh Wadinga Fomba, Fabian Rasch, Johannes Größ, Kay Weinhold, Wolfram Birmili, Alfred Wiedensohler, Hartmut Herrmann

Viele grundlegende physikalische und chemische Prozesse bei der Bildung und Transformation atmosphärischer Partikel, sowie viele ihrer Auswirkungen auf global bedeutende Fragen sind bisher nur unzureichend verstanden. TROPOS nimmt regelmäßig an Feldmesskampagnen teil, um durch integrierte physikalische und chemische Messungen zu einem besseren Prozessverständnis in aktuellen Themengebieten der Atmosphärenwissenschaft beizutragen. In diesem Beitrag werden stellvertretend für viele weitere in 2012 und 2013 durchgeführte Feldkampagnen erste Ergebnisse aus den Projekten PEGASOS (Bildung und Transformation des atmosphärischen Aerosols), CARE-Beijing NCP 2013 (Luftverschmutzung in Megacities), Aerosol 2013 (Luftverschmutzung in Sachsen) und Polarstern ANT XXVII/4 (Ozean/Atmosphärenaustausch organischer Gase und Partikel) vorgestellt.

## Introduction

Aerosol particles are involved in a multitude of processes affecting life on earth. These range from influencing the radiation budget by light absorption and scattering via providing a medium for unique chemical transformation reactions to affecting human health through their penetration into the respiratory system. Many of these processes are not well enough understood to answer pressing questions related to issues with high societal importance such as climate change and urban air pollution. Field campaigns are an essential tool to address such questions as they provide the opportunity to explore the unknown and validate the known at the same time.

TROPOS has been conducting many field campaigns to study fundamental processes in urgent atmospheric topic areas, following an integrated approach of determining both the physical properties and the chemical composition of aerosol particles in parallel. Four of such campaigns are presented within the present contribution, representing examples for the institute's field activities in the following areas:

- **Formation and transformation of aerosol**

Despite of their utmost importance, neither the formation of aerosol particles, nor the transformation during their atmospheric lifetime is fully understood at present. In a field campaign within the EU project PEGASOS, measurements were done in summer 2012 in the Po Valley with a

focus on the formation of secondary organic aerosol (SOA).

- **Air pollution in megacities**

Anthropogenic emissions in megacities and large urban agglomerations are posing a severe threat to human health. The CAREBeijing NCP 2013 project aimed at studying the present state and the effects of air pollution in Beijing, China, and its surrounding areas.

- **Air pollution in developed regions**

Even though the level of air pollution in developed regions has fallen substantially during past decades, urban citizen's exposure to particulate matter (PM) has recently been judged by the European Environment Agency (EEA) to remain a threat to public health and ecosystems [EEA, 2013]. The Aerosol 2013 project, funded by the Saxon State Agency of Environment, Agriculture and Geology, aims at documenting the main sources of present-day particulate pollution in Leipzig and Saxony and deducing recommendations for mitigation strategies and policies.

- **Air/sea exchange of gases and particles**

Oceans cover most of the Earth's surface and can act as source and sink for atmospheric gases and particles. The complex interactions of these two compartments are largely unexplored at present, especially with regards to organic compounds. Measurements during several Polarstern cruises together with closely related laboratory studies aim at a better understanding

of potentially important processes at the air/sea interface.

### Formation and transformation of aerosol: PEGASOS Po Valley 2012

Pan-European Gas-Aerosol-Climate Interaction Study (PEGASOS) is a EU Framework Programme 7 Large Scale Integrating Project aimed to (1) quantify the magnitude of regional to global feedbacks between atmospheric chemistry and a changing climate and to reduce the corresponding uncertainty of the major ones and (2) identify mitigation strategies and policies to improve air quality while limiting their impact on climate change. Within the project, the field campaign is designed to investigate the formation and transformation of gaseous and aerosol species in both horizontal and vertical spaces.

The campaign was carried out at the San Pietro Capofiume site in the North Eastern part of the Po Valley, Northern Italy in June and July 2012. The sampling site is approximately 40 km away from Bologna and impacted by both anthropogenic and natural emissions from surrounding sites and agricultural fields. PM<sub>1</sub> samples were collected using a Digitel High-Volume sampler twice a day (daytime, 9 a.m. to 9 p.m., and night-time, 9 p.m. to 9 a.m.). In parallel, online aerosol measurements were performed with Scanning Mobility Particle Sizer

(SMPS), Aerosol Mass Spectrometer (AMS), Multi-Angle Absorption Photometer (MAAP), Nephelometer and High Humidity Tandem Differential Mobility Analyser (HH-TDMA). Additionally, Volatile Organic Carbon (VOC) samples were collected with Tenax TA cartridges six times a day (1:00-5:00, 5:00-9:00, 9:00-13:00, 13:00-17:00, 17:00-21:00, 21:00-1:00) and subsequently analysed by Thermal Desorption Gas Chromatography Mass Spectrometry (TD-GC/MS).

Figure 1 shows a time series of SMPS derived particle size number distributions, AMS derived chemical mass concentrations and mass fractions during the campaign period. Twenty-eight new particle formation events were observed within 30 measurement days. The particle number size distributions show a series of nucleation events that start in the morning. The AMS mass concentrations do not show corresponding species to these nucleation events, most likely due to a relatively small mass contribution of nucleating particles to the total particle mass. Approximately 50% of the PM<sub>1</sub> mass determined by the AMS at the sampling site was organics, followed by sulphate and ammonium. The concentration of nitrate is often much higher during the night than the daytime, indicating that particle bound nitrate evaporates as the temperature increases with sunrise.

Figure 2 shows the diurnal cycles of average VOC mixing ratios determined for the whole campaign period. The highest mixing ratios were observed in

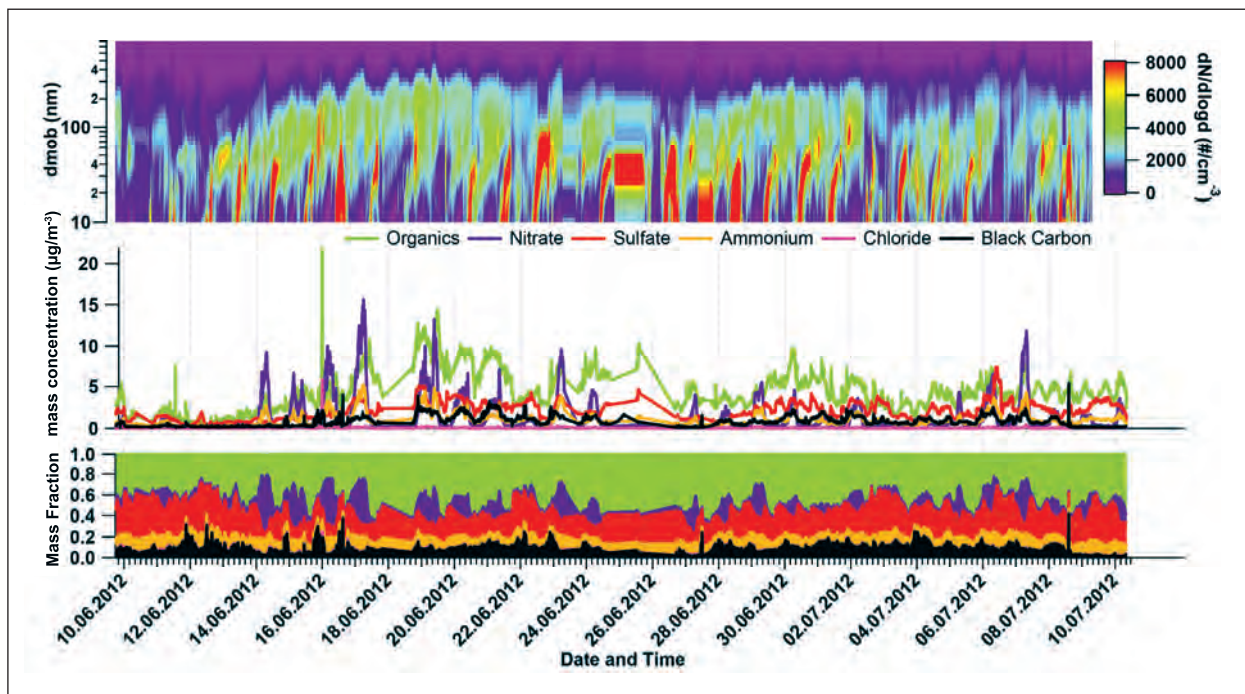


Fig. 1: Overview of the aerosol number size distribution (top) measured by SMPS and the aerosol chemical composition (middle) and mass fraction (bottom) measured by AMS at the San Pietro Capofiume site during the PEGASOS campaign.

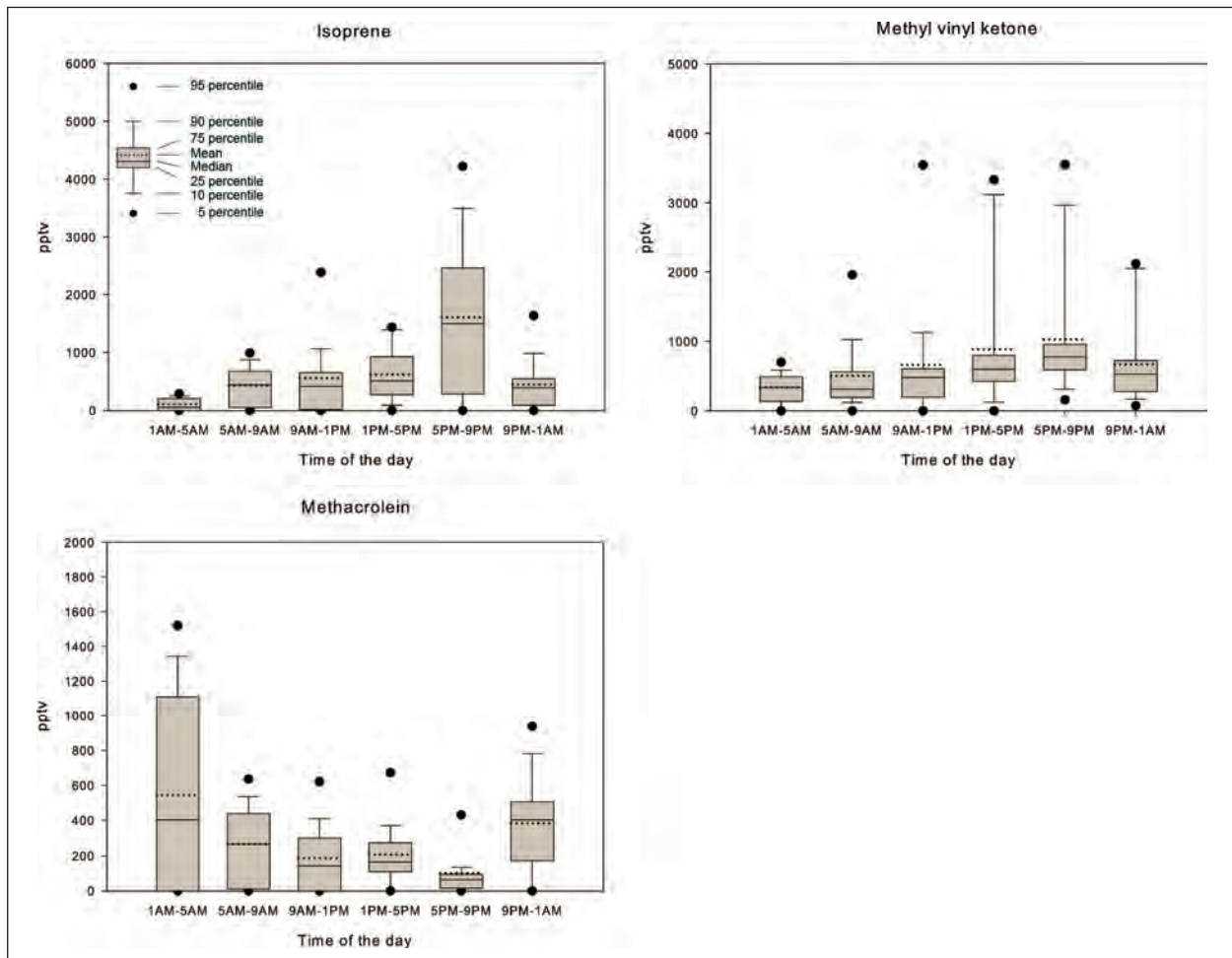


Fig. 2: Diurnal cycles of VOC mixing ratios observed during PEGASOS Po Valley 2012.

late afternoon for isoprene and methyl vinyl ketone (MVK) whereas the opposite was the case for methacrolein (MACR). The diurnal cycle of isoprene mixing ratio is consistent with its dependency on both temperature and light for its biogenic emission. MVK follows a similar diurnal cycle to isoprene, indicating that its formation relates to isoprene oxidation. However, MACR, another known isoprene oxidation product, shows an opposite pattern to both isoprene and MVK. It is not clear at this point if this is related to physical and chemical loss processes or the existence of MACR sources.

Figure 3 shows average diurnal variations of Secondary Organic Aerosol (SOA) compounds determined in the Hi-Vol aerosol samples collected during the campaign. Average glyoxal (GLY) and methylglyoxal (MGLY) concentrations were higher in the night-time samples whereas organosulphates (OS) concentrations were lower in the night-time samples. Indeed, GLY and MGLY correlate well with a correlation coefficient ( $r^2$ ) of 0.76, indicating that they have common sources. Higher glyoxal and methylglyoxal concentrations in the night-time samples are likely

caused by a change in a boundary layer height and degradation by photo-oxidation during the daytime.

All the OS correlate very tightly with  $r^2$  values greater than 0.6. However, GLY and MGLY, and OS correlate poorly with  $r^2$  values less than 0.2, indicating their formation mechanisms are not strongly linked even isoprene oxidation likely contributes significantly to their formation in the atmosphere. OS concentrations were higher in the daytime samples, indicating that they are photochemically formed. The m/z 215 OS showed only a small difference between daytime and night-time samples, indicating that there is a night-time source of a precursor compound. During the night-time, the reaction of isoprene with  $\text{NO}_3$  radical likely yields the C5 epoxydiol that serves as a precursor for the m/z 215 OS.

#### Air pollution in megacities: CAREBeijing NCP 2013

The rapidly increasing population and economy in China resulted in an enormous increase in emissions like  $\text{NO}_x$  and VOCs [e.g. Zhang et al., 2009]

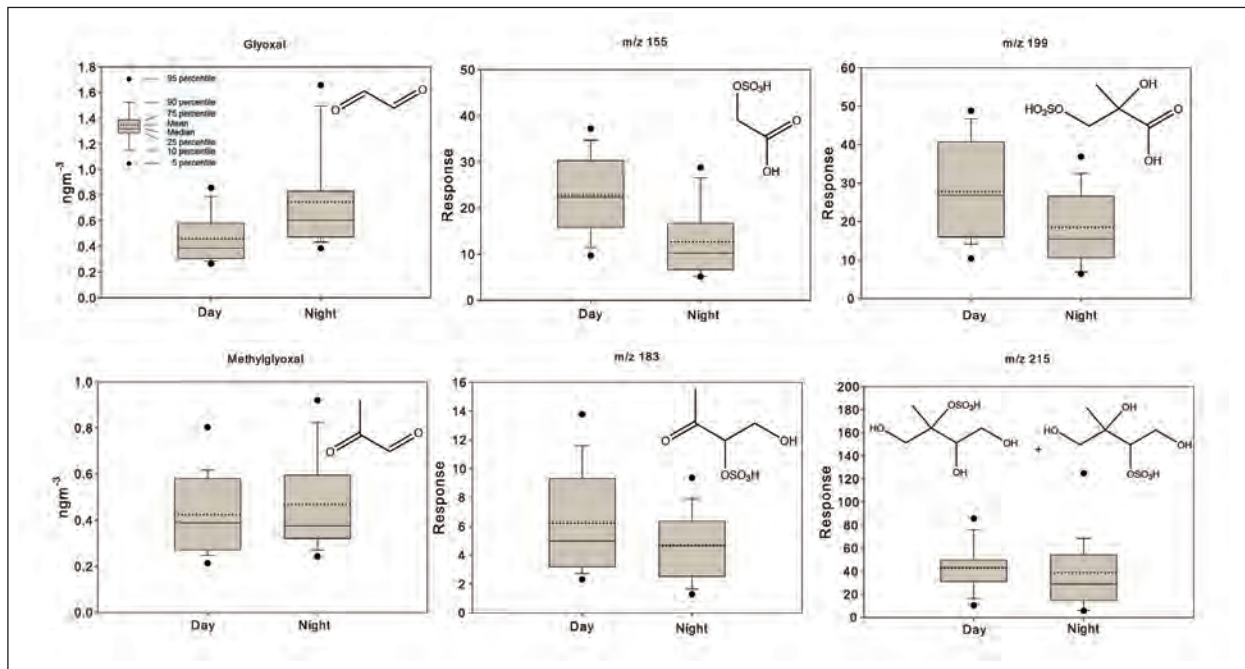


Fig. 3: Day/Night concentrations of SOA compounds during PEGASOS Po Valley 2012.

leading to severe photochemical smog and aerosol pollution. Consequences are reduced visibility and a strong impact on public health.

In July and August 2013, field measurements were performed at Xianghe which is located about 50 km south east of Beijing as part of CAREBeijing North China Plain 2013 (Campaigns of Air Quality Research in Beijing and Surrounding Regions). CAREBeijing aims to study the state and effects of air pollution in the megacity of Beijing and surrounding regions by characterizing physical, optical and chemical aerosol properties. Ground based measurements were carried out in-situ using a variety of instruments, e.g., Volatility Tandem Differential Mobility Analyser (V-TDMA), Hygroscopic Tandem Differential Mobility Analyser (HTDMA) and Multi-Angle Absorption Photometer (MAAP). Filter samples for offline chemical analysis including Organic Carbon and Elemental Carbon (OC/EC), Water-Soluble Organic Carbon (WSOC), inorganic ions and several individual organic compounds were collected during day and night-time using a  $\text{PM}_{10}$  high-volume DHA80-Digitel sampler and a 10-stage Berner impactor.

A preliminary result is shown in Fig. 4 where non-volatile particle number fractions determined for four different particles sizes (50, 100, 250 and 300 nm) by the V-TDMA measurements are plotted against the wind direction and the time of the day as an average over the whole campaign period. It shows that the 50 nm non-volatile particle number fraction is nearly constant for all wind directions. The observed reduction in non-volatile fraction during midday most

likely corresponds to new formed particles containing a high volatile fraction. Regarding the other three particle number sizes a more specific dependence on time of day and wind direction is observed. Predominating refractory particles during night time indicate the importance of local primary pollutant emissions.

Further data analyses are underway. Overall, the results of this campaign will allow for investigations of the evolution of aerosol by combining the chemical information with aerosol volatility and hygroscopicity data. Furthermore, developing parameterizations of the hygroscopic growth of the aerosol will help to quantify the influence of water in remote sensing observations so that a better link can be drawn between satellite observations and the pollution. Determination of mass concentrations of the aerosol, chemical composition and number size distribution will improve the understanding of the variability and magnitude of aerosol pollution for health risks studies.

### Air pollution in Saxony: Aerosol 2013

Air quality in the state of Saxony, Germany, is continuously monitored by the Saxon State Agency of Environment, Agriculture and Geology (Sächsisches Landesamt für Umwelt, Landwirtschaft und Geologie, LfULG). This monitoring provides long-term measurement data at many different places, while being limited to a rather low number of legally defined parameters only (mainly  $\text{PM}_{10}$  mass and trace gas concentrations). To provide a more comprehensive

basis for air quality and health related issues in the state legislation, the LfULG has been funding scientific projects focussing on important aspects of local and regional air pollution [e.g. *Birmili et al.*, 2008; *Brüggemann et al.*, 2000]. In 2013, TROPOS started to implement a project ("Size-segregated chemical and physical aerosol characterisation as indicator of air quality changes since 2000 in Leipzig and Saxony - Aerosol 2013") for the LfULG comprising a detailed characterisation of aerosol at four sites in parallel by means of in-situ measurements of particle number distributions and soot as well as discontinuous particle sampling for comprehensive offline chemical analysis. The project aims at i) documenting air quality changes within the last decade beyond the legally defined measures, ii) identifying the main sources of present-day air pollution in Saxony, iii) analysing the impact of biomass burning and pollutant long-distance transport, and iv) deducing recommendations for sustainable air quality control and corresponding legislation.

The four measurement sites were chosen to represent different air pollution characteristics: Two traffic sites were installed at a large street crossing in the city centre of Leipzig (Leipzig-Mitte, LMI) and next

to a narrow street canyon (Eisenbahnstrasse, EIB), urban background conditions were characterised by sampling on the roof of the TROPOS institute (TRO), and the TROPOS research site in Melpitz (MEL) served as a regional background site. At all sites, the in-situ measurements of particle number distributions and soot (black carbon, BC) will run for at least one year in parallel, while detailed chemical particle analysis is done in a summer and a winter campaign. The summer campaign was conducted between mid of June and end of September 2013. A total of 21 24-hour particle samples were collected applying 5-stage Berner low-pressure cascade impactors at all four sites. The samples were analysed for PM mass, inorganic ions, OC/EC, WSOC, monosaccharides including the biomass burning tracer levoglucosan, unpolar organic compounds including alkanes, polycyclic aromatic hydrocarbons (PAHs), and hopanes (traffic tracers), as well as a suite of trace metals.

In Fig. 5 a comparison of observed concentrations is shown for EC at all sites during the summer campaign. EC is one of the major air pollutants in urban areas and as can be seen for its  $\text{PM}_{10}$  concentrations (sum of 5 impactor stages) it is strongly elevated at the two traffic sites EIB and LMI. The

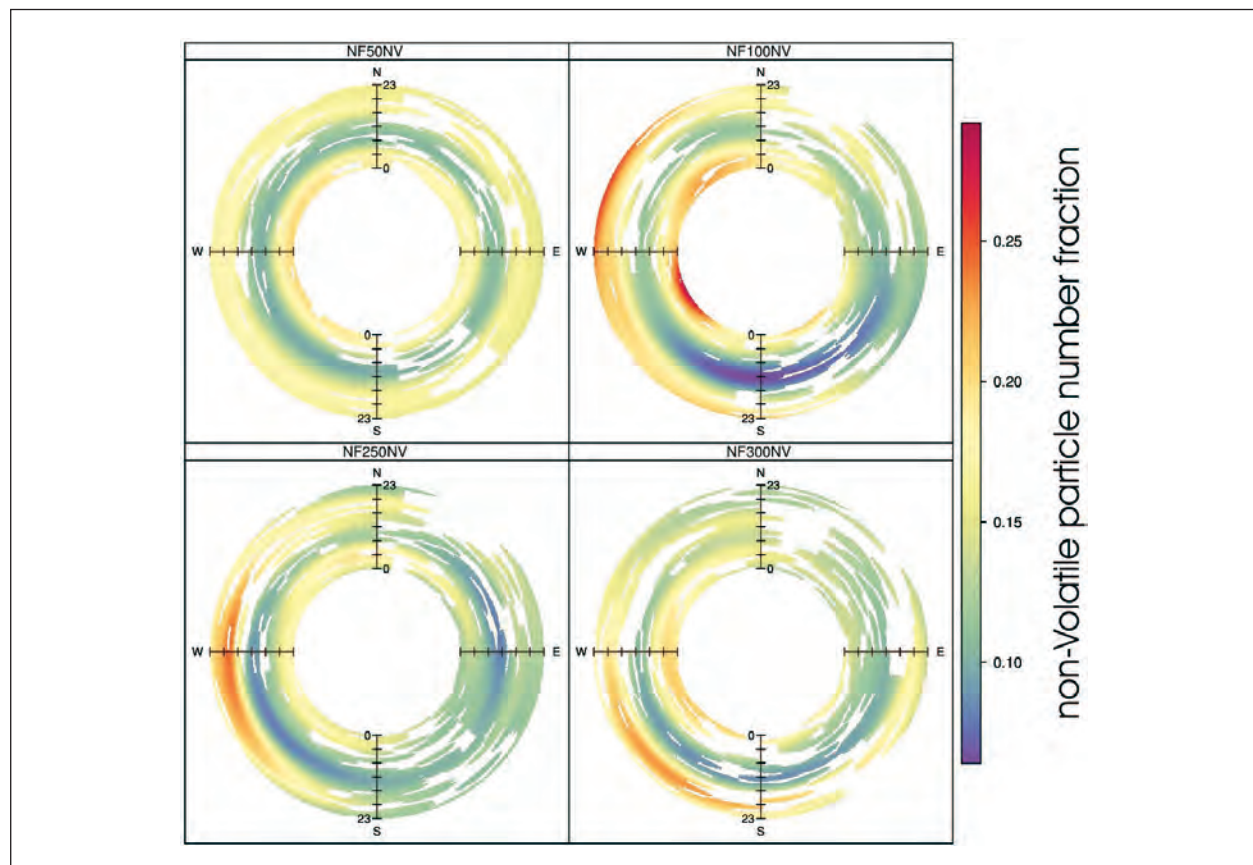


Fig. 4: Non-volatile particle number fractions for four selected particle sizes (50, 100, 250 and 300 nm).

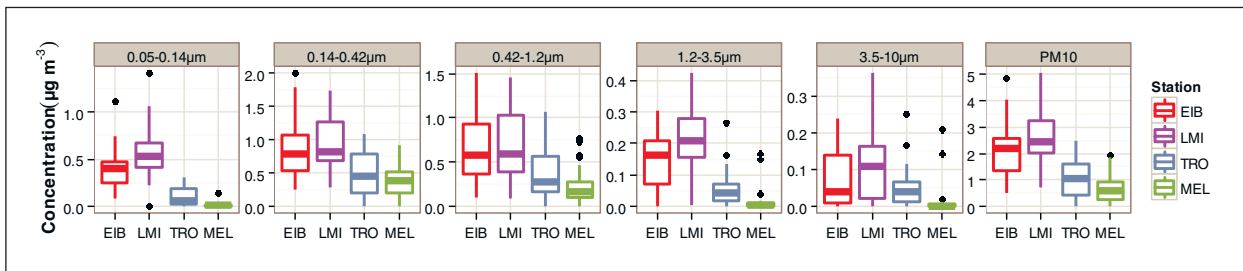


Fig. 5: Boxplots of observed EC concentrations in  $\mu\text{g m}^{-3}$  for 5 impactor stages (panels 1-5, left to right) and  $\text{PM}_{10}$  (sum of impactor stages) at all four project sites.

largest increases with regards to urban background concentrations at TRO are observed for ultrafine (aerodynamic diameter  $D_{\text{p,aer}} = 0.05\text{-}0.14 \mu\text{m}$ ) and for coarse particles (esp.  $D_{\text{p,aer}} = 1.2\text{-}3.5 \mu\text{m}$ ). While ultrafine particles represent direct exhaust emissions, coarse particle emissions are caused by road, tire and brake abrasion. Applying the concentrations measured at TRO as reference for the urban background [Lenschow et al., 2001], a median traffic contribution of ca.  $0.3\text{-}0.4 \mu\text{g m}^{-3}$  for ultrafine EC can be deduced, while traffic contributes ca.  $1.2 \mu\text{g m}^{-3}$  to  $\text{PM}_{10}$  EC concentrations. Traffic contributions from the Lenschow approach applied to total  $\text{PM}_{10}$  mass concentrations amount to ca.  $3\text{-}4 \mu\text{g m}^{-3}$  in this dataset. Another  $4 \mu\text{g m}^{-3}$  can be deduced for the urban increment (as compared to the regional background concentrations), indicating giving a total of ca.  $8 \mu\text{g m}^{-3}$   $\text{PM}_{10}$  mass concentration (as median value) which can be related to urban sources. As compared to the median concentrations of  $6.5 \mu\text{g m}^{-3}$  in the regional background, this indicates a rather large potential for local abatement strategies to significantly reduce urban pollution levels.

In the final evaluation of the project data (together with the results from the winter campaign), more detailed source apportionment approaches will be applied in order to obtain a detailed picture of present-day main PM sources within different particle size classes and to provide a scientific basis for legislation strategies of the LfULG agency.

#### Air/Sea exchange of organics: Polarstern cruises

It has recently been reported that marine aerosol particles contain unexpectedly large amounts of organic material that may significantly influence their physicochemical properties [Cavalli et al., 2004]. To study marine organic matter and its exchange between air and sea, marine aerosol particles ( $\text{PM}_1$ ) and the sea surface microlayer (SML) were sampled during the Polarstern cruises in 2011 and 2012. Aerosol sampling was carried out with a high

volume Digitel filter sampler during the Polarstern cruises in 2011 and 2012. The sampling time was typically 24 hours to allow for a sensitive determination of atmospherically relevant trace compounds in the particles. Chemical analysis of the samples comprised the determination of inorganic ions, OC/EC, WSOC, and different groups of organic species, including organic carbonyl compounds. The results for inorganic ions were in good agreement with the online AMS measurements and showed a majority of sulfate, ammonium and smaller concentrations of sea salt. The focus of the aerosol analysis was however on the determination of organic matter.

One major source for organic matter on marine aerosols is the ocean and especially the SML – the uppermost layer with a thickness of ca.  $1 \mu\text{m}$  that is the direct interface between the sea water and the atmosphere. The SML has shown to be often enriched with organic compounds. Sampling of the SML was carried out with a glass plate (sampling area  $2000 \text{ cm}^2$ ) that was vertically put in the water and slowly drawn upwards. The film adheres to the surface of the glass and is taken off by framed Teflon wipers [van Pinxteren et al., 2012]. For studying enrichment processes, corresponding bulk water from  $1 \text{ m}$  depth was collected using a self-made device consisting of a glass bottle mounted on a telescopic rod that regulates sampling depth.

A focus of organic analysis in the SML and in marine aerosol particles was on two  $\alpha$ -dicarbonyls glyoxal (GLY) and methylglyoxal (MGLY) that have attracted increasing attention over the past years because of their potential role in SOA formation. In the atmosphere, these carbonyls can be produced via oxidation of VOCs and typical precursors are isoprene, toluene, acetylene and acetone [Fu et al., 2008]. Besides secondary formation, direct emission of both GLY and MGLY to the atmosphere is also reported [Fu et al., 2008; Sinreich et al., 2010]. Although the volatility of GLY and MGLY is high and these compounds are found in the gaseous phase, large shifts of GLY and MGLY in the atmosphere towards the particle phase are reported [Ervens

und Volkamer, 2010]. Recently, Sinreich et al. [2010] attributed the open ocean as an important (so far unknown) source for GLY in the atmosphere and marine interactions are suggested to play a role in the carbonyl cycle. However, to date, there are few available field data of these compounds in the marine area. Therefore these carbonyls were investigated in the SML and marine aerosol particles sampled during the Polarstern Cruise ANT XXVII/4.

Chemical analysis of carbonyls in seawater is challenging as these compounds are mostly present in trace levels and the salt matrix can interfere with the analytical instrumentation. Therefore, at first a detailed method optimization was performed applying an analytical approach based on derivatisation with o-2,3,4,5,6-pentafluorobenzyl-hydroxylamine reagent (to convert the carbonyls into less volatile and less reactive species), solvent extraction with hexane (to transfer the derivatives into a compatible solvent for subsequent analysis) and gas chromatography-mass spectrometry in single ion monitoring mode (to ensure high selectivity and sensitivity of analytical determinations). The method was found to be suitable to analyse GLY and MGLY in marine aerosol particles and seawater in the nmol L<sup>-1</sup> range.

The results of water analysis showed that GLY and MGLY are present in the SML of the ocean and corresponding bulk water with average concentrations of 228 ng L<sup>-1</sup> (GLY) and 196 ng L<sup>-1</sup> (MGLY). Significant enrichment (factor of 4) of GLY and MGLY in the SML was found implying photochemical production of the two carbonyls though a clear connection to global radiation was not observed (Fig. 6).

In the marine aerosol particles samples during ANT XXVII/4, both carbonyls were detected (average concentration was 0.2 ng m<sup>-3</sup>) and are strongly connected to each other, suggesting similar formation

mechanisms. Both carbonyls show a very good correlation with particulate oxalate, supporting the idea of a secondary formation of oxalic acid via GLY and MGLY. A slight correlation of the two carbonyls in the SML and in the aerosol particles was found at co-located sampling areas [van Pinxteren und Herrmann, 2013]. This correlation of the  $\alpha$ -dicarbonyls in the SML and in the aerosol particles reported here could be a hint for interactions of these compounds – especially GLY – in seawater and in the atmosphere although specific mechanisms cannot be concluded from these data.

Photochemical carbonyl production from oceanic precursors has been observed before, where SML samples were irradiated using natural sunlight [de Bruyn et al., 2011]. To confirm these findings, SML sample irradiation was also carried out in the present study but using artificial Xe lamp irradiation ( $\lambda \geq 290$  nm) under controlled laboratory conditions. SML sample aliquots of 100 ml each were irradiated in a sealed reaction cell through a fused silica window in variable time steps up to several hours. The samples were then analysed for the GLY and MGLY concentrations. Interestingly, the resulting concentration time profiles do not always show carbonyl increase with increasing irradiation time as expected (Fig. 7).

Some profiles even show a carbonyl decrease or a mixed behaviour. Simultaneously to carbonyl production, the incident radiation could cause carbonyl decomposition by photosensitized production of halogen radicals [Jammoul et al., 2009] or direct photolysis of the carbonyls. Future measurements will involve the analysis of dissolved organic carbon because it was suggested that the formation of small carbonyl compounds can be caused by the photolysis of larger organic material of biogenic origin [de Bruyn et al., 2011]. More detailed process investigations will

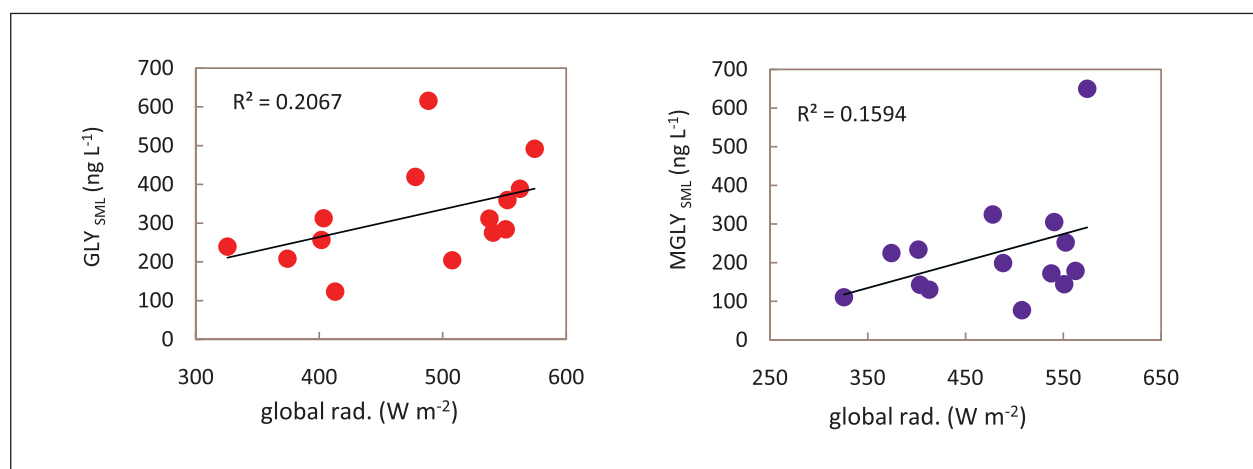


Fig. 6: Correlations between global radiation and GLY/MGLY concentrations in the SML during ANT XXVII/4.

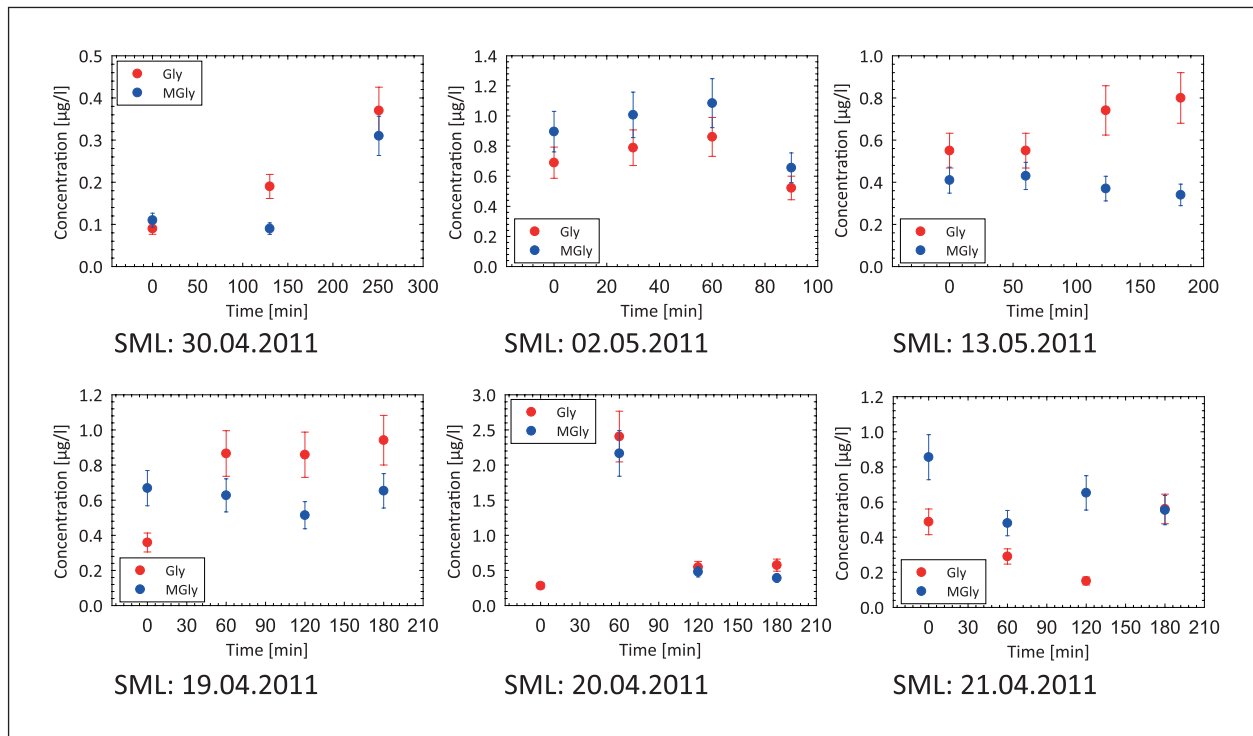


Fig. 7: Concentration-time profile of GLY and MGLY in SML samples from ANT XXVII/4 and ANT XXVIII/5 being exposed to different radiation times.

be necessary to elucidate the underlying mechanisms of this aqueous photochemistry and its potential impact on the marine atmosphere.

### Summary

Multiple field campaigns have been conducted by TROPOS during 2012 and 2013, four of which are presented as examples in the present contributions. During the PEGASOS field campaign in the Po Valley, Italy, different diurnal patterns for a number of SOA compounds were observed and related to photochemistry as a driving force for their formation as well as different sources and/or loss mechanisms such as photolysis. Data from the CAREBeijing NCP 2013 campaign is for the most part still under analysis but will improve the understanding of the variability

and magnitude of aerosol pollution in the Beijing area. First results from the Aerosol 2013 summer campaign indicate a rather large impact of urban emissions to the total PM pollution. Traffic could be shown to be one of the dominant factors which could be directly addressed by local abatement strategies to reduce urban air pollution levels. Measurements of organic carbonyl compounds in both the sea surface microlayer and marine particles during Polarstern cruises gave first insights into poorly studied interaction processes of these species between ocean and atmosphere.

Overall, results from these as well as other field campaigns with TROPOS participation help to improve knowledge in many important topic areas of atmospheric multiphase chemistry and aerosol physics.

### References

- Birmili, W., E. Brüggemann, T. Gnauk, H. Herrmann, Y. Iinuma, K. Müller, L. Poulin, K. Weinhold, and A. Wiedensohler (2008), Einfluss kleiner Holzfeuerungen auf die Immissionssituation - Teil Immissionsmessung. Sächsisches Landesamt für Umwelt und Geologie.
- Brüggemann, E., U. Franck, T. Gnauk, H. Herrmann, K. Müller, C. Neusüß, A. Plewka, G. Spindler, H.-J. Stark, and R. Wennrich (2000), Korngrößendifferenzierte Identifikation der Anteile verschiedener Quellgruppen an der Feinstaubbelastung., Sächsisches Landesamt für Umwelt und Geologie.
- Cavalli, F., M. C. Facchini, S. De Cesari, M. Mircea, L. Emblico, S. Fuzzi, D. Ceburnis, Y. J. Yoon, C. D. O'Dowd, J. P. Putaud, and A. Dell'Acqua (2004), Advances in characterization of size-resolved organic matter in marine aerosol over the North Atlantic, *J. Geophys. Res. - Atmos.*, 109(D24), -, doi: 10.1029/2004jd005137.
- de Bruyn, W. J., C. D. Clark, L. Pagel, and C. Takehara (2011), Photochemical production of formaldehyde, acetaldehyde and acetone from chromophoric dissolved organic matter in coastal waters, *J. Photochem. Photobiol. A*, 226(1), 16-22.

- EEA (2013), Air quality in Europe. 9/2013, 112 pp, European Environmental Agency, Copenhagen, Denmark.
- Ervens, B., and R. Volkamer (2010), Glyoxal processing by aerosol multiphase chemistry: towards a kinetic modeling framework of secondary organic aerosol formation in aqueous particles, *Atmos. Chem. Phys.*, 10(17), 8219-8244, doi: 10.5194/acp-10-8219-2010.
- Fu, T. M., D. J. Jacob, F. Wittrock, J. P. Burrows, M. Vrekoussis, and D. K. Henze (2008), Global budgets of atmospheric glyoxal and methylglyoxal, and implications for formation of secondary organic aerosols, *J. Geophys. Res. - Atmos.*, 113(D15), doi: 10.1029/2007jd009505.
- Herrmann, H., E. Brüggemann, U. Franck, T. Gnauk, G. Löschau, K. Müller, A. Plewka, and G. Spindler (2006), A source study of PM in saxon by size-segregated characterisation, *J. Atmos. Chem.*, 55(2), 103-130.
- Jammoul, A., S. Dumas, B. D'Anna, and C. George (2009), Photoinduced oxidation of sea salt halides by aromatic ketones: a source of halogenated radicals, *Atmos. Chem. Phys.*, 9(13), 4229-4237.
- Lenschow, P., H. J. Abraham, K. Kutzner, M. Lutz, J. D. Preuss, and W. Reichenbacher (2001), Some ideas about the sources of PM10, *Atmos. Environ.*, 35, S23-S33.
- Sinreich, R., S. Coburn, B. Dix, and R. Volkamer (2010), Ship-based detection of glyoxal over the remote tropical Pacific Ocean, *Atmos. Chem. Phys.*, 10(23), 11359-11371, doi: 10.5194/acp-10-11359-2010.
- van Pinxteren, M., and H. Herrmann (2013), Glyoxal and Methylglyoxal in Atlantic Seawater and marine Aerosol Particles: Method development and first application during the Polarstern cruise ANT XXVII/4, *Atmos. Chem. Phys.*, 13, 11791-11802, doi: 10.5194/acp-13-11791-2013.
- van Pinxteren, M., C. Müller, Y. Iinuma, C. Stolle, and H. Herrmann (2012), Chemical Characterization of Dissolved Organic Compounds from Coastal Sea Surface Micro layers (Baltic Sea, Germany), *Environ. Sci. Technol.*, 46(19), 10455-10462, doi: 10.1021/es204492b.
- Zhang, Q., D. G. Streets, G. R. Carmichael, K. B. He, H. Huo, A. Kannari, Z. Klimont, I. S. Park, S. Reddy, J. S. Fu, D. Chen, L. Duan, Y. Lei, L. T. Wang, and Z. L. Yao (2009), Asian emissions in 2006 for the NASA INTEX-B mission, *Atmos. Chem. Phys.*, 9(14), 5131-5153.

---

## Funding

European Union (EU), Brussels, Belgium

German Federal Ministry of Education and Research (BMBF), Bonn, Germany

German Research Foundation (DFG), Bonn, Germany

Saxon State Agency of Environment, Agriculture and Geology (LfULG), Dresden, Germany

---

## Cooperation

Multiple national and international project partners

# Regional Scale Amine Chemistry Dispersion Modelling with COSMO-MUSCAT

Ralf Wolke<sup>1</sup>, Andreas Tilgner<sup>1</sup>, Detlef Hinneburg<sup>1</sup>, Roland Schrödner<sup>1</sup>, Claus Nielsen<sup>2</sup>, Hartmut Herrmann<sup>1</sup>

<sup>1</sup>Leibniz Institute for Tropospheric Research (TROPOS), Leipzig, Germany

<sup>2</sup>University of Oslo, Oslo, Norway

Die Abtrennung von CO<sub>2</sub> aus dem Abgas von Kraftwerken durch industrielle Aminwäscheverfahren (Post-Combustion-Capture) ist eine CCS-Technologie, um anthropogene Emissionen des Treibhausgases CO<sub>2</sub> zu verringern. Geringe Mengen der verwendeten Amine, wie Monoethanolamin (MEA), können aus dem Aminwäsche-Prozess in die Atmosphäre emittiert werden und dort potentiell krebserregende Substanzen, wie Nitramine, bilden. Um die Prozessierung von emittierten MEA und dessen karzinogener Oxidationsprodukte in der Troposphäre sowie deren Eintrag in andere Umweltkompartimente zu untersuchen, wurde am TROPOS ein detaillierter MEA-Mehrphasenphasenchemie-mechanismus entwickelt und in einer Vielzahl von Modellstudien angewendet. Ferner wurde ein kondensiertes Reaktionsschema für 3D Ausbreitungsrechnungen erarbeitet. Mit diesem wurden 3D Ausbreitungssimulationen mit dem gekoppelten Chemie-Transport Modell COSMO-MUSCAT durchgeführt, um die regionale Prozessierung von MEA sowie zu erwartende regionale Umweltbelastungen und Gesundheitsrisiken durch karzinogene Reaktionsprodukte, wie Nitramine und Nitrosamine, im Umfeld einer CCS-Pilotanlage in Norwegen zu quantifizieren. Mit Hilfe der durchgeführten Umweltstudien konnte gezeigt werden, dass durch die zu erwartenden Amine-Emissionen und unter den meteorologischen Bedingungen in der Region Mongstad die norwegischen Grenzwerte für eine langfristige Exposition sowie die Gesamtkonzentrationen von Nitrosaminen und Nitraminen in der Luft nicht überschritten werden.

## Introduction and Motivation

CO<sub>2</sub> capture and store (CCS) technologies, for example amine-based post-combustion CO<sub>2</sub> capture techniques, are designed to reduce anthropogenic CO<sub>2</sub> emissions into the atmosphere and are thus an attempt to mitigate the climate change. At present, amine-based post-combustion CO<sub>2</sub> capture techniques of power plants will release discharged air into the environment, which will contain a small but still significant amount of amines and their oxidation products. Moreover, it is known that the atmospheric oxidation of amines can lead to the formation of harmful (potentially carcinogenic) compounds such as nitramines and nitrosamines [Nielsen et al. 2012, see Fig. 1]. Thus, an improved knowledge about the tropospheric chemical fate and physical removal processes of released amines and their oxidation products is required in order to assess the environmental impact and risks resulting from amine-based capturing operations.

Recent box model studies performed at TROPOS [Herrmann et al., 2011] have implicated the importance of multiphase chemical interactions for the

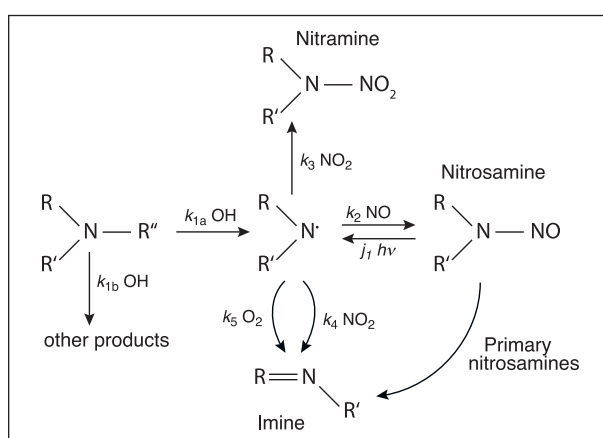


Fig.1: Atmospheric photo-oxidation scheme for amines showing the routes to imines, nitramines and nitrosamines. Modified after Nielsen et al. [2012].



Fig. 2: Industrial site at Mongstad (Norway).

tropospheric processing of emitted amines from CCS techniques. However, complex chemical interactions were not yet considered in former simple dispersion modelling [see e.g. Berglen et al., 2010]. For a better understanding of the regional fate and distribution of these compounds in the complex dynamic atmospheric multiphase system, further investigations with advanced higher-scale models are needed, which consider a detailed representation of amine chemistry.

The present air pollution study focuses mainly on the regional scale modelling of the tropospheric fate and deposition of monoethanolamine (MEA) and its oxidation products using the modelling system COSMO-MUSCAT. The present modelling work was specifically designed to investigate conditions and impacts at the planned CO<sub>2</sub> capture power plant at Mongstad and the surrounding area close to Bergen, Norway (see Fig. 2). The primary amine MEA was selected as test amine for the amine-based post-combustion facility at Mongstad.

In the present study, both detailed chemical process model studies are performed in order to develop a reduced chemical mechanism for MEA and complex 3-dimensional dispersion model investigations were carried out focusing mainly on the multiphase chemical fate and lifetime of MEA and its reaction products such as amides, nitramines and nitrosamines in the troposphere as well as their tropospheric removal. The present study aims to provide detailed and conclusive concentration/deposition charts. These charts provide details on the regional fate of MEA and its oxidation products, the regional distribution of such pollutants and characterize locally the potential input of those pollutants into other environmental compartments. The performed annual simulations were accompanied by extensive sensitivity and process studies to evaluate the associated uncertainties. Overall, the model results might allow future evaluations of possible environmental impacts

and human health effects of pollutants emitted from CCS processes.

In detail, the present work focused mainly on:

1. Development of an improved detailed multiphase chemistry mechanism for MEA and its oxidation products and subsequently on the development of a reduced multiphase MEA chemistry mechanism
2. Characterization of the multiphase chemical processing of MEA and its degradation products by detailed parcel model and 2D model simulations
3. Characterization of the regional transport and chemical transformation of the emitted aerosol constituents (MEA) including the potential formation of nitrosamines, nitramines and amides as well as the regional deposition of such pollutants
4. Characterization of compound concentrations in the surrounding of the industrial site Mongstad and deposition patterns (wet and dry deposition) under different synoptic/seasonal conditions allowing for future estimates on potential environmental impacts and human health effects

### Modelling System COSMO-MUSCAT

The physical and chemical processes in the atmosphere are very complex. They occur simultaneously, coupled and in a wide range of scales. These facts have to be taken into account in the numerical methods for the solution of the model equations. The numerical techniques should allow the use of different resolutions in space and also in time. The lack of adequate resolution limits the ability for accurate modelling of individual processes and their interactions. For example, when plumes are injected into coarse grid cells in regional models with a uniform grid, the emitted material is diluted immediately within the cell and the details of the near field chemistry are lost. Multiscale models can provide finer resolution in certain key regions, e.g. around large sources or urban areas.

The modelling department of the TROPOS has developed the state-of-the-art multiscale model system COSMO-MUSCAT [Wolke et al., 2004, 2012]. It is qualified for process studies as well as the operational forecast of pollutants in local and regional areas [Heinold et al., 2012; Hinneburg et al., 2009; Renner and Wolke, 2010]. The model system consists of two online-coupled codes. The operational forecast model COSMO is a non-hydrostatic and compressible meteorological model and solves the governing equations on the basis of a terrain-following grid

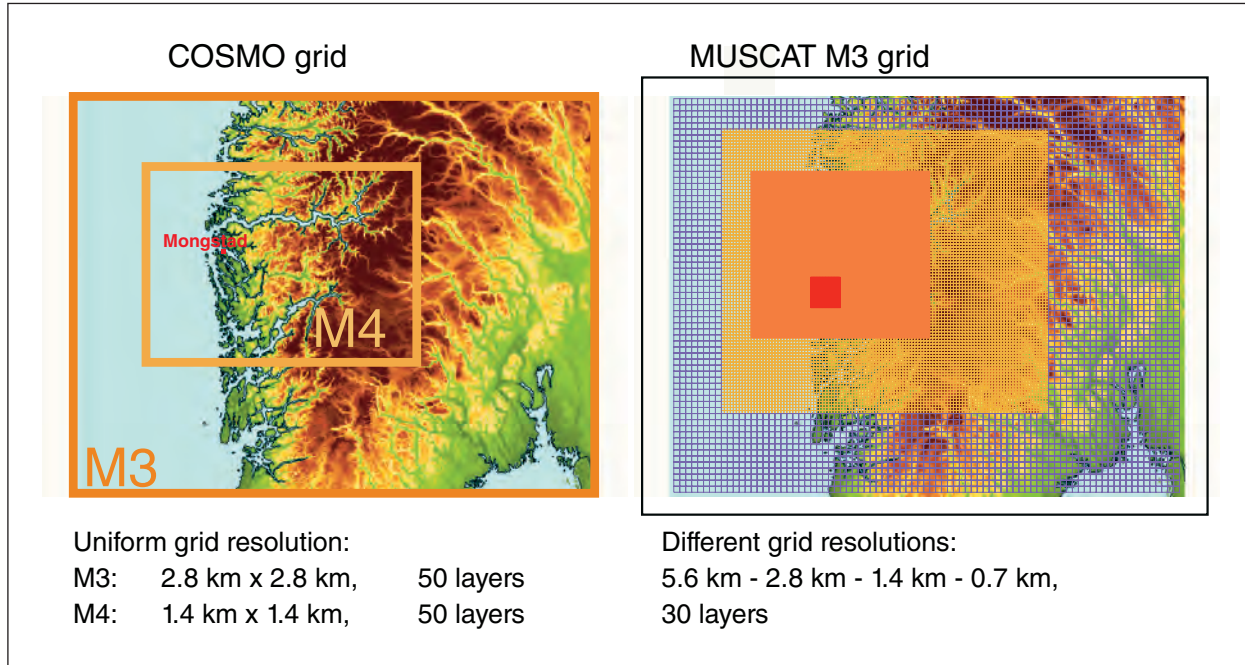


Fig. 3: COSMO and MUSCAT grids for the M3 model simulations.

[Baldauf et al., 2011; Schättler et al., 2009]. Driven by the meteorological model, the chemistry transport model MUSCAT treats the atmospheric transport as well as chemical transformations for several gas phase species and particle populations. The transport processes include advection, turbulent diffusion, sedimentation, dry and wet deposition.

The modelling system is used for several air quality applications [Stern et al., 2008; Hinneburg et al., 2009; Renner and Wolke, 2010] and the investigation of the large-scale transport of Saharan dust, including its sources and sinks [Heinold et al., 2007]. The simulation results are evaluated by ground-based measurements and satellite data.

### Model setup

Dispersion model simulations are performed with horizontal resolutions down to 700 m around the Mongstad absorber. A hierarchical nesting strategy provides the required boundary fields from the European to the local scale. Hereby, runs for West Norway (M2 domain) are performed with a horizontal grid resolution of 8 km. The nests M3 and M4 are given in Fig. 3. In this configuration, the domain M4 covers the region of interest around Mongstad of 60 km x 60 km. In each of the regions M2-M4, the meteorological code COSMO runs on a uniform grid. The online-coupled chemistry-transport model MUSCAT uses different resolutions (coarse near the boundaries and finer in the inner regions) for each of the domains M2-M4 (Fig. 3). This corresponds to a

two-way nesting for the chemistry-transport part and allows finer resolutions in the near of the Mongstad plume. 50 layers are used for the vertical discretization in all COSMO model runs. In this study, MUSCAT treats only the lower troposphere up to about 5 km and uses 30 vertical layers. The resolution is around 20 m near the surface.

The simulations are performed in a “forecast regime,” that means, only by forcing via the boundaries without any data assimilation and nudging. The usual nesting technique is applied for the COSMO-MUSCAT simulations on the inner domains (M3, M4). The COSMO run of the M2 domain is initialized and forced by reanalysed data provided by the global meteorological model GME (Global Model of the Earth) of the DWD (Deutscher Wetterdienst). The M2 boundary data for the gas phase species are generated from global data from the ECMWF (European Centre for Medium-Range Weather Forecasts). The inventories of the anthropogenic emissions are based on EMEP (European Monitoring and Evaluation Programme). The dataset consists in European anthropogenic emissions for the 10 SNAP sectors and international shipping on a 0.125 by 0.0625 degree lon-lat resolution. This emissions dataset did not include dust. The biogenic emissions and radiation activity are calculated by MUSCAT, whereas information on the cloud cover, temperature, and other meteorological parameters are taken from the coupled meteorological model. Consequently, the meteorological situation has a direct influence on the emission amount. Two different emission scenarios for the absorber

were provided by TCM [“expected” and “worst” case scenario; *Tønnesen*, 2011]. Additionally, 8 further point emission sources from Mongstad industrial area are also incorporated in the model calculations.

### Meteorological evaluation and tracer simulations

Meteorological values from COSMO-MUSCAT-simulations are compared with available measurements for November 2006 until October 2007. The model can reproduce the measured temperature

time series and the monthly wind roses relatively well (Fig. 4a, b). Precipitation is important for removal of atmospheric trace gases and particles due to wet deposition. For an accurate modelling of concentrations, which are sensitive to wet deposition, it is important that the occurrence of rain events matches the measurements in time and space and that the amount of rain is in the right range. A time series of precipitation (daily rain rate) at Kvitsoy is shown in Fig. 4c. An analysis of the spatial annual rain distribution shows that the precipitation is distributed homogeneously in the near source region with an annual

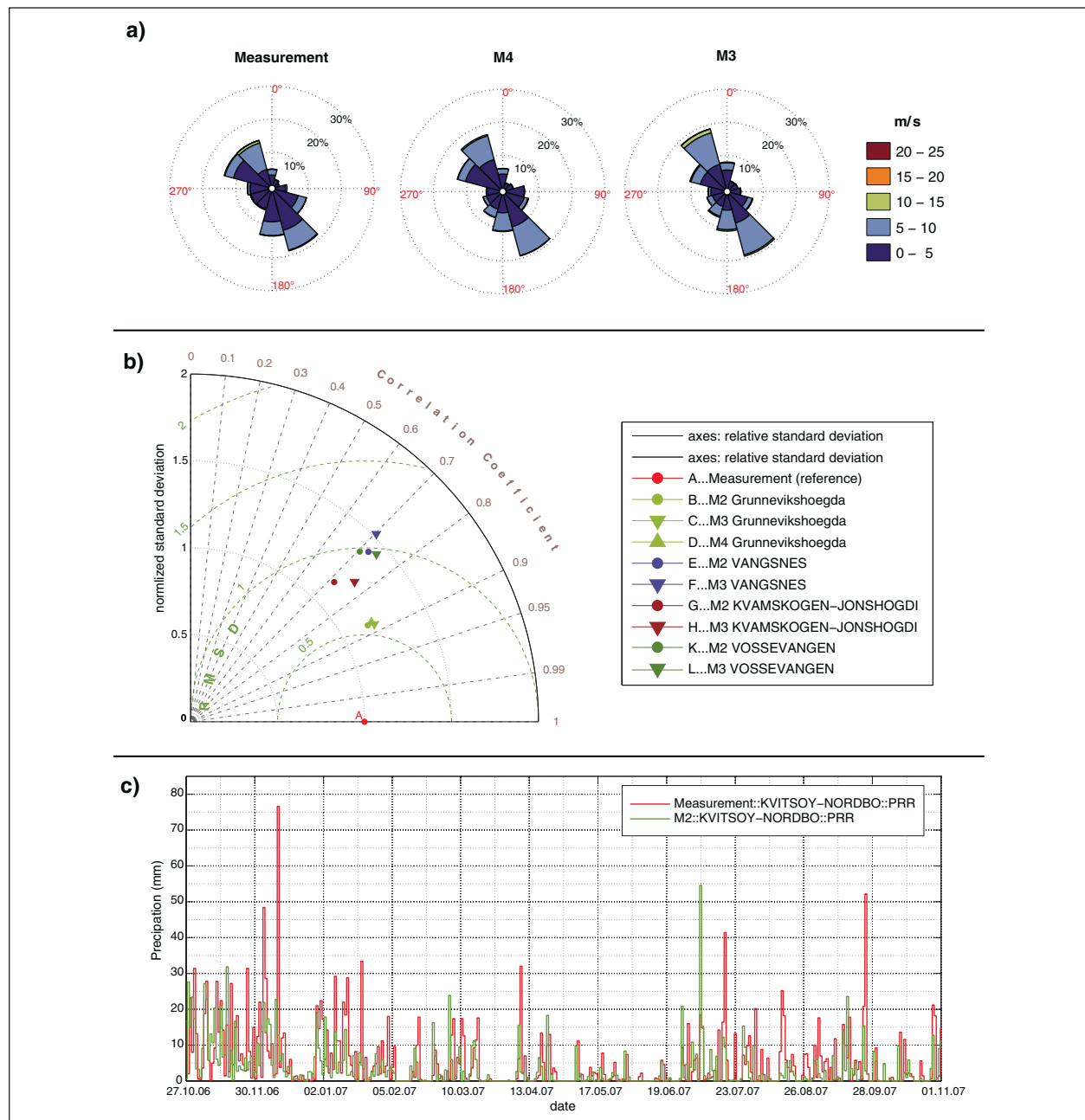


Fig. 4: Meteorological evaluation: (a) Measured and modelled annual wind roses at Grunnevikhoegea; (b) Taylor diagram of wind direction; (c) Time series of precipitation at Kvitsoy for November 2006 - October 2007.

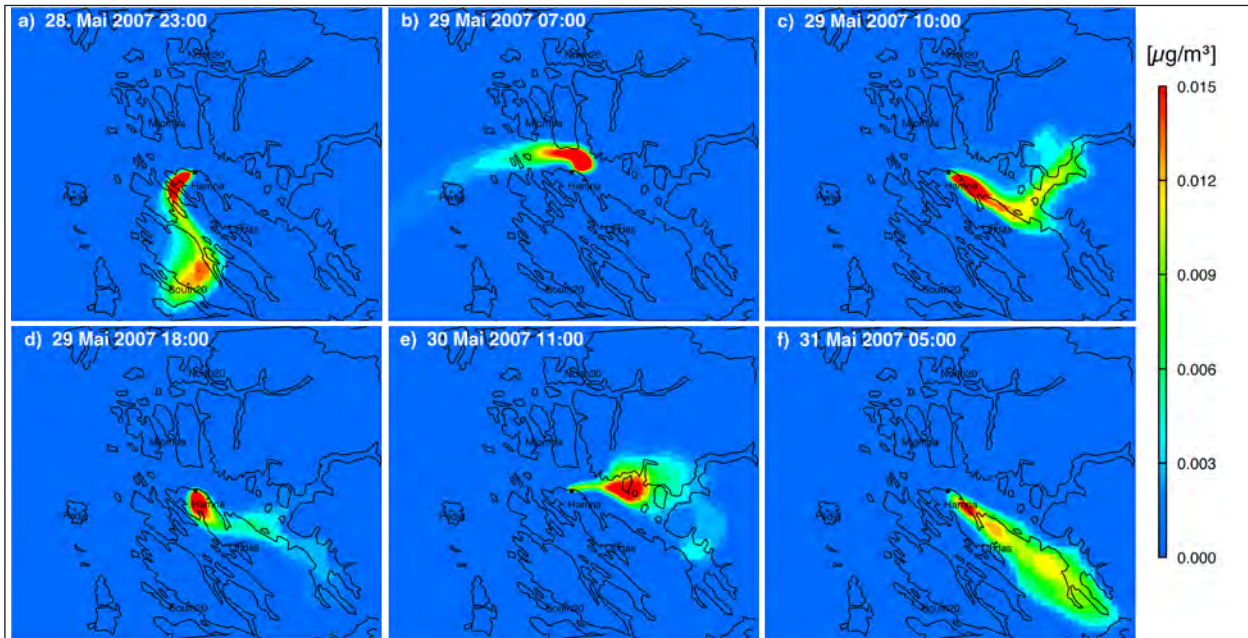


Fig. 5: Snapshots of the plume evolution end of May 2007: MEA concentration at ground level in [ $\mu\text{g}/\text{m}^3$ ].

average of around 1500 mm/year. In the Northwest, the precipitation rate is enhanced due to the elevating orography up to 3500 mm/year. Moreover, hit-statistics were analysed for evaluating the modelling performance. As analysed hit-statistics show, COSMO has some problems in the prediction of rainy days, which is shown by a false alarm rate of ~15-25%. Altogether, the amount of precipitation is represented with moderate accuracy, but the temporal behaviour is not always satisfying.

The active chemical species and their reactions are subject to the atmospheric conditions (wind, temperature, turbulent mixing, stability, cloudiness, ...), which in interaction with the surface structure vary in time and space very discontinuously. In order to conform to these simultaneous dynamic 3D relationships, the manifold processes of emission, transport, deposition, chemistry, and meteorology have to be completely coupled online as is managed in the applied simulation model. As worst-case estimation the emitted MEA is treated as an inert tracer including dry and wet deposition. These simulations without chemical transformations are carried out to study especially the plume rise, the dilution, the transport and deposition processes of pollutants in the plumes of the Mongstad stacks. Furthermore, the calculations should demonstrate the robustness and sensitivity of the results against changes in the model configuration as well as in the initial and boundary conditions. For this reason, some additional inert tracers have been introduced, where some process descriptions (e.g. plume rise formula) are modified or the point sources around the original position are varied. Such

investigations are performed for annual simulations as well as for selected periods. In this study, the dry and wet deposition of amines is described similar to  $\text{NH}_3$  due to the expected comparable chemical behaviour. The sensitivity of concentration fields against changes in the deposition parameterization was also quantified for two 10-day simulations in December 2006 and May 2007.

The dynamics of the plume evolution is illustrated in Fig. 5. The plots show six snapshots of plume concentrations within 60 hours. Different situations are presented, where rotating, alternating, retrograde, and fast variable wind leads to very complex structures such as evasion of the mountains, advance into the fjords, transport of former plume fractions, and oscillating plumes. The finer the horizontal and vertical grid resolution for the simulations was chosen, the more sophisticated patterns in the resulting concentration distributions can be diagnosed. Not only the spatial resolution plays an important role in a realistic simulation of the plumes, but also the (fast) temporal development of the meteorological situation. Such changes, e.g. of the dynamic stability of the atmosphere, can occur abruptly, which necessarily affords an online-coupled combined treatment of all processes as is implemented in the applied model system. All these influences are of crucial importance for the actual situation, even if they are smeared and get not interpretable by temporal averaging. Furthermore, the influence of three different applied plume rise approaches was compared. The general impact of the plume rise on the dispersion is a delayed touchdown of the plume on the surface.

Depending on the vertical mixing situation, the plume can reach the surface at a distance of up to a few tens of kilometres (Fig. 5e).

The performed “worst case” tracer simulations (MEA without chemistry) have revealed maximum concentrations of MEA of about 6 ng / m<sup>3</sup>, i.e., well below reported limits of long-term exposure [10 µg / m<sup>3</sup>, see Låg et al., 2008]. Furthermore, the studies have shown, that both dry and wet depositions are equally important for the tropospheric removal of MEA. Deposition reduces the predicted MEA concentrations by about 10-30% depending on the meteorological conditions and the surface properties. Dry deposition is closely correlated to the land-use data. The pattern of wet deposition is due to the occurrence of precipitation and high concentration in the same region at the same time. For the simulated year, the deposition of the MEA-tracer does not reach the limits prescribed in the guidelines.

### Chemical modelling of the multiphase MEA chemistry

To investigate the chemical fate of MEA emitted from CO<sub>2</sub> capturing processes and the MEA oxidation products in the tropospheric multiphase system by means of both box and later regional dispersion models, (i) the development of a complex multiphase chemical mechanism, (ii) subsequent simulations with the complex Lagrangian parcel model SPACCIM [SPectral Aerosol Cloud Chemistry Interaction Model, Wolke et al. 2005], (iii) a mechanism reduction (development of a condensed mechanism for the regional dispersion model COSMO-MUSCAT) and (iv) first 2D COSMO-MUSCAT simulations are performed within this study.

Based on former laboratory investigations and mechanism developments, an up-to-date multiphase mechanism describing the gas and aqueous phase chemistry of MEA has been developed in the present study. The developed multiphase phase oxidation scheme of MEA and its oxidation products, including nitrosamines, nitramines and amides, was coupled to the existing multiphase chemistry mechanism [RACM-MIM2ext-CAPRAM3.0i-red, Deguillaume et al. 2010] and the CAPRAM Halogen Module 2.0 [Bräuer et al. 2013]. Overall, the built multiphase mechanism comprises 1276 chemical processes including 668 gas and 518 aqueous phase reactions as well as 90 phase transfers. The multiphase amine module contains in total 138 processes. The final mechanism was used in the Lagrangian parcel model SPACCIM to investigate e.g. the main oxidation pathways, the formation of environmental hazardous oxidation products and seasonal differences. Simulations

were performed using a meteorological scenario with non-permanent clouds, different environmental trajectories and seasonal conditions using chemical mechanisms of different complexity (gas-only/gas+aq: mechanism with MEA gas phase chemistry only/with both MEA gas and aqueous phase chemistry considered). Further details on the developed mechanism and the performed model studies are given in [Herrmann et al. 2013].

The SPACCIM studies have shown that the partitioning of MEA is shifted towards the aqueous phase and thus the aqueous phase (cloud droplets and deliquescent particles) represents the main oxidizing compartment for MEA and the multiphase processing its products. The model investigations implicated that aqueous phase oxidation by OH radicals represents the main sink for MEA under daytime cloud summer conditions (see Fig. 6). Reaction flux analyses have shown that under deliquescent particle conditions, the Cl radical represents an important oxidant. The simulations with different mechanisms (e.g., with and without aqueous phase chemistry) have shown that the aqueous phase suppresses N-nitrosamine/N-nitramine formation in the gas phase by taking up MEA. Furthermore, the model implicated that aqueous phase chemistry treatment slows down the overall decay of MEA and increases its tropospheric residence time except rain is occurring. Simulations without aqueous phase chemistry treatment were characterized by much higher concentrations of MEA-nitramine implicating that pure gas phase simulations provide elevated “case concentrations” and might be used for “upper limit” estimations of harmful MEA products, which, however, have to be applied with care. Also, simulations revealed that the aqueous formation of N-nitrosoamines from MEA is not a relevant process under tropospheric conditions and thus the investigations were focused on the formation of MEA-nitramine. Moreover, the simulations showed that MEA oxidations are quite restricted under low photochemical winter conditions leading to much longer tropospheric residence times (see Fig. 6). Furthermore, performed sensitivity studies (not presented here) on the importance of mass accommodation coefficients ( $\alpha$ ) for multiphase processing of MEA have revealed that the applied  $\alpha$ -value in the performed multiphase chemistry simulations is a very crucial parameter, e.g., for MEA and particularly for MEA-nitramine, which can significantly influence the predicted concentration levels. In the range of the used  $\alpha$ -values the predicted MEA-nitramine can vary over orders of magnitude. However, the model runs have also revealed that the gas-only simulations ( $\alpha = 0$ ) represent an upper limit. Overall, the sensitivity studies have implied that adequately

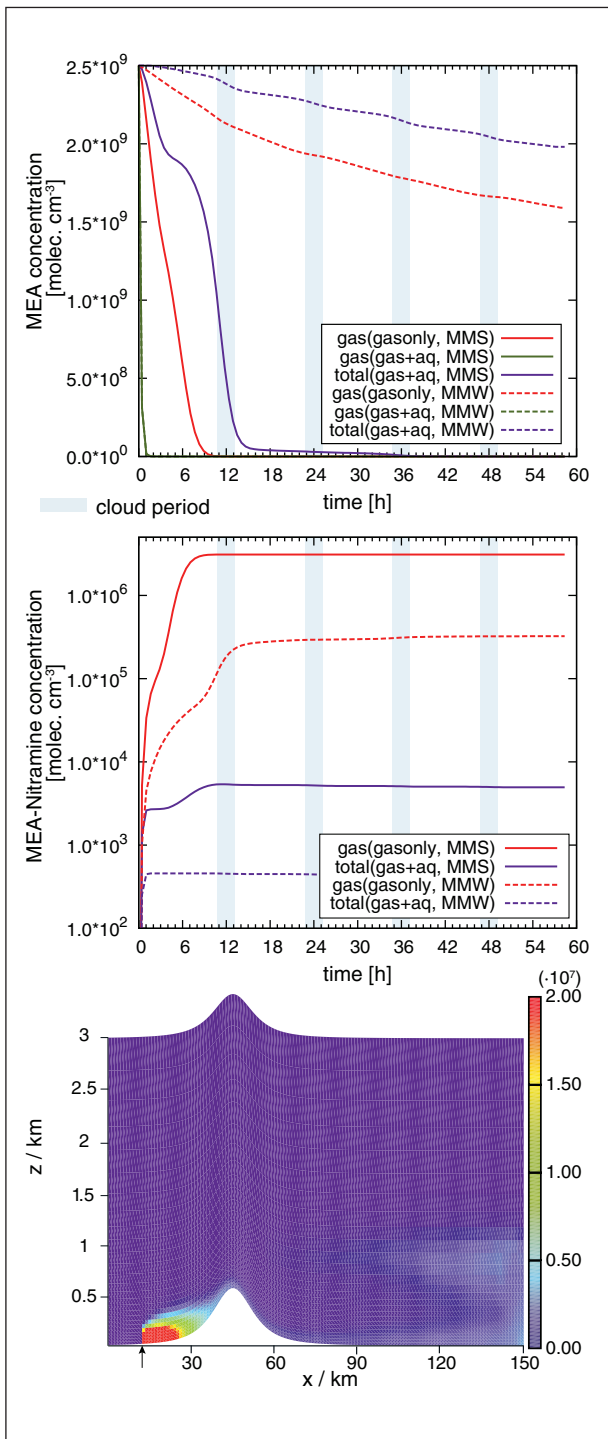


Fig. 6: Modelled concentration profiles (in molecules  $\text{cm}^{-3}$ ) of monoethanolamine (MEA, top) and MEA-Nitramine (center) for the scenarios MMS/MMW (marine summer/winter case) in the different mechanism cases (gas-only/gas+aq run). In the 2D plot (down), a vertical cross section of the concentration of MEA (gas + aq. phase) in molecules  $\text{cm}^{-3}$  at 12:00 (after 36 hours of simulation time). Calculations were conducted with the fully coupled chemistry transport model COSMO-MUSCAT. The main wind direction is from left to right. An orographic cloud is evolving at the top of the hill.

experimentally obtained  $\alpha$ -values of soluble amines such as MEA are a substantial must to improve the model predictions of nitramine and nitrosamine concentration levels and to lower the current uncertainties in the predicted concentrations.

In order to provide a condensed mechanism applicable for regional scale dispersion modelling, a mechanism reduction was performed based on comprehensive reaction flux investigations. The developed reduced mechanism contains just 303 gas and 112 aqueous phase reactions and 32 phase transfers. The reduced mechanism describes adequately the multiphase chemistry of MEA and its key oxidation products. The required computational costs are reduced by about 45% compared to the full MEA mechanism. Thus, the reduced mechanism provides the basis for further regional dispersion model studies. As a first step into this direction, first 2D simulations have been performed using the COSMO-MUSCAT chemistry transport model [Wolke et al. 2012] investigating the multiphase processing of MEA and its products in an orographic cloud. The 2D model studies have reproduced the output of the box model simulations considering the different mixing behaviour due to more dimensions. Furthermore, 2D sensitivity studies showed that the stack height is important for the mixing to the ground and transport effects (increasing stack height reduces the ground level concentrations and enhances transport over longer ranges).

### 3D simulations with MEA chemistry

Based on the results of the process model studies, further COSMO-MUSCAT studies were aimed at the examination of the importance of tropospheric gas phase oxidations for the fate of MEA, the production of harmful compounds such as nitramines and the dispersion of MEA and its products including their regional concentration levels. Chemical transformations of emitted pollutants are closely coupled with atmospheric transport (advection, vertical turbulent mixing, deposition) and meteorological conditions (temperature, humidity, cloudiness, photolysis, ...). The nature of these processes is that they occur simultaneously and dynamically in time and space. Additionally, the huge variety of atmospheric trace gases is responsible for the need of detailed chemical mechanisms. Therefore, an appropriate modeling is only possible by 3D chemistry transport models (CTM). For this study, realistic concentrations of reactants ( $\text{OH}$ ,  $\text{NO}_3$ ,  $\text{NO}_2$ ) for MEA chemistry were provided by applying the RACM chemistry and anthropogenic emission inventories [Pouliot et al., 2012]. The physical loss processes of dry and wet

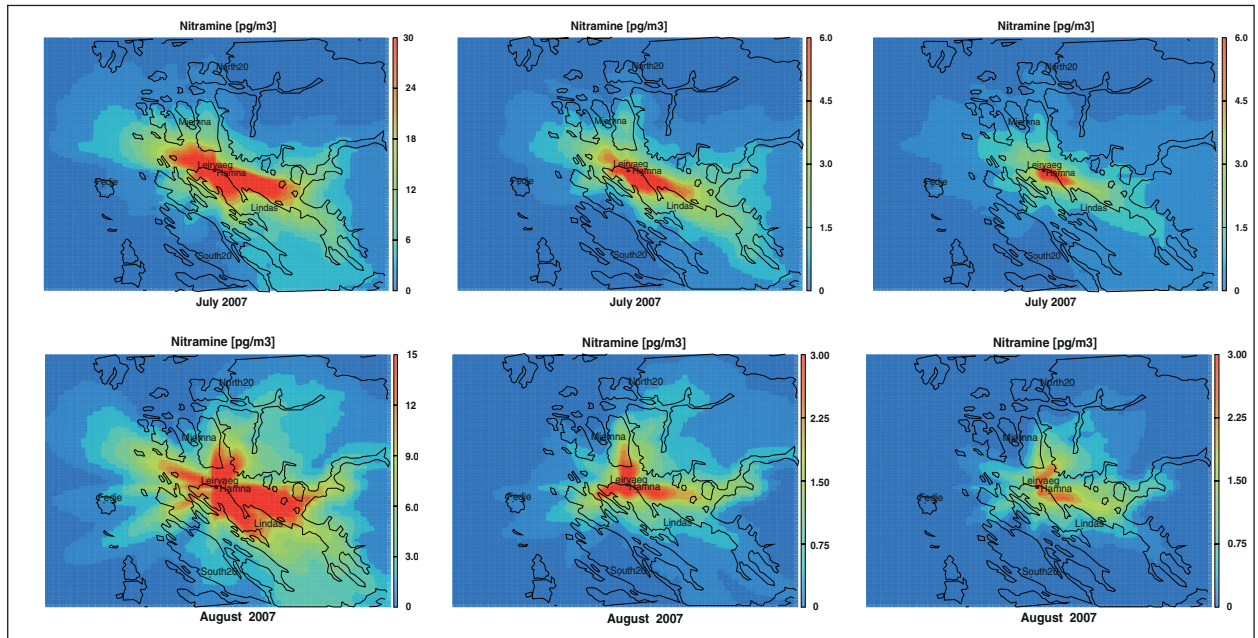


Fig. 7: Modelled monthly mean concentration of nitramine [ $\text{pg}/\text{m}^3$ ] at ground level for July (top) and August 2007 (bottom): Branching Factor equal to 1 (left column); variable branching factor in dependence on  $\text{NO}_x$  concentration (center column); explicit MEA gas phase chemistry (right column). Note that the scale of the left column is increased by a factor of 5.

deposition are described in dependence on meteorological conditions and land use properties.

The simulations and analysis were performed for the whole annual period Nov 2006 – Oct 2007. The annual COSMO simulations have predicted on average an about 20% lower MEA concentration considering gas phase oxidations. However, the observed differences between model runs with and without chemical gas phase processing are shown to be quite seasonal dependent. Because of the photochemical origin of the most important reaction partner OH this oxidation is most active in summer. Therefore, the highest product concentrations are found south-east of the source due to prevailing north-westerly winds in summer 2007. The predicted concentration pattern can be almost equal to the simulations without chemical processing. The produced nitrosamine is much smaller concentrated than the emitted one. The dispersion simulations have modelled total produced MEA-nitramine and emitted nitrosamine concentrations in the near of Mongstad of up to  $0.01\text{-}0.02 \text{ ng}/\text{m}^3$ , which are factor  $\sim 20$  lower than the long-term exposure limit values [ $0.3 \text{ ng}/\text{m}^3$ ; Låg et al., 2011]. The studies have revealed that the secondarily formed MEA-nitramine concentrations are in the same order than the primarily emitted nitrosamine, which is in agreement with former model studies.

The studies have predicted annual maximum deposition for nitrosamines and nitramines, which are clearly below the critical deposition rates. The importance (i.e. the magnitude) of dry and wet deposition

is nearly the same but the spatial patterns differ from each other. Dry deposition is strongly correlated with the land-use data whereas for wet deposition it is essential that the plume is advected into a precipitation event.

The nitramine concentrations modelled by the explicit MEA chemistry mechanism were compared with two simplified schemes [see Herrmann et al., 2013], which provide upper limits for the nitramine concentrations. In the first approach (BFe1), the product of the OH-reaction (see Fig. 1) gives an upper limit. In the second approach (BFvar), the branching by the  $\text{NO}_x$  and  $\text{O}_2$  reaction pathways of the product is also taken into account (cp. Fig. 1). In the explicit scheme, additionally the further oxidation of MEA degradation products is considered. For the modelling of all three approaches, the modelled OH,  $\text{NO}_x$  and  $\text{O}_2$  concentrations are used calculating the chemical turnovers. The results for July and August 2007 are presented in Fig. 7. As expected, the explicit mechanism produces the smallest concentrations. The values are 10-30% smaller than for the BFvar scheme and reduces the simple BFe1 estimation by a factor about 10. We find also some differences in the concentration pattern due to the heterogeneity of the surrounding concentration fields of the reaction partners. In agreement to the above-mentioned conclusions for the annual deposition rates, the dry and wet depositions in July 2007 are in the same range and show comparable pattern as in the annual run (Fig. 8).

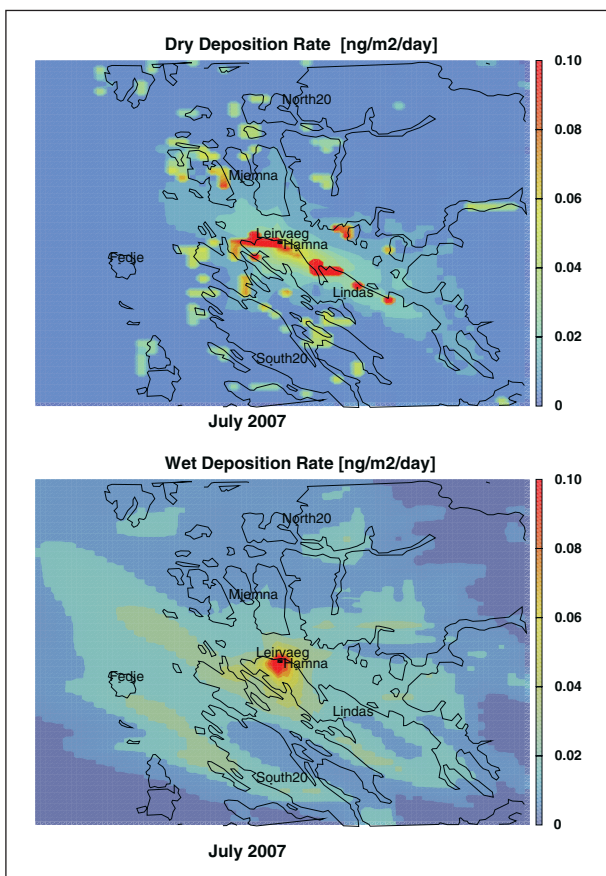


Fig. 8: Modelled monthly mean deposition rates of nitramine [ng/m<sup>2</sup>/day]: Dry deposition (top) and wet deposition (bottom).

## Summary and Conclusion

Based on the results of the process model studies, further COSMO-MUSCAT studies were aimed at the examination of the importance of tropospheric gas phase oxidations for the fate of MEA, the production of harmful compounds such as nitramines and the dispersion of MEA and its products including their regional concentration levels. In conclusion, the present dispersion model study has revealed that based on the available emissions and the meteorological conditions in the Mongstad region, the proposed guidelines for long-term exposure in air for MEA and also the total amount of nitrosamines and nitramines should not be exceeded. Moreover, the modelled annual deposition rates of MEA are clearly below the critical deposition rates representing the limit of long-term exposure in drinking water. However, for nitrosamines and nitramines, this conclusion cannot be safely given due to the large uncertainties about residence times of these compounds in the soil water.

## References

- Baldauf, M., A. Seifert, J. Förstner, D. Majewski, M. Raschendorfer, and T. Reinhardt (2011), Operational Convective-Scale Numerical Weather Prediction with the COSMO Model: Description and Sensitivities, *Mon. Wea. Rev.*, 139(12), 3887-3905, doi: 10.1175/mwr-d-10-05013.1.
- Berglen, T. F., D. Tønnesen, C. Dye, M. Karl, S. Knudsen, and L. Tarrasón (2010), CO<sub>2</sub> Technology Centre Mongstad – updated air dispersion calculation. Update of NILU report OR 12/2008, OR 41/2010.
- Bräuer, P., A. Tilgner, R. Wolke, and H. Herrmann (2013), Mechanism development and modelling of tropospheric multiphase halogen chemistry: The CAPRAM Halogen Module 2.0 (HM2), *J. Atmos. Chem.*, 1-34, doi: 10.1007/s10874-013-9249-6.
- Deguillaume, L., A. Tilgner, R. Schrödner, R. Wolke, N. Chaumerliac, and H. Herrmann (2009), Towards an operational aqueous phase chemistry mechanism for regional chemistry-transport models: CAPRAM-RED and its application to the COSMO-MUSCAT model, *J. Atmos. Chem.*, 64, 1-35, doi:10.1007/s10874-010-9168-8.
- Heinold, B., J. Helmert, O. Hellmuth, R. Wolke, A. Ansmann, B. Marticorena, B. Laurent, and I. Tegen (2007), Regional modeling of Saharan dust events using LM-MUSCAT: Model description and case studies, *J. Geophys. Res. - Atmos.*, 112(D11), D11204, doi:11210.11029/12006JD007443.
- Heinold, B., I. Tegen, R. Wolke, A. Ansmann, I. Mattis, A. Minikin, U. Schumann, and B. Weinzierl (2012), Simulations of the 2010 Eyjafjallajökull volcanic ash dispersal over Europe using COSMO-MUSCAT, *Atmos. Environ.*, 48, 195-204, doi:10.1016/j.atmosenv.2011.05.021.
- Herrmann, H., D. Hinneburg, A. Tilgner, R. Schrödner, R. Wolke, and C. J. Nielsen (2013), Regional Scale Amine Chemistry Dispersion Modelling with COSMO-MUSCAT. CO<sub>2</sub> Technology Centre Mongstad (TCM).
- Herrmann, H., C. Weller, and A. Tilgner (2011), Atmospheric Chemistry – Aqueous Phase Chemistry, Multiphase Modelling – Final report. Tel-Tek report no. 2211030-AQ05.
- Hinneburg, D., E. Renner, and R. Wolke (2009), Formation of secondary inorganic aerosols by power plant emissions exhausted through cooling towers in Saxony, *Environ. Sci. Pollut. Res.*, 16(1), 25-35, doi:10.1007/s11356-11008-10081-11355.
- Låg, M., C. Instanes, B. Lindemann, and Å. Andreassen (2008), Health effects of possible degradation products of different amines relevant for CO<sub>2</sub> capture. Final report. Oslo/Kjeller (NILU OR 06/2009).
- Låg, M., B. Lindeman, C. Instanes, G. Brunborg, and P. Schwarze (2011), Health effects of amines and derivatives associated with CO<sub>2</sub> capture. Oslo, The Norwegian Institute of Public Health.

- Nielsen, C. J., H. Herrmann, and C. Weller (2012), Atmospheric chemistry and environmental impact of the use of amines in carbon capture and storage (CCS), *Chem. Soc. Rev.*, 41(19), 6684-6704, doi:10.1039/c2cs35059a.
- Renner, E., and R. Wolke (2010), Modelling the formation and atmospheric transport of secondary inorganic aerosols with special attention to regions with high ammonia emissions, *Atmos. Environ.*, 44(15), 1904-1912.
- Schättler, U., G. Doms, and C. Schraff (2009), A description of the nonhydrostatic regional COSMO-Model. Part I: Users Guide. Deutscher Wetterdienst, Offenbach, 2008 [available from <http://www.cosmo-model.org>].
- Stern, R., P. Builjet, M. Schaap, R. Timmermans, R. Vautard, A. Hodzic, M. Memmesheimer, H. Feldmann, E. Renner, R. Wolke, and A. Kerschbaumer (2008), A model intercomparison study focussing on episodes with elevated PM10 concentrations, *Atmos. Environ.*, 42(19), 4567-4588.
- Tønnesen, D. (2011), Update and Improvement of Dispersion Calculations for Emissions to Air from TCM's Amine Plant: Part II – Likely case Nitrosamines, Nitramines and Formaldehyde, NILU report OR 52/2011.
- Wolke, R., O. Knoth, O. Hellmuth, W. Schröder, and E. Renner (2004), The parallel model system LM-MUSCAT for chemistry-transport simulations: Coupling scheme, parallelization and application, in *Parallel computing: Software technology, algorithms, architectures and applications*, edited by G. R. Joubert, W. E. Nagel, F. J. Peters and W. V. Walter, pp. 363-370, Elsevier, Amsterdam, The Netherlands.
- Wolke, R., W. Schröder, R. Schröder, and E. Renner (2012), Influence of grid resolution and meteorological forcing on simulated European air quality: A sensitivity study with the modeling system COSMO-MUSCAT, *Atmos. Environ.*, 53(SI), 110-130, doi:10.1016/j.atmosenv.2012.02.085.
- Wolke, R., A. M. Sehili, M. Simmel, O. Knoth, A. Tilgner, and H. Herrmann (2005), SPACCIM: A parcel model with detailed microphysics and complex multiphase chemistry, *Atmos. Environ.*, 39(23-24), 4375-4388.

---

## Funding

Technology Center Mongstad (TCM), Mongstad, Norway

---

## Cooperation

University of Oslo, Oslo, Norway

NILU - Norwegian Institute for Air Research, Kjeller, Norway

Deutscher Wetterdienst (DWD), Offenbach, Germany

Jülich Supercomputing Centre (JSC), Jülich, Germany

TU Dresden, Center for Information Services and High Performance Computing (ZIH), Dresden, Germany

# Insights on ice nuclei gained with LACIS

Heike Wex<sup>1</sup>, Stefanie Augustin<sup>1</sup>, Dennis Niedermeier<sup>1</sup>, Michael Rösch<sup>1</sup>, Susan Hartmann<sup>1</sup>, Tina Clauss<sup>1</sup>, Martin Ebert<sup>2</sup>, Bernhard Pummer<sup>3</sup>, Hinrich Grothe<sup>3</sup>, Susan Schmidt<sup>4</sup>, Johannes Schneider<sup>4</sup> and Frank Stratmann<sup>1</sup>

<sup>1</sup> Leibniz Institute for Tropospheric Research (TROPOS), Leipzig, Germany

<sup>2</sup> Institute of Applied Geosciences, Darmstadt, Germany

<sup>3</sup> Institute of Material Chemistry, Vienna University of Technology, Vienna, Austria

<sup>4</sup> Max Planck Institute for Chemistry, Mainz, Germany

**Im Rahmen von verschiedenen Kooperationen wurden Messungen zum Immersionsgefrieren verschiedenster Substanzen an LACIS (Leipzig Aerosol Cloud Interaction Simulator) durchgeführt. Partikel folgender unterschiedlicher Substanzen wurden untersucht: Mineralstäube sowohl in ihrem ursprünglichen Zustand als auch nach Beschichtung mit Schwefelsäure, eisaktive Makromoleküle aus biologischen Proben und Mischungen aus Mineralstäuben mit biologischem Material. Der Mineralstaub mit der stärksten Eisaktivität war Mikroklin, ein trikliner Kalium-Feldspat. Atmosphärische Alterung, die durch Beschichtung mit Schwefelsäure imitiert worden war, setzte die Eiskeimfähigkeit der Mineralstäube herab, was besonders ausgeprägt im Fall des untersuchten Feldspats auftrat. Bezuglich der biologischen Materialien, die zu den eisaktivsten Substanzen gehören, die bekannt sind, waren wir in der Lage, das Eisaktivierungsverhalten einzelner eisaktiver Makromoleküle zu quantifizieren und zu parametrisieren. Wir fanden Hinweise dafür, dass im Fall von Partikeln aus Mischungen von Mineralstäuben mit biologischem Material die eisaktiven Makromoleküle das Gefrierverhalten des ganzen Partikels bestimmen. Diese Makromoleküle können getrennt von ihren Trägern (z.B. Bakterien oder Pollen) auftreten, und es besteht die Möglichkeit, dass sie, zusammen mit Mineralstaub- bzw. Boden-Partikeln, in die Atmosphäre eingetragen werden. Damit könnte erklärt werden, warum in atmosphärischen Wolken Gefriertemperaturen beobachtet werden, die über denjenigen liegen, die für Mineralstäube in Laboruntersuchungen gefunden werden.**

## Introduction

In the atmosphere, ice containing clouds play important roles, influencing radiative processes and also the formation of precipitation. Of the latter, the majority is produced via the ice phase in mixed phase clouds, particularly outside of the tropics. The first step on the way to having ice in clouds is ice formation, and therefore this process is of large interest. But till today, our understanding of the related mechanisms is still incomplete [Murray *et al.*, 2012]. Among different freezing processes, immersion freezing, a heterogeneous process which requires the presence of an ice nucleus in a droplet, is one of the most important processes, particularly for mixed phase clouds [Ansmann *et al.*, 2009; Wiacek *et al.*, 2010; de Boer *et al.*, 2011].

Atmospheric observations indicate that heterogeneous ice nucleation in mixed-phase clouds can already occur at temperatures higher than  $-20^{\circ}\text{C}$

[Ansmann *et al.*, 2009; Seifert *et al.*, 2010; Kanitz *et al.*, 2011]. Dust particles are generally assumed to be the most abundant ice nuclei (IN) in the atmosphere, but laboratory studies showed that the majority of naturally occurring mineral dusts are only ice active at lower temperatures [Hoose and Möhler, 2012; Murray *et al.*, 2012]. This even holds for the most ice active mineral dust found so far, potassium feldspar [Atkinson *et al.*, 2013]. One possible explanation for the observed temperature differences might be the presence of biological material (e.g. from bacteria, pollen or fungi), initiating freezing already at higher temperatures. This biological material may be internally or externally mixed with other substances in atmospheric aerosol particles [Pratt *et al.*, 2009; Conen *et al.*, 2011; O'Sullivan *et al.*, 2013; Hartmann *et al.*, 2013; Augustin *et al.*, 2013].

To shed more light on these open issues, we set out using LACIS, the Leipzig Aerosol Cloud Interaction Simulator [Hartmann *et al.*; 2011], to

perform studies on immersion freezing for a variety of different substances which can act as IN. Some of these studies were done in close cooperation with other groups. Furthermore, we are a member of the "Ice Nucleation research UnIT" (INUIT, a DFG funded Research Unit, FOR 1525), and some investigations carried out within this unit contributed to the overview given here. Overall, in this article we summarize investigations of immersion freezing induced by particles from different mineral dust samples (feldspar (from Minas Gerais, Brazil), ATD (Arizona Test Dust from Powder Technology Inc.), illite (illite-NX from Arginotec) and kaolinite (from Fluka)), from biological material (originating from non-viable *Pseudomonas syringae* bacteria (Snomax) and from Birch pollen (washing water was used, here)), and from mixtures of one of the mineral dusts (illite) with the biological materials. Size selected, quasi mono-disperse particles were used in all cases, and the ice nucleation ability of the mineral dusts was examined for both, pure particles and surface modified particles, i.e., particles coated with sulfuric acid. It should be mentioned that the feldspar, illite and Snomax samples are all substances which were distributed within the INUIT network and which undergo thorough examination within this research unit.

## Methods

To generate mineral dust particles, a dry particle dispersion method, namely a fluidized bed generator, was used. The sulfuric acid coatings were applied by means of a vapor diffusion tube, heated to 70°C unless otherwise mentioned and followed by the addition of water vapor to enhance the reactivity of the sulfuric acid. For all dusts, the complete procedures for particle generation closely follow those described in detail in *Niedermeier et al.* [2011]. To generate particles containing biological material, suspensions were made and particles were then generated by atomization of the suspension and subsequent diffusion drying of the generated droplets. Details concerning the particle generation can be found in *Hartmann et al.* [2013] (for bacteria) and *Augustin et al.* [2013] (for pollen). It should be mentioned here, that the particles we generated from biological material contained both, substances which do not induce ice nucleation, together with ice nucleation active (INA) macromolecules, where the latter are INA protein complexes in case of the bacteria we examined [*Southworth et al.*, 1988] and polysaccharides in case of the birch pollen [*Pummer et al.*, 2012]. For examinations of mixtures of dust and biological material, the suspensions containing biological IN were mixed with suspension containing illite.

In all cases, particles were size selected with a Differential Mobility Analyzer (DMA, *Knutson and Whitby* [1975], type Vienna Medium). Examined mineral dust particles had a mobility diameter of 300 nm unless otherwise mentioned. Differently sized particles were studied in case of the biological samples, while for mixtures of dust and biological material, particles with mobility diameters of 500 nm were examined. Care was taken to avoid doubly charged particles by installing a Micro-Orifice Uniform-Deposit Impactor (MOUDI) and a cyclone in the aerosol flow prior to the size selection.

The amount of coating on the coated dust particles was determined following the procedure described in e.g. *Sullivan et al.* [2010] and *Wex et al.* [2013]. For that purpose, activation of the particles to cloud droplets was measured using a Cloud Condensation Nucleus counter (CCNC, *Roberts and Nenes* [2005]). Assuming spherical particle shape, it was found that coating thicknesses on the particles were on the order of a few nanometers. The largest coating thickness of 15 nm was achieved when a temperature of 80°C was used for coating of feldspar particles. Mineral dust particles are not spherical, but for the determined coating thickness, it is safe to assume that at least a major fraction of the particles' surfaces is covered by the coating. As an example, in Fig. 1 an electron microscope picture of the feldspar particles coated at 80°C is shown. A weak halo originating from small droplets of sulfuric acid can be seen around the particles. These droplets were released from the coated particle upon impact during sampling.

The immersion freezing behavior of all particles was examined using LACIS. LACIS is a 7 m long



*Fig. 1: Electron microscope picture of feldspar particles coated with sulfuric acid. Around the particles, thin sulfuric acid halos can be seen.*

laminar flow tube, for which each 1 m section can be temperature controlled separately. In LACIS, the particles were fed into the center of the tube and formed a particle beam along the center line, surrounded by slightly humidified sheath air. Supersaturated conditions were reached by cooling the tube walls, resulting in the particles being activated to droplets, where each droplet contained exactly one size selected particle. These droplets could then freeze due to further cooling. For detailed information about the operation mode of LACIS see Hartmann et al. [2011]. At the outlet of LACIS, TOPS-Ice [Clauss et al., 2013] was used to discriminate between frozen and unfrozen droplets. With this, the frozen fraction ( $f_{ice}$ , number of frozen droplets divided by the total number of droplets (i.e. frozen and unfrozen)) was determined. For the investigations presented here,  $f_{ice}$  was measured in the temperature range between -7°C to -41°C.

## Results

**Mineral dust particles as IN.** Figure 2 shows the results of the immersion freezing experiments for uncoated and coated mineral dust particles. Clearly by far the best mineral IN were uncoated feldspar particles, for which an  $f_{ice}$  of 1% was already detected at -23°C. Our feldspar sample roughly contained 80% of microcline (which is a K-feldspar), and 20% albite (a Na-feldspar). Hence our findings support Atkinson et al. [2013] who claim that K-feldspar minerals dominate ice nucleation by mineral dusts for freezing in the immersion mode. Good agreement is found when we directly compare our data to those presented in Atkinson et al. [2013] for a comparable feldspar.

This is discussed in detail in Augustin et al. [2014]. A close examination of the feldspar data reveals that we find a plateau at a value of  $f_{ice}$  of roughly 0.8, with  $f_{ice}$  going up to 1 only at around -38°C (where homogeneous freezing occurs) which indicates that not all of the produced particles show a good IN activity. When we examined feldspar particles with a mobility diameter of 500 nm (not shown here), the freezing temperatures were increased slightly (by 1.5 K), while the plateau value agreed to that found for the 300 nm particles within uncertainty. The formation of the plateau can be explained when we assume that grinding of the feldspar sample leads to an external mixture of microcline and albite. Different minerals can be present in separate particles when the crystal size in the original mineral sample is above that of the particle sizes we selected. So it could be assumed that roughly 80% of the particles we examined consisted purely or at least mainly of microcline and caused the observed immersion freezing. In other words, we suggest microcline to be the ice nucleating mineral component.

Uncoated ATD particles were found to be the second best IN. Yakobi-Hancock et al. [2013] examined ATD and its mineral components with respect to deposition ice nucleation. At -40°C, they determined the relative humidity necessary for the onset of freezing (i.e. for an  $f_{ice}$  of 0.1%). They found that the ice nucleation ability of ATD particles themselves was similar to that of orthoclase, which contributes roughly 20% of the overall mass of ATD, while any other of its components showed a lower ice activity. Orthoclase is also a K-feldspar. But when we compare the results for feldspar to that for ATD, it can be hypothesized

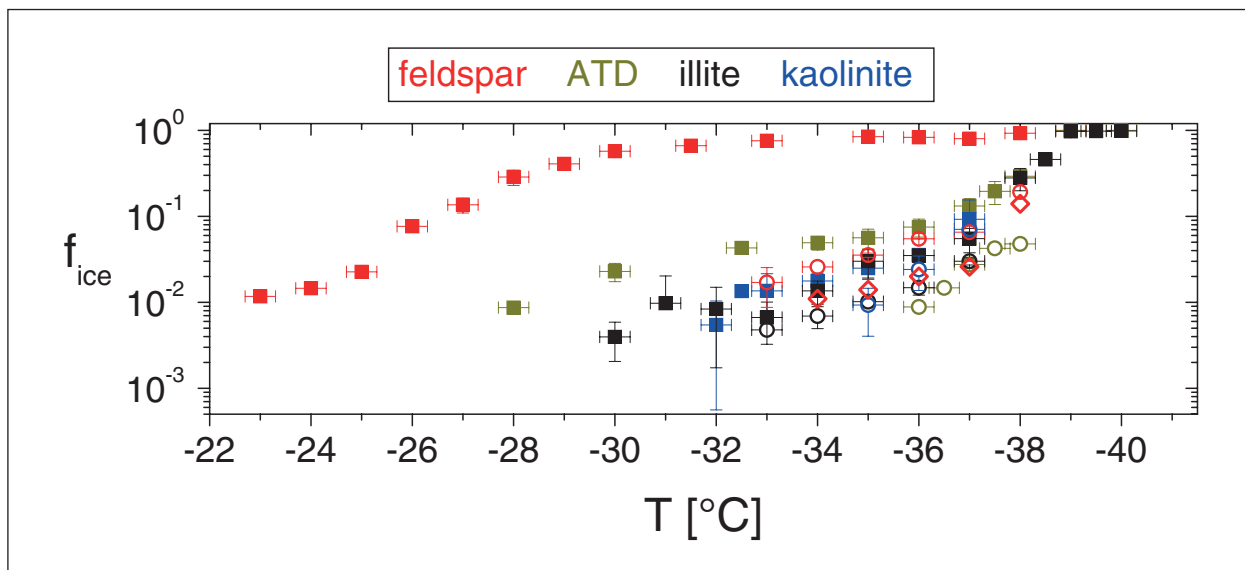


Fig. 2: Frozen fractions ( $f_{ice}$ ) determined for different mineral dust samples (squares and open circles indicate data obtained for uncoated particles and for particles coated at 70°C, respectively; red open diamonds represent data for feldspar particles coated at 80°C).

that microcline has a larger ice nucleating ability than orthoclase. This could originate from the fact that the two K-feldspars have a different crystal structure: while microcline has a triclinic crystal structure, orthoclase is monoclinic.

The mass fraction of K-feldspar contained in illite and kaolinite is 8% and 5%, respectively. However, it has not been clarified, yet, if these fractions of K-feldspar are orthoclase or microcline. But in any case, corresponding to the rather low fractions of K-feldspar included in these two mineral dusts is the fact that they both showed the lowest IN activity of the examined dusts. This can be interpreted as another hint that it really are the K-feldspars, and here particularly microcline, which are the most ice active mineral dusts for immersion freezing.

Now we focus on the effect of the coating on the ice nucleation ability of the examined mineral dusts. Before the data is interpreted, it should be explicitly mentioned that droplets which are activated in LACIS grow to sizes of 2  $\mu\text{m}$  and above, so that the soluble coatings will form highly dilute solutions around the insoluble dust particles, featuring water activities above 0.999. Therefore, even in the case of coated particles, a freezing point depression can be neglected.

Figure 2 clearly shows that in general the ice nucleation ability of the dusts decreased upon coating. This decrease is comparably small for illite and kaolinite, where the decrease could be described as a shift in  $f_{\text{ice}}$  by about 1.5 K towards lower temperatures. Values of  $f_{\text{ice}}$  for coated ATD particles are similar to those of coated illite and kaolinite, i.e. the loss in ice nucleation ability for ATD is larger than for illite and kaolinite. A value of  $f_{\text{ice}}$  of 1% for the uncoated ATD particles had been found at roughly -28°C, but for the coated ATD particles it is now only found at roughly -36°C.

The strongest change due to the coating was observed for the feldspar particles. Feldspar particles coated at 70°C lost most of their ice nucleation ability and only induced freezing at about the temperature-range previously observed for the two most inactive dusts. Coating at a higher coating temperature (80°C), i.e. with a larger amount of sulfuric acid, which was only done for the feldspar particles, reduced the ice nucleation ability further, so that it became comparable to that of the other coated mineral dusts. The loss in ice nucleation ability of the feldspar particles could alternatively be described as a shift of the curve of  $f_{\text{ice}}$  by roughly 12 K towards lower temperatures.

For ATD it had been found in the past that an increase in the coating temperature from 70°C to 85°C did only cause a negligible further reduction of the IN activity of the particles (decrease within

measurement uncertainty, Niedermeier et al. [2011]). However, while ATD particles coated at 70°C did carry no traces of unreacted sulfuric acid, those coated at 85°C did [Reitz et al., 2011]. Likely in the case of the feldspar particles, a larger amount of coating was needed to chemically alter the particles' surface such that all of the good ice nucleation sites were destroyed. The following paragraph gives a reason for this argument.

It is a well known fact that K-feldspar is converted to illite or kaolinite by acidic weathering in nature, or, more generally, that weathering of feldspar forms the common clay minerals [e.g. Blum, 1994]. Therefore we assume that a similar reaction transforms the feldspar in our samples and leads to a loss in IN activity. Hence more sulfuric acid is needed for the chemical reaction on the surface when there is more feldspar on the surface. Our hypothesis of a chemical transformation of the feldspar being responsible for the reduction in IN activity also agrees with the observations that the loss in IN activity is the largest for the sample containing the largest amount of K-feldspar (or more precisely of microcline), and that a modest loss is observed for ATD, which contains a much smaller amount of K-feldspar (and then only of orthoclase), while the IN activity of the mineral dusts containing only small amounts of a K-feldspar is altered comparably little.

Our results might also have implications for the atmosphere. In the atmosphere the formation of sulfuric acid occurs via wet phase chemistry, which is one pathway of chemical aging of atmospheric aerosol particles. This formation of sulfuric acid can potentially reduce the IN activity of mineral dust particles once they become airborne, causing aged particles to generally show lower IN activities. Although further chemical and/or mineralogical analysis are necessary to clarify what exactly has changed in the structure and composition of the feldspar particles used in our study, our results might contribute a key information to the question: "What makes a mineral dust particle an effective ice nuclei?"

**IN in biological materials.** In Fig. 3,  $f_{\text{ice}}$  measured for particles generated from biological material is shown. In all cases a steep increase in  $f_{\text{ice}}$  was found, followed by a plateau region with  $f_{\text{ice}} < 1$  towards lower temperatures. The plateau region originates from the fact that only a fraction of the generated particles contained an INA macromolecule [Hartmann et al., 2013; Augustin et al., 2013]. The distribution of the INA macromolecules over the particle population followed a Poisson distribution, with larger particles having a larger number of INA macromolecules, on average. Based on our data, it was possible to

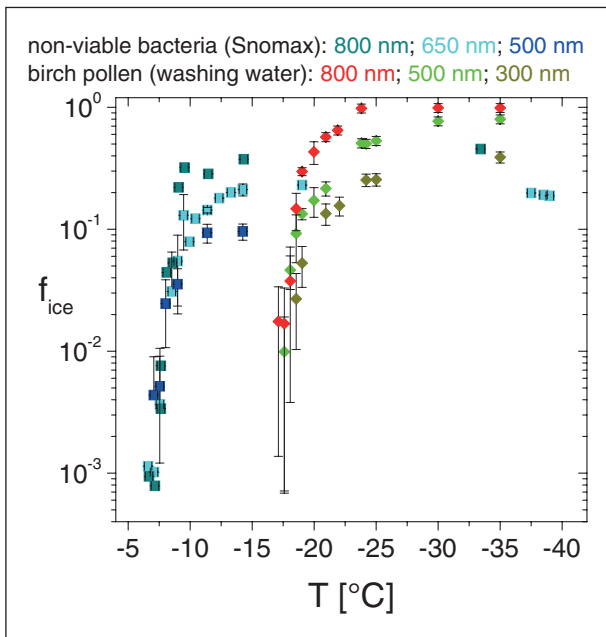


Fig. 3: Frozen fractions ( $f_{ice}$ ) determined for particles generated from non-viable *Pseudomonas syringae* bacteria (Snomax) and from birch pollen washing water. Different particle types and sizes are distinguished by color (see legend on top).

determine the average number of INA macromolecules in dependence on particle size, and from this nucleation rates for immersion freezing for single INA macromolecules. This is described in detail in Hartmann *et al.* [2013] and Augustin *et al.* [2013]. We developed parameterizations for these nucleation rates, based on two different methods: Classical Nucleation Theory (CNT) and a simpler empirical description. Both methods were able to describe the datasets well. With this, now, parameterizations for the ice nucleation ability of single INA macromolecules are available for modeling. Details can also be found in Hartmann *et al.* [2013] and Augustin *et al.* [2013].

In case of the birch pollen, we found that immersion freezing was already induced at around  $-17^{\circ}\text{C}$ , i.e., at temperatures higher than those found for any of the mineral dusts. Our studies on birch pollen also corroborated the results first found by Pummer *et al.* [2012], i.e., that freezing by pollen is indeed due to an INA macromolecule, a polysaccharide in this case, with a size of roughly 20 nm, which can easily be washed off the pollen grains. We estimated that several thousands of these macromolecules were present on each single one of the examined birch pollen grain [Augustin *et al.*, 2013].

INA macromolecules from *Pseudomonas syringae*, i.e., INA protein complexes, were found to induce freezing already at roughly  $-7^{\circ}\text{C}$ . They belong to the best IN known so far [e.g. Morris *et al.*, 2004]. As mentioned above, we were able to observe and

quantify ice nucleation by single INA macromolecules, which, in the case of Snomax, were single protein complexes. These protein complexes were attached to non-viable bacteria or fragments of those and still retained their ice nucleation ability. It was even found by Kleber *et al.* [2007], that INA protein complexes are well preserved – and maybe accumulated – when being connected to mineral surfaces.

The fact that INA macromolecules can exist separated from their original carrier, i.e., from pollen or bacteria, might make them much more important for atmospheric ice nucleation than assumed in the past, as they might accumulate in soils, become airborne again while attached to other particles, e.g. from mineral or soil dust, and stay airborne much longer and in much larger numbers than previously thought. This motivated us to look into the freezing behavior of mixtures of mineral dust and biological material.

However, before describing the respective investigations and results concerning mixtures in the next section, another result of our studies on both bacteria and pollen should be mentioned. We were able to clearly show that the observed freezing temperatures shift to higher values with an increase of the average number of INA macromolecules per particle, and hence per droplet. In former times, often droplets containing a vast number of bacteria or pollen were examined [e.g. Yankofsky *et al.*, 1981; Wood *et al.*, 2002; Diehl *et al.*, 2002]. Our results show that e.g. the resulting freezing temperatures for the onset of freezing, which are often reported, are higher than they were if droplets had contained only a single INA macromolecule. However, in the atmosphere likely only single INA macromolecules are present in separate droplets, a fact which has to be accounted for when using data obtained from highly concentrated droplets e.g. in atmospheric modeling.

Immersion freezing measurements of Snomax done with LACIS were also compared to data from a cold stage operated by the University of Bielefeld (BINARY, Bielefeld Ice Nucleation ARraY) in the framework of INUIT. When data from LACIS and BIANRY is expressed in terms of number of nucleation entities per mass of Snomax [Vali, 1971], both datasets agree very well. BINARY data cover a much larger range in the concentration of Snomax per examined droplet, and the trend which was seen for data from LACIS continued towards larger concentrations of Snomax, i.e. freezing temperatures increased even more. A comparison of results from LACIS and BIANRY to those from other measurement devices which are operated by partners in the INUIT project is ongoing.

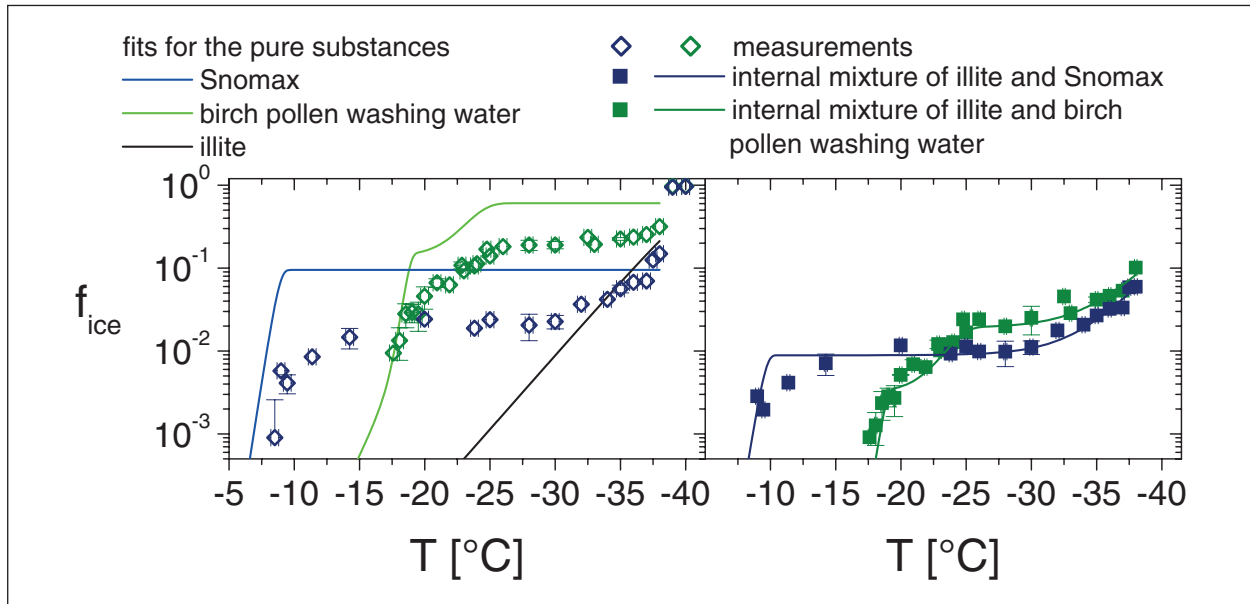


Fig. 4: Left panel:  $f_{\text{ice}}$  measured for particles generated from suspensions consisting of mixtures of biological material with illite. Solid lines indicate  $f_{\text{ice}}$  for the different separate compounds (based on fits). Right panel: Similar to left panel but displaying the fractions of the measured  $f_{\text{ice}}$  which were internally mixed and the respective composite curves (see text).

**Mixtures of mineral dust and biological material.** When we now compare the results obtained for mineral dust particles to those obtained for particles containing biological material, it becomes clear that even the microcline particles, i.e. those particles featuring the highest IN activity among the mineral dusts, induce freezing only at temperatures below those observed for either bacteria or pollen. The IN activity of insoluble mineral dust particles is generally supposed to scale with particle surface area, hence larger mineral dust particles can be expected to be more ice active. We tested this on kaolinite particles in the size range from 300 nm to 1000 nm and indeed found a very good correlation of the IN activity with particle surface area. Assuming a surface area dependent IN activity, it can be estimated that even microcline particles need to have sizes above 3  $\mu\text{m}$  to become similarly ice nucleation active to the birch pollen washing water particles shown in Fig. 3. Such large particles have short residence times in the atmosphere, hence it can be speculated that atmospheric ice nucleation, which often is observed for temperatures above -20°C, is mostly induced by biological particles or by smaller mineral dust or soil dust particles which have INA biological macromolecules attached to them.

We therefore started to examine mixtures of mineral dust particles with biological material. These measurements were done during a joint INUIT measurement campaign. The left panel of Fig. 4 shows  $f_{\text{ice}}$  measured for particles generated from suspensions of illite to which either a suspension of Snomax or

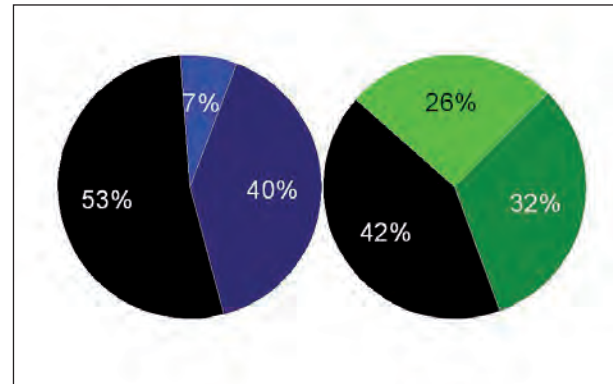


Fig. 5: Mixing state of particles consisting of mixtures of biological material with illite as determined by SPLAT. The color code follows that from Fig. 4, i.e. black denotes the fraction of pure illite particles, blue and green are the fractions of pure Snomax and birch pollen washing water particles, respectively, and dark blue and dark green represent the respective internally mixed particles.

a suspension from the birch pollen washing water had been added (depicted as blue or green open diamonds, respectively). Also shown are fits to the experimental data introduced in the above sections, i.e. for the respective pure particles: for 500 nm particles from suspensions containing only Snomax or birch pollen washing water (in blue or green, respectively) or illite (in black).

Within the INUIT cooperation, the particles generated from the investigated mixtures were also examined using a single particle mass spectrometer, SPLAT (Single Particle Laser Ablation Technique). SPLAT data show that at least a fraction of all generated particles was internally mixed (see Fig. 5). Based

on these data and the data for the pure particles, the frozen fractions originating from particles consisting purely of biological material and purely of mineral dust could be subtracted from the measured  $f_{ice}$  values. The respective values for only the internally mixed particles,  $f_{ice,mix}$ , are shown in the right panel of Fig. 4. Here the lines through the data are curves obtained assuming that the nucleation rate of the internally mixed particles is a mass fraction weighted composite of the nucleation rates of the separate components. These curves represent the measurements well. It is obvious that not every particle which contains biological material also contains an INA macromolecule, which was to be expected from measurements of the IN in biological materials introduced above. The first increase in  $f_{ice,mix}$  is seen at the same temperature at which the respective biological INA macromolecules induce ice nucleation. Hence in a particle composed of mineral dust and at least one INA macromolecule from either Snomax or birch pollen, the INA macromolecule controls the ice formation. Particles carrying no INA macromolecule feature the ice nucleation behavior of the pure mineral particles. In other words, the best ice nucleus in the particle determines the mixed particle's IN ability. This best ice nucleus can be an INA macromolecule or, in the case of pure mineral dust particles, a particular site on that particle. In any case, the IN which reduces the energy barrier for the formation of ice the most, determines the ice nucleation behavior of the overall particle.

## Summary and Conclusions

We investigated the ice nucleation behavior of pure and surface modified mineral dust particles, biological INA macromolecules, and particles containing both, mineral dust and biological material. We identified microcline, a triclinic K-feldspar, to be the most ice active mineral found up to now. Furthermore, we found strong indications that atmospheric aging processes may reduce the ice nucleation ability of minerals, depending on their K-feldspar content. We were able to quantify and parameterize the ice nucleation behavior of single biological INA macromolecules. We found evidence that for a particle composed of mineral dust and at least one INA macromolecule, the INA macromolecule controls the ice nucleation behavior of the whole particle. This together with the fact that biological INA macromolecules can exist separated from their original carrier, offers the possibility that e.g. mixed mineral-biological particles are responsible for the observed elevated freezing temperatures in atmospheric clouds, which are above those found for mineral dusts in laboratory studies.

Future research at LACIS will include the investigation of the ice nucleation behavior of fungal spores and natural mixed mineral-biological particles (e.g. soil dusts), and as new topic, homogeneous ice nucleation in concentrated solution droplets.

## References

- Ansmann, A., M. Tesche, P. Seifert, D. Althausen, R. Engelmann, J. Frunke, U. Wandinger, I. Mattis, and D. Müller (2009), Evolution of the ice phase in tropical altocumulus: SAMUM lidar observations over Cape Verde, *J. Geophys. Res.*, **114**(D17208), doi:10.1029/2008JD011659.
- Atkinson, J. D., B. J. Murray, M. T. Woodhouse, T. F. Whale, K. J. Baustian, K. S. Carslaw, S. Dobbie, D. O'Sullivan, and T. L. Mankin (2013), The importance of feldspar for ice nucleation by mineral dust in mixed-phase clouds, *Nature*, **498** (7454), 355–358, doi:10.1038/nature12278.
- Augustin, S., H. Wex, D. Niedermeier, B. Pummer, H. Grothe, S. Hartmann, L. Tomsche, T. Clauss, J. Voigtlander, K. Ignatius, and F. Stratmann (2013), Immersion freezing of birch pollen washing water, *Atmos. Chem. Phys.*, **13**, 10989–11003, doi:10.5194/acp-13-10989-2013.
- Augustin, S., H. Wex, S. Kanter, M. Ebert, D. Niedermeier, and F. Stratmann (2014), Effects of sulfuric acid coatings on the ice nucleation ability of feldspar and illite, *Geophys. Res. Lett.*, in preparation.
- Blum, A. E. (1994), *Feldspars in weathering*, 595–630 pp., Springer Netherlands.
- Clauss, T., A. Kiselev, S. Hartmann, S. Augustin, S. Pfeifer, D. Niedermeier, H. Wex, and F. Stratmann (2013), Application of linear polarized light for the discrimination of frozen and liquid droplets in ice nucleation experiments, *Atmos. Meas. Tech.*, **6**, 1041–1052, doi:10.5194/amt-6-1041-2013.
- Conen, F., C. E. Morris, J. Leifeld, M. V. Yakutin, and C. Alewell (2011), Biological residues define the ice nucleation properties of soil dust, *Atmos. Chem. Phys.*, **11** (18), 9643–9648, doi:10.5194/acp-11-9643-2011.
- de Boer, G., H. Morrison, M. D. Shupe, and R. Hildner (2011), Evidence of liquid dependent ice nucleation in high-latitude stratiform clouds from surface remote sensors, *Geophys. Res. Lett.*, **38**, doi:10.1029/2010gl046016.
- Diehl, K., S. Matthias-Maser, R. Jaenicke, and S. K. Mitra (2002), The ice nucleating ability of pollen: Part II. Laboratory studies in immersion and contact freezing modes, *Atmos. Res.*, **61**, 125–133.
- Hartmann, S., D. Niedermeier, J. Voigtlander, T. Clauss, R. A. Shaw, H. Wex, A. Kiselev, and F. Stratmann (2011), Homogeneous and heterogeneous ice nucleation at LACIS: Operating principle and theoretical studies, *Atmos. Chem. Phys.*, **11**, 1753–1767, doi:10.5194/acp-11-1753-2011.
- Hartmann, S., S. Augustin, T. Clauss, H. Wex, T. Santl Temkiv, J. Voigtlander, D. Niedermeier, and F. Stratmann (2013), Immersion freezing of ice nucleating active protein complexes, *Atmos. Chem. Phys.*, **13**, 5751–5766, doi:10.5194/acp-13-5751-2013.
- Hoose, C., and O. Moehler (2012), Heterogeneous ice nucleation on atmospheric aerosols: A review of results from laboratory experiments, *Atmos. Chem. Phys.*, **12**, 9817–9854, doi:10.5194/acp-12-9817-2012.

- Kanitz, T., P. Seifert, A. Ansmann, R. Engelmann, D. Althausen, C. Casiccia, and E. G. Rohwer (2011), Contrasting the impact of aerosols at northern and southern midlatitudes on heterogeneous ice formation, *Geophys. Res. Lett.*, 38, doi:10.1029/2011gl048532.
- Kleber, M., P. Sollins, and R. Sutton (2007), A conceptual model of organo-mineral interactions in soils: self-assembly of organic molecular fragments into zonal structures on mineral surfaces, *Biogeochem.*, 85, 9-24.
- Knutson, E. O., and K. T. Whithy (1975), Aerosol classification by electric mobility: apparatus, theory and applications, *J. Aerosol Sci.*, 6, 75-76.
- Morris, C. E., D. G. Georgakopoulos, and D. C. Sands (2004), Ice nucleation active bacteria and their potential role in precipitation, *J. Phys. IV France*, 121, 87-103, doi:10.1051/jp4:2004121004.
- Murray, B. J., D. O'Sullivan, J. D. Atkinson, and M. E. Webb (2012), Ice nucleation by particles immersed in supercooled cloud droplets, *Chem. Soc. Rev.*, 41, 6519-6554.
- Niedermeier, D., S. Hartmann, T. Clauss, H. Wex, A. Kiselev, R. C. Sullivan, P. J. DeMott, M. D. Petters, P. Reitz, J. Schneider, E. Mikhailov, B. Sierauf, O. Stetzer, B. Reimann, U. Bundke, R. A. Shaw, A. Buchholz, T. F. Mentel, and F. Stratmann (2011), Experimental study of the role of physicochemical surface processing on the IN ability of mineral dust particles, *Atmos. Chem. Phys.*, 11, 11131–11144, doi:10.5194/acp-11-11131-2011.
- O'Sullivan, D., B. J. Murray, T. L. Malkin, T. Whale, N. S. Umo, J. D. Atkinson, H. C. Price, K. J. Baustian, J. Browse, and M. E. Webb (2013), Ice nucleation by soil dusts: relative importance of mineral dust and biogenic components, *Atmos. Chem. Phys. Discuss.*, 13, 20275-20317.
- Pratt, K. A., P. J. DeMott, J. R. French, Z. Wang, D. L. Westphal, A. J. Heymsfield, C. H. Twohy, A. J. Prenni, and K. A. Prather (2009), In situ detection of biological particles in cloud ice-crystals, *Nat. Geosci.*, 2 (6), 397-400, doi:10.1038/ngeo521.
- Pummer, B. G., H. Bauer, J. Bernardi, S. Bleicher, and H. Grothe (2012), Suspendable macromolecules are responsible for ice nucleation activity of birch and conifer pollen, *Atmos. Chem. Phys.*, 12, 2541-2550, doi:10.5194/acp-12-2541-2012.
- Reitz, P., C. Spindler, T. F. Mentel, L. Poulain, H. Wex, K. Mildnerberger, D. Niedermeier, S. Hartmann, T. Clauss, F. Stratmann, R. C. Sullivan, P. J. DeMott, M. D. Petters, B. Sierauf, and J. Schneider (2011), Surface modification of mineral dust particles by sulphuric acid processing: implications for CCN and IN abilities, *Atmos. Chem. Phys.*, 11, 7839–7858, doi:10.5194/acp-11-7839-2011.
- Roberts, G., and A. Nenes (2005), A continuous-flow streamwise thermal-gradient CCN chamber for atmospheric measurements, *Aerosol Sci. Technol.*, 39, 206-221.
- Seifert, A., A. Ansmann, I. Mattis, U. Wandinger, M. Tesche, R. Engelmann, D. Müller, C. Perez, and K. Haustein (2010), Saharan dust and heterogeneous ice formation: Eleven years of cloud observations at a central-European EARLINET site, *J. Geophys. Res.*, 115 (D20201), doi:10.1029/2009JD013222.
- Southworth, M. W., P. K. Wolber, and G. J. Warren (1988), Nonlinear relationship between concentration and activity of a bacterial ice nucleation protein, *J. Biol. Chem.*, 263 (29), 15211-15216.
- Sullivan, R. C., M. D. Petters, P. J. DeMott, S. M. Kreidenweis, H. Wex, D. Niedermeier, S. Hartmann, T. Clauss, F. Stratmann, P. Reitz, J. Schneider, and B. Sierauf (2010), Irreversible loss of ice nucleation active sites in mineral dust particles caused by sulphuric acid condensation, *Atmos. Chem. Phys.*, 10, 11471–11487, doi:10.5194/acp-10-11471-2010.
- Vali, G. (1971), Quantitative evaluation of experimental results on heterogeneous freezing nucleation of supercooled liquids, *J. Atmos. Sci.*, 28 (3), 402-409.
- Wex, H., P. J. DeMott, Y. Tobo, S. Hartmann, M. Rösch, T. Clauss, D. Niedermeier, and F. Stratmann (2013), Kaolinite particles as ice nuclei: learning from the use of different types of kaolinite and different coatings, *Atmos. Chem. Phys. Discuss.*, 13, 30311-30348.
- Wiacek, A., and T. Peter (2009), On the availability of uncoated mineral dust ice nuclei in cold cloud regions, *Geophys. Res. Lett.*, 36 (L17801), doi:10.1029/2009gl039429.
- Wood, S. E., M. B. Baker, and B. D. Swanson (2002), Instrument for studies of homogeneous and heterogeneous ice nucleation in free-falling supercooled water droplets, *Rev. Sci. Instrum.*, 73, 3988-3996.
- Yakobi-Hancock, J. D., L. A. Ladino, and J. P. D. Abbatt (2013), Feldspar minerals as efficient deposition ice nuclei, *Atmos. Chem. Phys.*, 13, 11175–11185, doi:10.5194/acp-13-11175-2013.
- Yankofsky, S. A., Z. Levin, T. Bertold, and N. Sanderman (1981), Some basic characteristics of bacterial freezing nuclei, *J. Appl. Meteor.*, 20 (9), 1013-1019.

## Funding

German Research Foundation (DFG), Bonn, Germany  
EU FP-7 Infrastructure Project EUROCHAMP 2

## Cooperation

INUIT, the DFG funded “Ice Nuclei research UniT” (FOR 1525)  
Colorado State University, Fort Collins, Colorado, USA  
TU Wien, Vienna, Austria  
Aarhus University, Aarhus, Denmark

# Saharan Dust Long-range Transport and Aerosol-Cloud-Interaction Experiment SALTRACE: Observations and Modelling

Albert Ansmann, Ina Tegen, Thomas Müller, Dietrich Althausen, Thomas Bjerring Kristensen, Ronny Engelmann, Kharneha Wadinga Fomba, Moritz Haarig, Bernd Heinold, Hartmut Hermann, Michael Jaehn, Thomas Kanitz, Andre Klepel, Andreas Macke, Franziska Rittmeister, Annett Skupin, Alfred Wiedensohler

Die SALTRACE-Forschergruppe untersucht von 2013-2016 physikalische, chemische und optische Eigenschaften des Saharastaubs und die Verteilung des Mineralstaubes sowie seiner Wirkung auf Strahlungshaushalt und atmosphärische Dynamik im Fernfeld des Transportbereichs 2000-8000 km westlich der Staubquellen über dem tropischen Nordatlantik. Dabei werden In-situ-Aerosolmesungen und fernerkundliche, vertikal auflösende Beobachtungen auf Barbados und dem Forschungsschiff Meteor mit entsprechenden Transport-Modellrechnungen verknüpft.

## Introduction

The recent report of the Intergovernmental Panel on Climate Change (IPCC 2013) describes, for the first time, the direct effect (effective radiative forcing due to aerosol-radiation interaction, ERF-ari) and indirect effect (ERF-aci with aci = aerosol-cloud interaction) of aerosol particles on climate in large detail in order to explain why the uncertainties in the estimates of ERF-ari and especially of ERF-aci are so large. Many aspects dealing with cloud processes, in particular with heterogeneous ice formation are poorly understood and thus only crudely or practically not considered in climate models.

Desert dust is a major component of the atmospheric aerosol system and can be regarded to be omnipresent in the atmosphere. However, even the uncertainties in the direct climate effects (ERF-ari) of mineral dust are still high because of the variability in the global dust load associated with complex long-range transport pattern in the northern hemisphere (outflow regimes of African and Asian dust) as well as in the southern hemisphere (outflow regimes of Australian and Patagonian dust), not well described removal processes, and complex composition characteristics which determine the absorption and light-scattering efficiencies. Mineral dust particles are favorable cloud condensation (CCN) and ice nuclei (IN) and thus have a strong influence on the evolution

and glaciation of water clouds. Ice formation is the main driver to trigger significant amounts of rain.

Many large and comprehensive field campaigns were conducted during the last years (AMMA, DABEX, DODO, SAMUM-1, SAMUM-2, GERBILS, FENNEC, CHARMEx) to improve our knowledge on the role of mineral dust in the climate system. However, all of them were performed close to the Earth's largest dust source (Sahara). Long-range dust transport, associated changes in dust microphysical, chemical, and optical properties and resulting effects on climate-relevant processes cannot be investigated in this way.

SALTRACE (Saharan Aerosol Long-range Transport and Aerosol Cloud Interaction Experiment) is now the first large field campaign far away from the dust source. For the first time, state-of-the-art active remote sensing and ground-based and airborne in-situ particle measurement instrumentation (especially designed for dust studies) were involved in a large field experiment at Barbados ( $13^{\circ} 10' N$ ;  $59^{\circ} 31' W$ ) in the summer of 2013 (see Fig. 1). A cruise of the research vessel Meteor from the Caribbean to western Africa (more than 4000 km from West to East) in April-May 2013 with a multiwavelength Raman/polarization lidar aboard complemented our SALTRACE activities.

The focus of SALTRACE is on the characterization of dust over the tropical North Atlantic



Fig. 1: Field sites (yellow circles) of large dust field campaigns coordinated by TROPOS, Morocco (SAMUM-1), Cape Verde (SAMUM-2), and Barbados (SALTRACE).

in the Saharan air layer (SAL) from Cape Verde to Barbados, and dust-cloud interactions in this tropical region of dust transport. More specific, the SALTRACE objectives are:

- Investigation of dust transport and changes in dust properties during long-range transport,
- Impact of cloud processes, sedimentation, and turbulent downward mixing on aerosol vertical distribution and removal of dust,
- Impact of aged Saharan dust on the radiation field and atmospheric dynamics (and feedbacks on dust transport),
- Impact of aged Saharan dust on cloud processes: CCN characterization, heterogeneous ice formation in layered clouds.

The long-range transport regime over the tropical North Atlantic is an excellent area to investigate all aspects of aging (changes in the physical, optical, and composition characteristics), mixing of desert

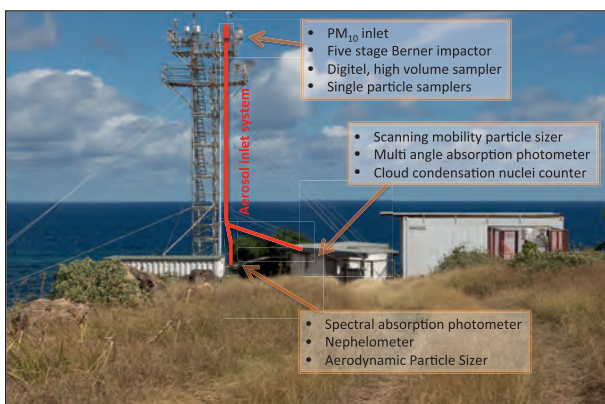


Fig. 2: Arrangement of instrumentation and aerosol sampling system at the atmospheric research station Ragged Point.

dust with marine and African smoke particles (during the winter half year), and downward transport of dust particles from the SAL to the ocean surface (removal of dust). Aerosol transformation processes in clear and cloudy air during the roughly 10-day travel over the Atlantic can be studied under nearly undisturbed conditions. No significant anthropogenic aerosol sources exist upwind of Barbados for more than 4000 km kilometers, making it an ideal site to investigate advected dust layers. The west-to-east RV Meteor cruise is a unique SALTRACE contribution along the main Saharan dust transport route. Such a ship borne field study has never been realized before.

## Observational and modelling results

In this contribution we provide a first impression of our ship borne and ground-based observations and modeling efforts. We start with the ground-based in-situ observations at Ragged Point at the east coast of Barbados. The atmospheric research station at Ragged Point is placed at a cliff at the outermost eastern point of Barbados (Fig. 2). Aerosol inlets for in-situ measurements were installed on top of a tower in a height of about 50 meters above sea level and in a cabinet and a container at ground level. Mass concentrations were obtained from gravimetrically weighting of daily samples collected with a five stage PM<sub>10</sub> Berner impactor, and volume concentrations were determined from measurements with a scanning mobility particle sizer (SMPS) and an aerodynamic particle sizer (APS) which cover the size range from 10 nm to 10 µm. The measured volume concentrations were converted to mass concentrations using an effective particle density of 2.25 g/cm<sup>3</sup>, a value typical for mineral-dust-dominated aerosol. Time series of mass concentration determined from the samples of the Berner impactor and from the particle sizers are shown in Fig. 3. The particle composition was investigated by a chemical offline analysis of the samples of the Berner impactor. Figure 4 shows the size-resolved masses of major ions and dust concentrations of these compounds for a day with moderate dust concentrations. Even in that case a high abundance of dust can be found. The remaining composition is dominated by sea salt (NaCl), and only a minor fraction consists of sulphate (SO<sub>4</sub><sup>2-</sup>). In the size stage 0.42-1.2 µm the dust fraction is higher than the locally produced NaCl, indicating that mineral dust can be the dominating composition in the accumulation mode aerosol even after long-range transport.

The concentrations of cloud condensation nuclei (CCN) were measured continuously with a CCN counter (DMT) at ground level at Ragged Point for different supersaturations throughout the campaign.

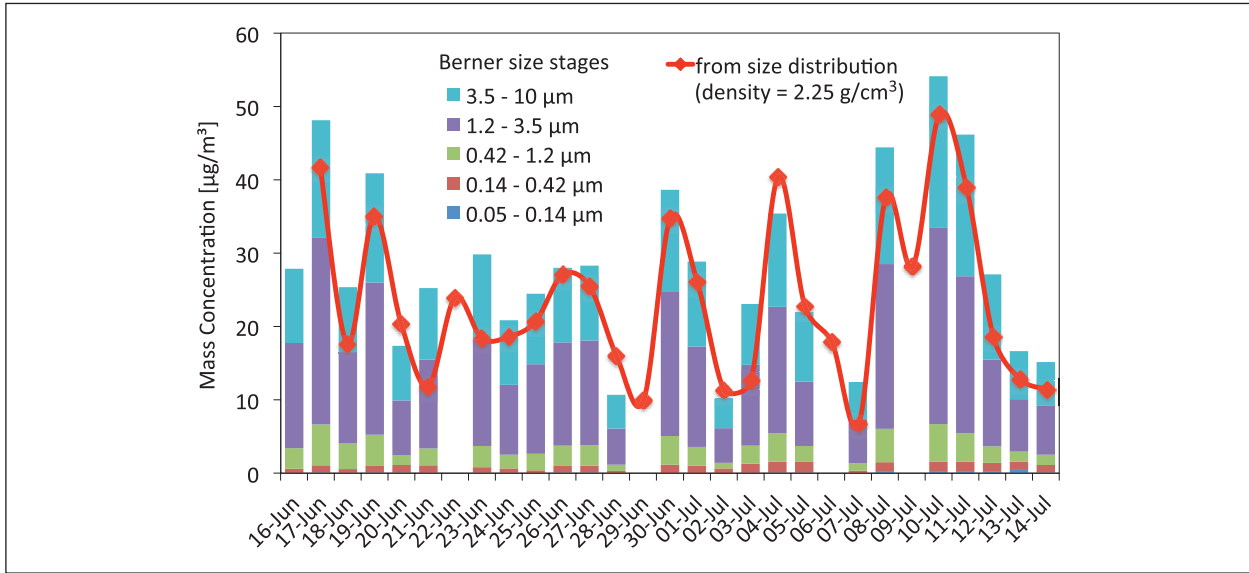


Fig. 3: Time series of mass concentrations from gravimetric weighting of samples of the 5-stage Berner impactor and from measured particle size distributions assuming a density of 2.25  $\text{g}/\text{cm}^3$ .

Airborne measurements of CCN were carried out with a similar instrument by Bernadett Weinzierl and Maximilian Dollner aboard the DLR Falcon research aircraft. A vertical profile from 5 July 2013 of the median concentration of CCN for a supersaturation of 0.2% is shown in Fig. 5. The error bars cover the 25%-75% quartile range so that 50% of all the measurements were found within the error bar. Clouds were present in altitudes between 2000 and 3000 m and the measurements carried out in this range are not included in the figure. On 5 July 2013, Saharan dust was observed in the air masses. Concentrations

of CCN for a superstation of 0.2% were typically at the order of  $200 \text{ cm}^{-3}$  in the boundary layer when dust was present, while it typically was at the order of  $50 \text{ cm}^{-3}$  without dust being present. Hence, Saharan dust significantly contributes to the number concentration of CCN in the Caribbean, which is expected to be even more pronounced above the boundary layer.

Optical properties measured at Ragged Point are the spectral absorption coefficients for wavelengths between 300 and 950 nm and scattering coefficients at wavelengths of 450, 535 and 635 nm. Figure 6 shows absorption and scattering coefficients for cases

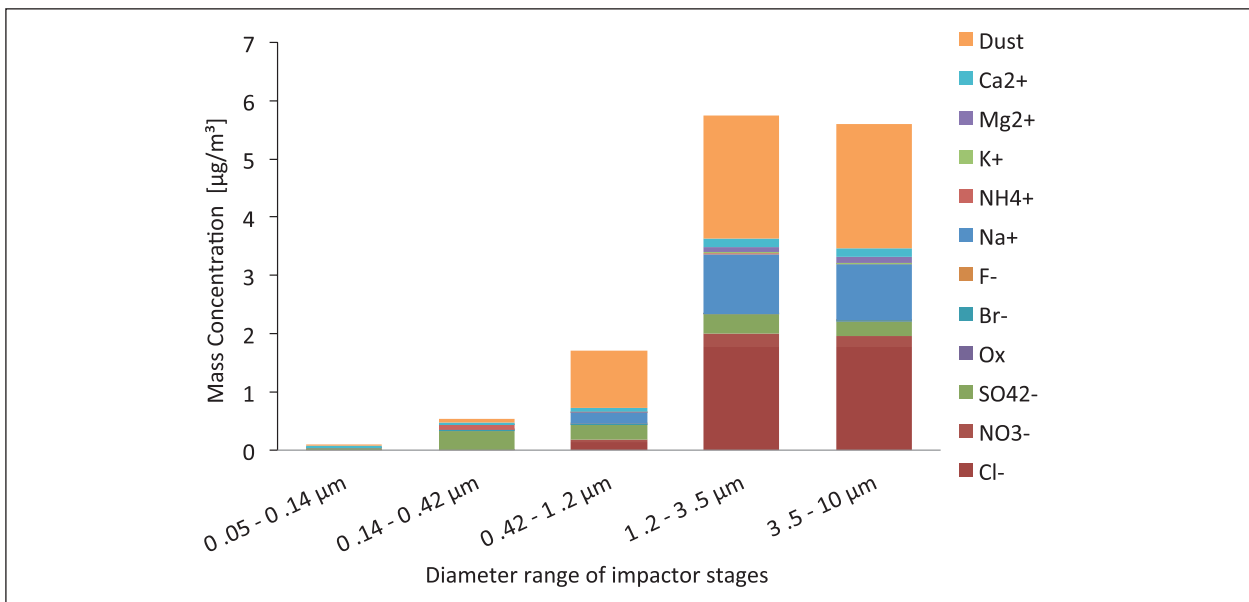


Fig. 4: Size-resolved composition, major ions, and dust concentrations from chemical analysis of Berner impactor samples. The data are for a day with relative moderate dust concentrations (3 July 2013).

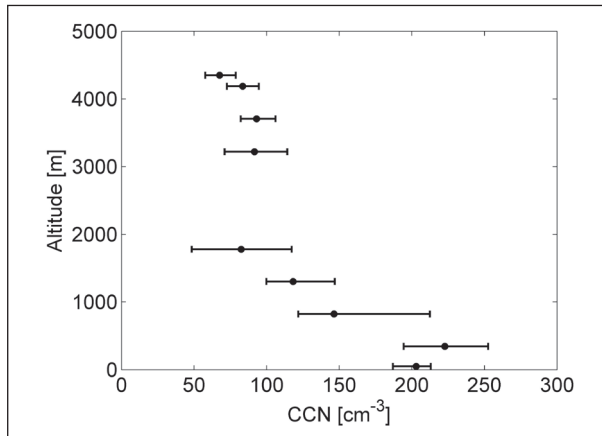


Fig. 5: Median concentrations of CCN measured at different altitudes on 5 July 2013 at the east coast or east of Barbados. The error bars represent  $\pm 1$  quartiles. Saharan dust was present on this particular day. Airborne measurements are kindly provided by Bernadett Weinzierl and Maximilian Dollner, DLR.

with high and low dust concentrations. The increase of the scattering with increasing wavelength indicates that the particle scattering is dominated by coarse mode particles, what is in agreement with the mass size distributions. One feature of mineral dust is the unique spectral run of the absorption coefficient. The increasing absorption towards smaller wavelength is caused by iron as the main absorbing compound in mineral dust. This spectral feature is used to determine the dust mass concentrations. Dust mass concentrations determined by optical absorption spectroscopy are shown in Fig. 7. One important intensive optical property is the single scattering albedo, which is a relative measure of the fraction of light scattering compared to the total extinction of light. The high single scattering albedo in Fig. 6 indicates that most of the light is scattered and only a small fraction is absorbed with increasing relative absorption towards shorter wavelengths.

During the entire measurement period the dust concentration was relatively high with only short periods of low dust concentrations. This periodical pattern was caused by the synoptic situation, which was dominated by westward traveling tropical easterly waves with a period of 3 to 4 days. The dominating aerosol type was long-range-transported mineral dust from the African continent. The dust was omnipresent in all heights up to 4.5–5 km according to the lidar observations at CLIMH. This is corroborated by comparison of in-situ measured dust concentration and the aerosol optical depth measured with sunphotometers. The aerosol optical depth is the column-integrated extinction of sunlight in the atmosphere. The aerosol optical depth is well correlated with the dust concentration measured near ground (Fig. 7). The high correlation between these properties indicates

that the dust concentration is directly coupled to the columnar dust concentration. According to the lidar observations, the highest dust concentrations occur above 2 km height. The close correlation between columnar integrated and near-ground-measured dust concentrations suggests a steady turbulent downward mixing of dust from the SAL to the ocean surface.

From 29 April to 23 May 2013 aerosol observations with lidar and Sun photometer were performed aboard the RV Meteor to determine Saharan dust properties in dependence of its atmospheric residence time. The ship and the route are shown in Fig. 8. Figure 9 provides an overview of the sunphotometer observations (aerosol particle optical depth, AOT, and spectral AOT slope in terms of the Angström exponent), lidar observations, and model calculations of the dust plumes along the RV Meteor cruise. The contribution of marine particles to AOT is about 0.05, the pure marine Angström exponent is around 0.6.

Figure 9b presents a composite of all ship borne lidar measurements of the cruise in terms of the 1064 nm range-corrected backscatter signal. Red and orange colors in the lowermost 2 km indicate the marine boundary layer (BL). The BL height varied

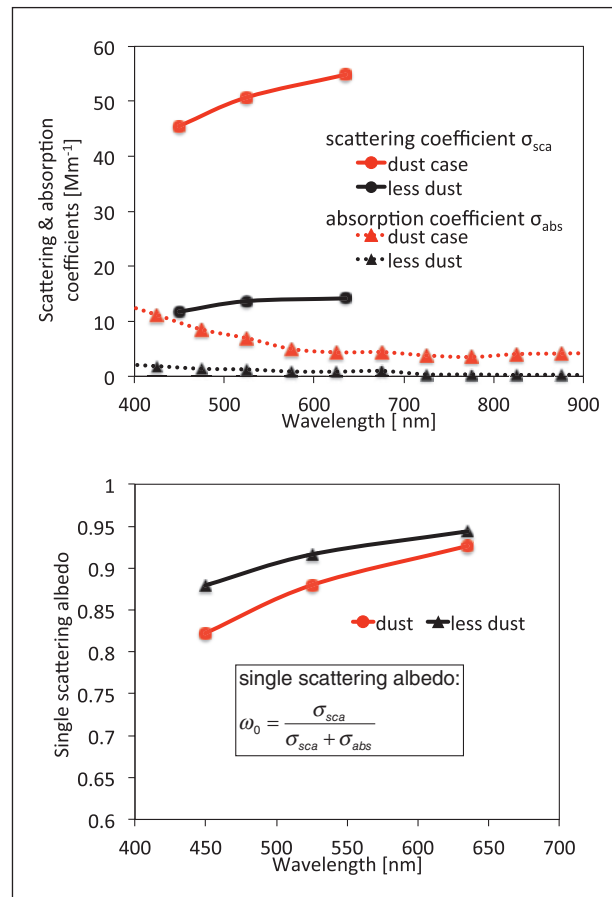


Fig. 6: Scattering and absorption coefficients for cases with high and low dust concentration (top) and single scattering albedo (bottom).

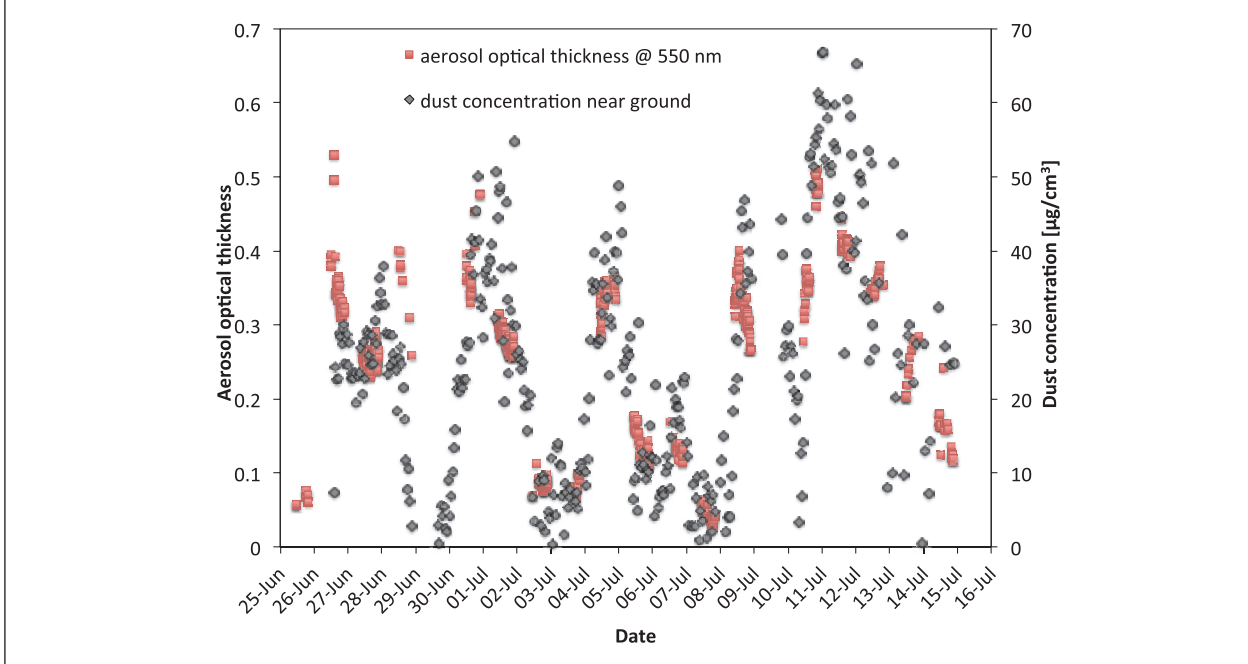


Fig. 7: Comparison of column-integrated aerosol optical depth at 500 nm and dust concentration measured at ground (Ragged Point).

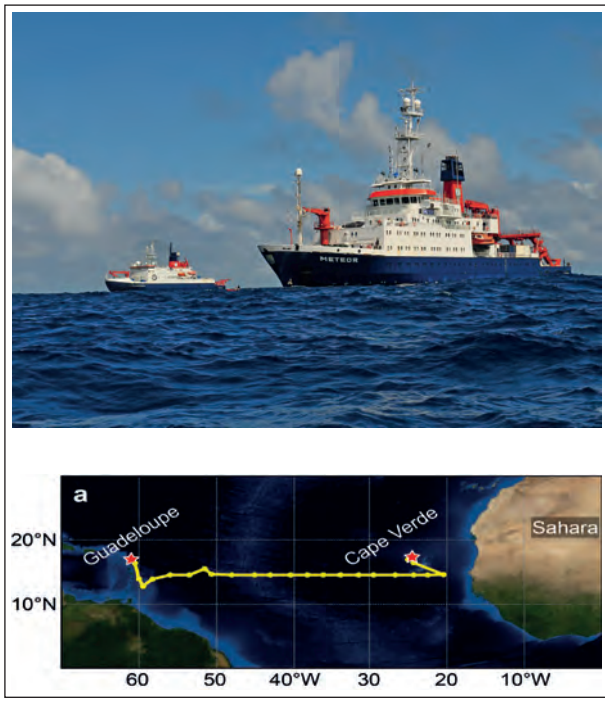


Fig. 8: RV Meteor (and RV Polarstern in the background) and track of the RV Meteor cruise from 29 April to 23 May 2013.

between 300 and 1700 m. From 45°W-25°W (Cape Verde) dust was observed up to 5 km height (green and yellow colors). The volume linear depolarization ratio at 532 nm shown in Fig. 9c clearly indicates the dominance of Saharan dust (non-spherical particles) in these layers (yellow to red colors). Figure 9c shows also an aged dust layer in the area around 55°W

observed from 4-6 May 2013. This plume reached to 2.5 km height only and was observed after a travel time of 12 days (7500 km). Figure 9d presents the height-time display of the lidar-derived water-vapor mixing ratio. The highest mixing ratios were found in the boundary layer with values up to 20 g/kg. In the dust layers, the specific humidity ranged mostly between 4-5 g/kg.

COSMO-MUSCAT simulations were performed to estimate the atmospheric dust concentration as shown in Fig. 9e. The simulated vertical dust distribution is in good agreement with the lidar observations (cf. Fig. 9b and e). Especially, patterns in the height-time display showing high volume depolarization ratios (Fig. 9c) from 11-13 May and 21-23 May 2013 are well reproduced by the simulations. The derived dust load varies between 10 and 20 µg m⁻³ during the first observed dust layer (4-6 May 2013) and from 10 to 150 µg m⁻³ during the second observed dust layer (10-23 May 2013).

For the Barbados SALTRACE field studies dust transport is simulated in order to understand the controls of long-range transport of dust across the tropical Atlantic, including mixing and deposition processes. The comprehensive field measurements will be used for a detailed evaluation of model results, which in turn can provide spatiotemporal context to the observations.

COSMO-MUSCAT is based on the dust model that was developed within the Saharan Mineral Dust Experiment (SAMUM). The model components are the COSMO model, which is the operational forecast

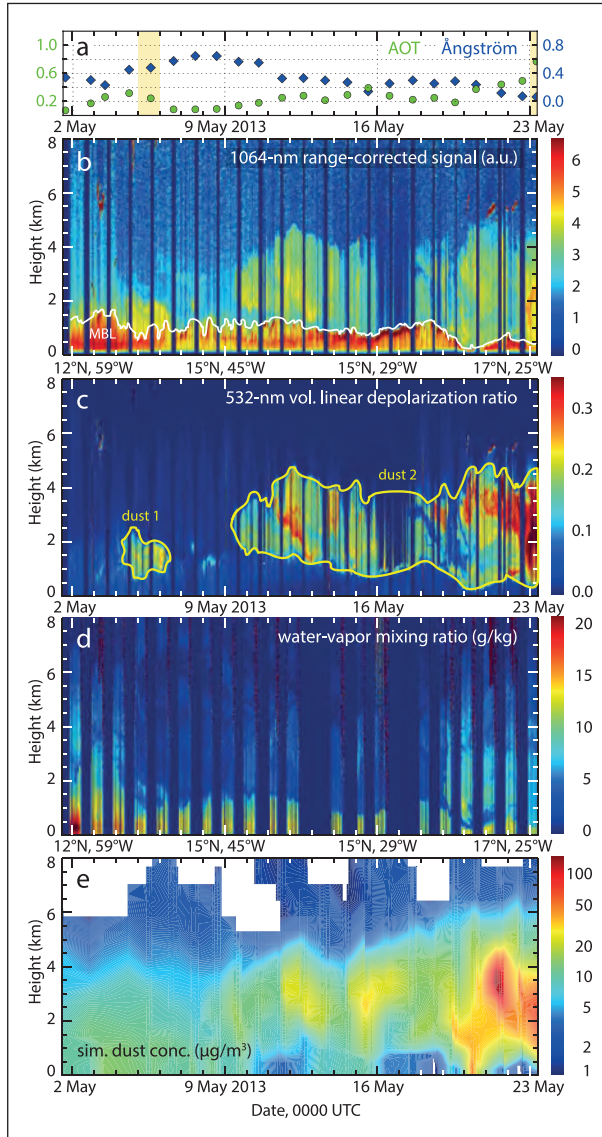


Fig. 9: (a) Daily mean aerosol optical thickness at 500 nm (green circles) and Angström exponent (440/870 nm) as determined with sunphotometer aboard RV Meteor from 60°–20°W in May 2013. Orange-shaded sections highlight the measurement days of the in-depth analysis. (b-d) Height-time display of lidar measurements during the cruise in terms of (b) 1064 nm range-corrected backscatter signal, (c) 532 nm volume linear depolarization ratio, and (d) water-vapor mixing ratio. White line in (b) indicates the marine boundary layer (MBL) height. Yellow lines in (c) highlight the main part of the lofted aerosol layers which contain considerable amounts of non-spherical dust. (e) COSMO-MUSCAT simulation of the vertical distribution of dust concentration.

model of the Deutscher Wetterdienst (DWD), and the coupled chemistry-transport model MUSCAT. The model system computes emission, transport, dry and wet deposition of Saharan dust as well as the effect of dust radiative forcing on heating rates and related feedbacks on atmospheric dynamics. For dust emission calculations, the location of dust sources derived from Meteosat Second Generation (MSG) satellite observations is used. The model-predicted dust is

transported as dynamic tracer in five independent size classes with radius limits between 0.1 and 24  $\mu\text{m}$ . While the model has been previously applied in the vicinity of the Saharan desert, here, the model domain is extended to include the Caribbean. The model is run with 28 km grid spacing and 40 vertical layers from surface to tropopause with a first-layer depth of about 20 m.

Another modelling activity will focus on the impact of mineral dust on the evolution of the tropical storm Chantal, which developed during the last week of the SALTRACE summer 2013 campaign. Figure 10 illustrates the impact of the tropical storm Chantal on Saharan dust transport. The storm reduces the dust load in the Caribbean by precipitation and mixing in of clean Southern Hemispheric air. Behind the tropical depression, the amount of Saharan dust advected westwards is strongly increased, which results from intense dust emission over West Africa in the wake of the former African easterly wave. Using sensitivity studies, it is planned to further explore the influence of the tropical storm on dust transport and mixing.

In agreement with these model results in Fig. 10, the lidar observation in Fig. 11 shows a steady decrease of the dust load until the morning of 9 July 2013, when the storm was closest to Barbados. The center of the cyclone was 50 km northeast of Barbados at 1000 UTC. The lidar observations had to be interrupted for about 15 hours, until the evening of 9 July 2013. Immediately, after last clouds dissolved, a strong Saharan dust layer appeared and remained for the next three days. The lidar field site at CIMH is shown in Fig. 12.

To get a deeper understanding of the spatiotemporal structure boundary layer (BL) dynamics and dynamic mixing processes, Large Eddy Simulations

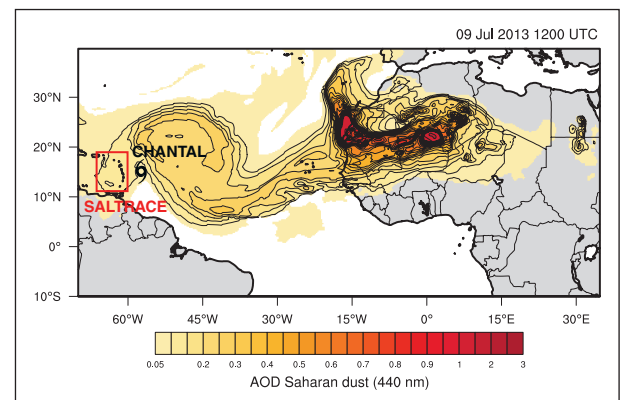


Fig. 10: COSMO-MUSCAT simulation of the dust-related aerosol particle optical depth (AOD) over the tropical Atlantic on 9 July 2013. The red box roughly indicates the SALTRACE area. The tropical cyclone Chantal (indicated by a black symbol) was about 50 km northeast of Barbados on 9 July 2013, 1200 UTC.

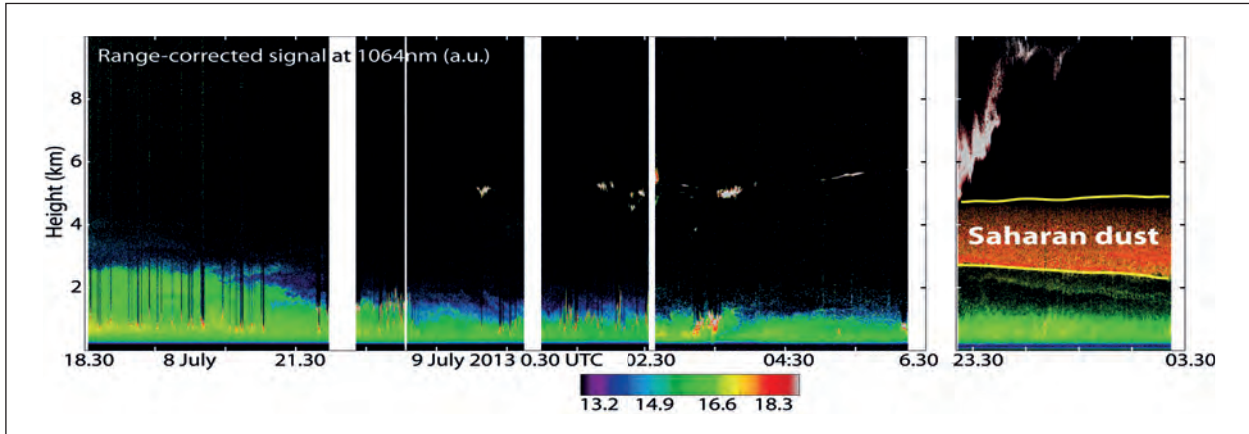


Fig. 11: Height-time display of the decreasing dust load as observed with the TROPOS lidar at CIMH, when Chantal approached Barbados (measurements before 0630 UTC). Afterwards (after 2330 UTC), when the tropical storm had left the eastern Less Antilles, a rather strong and coherent Saharan dust layer was observed for the next three days in full agreement with the COSMO-MUSCAT simulations (Fig. 10).



Fig. 12: TROPOS lidar/photometer station at the west coast of Barbados, 21 km west of Ragged Point. The remote sensing facility was deployed at the Caribbean Institute for Meteorology and Hydrology (CIMH), and will take observations until the summer of 2014. (Photo: Maximilian Dollner/DLR)

are performed with the All Scale Atmospheric Model (ASAM). The model results will help to better interpret measurements performed at Ragged Point (east coast) and CIMH (west coast). First model studies with idealized initial profiles show that ASAM is able to simulate island-induced low-level cumulus cloud generation. Because of the mostly uniform trade wind flow and the shape of the island, convective updraft cells are advected leewards and can form cloud streets (if the synoptical forcing is not dominant). Figure 13 shows the vertical wind component over Barbados derived from the LES model in 400 m height above sea level at the afternoon hours. West of the island one can observe a wide-spread propagating lee wave and a narrow updraft band with its starting point at the central west coast. Furthermore, passive aerosol tracers can be used to study BL development and can give an idea about vertical mixing processes. Figure 14 shows such a BL tracer, which was initialized with a relative number

concentration of 1 between the bottom and 700 m height at the beginning of the simulation. The island BL height goes up to 1.0–1.2 km height, especially at the southern part of the island, which is most likely caused by the larger landmass that is overflowed. Therefore, larger convective cells can evolve.

Further steps are model initialization with real vertical profiles gained from radiosonde, drop sonde and FALCON aircraft data. The impact of aerosol properties on cloud development will also be studied with the model for the shallow precipitating cumulus clouds that were observed in the lee of Barbados. In

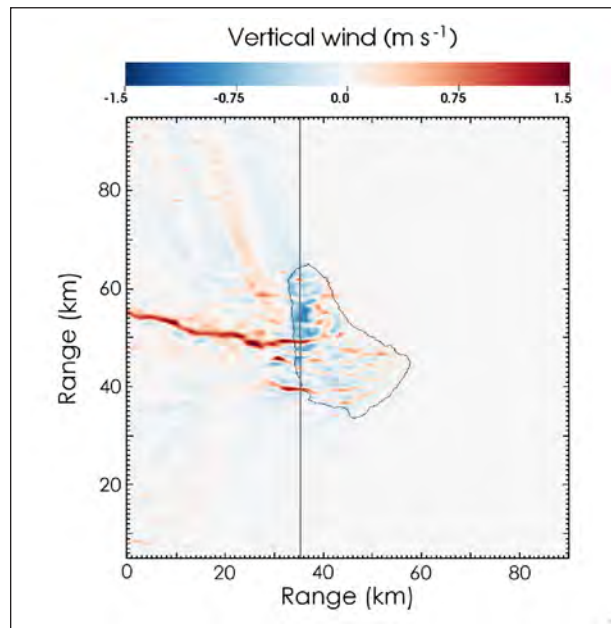
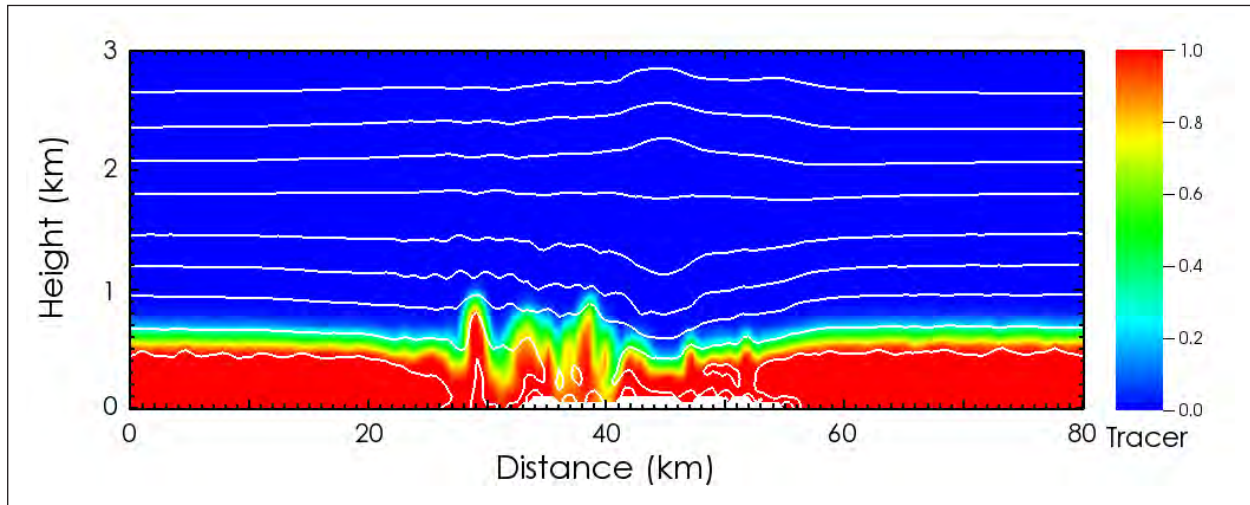


Fig. 13: Vertical wind at 400 m altitude for the LES run with 5 m/s horizontal mean flow from east. The snapshot is taken at 1500 local time (1900 UTC). The thin grey line indicates the cut-plane for the next figure.



*Fig. 14:* Height-distance profile (south-north cross section, thin vertical line in Fig. 13) of a passive boundary layer tracer for the same LES run as in Fig. 13. The tracer was initialized with a relative number concentration of 1 for  $0 \text{ m} < z < 700 \text{ m}$  height. The snapshot is taken at 1500 local time. Thin grey lines represent potential temperature isolines every 2 K.

addition to the aged dust particles that may be acting as CCN, possible effects from local aerosol sources (marine aerosol, smoke particles transported from island sources) will be estimated, too.

### Outlook

As an outlook, an intensive day-by-day, case-by-case data analysis will be performed during the next three years. The SALTRACE data set comprises the ground-based observations at Barbados, over the tropical North Atlantic aboard the RV Meteor and aboard the DLR Falcon aircraft. Within close cooperations with the modeling group of TROPOS, the

long-range dust transport, removal processes, the impact of dust on the Earth's radiation budget and on cloud processes will be studied in detail. All observational products will be contrasted with the SAMUM-1 and SAMUM-2 measurements to quantify the changes in the physical, chemical, and optical properties during long-range transport. As a highlight, we will investigate the potential role of dust on tropical storm developments by using our unique dust observations and the modeling capabilities. For the first time, such a study can be based on comprehensive dust observations with lidars and aircraft. A special issue in an appropriate journal for atmospheric sciences is planned for 2015-2016.

---

### Cooperation

Ludwig-Maximilians-Universität, Munich, Germany  
 DLR, Institute of Atmospheric Physics, Oberpfaffenhofen, Germany  
 Technische Universität Darmstadt, Germany  
 Caribbean Institute for Meteorology and Hydrology, Barbados

# Lab and field studies on photocatalysis to improve urban air quality

Falk Mothes, Olaf Boege, Christian Weller, Gerald Spindler, Thomas Schaefer, Hartmut Herrmann

Neben den bekannten Luftschadstoffen Feinstaub und Ozon rücken die Stickoxide ( $\text{NO}_x$ ) immer mehr in den Fokus der Betrachtung. Aufgrund häufiger Grenzwertüberschreitungen, besonders in verkehrsreichen Gebieten, besteht aktuell sehr großes Interesse an Methoden zur Verbesserung urbaner Luftqualität. Eine viel diskutierte Variante, neben der Reduktion der Schadstoffemissionen, stellt der Einsatz photokatalytisch aktiver Baumaterialien dar. Im Rahmen des Life+ Projektes PhotoPAQ (Demonstration of PHOTOCatalytic remediation Processes on Air Quality) und eines Pilotprojektes in Leipzig verfolgt TROPOS das Ziel die Wirksamkeit derartiger Materialien im Labor und unter realen atmosphärischen Bedingungen nachzuweisen.

## Introduction

Air pollution is a local, regional and trans-boundary problem caused by the emission of specific pollutants. Due to their widespread environmental and health effects nitrogen oxides ( $\text{NO}_x = \text{NO} + \text{NO}_2$ ) and volatile organic compounds (VOCs) play an important role, especially, for urban air quality. They contribute to the acidification of soil and surface water and furthermore also to the formation of secondary pollutants, for example ozone and particulate matter with associated climate effects [EEA, 2012]. To protect human health, the EU introduced threshold values (e.g.,  $40 \mu\text{g m}^{-3}$  for  $\text{NO}_2$ ), which are often exceeded by car emissions at traffic hotspots in urban areas. Therefore, the interest in new methods to improve urban air quality is increasing. To use photocatalytic active materials is one idea in addition to reduce the direct emissions of the pollutants. Semiconductor photocatalysts such as titanium dioxide ( $\text{TiO}_2$ ) are added to different materials (e.g., paints or concrete). These materials are able to convert pollutants into less harmful products on their surfaces under actinic irradiation (UV-range). The TROPOS chemistry department has set up a variety of laboratory and chamber experiments where such materials can be investigated in detail to characterise their performance. Based on these results, the material was finally tested under real atmospheric conditions in different field campaigns. The data obtained will provide an overview on the behaviour of nitrogen oxides and other air pollutants on these surfaces under irradiation with UV-light and allow an initial assessment of this material with respect to the goal of "improving urban air quality."

## Lab studies

To investigate the photocatalytic activity of such materials in the lab, often small gas flow reactors are used [Chen et al., 2011; Hüskens et al., 2009; Laufs et al., 2010; Martinez et al., 2011]. First experiments to characterize the performance of a photocatalytic active concrete has been done in an established "iso-reactor" (construction and setup according to international standard 22197-1:2007(E)). The raw material was mixed with water and applied on sandblasted glass plates. Under conditions as they are recommended in the iso-standard the material showed the ability to depollute air contaminated with 100 ppb NO or  $\text{NO}_2$  by about 70-80%. In addition to these experiments, a special so-called runoff reactor (ROR) has been developed and characterised at TROPOS to identify also low volatile photocatalytic reaction products in the aqueous run off of the coated model surface. The ROR enables washing of the surface of the material after a test run without the necessity to open the complete system. This is an important advantage especially if experiments with hazardous compounds are performed. Furthermore, it is possible to simulate rain during an experiment to investigate the influence of surface water on the heterogeneous activity of these materials. After a test run with  $\text{NO}_x$ , where a "heavy rain" was simulated before, the depollution effect was almost completely lost. Obviously the water molecules block the active sites on the catalysts surface and therefore suppress the photocatalytic effect. Thus the relative humidity and rain (surface/water interaction) will play an important role for the depollution ability of the material under



Fig. 1: View inside the aerosol chamber equipped with the set up to investigate the photocatalytic active concrete applied on glass plates (UV-light on).

real atmospheric conditions. Additionally, aerosol chamber studies with the photocatalytic concrete have been performed. To use the TROPOS aerosol chamber (LEAK) a special construction was developed (Fig.1). Experimental results with NO under variation of the relative humidity (RH) with and without light are presented in Fig. 2. It can be clearly seen that the NO signal showed a significant change in its shape if the UV-light was switched on for all three investigated humidities. The decrease of the NO values is much stronger under light conditions and therefore underlined the photocatalytic activity of the concrete. Calculations of the uptake coefficient,  $\gamma$ , which is the rate of reactive collisions divided by the rate of all collisions [Laufs et al., 2010], confirmed the results of the small lab reactors. Based on these positive results, the next step was to test the material under real atmospheric conditions.

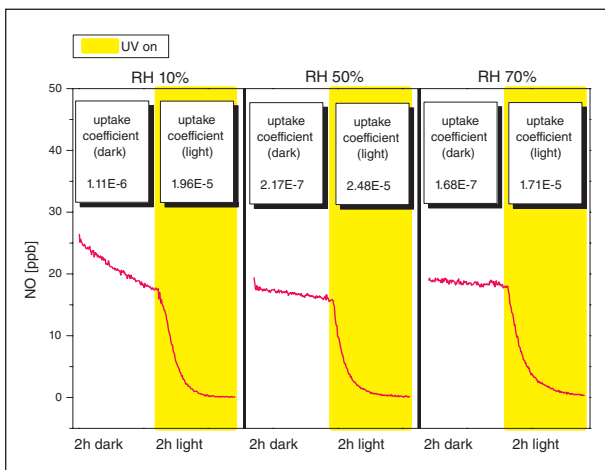


Fig. 2: Measured NO values in the aerosol chamber LEAK (equipped with the photocatalytic material) with and without light under variation of the relative humidity.

## Field studies

TROPOS as one partner in the Life+ project PhotoPAQ was involved in an outdoor campaign in Belgium 2013. The campaign took place in the Leopold II tunnel in Brussels, which is the longest tunnel (2,534 m) in Belgium. The tunnel consists of two separated tubes, 2 lanes in each direction. To perform this experiment the photocatalytic active concrete was applied on the wall and the ceiling of one tube over a length of about 160 m. Installation of additional UV-light sources should provide the necessary energy (Fig. 3). About 2,300 vehicles per hour (mainly private cars) pass this tunnel and cause very high pollutant concentrations. To investigate the photocatalytic depollution effect, the tunnel air was



Fig. 3: Test section Leopold II tunnel, Brussels with the applied photocatalytic concrete and 236 additional UV-light sources. (Photo: PhotoPaq consortium)

monitored before and after the test section. Switching the light on and off enabled also the possibility to observe directly a possible change in the measured pollutant concentrations, for example  $\text{NO}_x$ , volatile organic compounds (VOCs) and particles.

In contrast to estimations based on the positive lab experiments, the results in the tunnel showed no significant pollutant reduction. While the lab experiments proved the ability to remove  $\text{NO}_x$ , the reduction in the tunnel was lower than the statistical experiments uncertainty of 2%. One major reason, which was impossible to prevent, was the extremely dirty air in the heavily trafficked tunnel. The freshly coated surface was very fast contaminated through the dust, which lead to a deactivation of the material. Also the UV-lights were influenced by the dust. The measured light intensity was about  $2 \text{ W/m}^2$  (UV-A), a factor of 2 lower as it was intended. Due to the ambient weather conditions the temperature in the tunnel was very low

and the relative humidity was between 70 and 90%. The negative impact of high RH is known from the lab experiments. In conclusion, all these difficult conditions resulted in a ten times smaller reduction effect as expected for that tunnel.

### Summary and Outlook

Lab experiments with NO<sub>x</sub> and a photocatalytic active concrete using small horizontal gas flow reactors, proved a possible depollution effect of the material. Also during experiments with smaller and more realistic surface to volume ratios in the aerosol chamber, the photocatalytic activity of the concrete was observed. However the application of the material and installation of additional UV-light sources in a tunnel in Brussels did not show a significant change in the NO<sub>x</sub> concentrations. The reduction was below the uncertainty of the experimental setup. This field campaign underlined the difficulty to evaluate the benefit of using such TiO<sub>2</sub> based products under real

atmospheric conditions. TROPOS was also involved in 2 more field experiments.

The so called “street-canyon” campaign in Bergamo, Italy, basically consisted of two identical parallel street canyons (artificial), one coated with the active material and one without as reference. The canyons were located on a company site, next to a heavily trafficked road and the ambient air was monitored in parallel in each canyon. The second experiment is a pilot project of the Gesellschaft für Materialforschung und Prüfungsanstalt für das Bauwesen Leipzig mbH (MFPA), funded by Leipziger Wohnungs- und Baugesellschaft (LWB) where a photocatalytic active concrete is tested at the façade of an apartment building in Leipzig. The NO<sub>x</sub> concentrations will be compared before and after the application of the material, to evaluate the activity of the surface. TROPOS is in charge of the measuring instrumentation and also for data evaluation and interpretation. However, the data analysis for both campaigns is still ongoing.

---

### References

- Chen, J., S.-c. Kou, and C.-s. Poon (2011), Photocatalytic cement-based materials: Comparison of nitrogen oxides and toluene removal potentials and evaluation of self-cleaning performance, *Build. Environ.*, 46(9), 1827-1833, doi: 10.1016/j.buildenv.2011.03.004.
- EEA, E. E. A. (2012), Air quality in Europe - 2012 report.
- Hüsken, G., M. Hunger, and H. J. H. Brouwers (2009), Experimental study of photocatalytic concrete products for air purification, *Build. Environ.*, 44(12), 2463-2474, doi: 10.1016/j.buildenv.2009.04.010.
- Laufs, S., G. Burgeth, W. Dutlinger, R. Kurtenbach, M. Maban, C. Thomas, P. Wiesen, and J. Kleffmann (2010), Conversion of nitrogen oxides on commercial photocatalytic dispersion paints, *Atmos. Environ.*, 44(19), 2341-2349, doi: 10.1016/j.atmosenv.2010.03.038.
- Martinez, T., A. Bertron, E. Ringot, and G. Escadeillas (2011), Degradation of NO using photocatalytic coatings applied to different substrates, *Build. Environ.*, 46(9), 1808-1816, doi: 10.1016/j.buildenv.2011.03.001.

---

### Funding

EU-life+project

Leipziger Wohnungs- und Baugesellschaft (LWB)

---

### Cooperation

Photopaq Consortium

Gesellschaft für Materialforschung und Prüfungsanstalt für das Bauwesen Leipzig mbH (MFPA)

# Mechanistic investigations on the formation of ELVOCs

Torsten Berndt<sup>1</sup>, Tuija Jokinen<sup>1,2</sup>

<sup>1</sup> Leibniz Institute for Tropospheric Research, Leipzig, Germany

<sup>2</sup> University of Helsinki, Helsinki, Finland

**Die Oxidationsprodukte des Isoprens und der Terpene sind bedeutend für das Wachstum von Nanopartikeln und für die Bildung des Sekundären Organischen Aerosols generell. Unsere Ergebnisse aus Strömungsrohruntersuchungen zeigen, dass auf einer Zeitskala von Sekunden und für atmosphärische Konzentrationen von Ozon und Terpenen (hier für Limonen) hochoxidierte, organische Oxidationsprodukte (ELVOCs) gebildet werden mit einem O:C Verhältnis von ~1. Die nachgewiesenen Intermediate sowie deren Reaktion mit NO<sub>x</sub> unter Bildung von organischen Nitraten (RONO<sub>2</sub>) und Peroxonitratoren (RO<sub>2</sub>NO<sub>2</sub>) lassen den Schluss zu, dass die Bildung der hochoxidierten Produkte über Peroxylradikale (RO<sub>2</sub>) verläuft. Der Einsatz von <sup>18</sup>O markiertem Ozon erlaubt weitere Einblicke in den Bildungsmechanismus dieser Substanzen.**

## Introduction

Oxidation products of isoprene and terpenes are known to have an important impact on the global secondary organic aerosol burden and on the growth of nanoparticles. It is still a puzzling question how the essentially low-volatile organic oxidation products are formed in the atmosphere [Riipinen et al., 2012]. The traditional oxidation chemistry cannot explain the required production of low enough vapour pressure compounds and state-of-art models systematically fail to reproduce the observed concentrations and volatility of organic aerosol components. A possible solution of this problem was recently given by Ehn et al. [2014] who found that highly oxidized (O:C ratio of ~1) and extremely low-volatility organic compounds (ELVOC) are being formed as the first-generation products from the oxidation of  $\alpha$ -pinene. It is shown that after the initial attack by ozone (O<sub>3</sub>) or hydroxyl radicals (OH) and subsequent O<sub>2</sub> addition, the formed peroxy radicals (RO<sub>2</sub>) can undergo rapid intra-molecular hydrogen shifts followed by a consecutive reaction with O<sub>2</sub>. The repetition of the reaction sequence (intra-molecular hydrogen shift and O<sub>2</sub> addition) results promptly in high oxygenation levels.

Subject of this work are basic mechanistic investigations for a better understanding of the gas-phase processes leading to ELVOC formation starting from isoprene and a series of monoterpenes with special attention to limonene.

## Experimental

The experiments were carried out in the IfT-LFT (Institute for Tropospheric Research – Laminar Flow Tube, i.d. 8 cm; length 505 cm) at 293 ± 0.5 K, a relative humidity of 25% and atmospheric pressure using purified synthetic air as the carrier gas. The isoprene or terpene concentration was detected by means of proton transfer reaction mass spectrometry. ELVOC was measured using a NO<sub>3</sub><sup>-</sup>-CI-API-TOF (chemical ionisation - atmospheric pressure interface - time-of-flight) mass spectrometer sampling the centre flow at the tube outlet with a rate of 10 litre min<sup>-1</sup> (STP, standard temperature and pressure). Calibration of the CI-API-TOF was carried out using a well-defined source of sulphuric acid. The reaction time was varied between 8.2 and 40 s for a constant total flow of 30 litre min<sup>-1</sup> (STP).

## Results

First of all we studied ELVOC formation from the ozonolysis of limonene as a function of time. Figure 1 shows the most abundant RO<sub>2</sub> radicals, C<sub>10</sub>H<sub>15</sub>O<sub>8</sub> (325 Th) and C<sub>10</sub>H<sub>15</sub>O<sub>10</sub> (357 Th), and closed shell products, C<sub>10</sub>H<sub>14</sub>O<sub>9</sub> (340 Th) and C<sub>10</sub>H<sub>14</sub>O<sub>11</sub> (372 Th), for different reaction times in the flow tube. For close to atmospheric reactant concentrations, the highly oxidized radicals (8 or 10 O-atoms!) appear in the spectrum after a few seconds in the concentration range of ~10<sup>6</sup> molecule cm<sup>-3</sup>. The formation of the

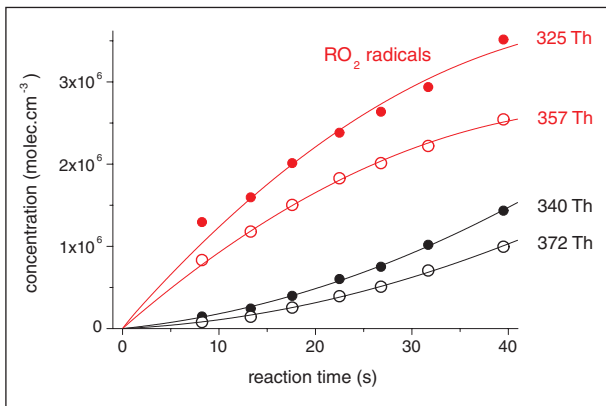


Fig. 1: Time dependent measurement of the most abundant radicals ( $\text{RO}_2$ ) and closed shell products rising from ozonolysis of limonene, initial concentrations:  $[\text{limonene}] = 5.0 \cdot 10^{10}$  molecule cm<sup>-3</sup> and  $[\text{O}_3] = 5.5 \cdot 10^{11}$  molecule cm<sup>-3</sup>. The products are measured as adducts with  $\text{NO}_3^-$ . Radicals are given in red,  $\text{C}_{10}\text{H}_{15}\text{O}_8(\text{NO}_3)^-$  (325 Th) and  $\text{C}_{10}\text{H}_{15}\text{O}_{10}(\text{NO}_3)^-$  (357 Th). Stable products presented in black are identified as  $\text{C}_{10}\text{H}_{14}\text{O}_9(\text{NO}_3)^-$  (340 Th) and  $\text{C}_{10}\text{H}_{14}\text{O}_{11}(\text{NO}_3)^-$  (372 Th).

stable products ( $\text{C}_{10}\text{H}_{14}\text{O}_9$  and  $\text{C}_{10}\text{H}_{14}\text{O}_{11}$ ) proceeds delayed in time. This behaviour reveals clearly that the ELVOC formation is a  $\text{RO}_2$  radical driven process taking place in the atmosphere at a time scale of seconds.

Furthermore, we tested for the chemical behaviour of the  $\text{RO}_2$  radicals. In the presence of  $\text{NO}_x$  in the reaction gas the occurrence of the corresponding organic nitrates ( $\text{RONO}_2$ ) and peroxy-nitrates ( $\text{RO}_2\text{NO}_2$ ) was detected in line with the expected behaviour of  $\text{RO}_2$  radicals. This fact confirms the  $\text{RO}_2$  structure of the compounds with the molecular formula  $\text{C}_{10}\text{H}_{15}\text{O}_8$  and  $\text{C}_{10}\text{H}_{15}\text{O}_{10}$ .

In a next set of experiments the origin of the O-atoms in the highly oxidized products was investigated, coming either from ozone ( $\text{O}_3$ ), from the ozonolysis itself, or from  $\text{O}_2$ , present in the pressure gas. For that we compared the product spectra of the limonene ozonolysis using either “normal” ozone ( $^{16}\text{O}_3$ ) or isotopically labelled ozone, the so-called “heavy” ozone ( $^{18}\text{O}_3$ ), see Fig. 2. The analysis showed that for the ELVOC main compounds two O-atoms arose from ozone and the others from  $\text{O}_2$ . Due to this finding we can speculate that the  $\text{RO}_2$  formation starts out from a limonene Criegee Intermediate after splitting off an OH radical.

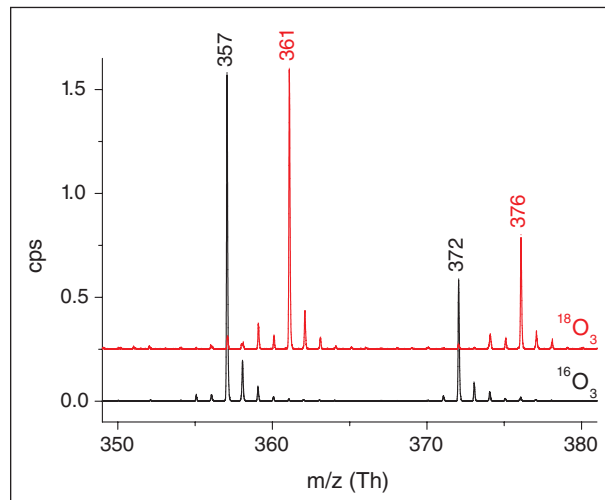


Fig. 2: Part of the product spectra (349 - 381 Th) of the limonene ozonolysis using either “normal” ozone ( $^{16}\text{O}_3$ ) or isotopically labelled ozone ( $^{18}\text{O}_3$ ), initial concentrations:  $[\text{limonene}] = 5.0 \cdot 10^{10}$  molecule cm<sup>-3</sup> and  $[\text{O}_3] = 6.2 \cdot 10^{11}$  molecule cm<sup>-3</sup>. The products are measured as adducts with  $\text{NO}_3^-$ . From ozonolysis with  $^{16}\text{O}_3$ :  $\text{C}_{10}\text{H}_{15}^{16}\text{O}_{10}(\text{NO}_3)^-$  (357 Th) and  $\text{C}_{10}\text{H}_{14}^{16}\text{O}_{11}(\text{NO}_3)^-$  (372 Th). From the usage of  $^{18}\text{O}_3$ :  $\text{C}_{10}\text{H}_{15}^{18}\text{O}_8^{16}\text{O}_2(\text{NO}_3)^-$  (361 Th) and  $\text{C}_{10}\text{H}_{14}^{16}\text{O}_9^{18}\text{O}_2(\text{NO}_3)^-$  (376 Th).

( $^{16}\text{O}_3$ ) or isotopically labelled ozone, the so-called “heavy” ozone ( $^{18}\text{O}_3$ ), see Fig. 2. The analysis showed that for the ELVOC main compounds two O-atoms arose from ozone and the others from  $\text{O}_2$ . Due to this finding we can speculate that the  $\text{RO}_2$  formation starts out from a limonene Criegee Intermediate after splitting off an OH radical.

This work demonstrates the rapid production of extremely low-volatility organic compounds (ELVOCs) for atmospheric reactant concentrations of ozone and organic compounds. The formation of ELVOCs can possibly contribute to secondary organic aerosol (SOA) formation and helps to close the existing gap in the understanding of SOA sources. Much more work is needed for a better understanding of the processes leading to ELVOCs.

## References

- Riipinen, I., T. Yli-Juuti, J. R. Pierce, T. Petäjä, D. R. Worsnop, M. Kulmala, and N. M. Donahue (2012), The contribution of organics to atmospheric nanoparticle growth, *Nature Geosci.*, 5, 453-458, DOI: 10.1038/ngeo1499.
- Ehn, M., J. A. Thornton, E. Kleist, M. Sipilä, H. Junninen, I. Pullinen, M. Springer, F. Rubach, R. Tillmann, B. Lee, F. Lopez-Hilfiker, S. Andres, I.-H. Acir, M. Rissanen, T. Jokinen, S. Schobesberger, J. Kangasluoma, J. Kontkanen, T. Nieminen, T. Kurtén, L. B. Nielsen, S. Jørgensen, H. G. Kjaergaard, M. Canagaratna, M. Dal Maso, T. Berndt, T. Petäjä, A. Wahner, V.-M. Kerminen, M. Kulmala, D. Worsnop, J. Wildt, and T. F. Mentel (2014), A large source of low-volatility secondary organic aerosol, *Nature*, in press.

## Cooperation

University of Helsinki, Helsinki, Finland  
University of Colorado, Boulder, USA

# Formation of organosulfates from sulfate radical reactions in atmospheric aerosols

Janine Schindelka, Yoshiteru Iinuma, Hartmut Herrmann

**Kleine C<sub>2</sub> – C<sub>4</sub>-Organosulfate, verwandt mit Isopren-Oxidationsprodukten, wurden bereits vielfach im atmosphärischen aber auch laborgeneriertem Aerosol nachgewiesen, aber der Mechanismus ihrer Bildung ist noch nicht vollständig verstanden. In der vorliegenden Arbeit wurde mit Hilfe von Flüssigphasen- und Kammerexperimenten deren Bildung durch die Oxidation von VOCs mit Sulfat-Radikalen untersucht. Als Vorläufer dienten Methacrolein und Methylvinylketon, beide mengenmäßig die wichtigsten Oxidationsprodukte von Isopren.**

## Introduction

Recent studies show that organosulfates are an important fraction of ambient secondary organic aerosol (SOA) which can contribute up to 30% to the organic mass of ambient aerosols [Surratt *et al.*, 2008]. The isoprene-derived organosulfate with *m/z* 215 ( $C_5H_{11}O_7S^-$ ) is often reported to be the most abundant single organosulfate compound. Besides, smaller C<sub>2</sub> to C<sub>4</sub> organosulfates are found in ambient and laboratory generated SOA that can be related to isoprene oxidation products [Surratt *et al.*, 2008; Froyd *et al.*, 2010]. These compounds have been suggested to form from the sulfate radical induced oxidation of semi-volatile isoprene oxidation products in the particle phase [Nozière *et al.*, 2010]. Especially, the formation of organosulfates originating directly from methacrolein (MACR) or methyl vinyl ketone (MVK) with *m/z* of 199 and 183, are of interest because their existence was shown in studies of ambient aerosols sampled in ground sites and free troposphere [Froyd *et al.*, 2010]. A sulfate radical reaction with unsaturated compounds is as fast as other organosulfate formation mechanisms and is even competitive to the reaction with hydroxyl radicals. Supporting the theory of the contribution of a radical mechanism in the formation, a very recent study reports a dependency of the fraction of organosulfates in particle mass on the season and photochemical activity. This might indicate the involvement of solution phase radical chemistry [Tolocka and Turpin, 2012].

## Experimental

An aqueous solution of 5 mM methacrolein or methyl vinyl ketone with 30 mM of potassium peroxodisulfate either acidified with sulfuric acid or not, was

irradiated with varying number of laser pulses from an excimer laser at a wavelength of 248 nm.

Two sets with three experiments each were performed on the formation of organosulfates from either MACR or MVK in the indoor aerosol chamber LEAK. The experiments were performed at a relative humidity of 75% with seed particles of either only sulfuric acid or a mixture of potassium peroxodisulfate and sulfuric acid. The three experiments consisted of two experiments under irradiation with UV/Vis light for each seed mixture as well as one experiment with sulfuric acid as seed in the dark. The particles were sampled on a borosilicate glass fibre filter coated with fluorocarbon. One half of the chamber sample filter was cut into small pieces and extracted with a solution of 250 µL methanol.

Samples obtained from the experiments performed in the bulk aqueous solutions and the aerosol chamber were analysed using an Acquity UPLC system coupled to Synapt HD TOFMS. The analytes were separated on an Acquity UPLC HSS T3 column (2.1 x 100 mm, 1.8 µm). As eluents ultrapure water with addition of 0.1% acetic acid and methanol were used.

## Results and discussion

A number of different C<sub>2</sub> - C<sub>4</sub> organosulfate species were found to form from the oxidation of MACR and MVK with sulfate radicals. In general, the intensities of the signals increased with an increase in number of laser pulses, indicating that their formation involved a sulfate radical induced oxidation. Methacrolein and methyl vinyl ketone showed both the formation of the hydroxyacetone sulfate ester (C<sub>3</sub> compound, *m/z* 153), whereas the glycolic acid sulfate ester (C<sub>2</sub> compound) with *m/z* 155 was only detected

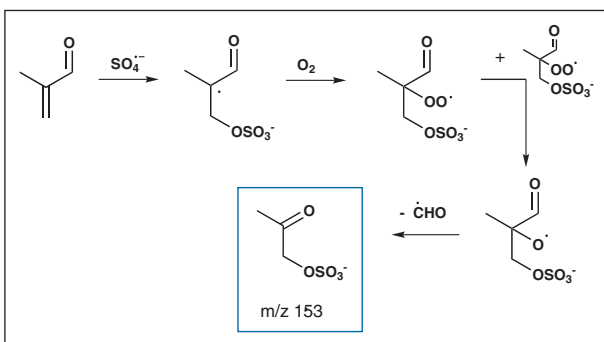


Fig. 1: Possible reaction mechanism for the formation of the hydroxyacetone sulfate ester  $m/z$  153 from MACR.

in the oxidation of MVK. Besides these small  $C_2$  -  $C_3$  compounds, the  $C_4$  compounds with the  $m/z$  183 and 199 were detected for both analytes. The detection of these species is of interest as evidence for their existence was shown by studies of ambient aerosols. Furthermore dimeric compounds with eight carbon atoms ( $m/z$  251 and  $m/z$  253) were detected in all experiments.

Figures 1 and 2 show suggested structures and reaction pathways for the formation of the compounds with the  $m/z$  153 from MACR and  $m/z$  251 and 253 from MVK. A sulfate radical abstracts an H atom or adds itself to a C-C double bond. In both cases a carbon-centred radical forms, which undergoes different successive reactions. For example, the formed radical may react with another unsaturated

compound to extend the carbon chain to form a dimeric carbon-centred radical. The other important reaction is the formation of peroxy radicals ( $\text{RO}_2$ ) from the addition of oxygen. Peroxy radicals can recombine to form tetroxides as intermediate species. The latter then decompose in different pathways producing compounds with carbonyl or alcohol functional groups (Fig. 2) or alkoxy radicals (see Fig. 1). Alkoxy radicals are unstable. They decompose producing smaller compounds by bond breakage as it

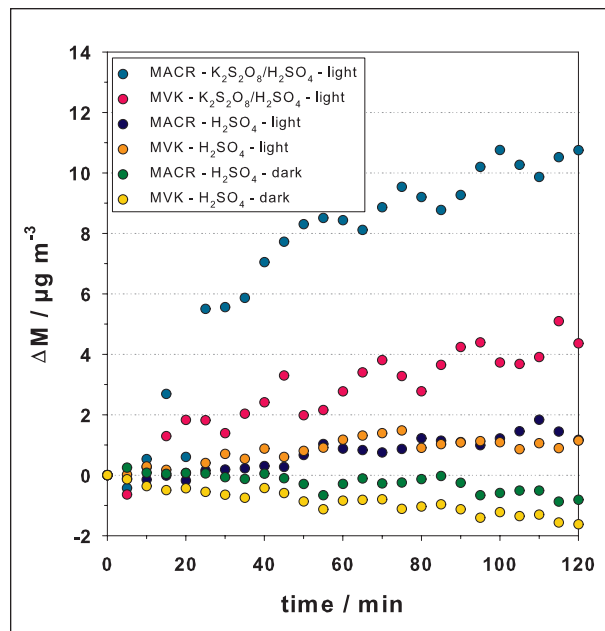


Fig. 3: Time series of particle mass increase ( $\Delta M$ ) for all six chamber experiments.

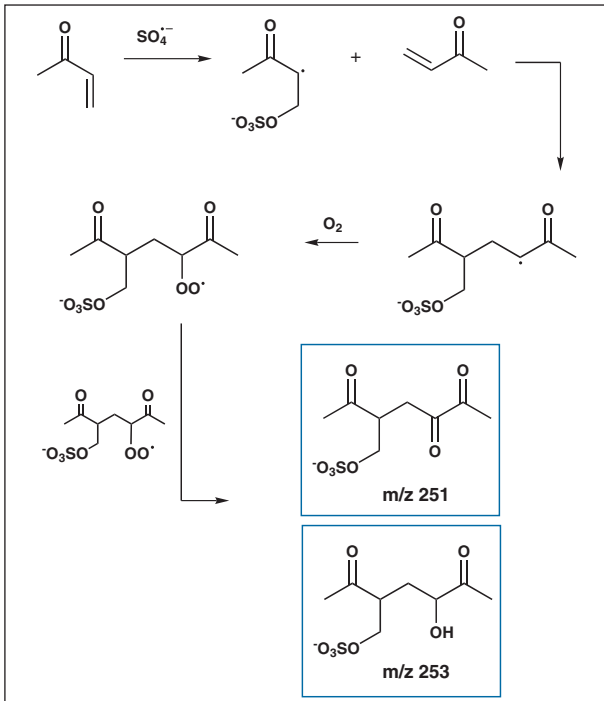


Fig. 2: Possible reaction mechanism for the formation of the dimeric organosulfates  $m/z$  251 and 253 from MVK.

is shown for the formation of hydroxyacetone sulfate ester ( $m/z$  153) in Fig. 1. With a radical chain reaction preceding the peroxy radical mechanisms as shown in Figure 2, higher molecular weight compounds can be formed. The other organosulfate compounds from MACR and MVK are expected to form from similar reactions but cannot be completely explained with these mechanisms.

The formation of organosulfate from MACR and MVK was further investigated under three different reaction conditions in the TROPOS aerosol chamber. All experiments were performed at elevated relative humidity and OVOC mixing ratios as well as sulfuric acid in the seed particles as latest studies have shown that these conditions enhance the formation of organosulfates and promote the partitioning of MACR and MVK into the particle phase. Experiments performed under dark and irradiated condition with sulfuric acid as seed showed no or only little organic mass growth (Fig. 3). This is consistent with the results of the filter analysis that showed no or

a few organosulfate species in these samples. The appearance of organosulfates in the experiments with irradiation can be explained with the production of a small amount of sulfate radicals formed in the presence of acidic sulfate seed particles and UV light due to background OH radical production. The addition of a sulfate radical source (potassium peroxodisulfate) to the seed solution led to an increase of the particle mass production and the formation of additional organosulfate species from both OVOCs. After 2 h of irradiation in the presence of acidified potassium peroxodisulfate seed particles,  $10 \mu\text{g m}^{-3}$  of particle mass was produced from MACR, and  $4 \mu\text{g m}^{-3}$  was produced from MVK (Fig. 3). This is consistent with the spate of monomeric organosulfate species ( $m/z$  153, 155, 183 and 199) detected in the filter samples. Furthermore, the oligomeric species  $m/z$  251 and 253 were detected in the sample of the experiment with MACR, which explains higher particle mass from MACR, as oligomeric species add more mass to the SOA in the MACR experiment.

The results of these experiments reveal different behaviours of MACR and MVK to partitioning, radical induced organosulfate formation and subsequent SOA formation:

- Acid-catalysed oligomerisation reactions such as aldol condensation and hydration/polymerisation were unimportant under the experimental conditions as no particle mass was produced in the dark experiments.
- The radical reaction was one of the determining factors for the organic mass production as the particle growth corresponds to an increasing concentration of sulfate radicals in the seed particles.
- The higher SOA formation of MACR accompanied with dimer formation likely originates from a more pronounced partitioning of MACR than MVK.

## Conclusion

In this study we found evidence for the sulfate radical-induced formation of organosulfates following reactive uptake of MACR and MVK. We suggest that the particle phase sulfate radical chemistry can play a role in SOA formation under appropriate conditions in which these OVOCs are likely present in aqueous particles but further studies are warranted to draw a clear conclusion about the importance of the radical and non-radical initiated organosulfate formation.

---

## References

- Froyd, K. D., S. M. Murphy, D. M. Murphy, J. A. de Gouw, N. C. Eddingsaas, and P. O. Wennberg (2010), Contribution of isoprene-derived organosulfates to free tropospheric aerosol mass, *Proc. Natl. Acad. Sci. U. S. A.*, 107(50), 21360-21365.
- Nozière, B., S. Ekström, T. Alsberg, and S. Holmström (2010), Radical-initiated formation of organosulfates and surfactants in atmospheric aerosols, *Geophys. Res. Lett.*, 37, DOI: 10.1029/2009GL041683.
- Surratt, J. D., Y. Gómez-González, A. W. H. Chan, R. Vermeylen, M. Shahgholi, T. E. Kleindienst, E. O. Edney, J. H. Offenberg, M. Lewandowski, M. Jaoui, W. Maenhaut, M. Claeys, R. C. Flagan, and J. H. Seinfeld (2008), Organosulfate formation in biogenic secondary organic aerosol, *J. Phys. Chem. A*, 112(36), 8345-8378.
- Tolocka, M. P., and B. Turpin (2012), Contribution of Organosulfur Compounds to Organic Aerosol Mass, *Environ. Sci. Technol.*, 46(15), 7978-7983.

---

## Funding

The work was supported by the European Community's Seventh Framework Programme ([FP7/2007-2013]) EU project PEGASOS under grant agreement no. 265307

# Oxidation of Glyoxal in the Tropospheric Aqueous Phase

Thomas Schaefer, Hartmut Herrmann

Die temperaturabhängigen Geschwindigkeitskonstanten der Oxidation von Glyoxal durch atmosphärisch relevante Radikale wurden mittels einer weiterentwickelten Laser-Photolyse-Langweg-Laser-Absorptionsapparatur ermittelt. Durch die Erweiterung war es möglich die Sauerstoffadditionsreaktion an Alkylradikale zu untersuchen und damit bestehende Diskrepanzen der Größenordnung der Geschwindigkeitskonstante aufzuklären.

## Introduction

Volatile and semivolatile organic compounds (VOCs) are introduced into the troposphere in large amounts from biogenic and anthropogenic sources. Oxidation products of these VOCs, e.g., glyoxal, are important for the formation of secondary organic aerosol (SOA). Glyoxal can partition into the aqueous phase of cloud droplets, fog, rain and deliquescent particles and is oxidized by radicals, like OH and  $\text{NO}_3^-$ .

Currently, there are still uncertainties concerning the rate constant after H-atom abstraction from glyoxal by, e.g., OH radicals, where alkyl radicals form peroxy radicals under addition of molecular oxygen. *Buxton et al.*, [1997] claims a rate constant of  $k = 1 \times 10^9 \text{ M}^{-1} \text{ s}^{-1}$  for the formation of the peroxy radical in dilute solutions ( $< 1 \text{ mM}$ , typical concentration for cloud water). A second study from *Lim et al.*, [2010] assumes that the formation of the peroxy

radicals in solutions with higher concentrations  $> 1 \text{ mM}$  is a minor reaction pathway because of a lower rate constant of  $k = 1 \times 10^6 \text{ M}^{-1} \text{ s}^{-1}$  that was estimated after *Guzman et al.*, [2006]. The difference in the oxygen addition rate constants is of about three orders of magnitude which might lead to different oxidation products and yields in the aqueous solution.

## Experimental

The kinetic investigation of radical reactions were carried out as a function of temperature ( $278 \text{ K} \leq T \leq 318 \text{ K}$ ), of pH ( $2 \leq \text{pH} \leq 9$ ), and of the oxygen concentration using a laser flash photolysis - long path laser absorption (LFP – LPLA) setup (Fig. 1). OH radicals were formed by photolysis of hydrogen peroxide at  $\lambda = 248 \text{ nm}$ . Rate constants for OH radical reactions were determined by applying the competition kinetics method with thiocyanate as

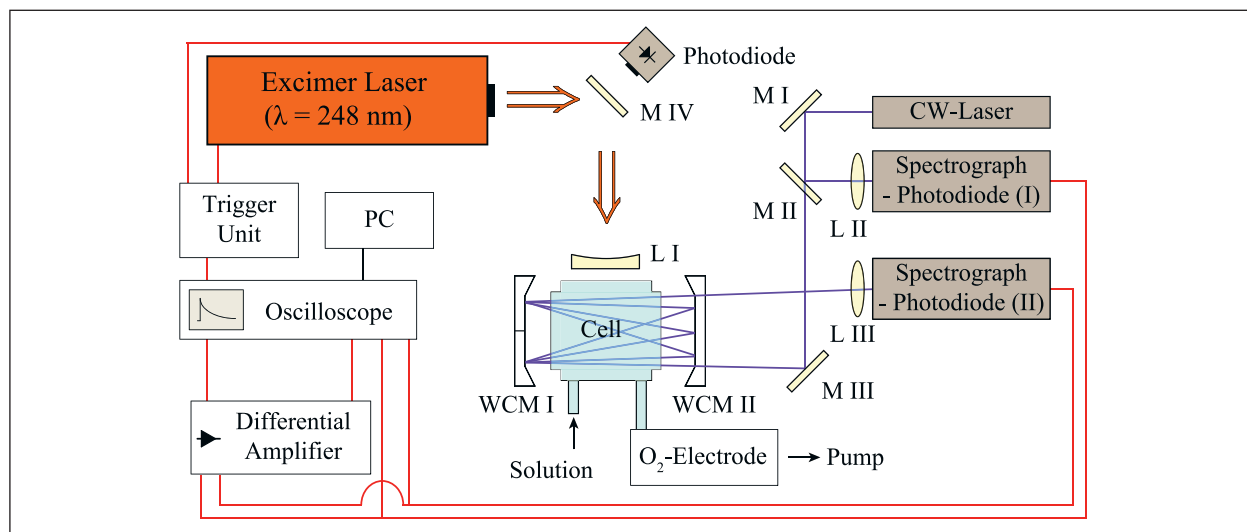


Fig. 1: Laser-Photolysis - Long Path Laser Absorption (LFP – LPLA) set-up for kinetic investigations in the aqueous solution.

Tab. 1: Kinetic data and activation parameters of investigated OH,  $\text{SO}_4^-$  and  $\text{NO}_3^-$  reactions with glyoxal in aqueous solution.

compound	$k_{298\text{ K}} [\text{M}^{-1} \text{s}^{-1}]$	$E_A [\text{kJ mol}^{-1}]$	$A [\text{M}^{-1} \text{s}^{-1}]$	pH
temperature dependent measurements				
Glyoxal + OH	$(9.6 \pm 0.5) \cdot 10^8$	$12 \pm 1$	$(1.2 \pm 0.1) \cdot 10^{11}$	6
Glyoxal + $\text{SO}_4^-$	$(2.4 \pm 0.2) \cdot 10^7$	$13 \pm 1$	$(5.4 \pm 0.1) \cdot 10^9$	6
Glyoxal + $\text{NO}_3^-$	$(9.0 \pm 0.9) \cdot 10^6$	$33 \pm 21$	$(4.5 \pm 1.3) \cdot 10^{12}$	6
pH dependent measurements				
Glyoxal + OH	$(9.7 \pm 0.4) \cdot 10^8$	-	-	2
	$(1.2 \pm 0.1) \cdot 10^9$	-	-	9
Glyoxal + $\text{SO}_4^-$	$(2.2 \pm 0.4) \cdot 10^7$	-	-	2
	$(2.6 \pm 0.1) \cdot 10^7$	-	-	9

reference reactant, [Hoffmann et al., 2009]. Contrary to this, sulfate ( $\text{SO}_4^-$ ) and nitrate ( $\text{NO}_3^-$ ) radicals were observed directly to determine the rate constant of the respective radical reaction. The  $\text{SO}_4^-$  radical was produced by the photolysis of peroxodisulfate anions at  $\lambda = 248$  nm. The nitrate radical was formed by the photolysis of peroxodisulfate anions at  $\lambda = 351$  nm in the presence of nitrate anions [de Semainville et al., 2007]. The alkyl radical reaction with molecular oxygen in aqueous solution was studied by using the competition kinetics method with ferricyanide  $[\text{Fe}(\text{CN})_6]^{3-}$  as reference system [Adams et al., 1969].

## Results

Results of the temperature and pH dependent measurements for the reaction of OH,  $\text{NO}_3^-$  and  $\text{SO}_4^-$  radicals with glyoxal are summarized in Tab. 1. The measured rate constant of the OH radical reaction at  $T = 298$  K is in close agreement with the value given by Buxton et al., [1997]  $k_{298\text{ K}} = (1.1 \pm 0.04) \cdot 10^9 \text{ M}^{-1} \text{s}^{-1}$ .

Furthermore, the method from Adams et al., [1969] to measure the rate constant of the oxygen

addition on alkyl radical was modified for laser flash photolysis conditions and successfully applied. The results given in Tab. 2 are in consistence with literature values obtained by pulse radiolysis studies,  $k_{\text{CH}_2\text{OH} + \text{O}_2} = (4.2 \pm 0.5) \cdot 10^9 \text{ M}^{-1} \text{s}^{-1}$  from Rabani et al., [1974] and  $k_{(\text{CH}_3)_2\text{COH} + \text{O}_2} = 3.5 \cdot 10^9 \text{ M}^{-1} \text{s}^{-1}$  from Willson et al., [1971]. The oxidation of the glyoxyl alkyl radical by  $\text{O}_2$  to the peroxy radical can be better described by Buxton et al., [1997] with  $k = (1.4 \pm 0.1) \cdot 10^9 \text{ M}^{-1} \text{s}^{-1}$ .

## Summary

The results of this study indicate that the oxidation of glyoxal by OH radicals via H abstraction reaction to the glyoxyl alkyl radical followed by the addition of oxygen to the glyoxyl peroxy radical can be better described by the concept of Buxton et al., [1997]. Furthermore, these results underline that the rate constants of the oxygen addition reaction to the peroxy radicals are in the range of  $10^9 \text{ M}^{-1} \text{s}^{-1}$ . Hence, mechanisms using the way too small rate constant have urgently to be corrected to avoid wrong conclusions.

Tab. 2: Kinetic data of investigated organic radical reactions with ferricyanide and molecular oxygen in aqueous solution.

compound	$[\text{Fe}(\text{CN})_6]^{3-} k_{298\text{ K}} [\text{M}^{-1} \text{s}^{-1}]$	$\text{O}_2 k_{298\text{ K}} [\text{M}^{-1} \text{s}^{-1}]$	pH
$\text{CH}_2\text{OH}$	$(4.2 \pm 0.9) \cdot 10^9$	$(4.2 \pm 0.9) \cdot 10^9$	2
$(\text{CH}_3)_2\text{C}(\text{OH})$	$(5.2 \pm 0.3) \cdot 10^9$	$(3.2 \pm 1.1) \cdot 10^9$	2
$(\text{OH})_2\text{CHC}(\text{OH})_2$	$(1.8 \pm 0.3) \cdot 10^9$	$(7.2 \pm 1.3) \cdot 10^8$	2

---

## References

- Adams, G. E., and R. L. Willson (1969), Pulse Radiolysis Studies on the Oxidation of Organic Radical in Aqueous Solution, *Trans. Faraday Soc.*, 65, 2981-2987
- Buxton, G. V., T. N. Malone, and G. A. Salmon (1997), Oxidation of glyoxal initiated by OH in oxygenated aqueous solution, *J. Chem. Soc. Faraday Trans.*, 93 (16), 2889-2891.
- de Semailville, P. G., D. Hoffmann, C. George, and H. Herrmann (2007), Study of nitrate radical ( $\text{NO}_3\cdot$ ) reactions with carbonyls and acids in aqueous solution as a function of temperature, *Phys. Chem. Chem. Phys.*, 9 (8), 958-968.
- Guzman, M. I., A. J. Colussi, and M. R. Hoffmann (2006), Photoinduced Oligomerization of Aqueous Pyruvic Acid, *J. Phys. Chem. A*, 110 (10), 3619-3626.
- Hoffmann, D., B. Weigert, P. Barzaghi and H. Herrmann (2009), Reactivity of poly-alcohols towards OH,  $\text{NO}_3$  and  $\text{SO}_4^{\cdot-}$  in aqueous solution, *Phys. Chem. Chem. Phys.*, 11 (41), 9351-9363.
- Lim, Y. B., Y. Tan, M. J. Perri, S. P. Seitzinger, and B. J. Turpin (2010), Aqueous chemistry and its role in secondary organic aerosol (SOA) formation, *Atmos. Chem. Phys.*, 10, 10521-10539.
- Rabani, J., D. Klug-Roth and A. Henglein (1974), Pulse radiolytic investigations of  $\text{OHCH}_2\text{O}_2$  radicals, *J. Phys. Chem.*, 78 (21), 2089-2093.
- Willson, R. L. (1971), Pulse Radiolysis Studies on Reaction of Triacetoneamine-N-oxyl with Radiation-Induced Free Radicals, *Trans. Faraday Soc.*, 67, 3008-3019.

---

## Funding

German Research Foundation (DFG), Bonn, Germany

---

## Cooperation

Laboratoire inter-universitaire des Systèmes Atmosphériques (LISA), Paris, France

# CAPRAM mechanism development and modelling

Peter Bräuer, Andreas Tilgner, Ralf Wolke, Hartmut Herrmann

**Ziel der hier beschriebenen Studie war die Entwicklung eines Protokolls für eine automatisierte Generierung expliziter Flüssigphasenmechanismen und dessen Implementierung in einem Expertensystem. Mittels des für die Flüssigphase erweiterten Expertensystems GECKO-A (Generator for Explicit Chemistry and Kinetics of Organics in the Atmosphere) wurde der Flüssigphasenmechanismus CAPRAM (Chemical Aqueous Phase RADical Mechanism) auf bis zu 7118 Prozesse in Zusammenarbeit mit Kooperationspartnern am Laboratoire Inter-universitaire des Systèmes Atmosphériques (LISA, Paris, Frankreich) erweitert. Mit dem Boxmodell SPACCIM (SPectral Aerosol Cloud Chemistry Interaction Model) wurden intensive Studien mit CAPRAM3.5 $\alpha$  für ein meteorologisches Szenario mit nicht-permanenten Wolken unter ländlichen und urbanen Bedingungen durchgeführt.**

## Introduction

The ubiquitous abundance of organic compounds in natural and anthropogenically-influenced eco-systems has put these compounds into the focus of environmental research. Organic compounds are involved in numerous atmospheric processes and environmental issues. They contribute to particle growth by secondary organic aerosol (SOA) formation and are widely discussed in relation with air quality and health issues. However, the multiphase and especially the aqueous phase chemistry of organic compounds is still poorly understood. The oxidation chain of organic compounds includes a large number of intermediate compounds, many of which with unknown or poorly investigated formation and degradation pathways. Modelling can provide a powerful tool to investigate the multiphase chemistry of organic compounds in the troposphere. The success of model simulations heavily relies on an accurate description of the microphysics and chemistry in the model simulations. However, previous attempts for explicit and detailed chemical mechanisms focused mainly on the gas phase for which large mechanisms, such as the Master Chemical Mechanism (MCM, Saunders *et al.*, 2003) with far more than 10,000 reactions exist. Therefore, the present study aimed to extend the currently most comprehensive aqueous phase mechanism CAPRAM 3.0n (Chemical Aqueous Phase RADical Mechanism, Tilgner and Herrmann, 2010, Bräuer *et al.*, 2013).

## CAPRAM mechanism development

With 777 reactions and equilibria, CAPRAM 3.0n is already the most comprehensive aqueous phase mechanism. The feasibility of a mechanism extension demanded automation routines due to the large number of reactions deriving from the explicit nature of CAPRAM. Moreover, the mechanism development aims at longer chained organic compounds. The number of intermediate products increases exponentially and for a complete description of the C4 chemistry, about 10.000 reactions are expected (see Aumont *et al.*, 2005). Therefore, a protocol has been developed for automated mechanism self-generation, which has then been implemented into the expert system GECKO-A (see Mouchel-Vallon *et al.*, 2013 for preliminary aqueous phase studies). When possible, the expert system uses available kinetic data, which was compiled from literature in advance. In most cases, rate constants have to be estimated using evaluated prediction methods. For hydroxyl radical reactions, structure-activity relationships are used (Doussin and Monod, 2011, Minakata *et al.*, 2009). For nitrate radical reactions, Evans-Polanyi-type correlations (see, e.g. Hoffmann *et al.*, 2009 and references therein) have been improved with the help of the kinetic database.

Three new mechanisms have been created: CAPRAM 3.0p, 3.5, and 4.0. Major advances are the extension of the organic oxidation schemes for compounds with up to 4 carbon atoms, branched

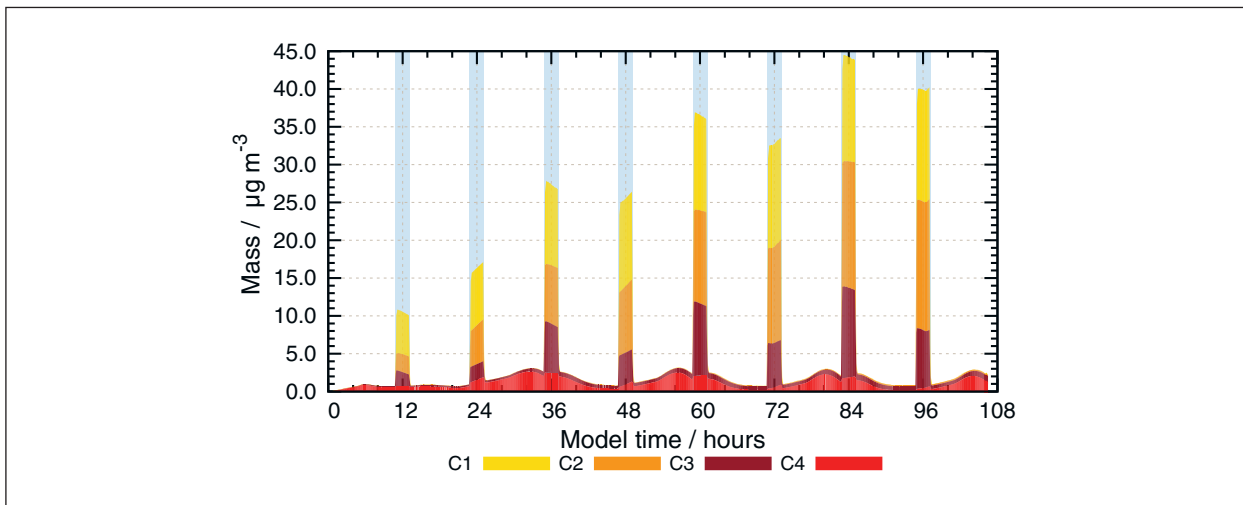


Fig. 1: Concentration-time profile of the organic particulate mass differentiated by chain length of the organic constituents in the model run with CAPRAM 3.5 $\alpha$  under urban conditions. Blue bars represent cloud periods.

radical attack, the introduction of peroxy radical cross reaction, and the addition of nitrate radicals to double bonds leading to organic nitrates. Moreover, for each new CAPRAM mechanisms, three subversions ( $\alpha$ ,  $\beta$  and  $\gamma$ ) with different levels of details concerning the nitrate radical chemistry exist. In the most comprehensive mechanism (CAPRAM 4.0 $\alpha$ ), 7118 aqueous phase processes are described.

### SPACCIM model studies

Model studies have been performed with the parcel model SPACCIM (Wolke et al., 2005) and the recently created multiphase chemical mechanism MCMv3.1-CAPRAM 3.5 $\alpha$  and 4.0 $\alpha$ . A standard meteorological scenario with non-permanent clouds under remote continental and urban conditions (see

Tilgner and Herrmann, 2010) was chosen for the model runs. Thorough analysis of the box model results on the concentration-time profiles and time-re-solved chemical fluxes has been performed with a focus on the multiphase budget of important tropospheric oxidants such as OH and  $\text{NO}_3$  radicals, or hydrogen peroxide, particle acidity, and secondary organic aerosol (SOA) formation. While detailed investigations were initially performed on single organic compounds, several lumping methods have been applied for a more convenient and clarified presentation and interpretation. The processing of the organic mass has been investigated by grouping all organic compounds either by their carbon number (Fig. 1) or by the compound class they belong to (Fig. 2). Both lumping techniques give new perspectives in the SOA processing. Figure 1 shows the organic

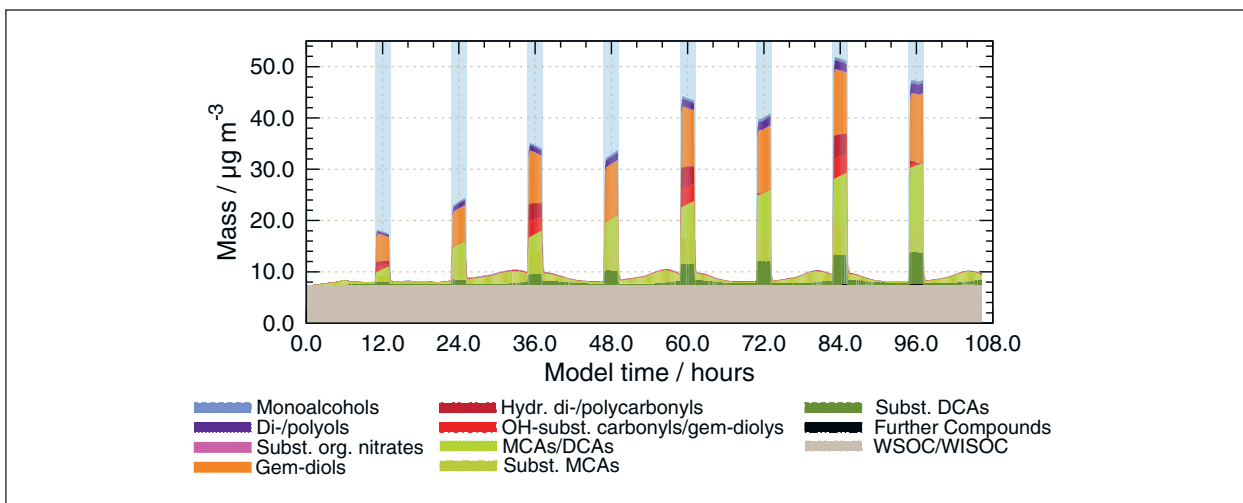


Fig. 2: Concentration-time profile of the organic particulate mass differentiated by compound classes in the model run with CAPRAM 3.5 $\alpha$  under urban conditions. Blue bars represent cloud periods.

mass grouped by carbon number in the model runs with CAPRAM 3.5 $\alpha$  under urban conditions. Organic mass increase is seen predominantly during daytime clouds, due to increased uptake. Organic matter consists to a large portion of smaller compounds. C4 chemistry is of minor importance. This changes during non-cloud periods, where chemistry is dominated by C4 compounds. This fact stresses the need for an extension of the organic scheme to even higher carbon numbers. In Fig. 2, the organic mass is analysed by compound classes for the model run with CAPRAM 3.5 $\alpha$  under urban conditions. Under cloud conditions a variety of compounds is found in the aqueous phase. Most compounds can be attributed to carbonyl compounds with one or more functional group as well as hydroxyl-substituted carbonyl compounds and carboxylic acid and diacids with possible hydroxyl and oxo substitutions. During non-cloud periods, only the carboxylic acids remain in the aqueous phase.

## Conclusions and outlook

In the model runs with the extended organic schemes, substantial improvements could be achieved in the simulation of inorganic and organic trace compounds and SOA processing. However, intensive testing of key parameters and a critical evaluation of single prediction methods is still necessary. Moreover, the protocol needs to be extended to further compound classes not yet considered including organic hydroperoxides, esters, ethers, and aromatic compounds. The extension of the aqueous phase mechanism leads to semi-volatile organic compounds that are currently not considered in the gas phase mechanism MCMv3.1. Therefore, the mechanism development needs to be extended to the gas phase to most precisely describe feedbacks between the two compartments in the tropospheric multiphase chemical processing. Further model studies should aim at higher carbon numbers (C $\geq$ 5).

---

## References

- Bräuer, P., A. Tilgner, R. Wolke, and H. Herrmann (2013), Mechanism development and modelling of tropospheric multiphase halogen chemistry: The CAPRAM Halogen Module 2.0 (HM2), *J. Atmos. Chem.*, 1-34, doi: 10.1007/s10874-013-9249-6.
- Hoffmann, D., B. Weigert, P. Barzaghi, and H. Herrmann (2009), Reactivity of poly-alcohols towards OH, NO<sub>3</sub> and SO<sub>4</sub><sup>2-</sup> in aqueous solution, *Phys. Chem. Chem. Phys.*, 11(41), 9351-9363.
- Minakata, D., K. Li, P. Westerhoff, and J. Crittenden (2009), Development of a Group Contribution Method to Predict Aqueous Phase Hydroxyl Radical (HO) Reaction Rate Constants, *Environ. Sci. Technol.*, 43(16), 6220-6227, doi: 10.1021/es900956c.
- Monod, A., and J. F. Doussin (2013), Structure–activity relationship for the estimation of OH-oxidation rate constants of carbonyl compounds in the aqueous phase, *Atmos. Chem. Phys.*, 13, 11625-11641, doi:10.5194/acp-13-11625-2013.
- Mouchel-Vallon, C., P. Brauer, M. Camredon, R. Valorso, S. Madronich, H. Herrmann, and B. Aumont (2013), Explicit modeling of volatile organic compounds partitioning in the atmospheric aqueous phase, *Atmos. Chem. Phys.*, 13(2), 1023-1037.
- Saunders, S. M., M. E. Jenkin, R. G. Derwent, and M. J. Pilling (2003), Protocol for the development of the Master Chemical Mechanism, MCM v3 (Part A): tropospheric degradation of non-aromatic volatile organic compounds, *Atmos. Chem. Phys.*, 3(1), 161-180.
- Tilgner, A., and H. Herrmann (2010), Radical-driven carbonyl-to-acid conversion and acid degradation in tropospheric aqueous systems studied by CAPRAM, *Atmos. Environ.*, 44, 5415-5422.
- Wolke, R., A. M. Sehili, M. Simmel, O. Knoth, A. Tilgner, and H. Herrmann (2005), SPACCIM: A parcel model with detailed microphysics and complex multiphase chemistry, *Atmos. Environ.*, 39(23-24), 4375-4388.

# Cloud Chemistry Modelling with COSMO-MUSCAT: A 2D Sensitivity Study

Roland Schrödner, Andreas Tilgner, Ralf Wolke, Hartmut Herrmann

**Das gekoppelte Chemie-Transport Modell COSMO-MUSCAT wurde um die Beschreibung der wolkenchemischen Aerosol-Prozessierung erweitert. Somit ist es möglich, detaillierte chemische Flüssigphasenmechanismen wie CAPRAM 3.0i zu verwenden. In Sensitivitätsstudien wurde die komplexe CAPRAM-Chemie mit einer einfacheren Repräsentation der Flüssigphasenchemie verglichen. Dabei haben sich deutliche Unterschiede im Oxidationsbudget, im pH-Wert der Wolkentropfen und in der Bildung organischer Partikelmasse gezeigt.**

## Introduction

The interaction of gases and aerosol particles with clouds entails a number of key environmental processes. On the one hand, they directly influence the life cycles of trace constituents and facilitate the multiphase oxidation budget. On the other hand, multiphase interactions strongly influence the physical properties of the processed aerosol.

A detailed description of both aqueous phase cloud chemistry and microphysics causes high computational costs. Therefore, most chemistry transport models (CTMs) use a highly parameterized description or simple aqueous phase chemical mechanisms focusing on sulphate production only.

In the present study, the comprehensive aqueous phase mechanism CAPRAM 3.0i (Chemical Aqueous Phase Radical Mechanism, [Tilgner and Herrmann et al., 2010]) was used in its reduced version (C3.0RED, [Deguillaume et al., 2009]) in the coupled regional CTM COSMO-MUSCAT [Wolke et al., 2004, 2012] and compared to the more simple inorganic mechanism INORG [Sehili et al., 2005]. Sensitivity studies on the behaviour of both mechanisms on several chemical targets (major oxidants ( $\text{OH}$ ,  $\text{HO}_2$ ,  $\text{H}_2\text{O}_2$ ,  $\text{NO}_3^-$ ,  $\text{O}_3$ ), sulphate mass, organic mass, pH) were conducted in an urban and a rural air mass.

## Representation of cloud chemistry in COSMO-MUSCAT

The bulk liquid water content (LWC) provided by COSMO is used as medium for the aqueous phase chemistry, which is switched on above a LWC

threshold of  $0.01 \text{ g m}^{-3}$ . To avoid numerical instability due to imbalanced fast dissociations and appropriate uptake reactions, these fast processes were balanced at this threshold in the whole domain. The droplet number of the monodisperse distribution is held constant at  $150 \text{ cm}^{-3}$  corresponding to droplet radii between  $2.5$  and  $9 \mu\text{m}$ .

## Model setup

Simulations lasting for 48 hours were conducted for a 2D vertical cross-section. The air streams over a bell-shaped hill (500 m high, 20 km half width), where a cap cloud forms shortly after the simulation starts. The initial chemical composition of air and particles is used as constant inlet boundary (left) during the whole simulation.

## Model results

All oxidants, except  $\text{O}_3$ , which is almost not affected by the aqueous phase, are strongly reduced in the gas phase during the cloud passage due to phase transfer and reactions in the aqueous phase. The reduction is between 20 and 99% with higher losses in the urban case. Besides  $\text{O}_3$ ,  $\text{H}_2\text{O}_2$  is the only oxidant present in both INORG and C3.0RED. Additionally, in both mechanisms its main fate in the aqueous phase is the production of sulphate. Therefore, only for these oxidants both mechanisms show similar concentration patterns. After the cloud passage,  $\text{H}_2\text{O}_2$  needs much time to refill the loss, whereas the reproduction of the other oxidants is quite fast.

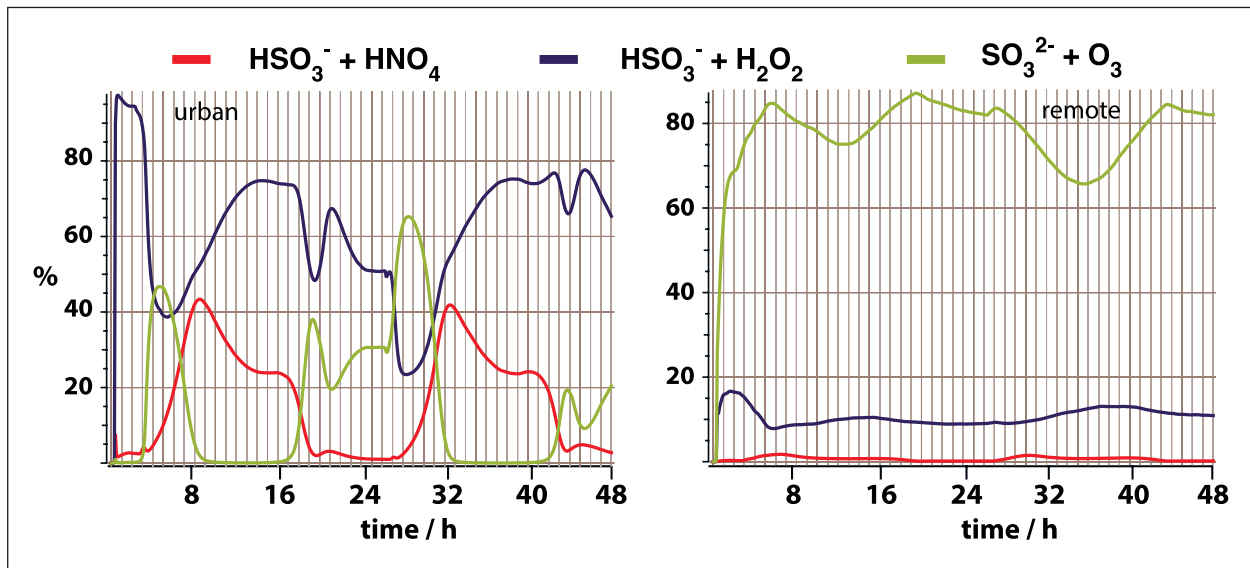


Fig. 1: Relative contribution of the modelled reaction fluxes converting S(IV) to S(VI) for the urban (left) and rural case (right) inside of the cloud.

The cloud water pH differences are up to 0.2 for the rural and up to 1 for the urban case between both mechanisms with more acidic cloud droplets for C3.0RED. Highest deviations occur during the day. The majority of the difference for the rural case can be explained by production of organic acids and to some extent by TMI-chemistry. For the urban air mass, this is more complex and also additional nitrate pathways come into consideration whereas TMI-chemistry seems to have only minor influence.

Due to cloud chemistry, the sulphate mass is increased by a factor of 1.3 - 3. Downwind of the cloud the sulphate mass is up to 5% lower for INORG compared to C3.0RED for the rural air mass. In

contrast, the urban daytime cloud shows an opposite difference, but high deviations can be seen during the night with up to 15% lower sulphate using INORG. Sulphate production is very sensitive to the pH. In the urban case, the oxidations via  $\text{H}_2\text{O}_2$  and  $\text{HNO}_4$  are the most important during daytime, whereas during the less acidic night-time also the  $\text{O}_3$ -pathway becomes essential (Fig. 1). Consequently, in the more alkaline rural air mass the production via  $\text{O}_3$  is responsible for the majority of sulphate present.

The modelled organic mass using C3.0RED (Fig. 2) reaches values of up to  $1.9 - 2.8 \mu\text{g m}^{-3}$  inside of the cloud. The organic mass on cloud residuals is increased compared to the pre-cloud values by  $\sim 0.6 \mu\text{g m}^{-3}$  and  $\sim 0.3 \mu\text{g m}^{-3}$ . The modelled mass of glyoxalic acid is in the range of available measurements [e.g. Sun and Ariya et al., 2006], whereas pyruvic acid is underestimated in the urban case and oxalic acid is underestimated in both air masses. Note that C3.0RED treats only some water-soluble organics with up to 4 C-atoms and that no oligomerization reactions are present.

### Conclusions and Outlook

The complex aqueous phase mechanism CAPRAM 3.0i RED was implemented in the CTM COSMO-MUSCAT. A test application was designed and the sensitivity of the mechanism on several chemical targets was analysed in comparison to a more simple aqueous phase approach. In the next step, this model system will be applied in 3D in comparison with the measurements of HCCT 2010 [van Pinxteren et al., 2012].

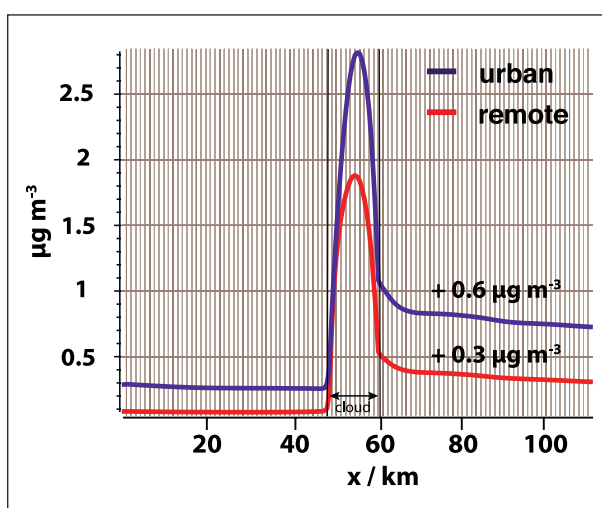


Fig. 2: Modelled processing of the organic mass in  $\mu\text{g}/\text{m}^3$  in the 2nd height level above ground midday of the second day. The cloud is located within the vertical bars.

---

## References

- Deguillaume, L., A. Tilgner, R. Schrodner, R. Wolke, N. Chaumerliac, and H. Herrmann (2009), Towards an operational aqueous phase chemistry mechanism for regional chemistry-transport models: CAPRAM-RED and its application to the COSMO-MUSCAT model, *J. Atmos. Chem.*, 64(1), 1-35, doi: DOI 10.1007/s10874-010-9168-8.
- Sehili, A. M., R. Wolke, O. Knoth, M. Simmel, A. Tilgner, and H. Herrmann (2005), Comparison of different model approaches for the simulation of multiphase processes, *Atmos. Environ.*, 39(23-24), 4403-4417, doi: Doi 10.1016/J.Atmosenv.2005.02.039.
- Sun, J. M., and P. A. Ariya (2006), Atmospheric organic and bio-aerosols as cloud condensation nuclei (CCN): A review, *Atmos. Environ.*, 40(5), 795-820, doi: Doi 10.1016/J.Atmosenv.2005.05.052.
- Tilgner, A., and H. Herrmann (2010), Radical-driven carbonyl-to-acid conversion and acid degradation in tropospheric aqueous systems studied by CAPRAM, *Atmos. Environ.*, 44(40), 5415-5422, doi: Doi 10.1016/J.Atmosenv.2010.07.050.
- van Pinxteren, D., A. Tilgner, L. Poulain, W. Fomba, T. Gnauk, A. Müller, Y. Iinuma, G. Spindler, B. Fahrlbusch, C. Müller, L. Schöne, P. Bräuer, S. Mertes, K. Dieckmann, M. Schäfer, P. Zedler, F. Stratmann, M. Merkel, W. Zhijun, K. Weinhold, W. Birmili, A. Wiedensohler, A. Roth, J. Schneider, S. Borrmann, E. Harris, B. Sinha, I. George, L. Whalley, D. Heard, M. Müller, B. D'Anna, C. George, A. Wéber, W. Haunold, A. Engel, D. Amedro, C. Schoemaeker, C. Fittschen, T. Lee, J. Collett, and H. Herrmann (2012), Hill Cap Cloud Thuringia 2010 (HCCT-2010): A ground based integrated study on aerosol cloud interaction, in *Biennial Report 2010/2011*, edited by A. Macke, H. Herrmann and I. Tegen, pp. 30-39, Leibniz Institute for Tropospheric Research, Leipzig.
- Wolke, R., O. Knoth, O. Hellmuth, W. Schröder, and E. Renner (2004), The parallel model system LM-MUSCAT for chemistry-transport simulations: Coupling scheme, parallelization and application, in *Parallel computing: Software technology, algorithms, architectures and applications*, edited by G. R. Joubert, W. E. Nagel, F. J. Peters and W. V. Walter, pp. 363-370, Elsevier, Amsterdam, The Netherlands.
- Wolke, R., W. Schroder, R. Schrodner, and E. Renner (2012), Influence of grid resolution and meteorological forcing on simulated European air quality: A sensitivity study with the modeling system COSMO-MUSCAT, *Atmos. Environ.*, 53, 110-130, doi: Doi 10.1016/J.Atmosenv.2012.02.085.

---

## Funding

The project was funded by the German Federal Environmental Foundation (Deutsche Bundesstiftung Umwelt, DBU) as part of their Doctoral Scholarship Programme

# Model study on the temperature dependence of primary marine aerosol emission

Stefan Barthel, Ina Tegen, Ralf Wolke

**Primäres marines Aerosol (PMA) bestehend aus Seesalz und organischen Anreicherungen dominiert die Aerosolphase (Massebetrachtung) über den Ozeanen und hat daher einen starken Einfluss auf alle atmosphärischen Prozesse, bei denen Aerosolpartikel beteiligt sind. Die Emission von PMA erfolgt durch das Platzen von Luftblasen, die infolge brechender Wellen entstanden sind, an der Meeresoberfläche. Dieser Prozess wird von vielen Parametern beeinflusst, wobei die Abhängigkeit von der Windgeschwindigkeit dominiert. Nahezu alle bisher existierenden Parametrisierungen zur Beschreibung des Emissionsflusses beachten nur diese Abhängigkeit. In den letzten Jahren wurde der Einfluss der Meeresoberflächentemperatur auf diesen Prozess näher betrachtet, so dass inzwischen drei Funktionen existieren, mit denen der Einfluss dieses Effektes in Modellen parametrisiert werden kann. Die Modellergebnisse stimmen besser mit Messwerten überein, wenn der Temperatureffekt beachtet wird.**

## Introduction

Primary marine aerosol (PMA) consisting of sea salt and organic enrichment influences cloud properties, incoming radiation as well as heterogeneous chemistry. These particles have a major impact in marine air, where they dominate the aerosol phase by mass. With 3 to 18 Tg/yr PMA has the highest emission rates of all aerosol types, but it has also the highest uncertainties in the quantification of the contribution to the global aerosol load as well as the global emission rates [Textor *et al.*, 2006]. One reason of this may be inaccurate parameterisations of the emission process.

PMA is emitted by the bursting of bubbles, which are produced through the entrainment of air into the ocean by breaking waves. This process is mainly forced by the surface wind speed, which is the only parameter in the majority of the currently available sea salt source functions. Besides others factors, the sea surface temperature became known to have a stronger impact on the PMA emission [e.g. Zábori *et al.*, 2012]. Three functions to describe the influence of the sea surface temperature on the PMA emission rates are available: Jaeglé *et al.* [2011] (J11), Sofiev *et al.* [2011] (S11) and a new one based Zábori *et*

*al.* [2012] (Zb13). These functions were implemented into the regional aerosol model COSMO-MUSCAT; the model results for the three different temperature dependence parameterizations were compared to each other and evaluated with measurements from an EMEP intensive campaign in January 2007.

## Method

**Model description.** COSMO-MUSCAT is an online-coupled model system consisting of the regional weather forecast model COMSO (Consortium of small scale modelling) from the Deutscher Wetterdienst (DWD) and the MUlti Scale Chemistry and Aerosol Transport model (MUSCAT) from TROPOS. The transport processes in the model include advection, turbulent diffusion, sedimentation and size dependent dry and wet deposition as well as chemical and microphysical transformations [Wolke *et al.*, 2012]. The aerosol size distribution is described with a spectral mass-based approach using 15 logarithmically spaced bins from 10 nm to 10 µm. The PMA emission rates are calculated with the approach from Long *et al.* [2011], which includes both sea salt and organic material.

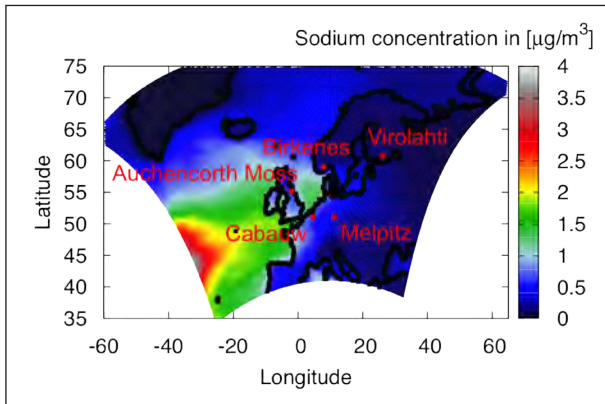


Fig. 1: Model domain for the case study together with the geographical position of the measurement sites, which have been included in the comparison.

**Case study.** For the case study the measurement stations Virolahti II (Finland), Birkenes (Norway), Auchencorth Moss (Great Britain), Cabauw (Netherlands) and Melpitz (Germany) were used. Therefore a model domain covering mid and northern Europe with the northeast Atlantic as potential source for PMA is needed (Fig. 1). The model uses a horizontal grid resolution of  $0.25^\circ$  and 30 vertical layers. The mid-height of the lowest level is at approximately 10 m. The spin up time of the model is five days.

## Results

For the comparison of the model results to the measurements the sodium concentration is used. This is a good tracer for sea salt since there are only minor sources of no marine origin [Tsyro et al., 2011]. The sodium concentrations were computed from the sea salt part of PMA concentrations with a conversion factor of 0.3061 [Seinfeld and Pandis, 2006]. The monthly averaged modelled sodium concentrations in PM10 in the first model layer are shown in Fig. 1. The high values west of Ireland are due to the high emission rates as result of high wind speeds there, but may also be partly affected by the boundary conditions. The sodium concentration decreases

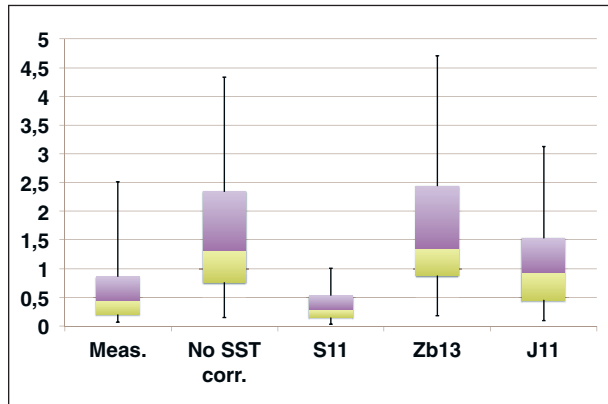


Fig. 2: Box plots (5 to 95-percentile) for the sodium mass concentration in PM10 including measurement and model values for all five EMEP stations (Virolahti II, Birkenes, Auchencorth Moss, Cabauw and Melpitz).

with the distance from the sea, as expected. Figure 2 shows boxplots for sodium concentrations in PM10 combined for the five stations for January 2007. This plot compares the measured concentration to the modelled results for the case (1) without any temperature dependence, (2) S11, (3) Zb13 and (4) J11 (from left to right). The model overpredicts the sodium concentration when the influence of the sea surface temperature is neglected. The correction function Zb13 leads to no significant changes, which is due to the fact that with this correction the reduction of coarse mode particles is partly compensated by a strong increase of fine mode particles especially near cold water. With the J11 correction the modelled concentrations decrease and are closer to the measurements, but some overprediction remains. Using the correction function by S11 the modelled concentrations are close to the measurements, especially the median of model and measurements agrees well. However, here the model tends to underestimate the measured peak concentrations. This leads to the conclusion that the use of a SST-correction function improves the model results compared with measurements. However, the remaining discrepancies indicate the need of further research on this topic.

## References

- Jaeglé, L., Quinn, P. K., Bates, T. S., Alexander, B., and Lin, J.-T. (2011), Global distribution of sea salt aerosols: new constraints from in situ and remote sensing observations, *Atmos. Chem. Phys.*, 11, 3137-3157, doi:10.5194/acp-11-3137-2011.
- Long, M. S., Keene, W. C., Kieber, D. J., Erickson, D. J., and Maring, H. (2011), A sea-state based source function for size- and composition-resolved marine aerosol production, *Atmos. Chem. Phys.*, 11, 1203-1216, doi:10.5194/acp-11-1203-2011.
- Wolke, R., Schröder, W., Schrödner, R. and Renner, E. (2012), Influence of grid resolution and meteorological forcing on simulated European air quality: A sensitivity study with the modeling system COSMO-MUSCAT, *Atmos. Environ.*, 53, 110-130, doi:10.1016/j.atmosenv.2012.02.085.
- Seinfeld, J. H., and Pandis, S. N. (2006), *Atmospheric Chemistry and Physics - From Air Pollution to Climate Change*, second ed. John Wiley & Sons, New York.

- Sofiev, M., Soares, J., Prank, M., de Leeuw, G., and Kukkonen, J. (2011), A regional-to-global model of emission and transport of sea salt particles in the atmosphere, *J. Geophys. Res. - Atmos.*, 116, D21302, doi:10.1029/2010JD014713.
- Textor, C., Schulz, M., Guibert, S., Kinne, S., Balkanski, Y., Bauer, S., Berntsen, T., Berglen, T., Boucher, O., Chin, M., Dentener, F., Diehl, T., Easter, R., Feichter, H., Fillmore, D., Ghan, S., Ginoux, P., Gong, S., Grini, A., Hendricks, J., Horowitz, L., Huang, P., Isaksen, I., Iversen, I., Kloster, S., Koch, D., Kirkevåg, A., Kristjansson, J. E., Krol, M., Lauer, A., Lamarque, J. F., Liu, X., Montanaro, V., Myhre, G., Penner, J., Pitari, G., Reddy, S., Seland, Ø., Stier, P., Takemura, T., and Tie, X. (2006), Analysis and quantification of the diversities of aerosol life cycles within AeroCom, *Atmos. Chem. Phys.*, 6, 1777-1813, doi:10.5194/acp-6-1777-2006.
- Tsyro, S., Aas, W., Soares, J., Sofiev, M., Berge, H., and Spindler, G. (2011), Modelling of sea salt concentrations over Europe: key uncertainties and comparison with observations, *Atmos. Chem. Phys.*, 11, 10367-10388, doi:10.5194/acp-11-10367-2011.
- Zábori, J., Matisáns, M., Krejci, R., Nilsson, E. D., and Ström, J. (2012), Artificial primary marine aerosol production: A laboratory study with varying water temperature, salinity, and succinic acid concentration, *Atmos. Chem. Phys.*, 12, 1070910724, doi:10.5194/acp-12-10709-2012.

---

### Funding

German Science Foundation (DFG), Grant No. TG 376/6-1

Federal Ministry of Education and Research (BMBF) as part of the SOPRAN project (FZK 03F0611J)

# UDINE: Ice formation in altocumulus clouds over Leipzig: Remote sensing measurements and detailed model simulations

Martin Simmel, Johannes Bühl, Ina Tegen, Albert Ansmann

Mit Hilfe von Lidar- und Radarsystemen wurde innerhalb der letzten zehn Jahre ein großer Datensatz über mittelhohe Schichtwolken (Altocumuluswolken, Altostratus) gesammelt. Die Messungen zeigen, dass ab Temperaturen kleiner -12 °C in der Hälfte dieser Wolken Eisbildung stattfindet. Die produzierte Menge an Eis variiert allerdings stark in allen Temperaturbereichen. Die vorliegende Studie untersucht zwei Wolkenfälle mit Hilfe des Modellsystems AK-SPECS (Kopplung des spektralen Mikrophysikmodells SPECS mit einem Dynamikmodell vom Asai-Kasahara-Typ). Die Beobachtungen werden ausreichend gut wiedergegeben, um Sensitivitätsstudien zum Einfluss verschiedener Parameter durchzuführen. Dabei zeigt sich, dass der Eisgehalt der Wolke bei ansonsten unveränderten Bedingungen am stärksten von der Form der Eispartikel abhängt.

## Introduction

Over Leipzig, altocumulus clouds are frequently observed by LACROS (Leipzig Aerosol and Clouds Remote Observations System) [Bühl et al., 2013]. These observations cover a wide range of heights and temperatures. The ratios of ice- to liquid-water path were found to vary between  $10^{-4}$  and 1.

## Case study: description and measurements

The altocumulus cloud shown in Fig. 1 was observed on 2012-08-02 between 21:00 UTC and 21:40 UTC. Liquid water was measured around 7500 m at about -25 °C (denoted by the red dashed line). The ice phase (virga) reached down to about 5500 m (Fig. 1a). Vertical windspeeds ranged from about -1.5 m/s to 1.0 m/s with a maximum of occurrence between -0.5 m/s and 0.5 m/s (Fig. 1b). Vertical motions at cloud base are visible in the Doppler lidar measurement showing the movement of small droplets at cloud base.

## Model description and initialization

For the current study the mixed-phase spectral microphysical model SPECS [Simmel and Wurzler, 2006; Diehl et al., 2006] was coupled to a dynamical model of the Asai-Kasahara type [Asai and

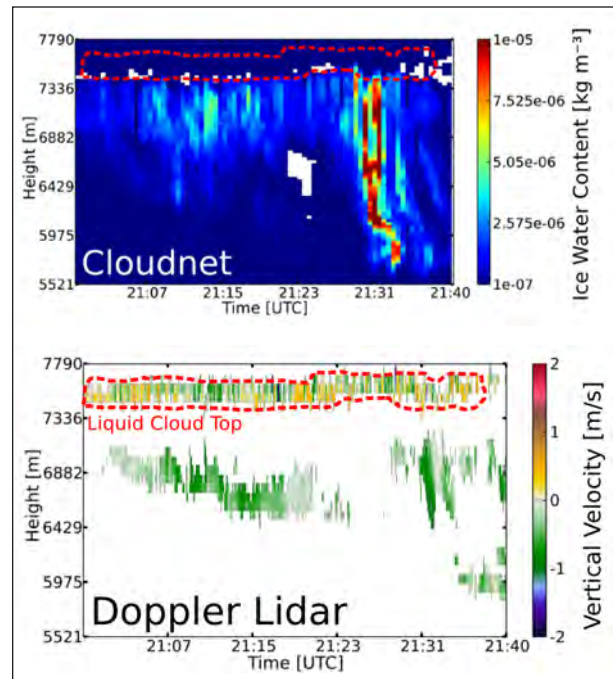


Fig. 1: Cloud observation on 2012-08-02 between 21:00 UTC and 21:40 UTC. (a) Ice water content derived by CLOUDNET and (b) vertical velocity measured by the Doppler Lidar WiLi. The red dashed line shows the upper part of the cloud consisting mainly of supercooled drops.

Kasahara, 1967] resulting in the model system AK-SPECS. The model geometry is axisymmetric and consists of an inner and an outer cylinder. The

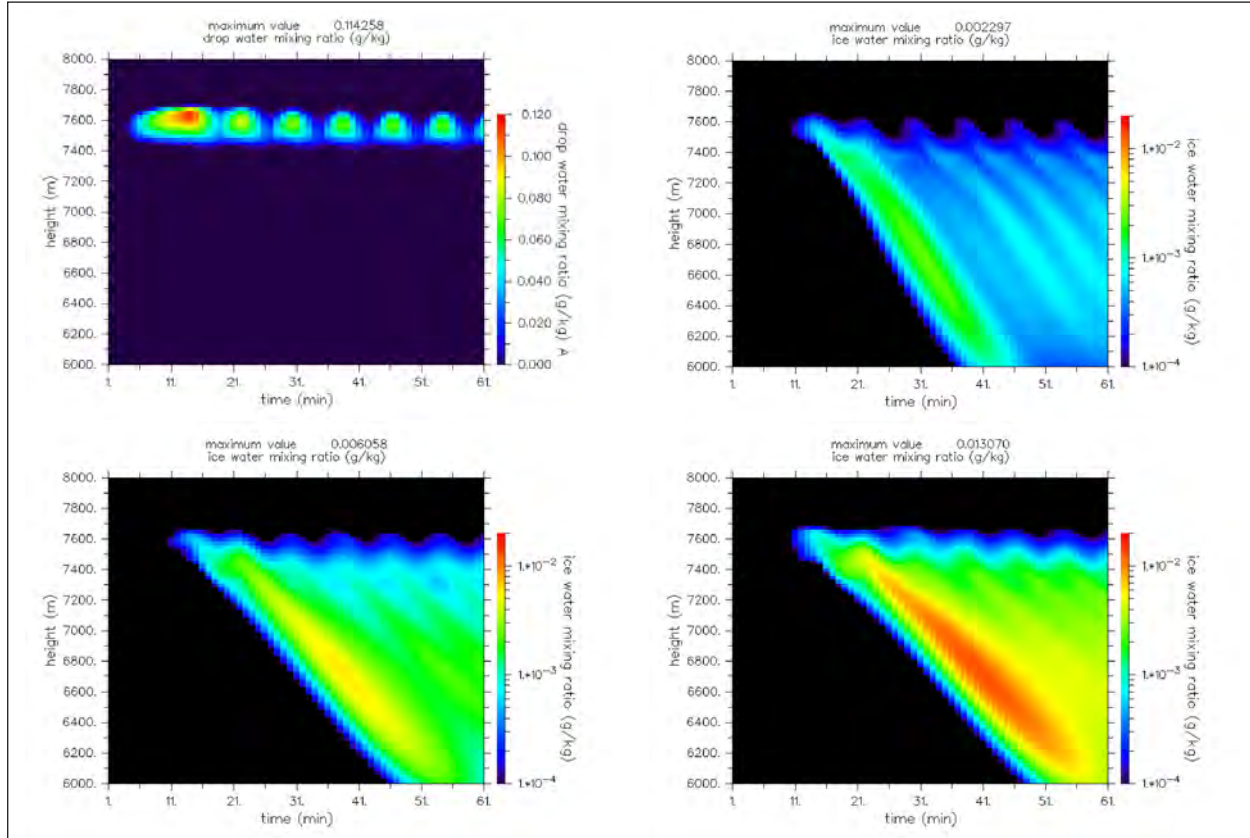


Fig. 2: Model result for (a) ar=1 liquid water mixing ratio, (b) ar=1 ice water mixing ratio, (c) columns ice water mixing ratio, and (d) plates ice water mixing ratio for the case study on 2012-08-02. Notice the logarithmic scale for the ice mixing ratios.

vertical resolution is constant with height and is chosen to be 25 m to give a sufficient resolution of the relatively shallow cloud layer. In contrast to a parcel model, the vertically resolved model grid allows for the description of hydrometeor sedimentation. This is important especially for the fast growing ice crystals to realistically describe their interaction with the vapour and liquid phase (Bergeron-Findeisen process). Since the focus is on the cloud microphysics, the dynamics in terms of vertical velocity profile is prescribed for the model runs (based on observation, cp. Fig. 1b) and the feedback of the microphysics on dynamics by release or consumption of latent heat due to phase transfer is not taken into account.

The microphysics is extended in two main aspects:

- **Ice particle shape:** In contrast to Diehl et al. [2006] ice particles of the hexagonal type (plates and columns) can be prescribed. The aspect ratio of the ice particles can be chosen either constant or size dependent following Mitchell [1996].
- **Ice nuclei (IN) budget:** A prognostic temperature resolved field of potential IN is introduced. We adapt the method of Fridlind et al. [2007]

assuming that all potential IN are active in the immersion freezing mode at the temperatures given by the parameterization of DeMott et al. [2010]. Immersion freezing occurs only when active IN and supercooled drops above a certain size threshold are present within a grid cell.

The model is initialized with vertical profiles of temperature and dewpoint temperature using the GDAS reanalysis data for Leipzig at 21 UTC. A sufficiently humid layer is present where the clouds were observed. Therefore, lifting of these layers leads to supersaturation and subsequent cloud formation. Since no in situ aerosol measurements are available, literature data is used. The Raman lidar observations do not show any polluted layers; therefore data from LACE98 for the upper free troposphere is used [Petzold et al., 2002].

## Results and conclusions

Figure 2a shows that the model results compare well enough with the measurements to justify sensitivity studies. Liquid water path for both is in the order of  $10^{-2}$  kg/m<sup>2</sup> (not shown) and the cloud geometry is rather similar. Figures 2 b-d show the sensitivity

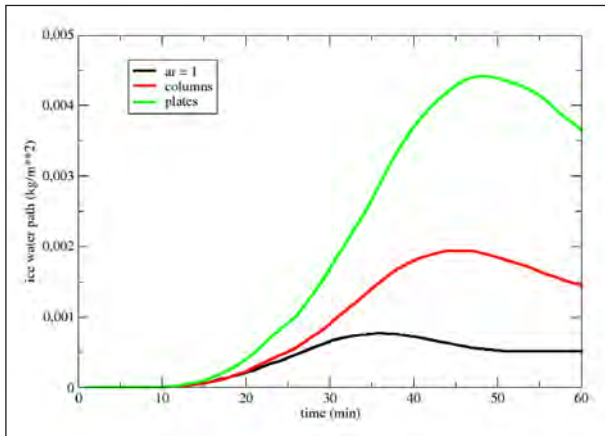


Fig. 3: Ice water path for  $ar=1$  (black), columns (red), and plates (green).

with respect to ice particle shape (aspect ratio  $ar=1$  vs. columns vs. plates). As in the measurements, virgae extend down to about 6000 m with a maximum between 6600 m and 6800 m. Ice maxima are increased by a factor of about 3 (5) for the columns (plates) case showing a much better agreement with observations than for  $ar=1$ . A closer look into the spectral microphysics reveals that for  $ar=1$  ice particles grow to maximum sizes of 0.2-0.3 mm falling at a terminal velocity of 0.63-1.14 m/s. If the ice particles are assumed to be columns (plates) they reach maximum sizes of 0.6-2 mm (0.8-1.8 mm)

and corresponding velocities of 0.47-0.76 m/s (0.42-0.75 m/s) with the size-dependent axis ratios of 4.3 to 9.2 (0.05-0.03). Despite these rather similar numbers for columns and plates, much more total ice mass is produced for the plates case. This can be attributed to the higher relative capacitance of plates, ranging from 1.6-1.9 for the relevant sizes compared to 1.3-1.6 for the columns. The relative capacitance describes the relative increase of water vapour deposition of a non-spherical particle compared to a sphere. Figure 3 compares the ice water path for the three runs and underlines the major influence of the ice habit due to lower terminal fall velocity and enhanced relative capacitance.

Similar results are obtained for a warmer case with a cloud base temperature of -6 °C. As expected, much less ice particles are abundant due to the higher temperatures but the high sensitivity with respect to the ice particle shape is present as well. Like in the observations, virgae are shorter and ice particles remain smaller. Following classical ice habit diagrams as in Pruppacher and Klett [1997] for the warmer temperatures of about -5 °C plates as well as columns could be expected, whereas for the colder case between -15 °C and -20 °C plates are more likely with aspect ratios depending on ice supersaturation. For  $T < -20$  °C column-like shapes can be expected.

## References

- Asai, T. and A. Kasahara (1967), A theoretical study of compensating downward motions associated with cumulus clouds, *J. Atmos. Sci.*, 24, 487–496.
- Bühl, J., A. Ansmann, P. Seifert, H. Baars, and R. Engelmann(2013), Toward a quantitative characterization of heterogeneous ice formation with lidar/radar: Comparison of CALIPSO/CloudSat with ground-based observations, *Geophys. Res. Lett.*, 40, 4404–4408, doi:10.1002/grl.50792.
- DeMott, P. J., A. J. Prenni, X. Liu, S. M. Kreidenweis, M. D. Peters, C. H. Twohy, M. S. Richardson, T. Eidhammer, and D. C. Rogers (2010), Predicting global atmospheric ice nuclei distributions and their impacts on climate, *PNAS*, 107, 11 217–11 222, doi:10.1073/pnas.091081810710.1073/pnas.0910818107.
- Diehl, K., M. Simmel, and S. Wurzler (2006), Numerical sensitivity studies on the impact of aerosol properties and drop freezing modes on the glaciation, microphysics, and dynamics of clouds, *J. Geophys. Res.*, 111, doi:10.1029/2005JD00588410.1029/2005JD005884.
- Fridlind, A. M., A. S. Ackerman, G. McFarquhar, G. Zhang, M. R. Poellot, J. P. DeMott, A. J. Prenni, and A. J. Heymsfield (2007), Ice properties of single-layer stratocumulus during the Mixed-Phase Arctic Cloud Experiment: 2. Model results, *J. Geophys. Res.*, 112, doi:10.1029/2007JD00864610.1029/2007JD008646.
- Heymsfield, A. J. and C. D. Westbrook (2010), Advances in the Estimation of Ice Particle Fall Speeds Using Laboratory and Field Measurements, *J. Atmos. Sci.*, 67, 2469–2482, doi:10.1175/2010JA3379.1.
- Petzold, A., M. Fiebig, H. Flentje, A. Keil, U. Leiterer, F. Schroder, A. Stifter, M. Wendisch, and P. Wendling (2002), Vertical variability of aerosol properties observed at a continental site during the Lindenbergs Aerosol Characterization Experiment (LACE 98), *J. Geophys. Res.*, 107, doi:10.1029/2001JD00104310.1029/2001JD001043.
- Pruppacher, H. R. and J. D. Klett, (1997), *Microphysics of Clouds and Precipitation*. Kluwer Academic, 954 pp.
- Simmel, M. and S. Wurzler (2006), Condensation and activation in sectional cloud microphysical models, *Atmos. Res.*, 80, 218–236, doi:10.1016/j.atmosres.2005.08.00210.1016/j.atmosres.2005.08.002.
- Westbrook, C. D., R. J. Hogan, and A. J. Illingworth (2008), The capacitance of pristine ice crystals and aggregate snowflakes, *J. Atmos. Sci.*, 65, 206–219, doi:10.1175/2007JAS2315.110.1175/2007JAS2315.1.

## Funding

German Research Foundation (DFG), Bonn, Germany

# ASAMgpu nested in WRF – on the way to an operational LES forecast

Stefan Horn

**Im Rahmen der HOPE-Kampagne im September 2013 in Melpitz wurde das Large Eddy Simulationsmodell ASAMgpu an ein operationelles regionales Wettervorhersagemodell gekoppelt. Das Ziel war es, eine experimentelle Vorhersage der Grenzschicht- und Wolkenentwicklung des kommenden Messtages bereitzustellen und im Nachlauf Simulationen ausgewählter Tage in höherer Auflösung für Analyse und Vergleichszwecke zu erstellen.**

## Introduction

In the context of the HOPE project a measurement campaign took place at the site in Melpitz from the 9th to the 27th of September 2013. The idea of the particular project presented in this report was to accompany the campaign with a large eddy simulation model (LES) to reproduce atmospheric parameters like boundary layer development and microphysical cloud properties on an operational basis. Therefore the possibility to nest the LES model ASAMgpu [Horn, 2012] into a larger scale regional weather forecast model to produce a daily large eddy forecast during the campaign was explored.

The results of those forecast runs were promising but not very satisfying yet. To check the theoretically applicability of the used model ASAMgpu in such a LES forecast framework, some of the days of the campaign were simulated at a much higher resolution afterwards.

The produced results can be used in comparisons with remote and in-situ data, for example from LIDAR, RADAR or the ACTOS platform or for further modelling studies like three dimensional radiation transfer codes.

## Boundary conditions

To produce a high resolution forecast, it is necessary to couple the LES model to an operational regional scale weather forecast model. During this work the boundary conditions were provided by Janek Zimmer (<http://www.modellzentrale.de>). The data was produced using the Weather Research and Forecast model (WRF). The used WRF setup covers Germany, runs at a resolution of 4km and is operational and

tested for several years already. The quality of the boundary data from the driving model is a crucial factor for any higher resolution forecast.

The model ASAMgpu uses three dimensional data fields for pressure, water vapour mixing ratio, cloud water mixing ratio, temperature, windspeed and two dimensional fields for the sensible and latent surface fluxes. A new boundary condition dataset was provided every 15 forecast minutes, covering the area from  $11.49^{\circ}$  to  $14.50^{\circ}$  longitude and  $49.99^{\circ}$  to  $52.00^{\circ}$  latitude. To get a hydrostatic balanced field without destroying the horizontal windspeed pressure gradient balance, every new three dimensional dataset was loaded into the ASAMgpu model and then integrated in time for a certain period with suppressed horizontal advection and damped vertical motions. Those fields are then linearly interpolated to the intermediate time steps and used as a nudging target at the boundaries for the continuously time integrated fields at the rest of the domain.

## The LES setup

The model ASAMgpu uses modern graphic adapters (GPUs) to provide the necessary computational power to perform fully compressible, high resolution simulations of the atmospheric boundary layer with sufficient domain sizes in computation times suitable for fore- and nowcasting.

The forecast mode runs currently with  $200 \times 200 \times 48$  cells at a for an LES very low resolution of  $500\text{m} \times 500\text{m} \times 200\text{m}$  resulting in a domain size of  $100\text{km} \times 100\text{km} \times 9.6\text{km}$ . The low resolution was chosen to limit the computation time to 5-6h for a 24h simulation using one single GPU. With that the forecast mode was more a technically study and not

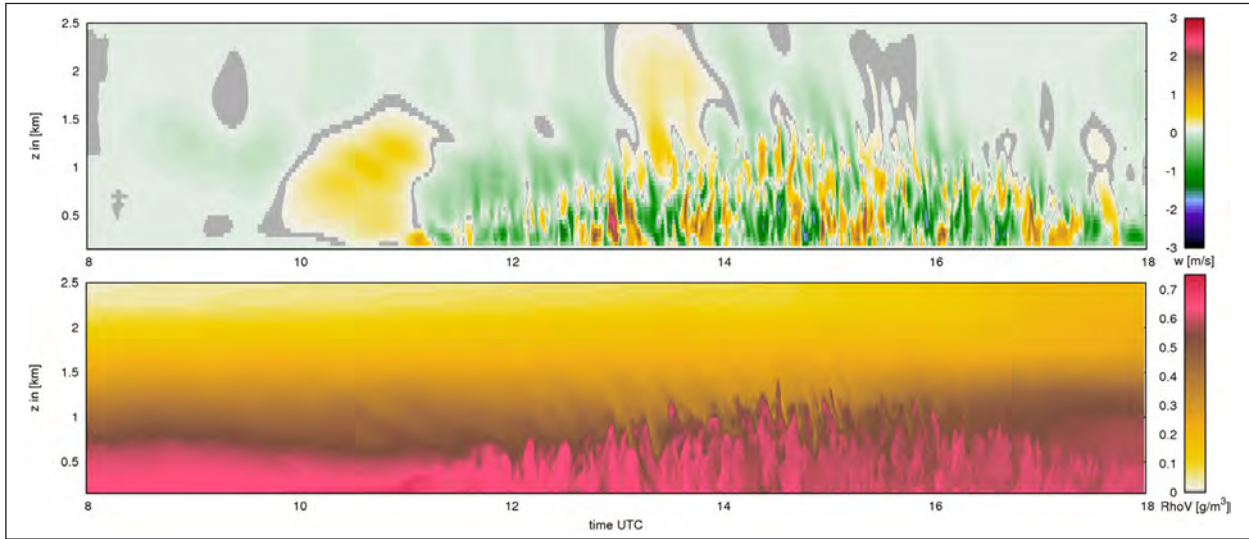


Fig.1: Simulated time evolution of vertical profiles of the vertical velocity (top) and the water vapour density (bottom) above the measurement site in Melpitz for the 27th of September 2013; boundary layer development starting at 11 UTC.

capable to reproduce the atmospheric properties with satisfactory results at the moment. But it is foreseeable that the technical development and the usage of more GPUs will enable predictive simulations at suitable resolutions in acceptable time ranges for LES forecasting during the next few years. To verify the model performance with focus on boundary layer development and cloud evolution higher resolution runs were performed using  $256 \times 256 \times 48$  cells with a size of  $45\text{m} \times 45\text{m} \times 45\text{m}$ , resulting in a domain size of  $11\text{km} \times 11\text{km} \times 2.8\text{km}$ . Those runs currently need about 3 days to finish.

## Results

Results from such a high resolution simulation for the 27th of September are presented in Fig. 1. During this day a very nice boundary layer development starting at 11 UTC up to a height of approximately

1km could be observed. The top of the figure shows a panel of vertical profiles of the vertical velocity over time at the centre of the domain, respectively the measurement site. It may be interpreted as a result from a doppler LIDAR looking upward. The lower panel shows the vertical distribution of the water vapour above the measurement site.

In Fig. 2 two vertical cut-planes are shown. The upper one shows the cloud droplet number concentration and the bottom one the cloud water density for the 14th of September at 16UTC. At this day small cumulus clouds developed during the late afternoon, while a warm front approaches from the west. First effects of the front are already recognizable in enhanced convection.

Figure 3 shows a horizontal plane of the corresponding liquid water path. Strong boundary effects can be observed near the inflow boundaries. Those are a result from the missing boundary layer

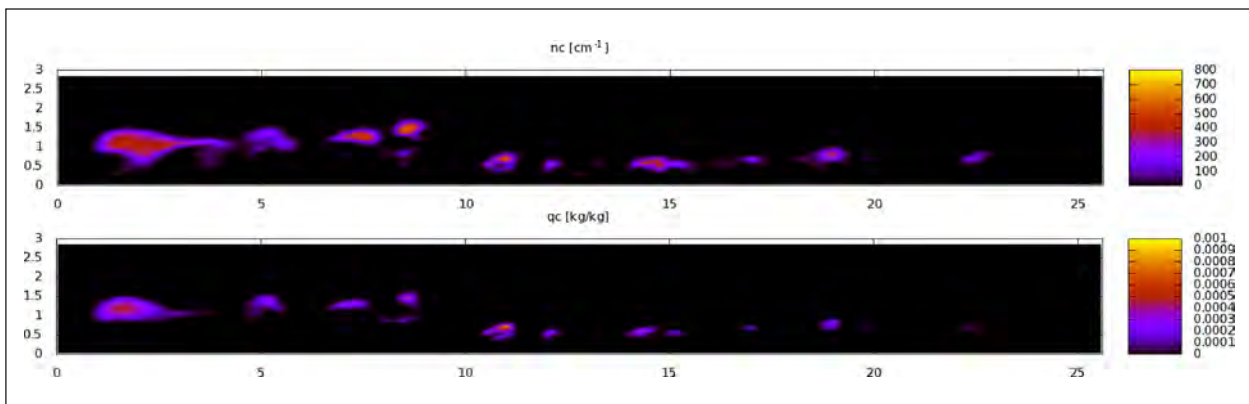


Fig.2: Vertical cut plane in west-east direction of cloud water density and cloud droplet number concentrations for the 14th of Sept. 2013 at 16 UTC.

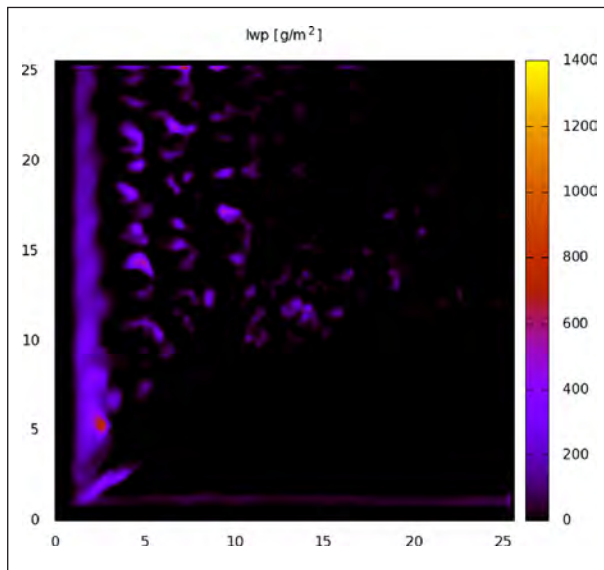


Fig.3: Horizontal plane of liquid water path for the 14th of Sept. 2013 at 16 UTC, first effects of approaching warm front from the west recognizable.

turbulence at the inflow, after a certain time a turbulent boundary layer structure evolves. That means boundary effects reach further into the domain at higher wind speeds. Another observable structure is a zone of enhanced convection diagonal from the inflow edge of the domain. This is most probably a result of enhanced convergence through missing turbulence and the simultaneously initiation of boundary layer turbulence leading to an amplification of convection.

### Outlook

The study showed the applicability of the ASAMgpu/WRF framework to produce high resolution simulations of the atmospheric boundary layer in acceptable computation times. For analysis purposes it is already possible to reproduce boundary layer development and cloud evolution and is also capable to provide microphysical information like droplet number concentrations for example. Future development will allow to perform high resolution large eddy simulation forecasts.

---

### References

Horn, S. (2012), ASAMgpu V1.0 – a moist fully compressible atmospheric model using graphics processing units (GPUs), *Geosci. Model Dev.*, 5, 345–353, doi: doi:10.5194/gmd-5-345-2012.

---

### Funding

HOPE - HD(CP)2 (High definition clouds and precipitation for advancing climate prediction) - German Federal Ministry of Education and Research (BMBF)

# Evaluation of Saharan dust source activation with regional model simulations and satellite observations

Kerstin Schepanski, Hartwig Deneke, Bernd Heinold, Thomas Kunze, Ina Tegen

Charakteristiken der raumzeitlichen Verteilung von Saharastaubemissionen werden mit Methoden regionaler Staubmodellierung und Satellitenfernerkundung untersucht. Ein Großteil der Emissionen wird durch nächtliche Grenzschichtstrahlströme verursacht. In Bergregionen ist die Modellierung solcher Ereignisse problematisch. Die atmosphärische Staubkonzentration wird jedoch nicht notwendigerweise durch die Anzahl der Emissionsereignisse sondern vielmehr durch die Stärke von Emissionsflüssen kontrolliert. Um quantitative Vergleiche von Modellergebnissen und Staubretrievalprodukten aus der Satellitenfernerkundung wie dem SEVIRI Staubindex zu ermöglichen, wurde dieser aus der modellierten Staubverteilung mit Hilfe eines Strahlungstransfermodells simuliert.

## Introduction

Soil dust aerosol originating from the Sahara desert is considered to be an important factor in the climate system. Regional-scale models can be used to study the meteorological features leading to dust

emissions. Such processes include synoptic scale features like cold fronts, low-level jets (LLJs), and convective activities [Knippertz and Todd, 2012]. Information on the spatiotemporal distribution of Saharan dust source activation (DSA) events is available from the geostationary Meteosat Second

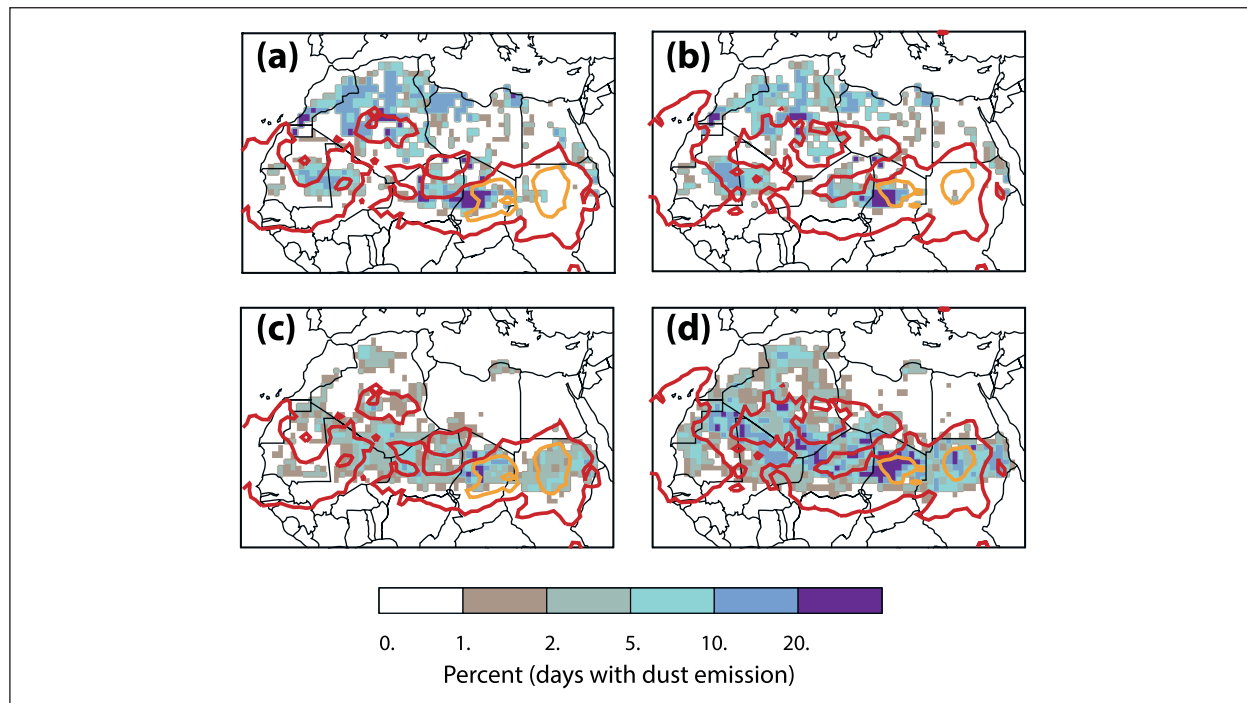


Fig. 1: Number of days per month with dust emission simulated with the COSMO-MUSCAT model (a, b) and derived from the MSG SEVIRI IR dust index (c, d). The red and orange contours indicate areas where the occurrence of low level jets in the model is higher than 5 and 10 days per months, respectively.

Generation (MSG) satellite infrared (IR) dust index [Schepanski et al., 2007]. The MSG observations suggest that the majority of the Saharan dust events are initiated in the morning hours, indicating the importance of turbulent downward mixing of momentum from nocturnal LLJs for activating dust sources [Schepanski et al., 2009]. Comparisons of the DSA from model results with the satellite observations reveal strengths and weaknesses of the dust model.

## Method

We use the regional-scale dust model COSMO-MUSCAT (COSMO: Consortium for Small-scale Modeling; MUSCAT: MultiScale Chemistry Aerosol Transport) to simulate the dust emission fluxes and size-resolved atmospheric dust concentrations for the years 2007 and 2008. Modeled dust emissions depend on surface wind friction velocities, surface roughness, soil particle size distribution, and soil moisture [Heinold et al., 2011]. DSA were counted when the emission flux in a model grid cell exceeded  $0.6 \times 10^{-4} \text{ kg m}^{-2} \text{ s}^{-1}$  in a 3-hour time interval [Laurent et al., 2010].

DSA events inferred from MSG SEVIRI (Spinning Enhanced Visible and InfraRed Imager) IR dust index data are used for evaluation of the spatiotemporal distribution of modeled dust emission events [Tegen et al., 2013]. The qualitative index indicating the presence of mineral dust is computed at 15-minute time intervals from brightness temperatures of the IR channels at 8.7  $\mu\text{m}$ , 10.8  $\mu\text{m}$ , and 12.0  $\mu\text{m}$ . [Schepanski et al., 2007]. This composite was used to localize DSA events by tracing dust plume patterns back to their origin [Schepanski et al., 2007, 2009]. The dust source regions inferred from this method differ from dust source regions that are based on daily satellite dust retrievals, e.g. from MODIS. The differences can be attributed to the temporal resolution of the different satellite retrievals [Schepanski et al., 2012].

## Results and Discussion

The observed morning maximum in DSA frequencies indicates that the breakdown of nocturnal LLJs is responsible for a considerable number of DSA events in the Sahara. The comparison of modeled and observed DSA shows that the onset of dust emission is delayed in the model compared to the observations. Also, the simulated number dust events associated with nocturnal LLJs in mountainous regions is underestimated in the model. The MSG dust index observations indicate a strong increase in dust source activation frequencies in the year 2008 compared to

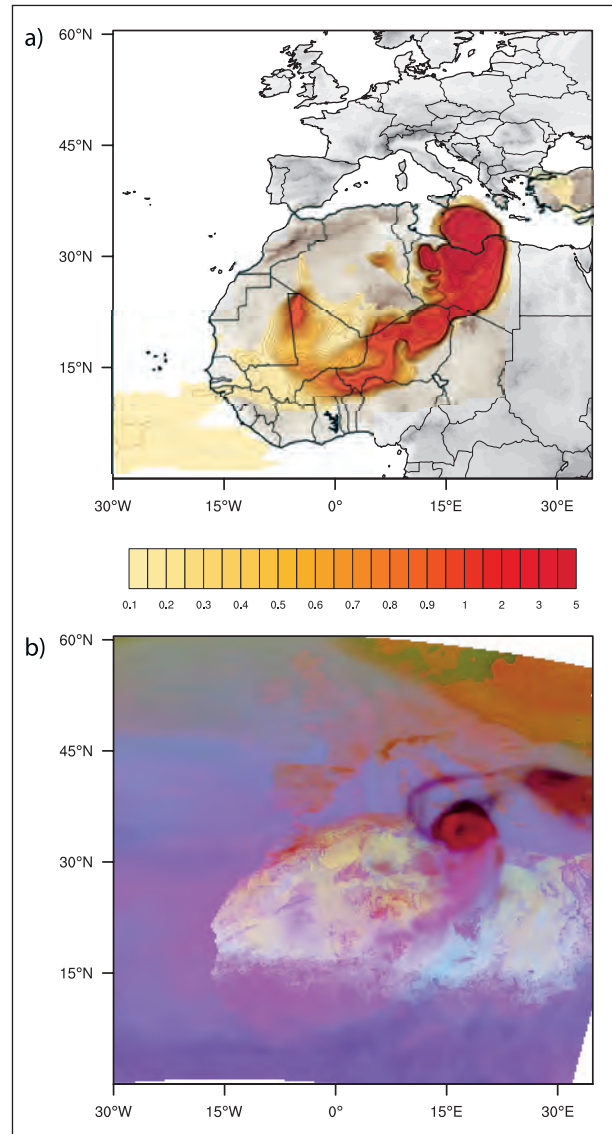


Fig. 2: (a) Dust optical thickness simulated with the COSMO-MUSCAT model for 23 February 2007, 03 UTC. Infra-red dust index as designed for MSG-SEVIRI brightness temperatures shown here for COSMO-MUSCAT radiances. Radiances are calculated from atmospheric fields and dust concentration distributions simulated by COSMO-MUSCAT for the same scene shown in (a). Airborne dust is indicated by pinkish color.

2007, the difference between the two years is less pronounced in the model (Fig. 1).

In both years the agreement between modeled and observed dust emission events is very good for the Bodélé region (Chad), the most active dust source worldwide, where almost all modeled dust emission events occur on days when a LLJ developed. Mismatches are evident in the Sudan and the central Saharan mountain region. LLJs develop in the model but do not always lead to dust emissions. Nevertheless, increased LLJ occurrence in 2008 compared to 2007 (Fig. 1) corroborates the importance of this phenomenon for the higher DSA

observations in 2008. The reason for the lack of modeled dust mobilization following the development of nocturnal LLJs in mountainous regions may be due to too weakly developed LLJs or insufficient turbulent mixing of momentum towards the surface during the breakdown of the LLJs in the morning hours in the COSMO model.

In contrast to the mismatch in modeled and observed DSA, the quantitative comparison of simulated dust optical thicknesses with sunphotometer observations at Aerosol Robotic Network (AERONET) stations shows good agreement for both years [Tegen *et al.*, 2013], indicating that the number of observed dust activation events is only of limited use for estimating actual dust emission fluxes in the Sahara. To clarify the role of different meteorological features for dust emissions, a quantitative comparison of the model results and the IR dust index would be needed. To directly compare model results to

satellite observations, radiative transfer models such as RTTOV can be used as an interface. Radiances at those wavelengths that are measured by satellite sensors are calculated from COSMO-MUSCAT simulations of atmospheric conditions and dust 3D dust concentrations. Radiances are converted into brightness temperatures, and used to compile the SEVIRI-like IR dust index. This approach allows for characterizing uncertainties in atmospheric conditions like humidity that are known uncertainty factors for interpreting IR dust retrievals. A model-based comparison between atmospheric dust optical thickness and simulated IR dust index is shown in Fig. 2. Substantial differences are found between quantitative dust loading (Fig. 2a) and intuitive understanding of dust concentration from the IR dust index (color intensity, (Fig. 2b)), which emphasizes the demand for quantifying the uncertainty of satellite dust retrievals.

## References

- Heinold, B., I. Tegen, M. Esselborn, K. Kandler, P. Knippertz, D. Müller, A. Schladitz, M. Tesche, B. Weinzierl, A. Ansmann, D. Althausen, B. Laurent, A. Massling, T. Müller, A. Petzold, K. Schepanski, and A. Wiedensohler (2009), Regional Saharan dust modelling during the SAMUM 2006 campaign, *Tellus B*, 61, 307-324.
- Knippertz, P., and M. C. Todd (2012), Mineral dust aerosols over the Sahara: Meteorological controls on emission and transport and implications for modeling, *Rev. Geophys.*, 50, doi: 10.1029/2011RG000362.
- Laurent, B., I. Tegen, B. Heinold, K. Schepanski, B. Weinzierl, and M. Esselborn (2010), A model study of Saharan dust emissions and distributions during the SAMUM-1 campaign, *J. Geophys. Res.*, 115, D21210, doi:10.1029/2009JD012995.
- Schepanski, K., I. Tegen, and A. Macke (2012), Comparison of satellite based observations of Saharan dust source areas, *Rem. Sens. Environ.*, 123, 90-97, doi:10.1016/j.rse.2012.03.019.
- Schepanski, K., I. Tegen, M. C. Todd, B. Heinold, G. Bönisch, B. Laurent, and A. Macke (2009), Meteorological processes forcing Saharan dust emission inferred from MSG-SEVIRI observations of subdaily dust source activation and numerical models, *J. Geophys. Res.*, 114(D10), D10201, doi:10.1029/2008JD010325.
- Schepanski, K., I. Tegen, B. Laurent, B. Heinold, and A. Macke (2007), A new Saharan dust source activation frequency map derived from MSG-SEVIRI IR-channels, *Geophys. Res. Lett.*, 34, L11803, doi:10.1029/2007GL030168.
- Tegen, I., K. Schepanski, and B. Heinold (2013), Comparing two years of Saharan dust source activation obtained by regional modelling and satellite observations, *Atmos. Chem. Phys.*, 13, 2381–2390, doi:10.5194/acp-13-2381-2013.

## Cooperation

Deutscher Wetterdienst (DWD), Offenbach, Germany

# Probing the atmospheric boundary layer aerosol using an unmanned aerial vehicle (UAV)

Birgit Wehner<sup>1</sup>, Markus Hermann<sup>1</sup>, Ralf Käthner<sup>1</sup>, Barbara Altstädtter<sup>2</sup>, Andreas Scholtz<sup>2</sup>, Astrid Lampert<sup>2</sup>, Andreas Platis<sup>3</sup>, Norman Wildmann<sup>3</sup>, Jens Bange<sup>3</sup>, and Alfred Wiedensohler<sup>1</sup>

<sup>1</sup> Leibniz Institute for Tropospheric Research, Leipzig, Germany

<sup>2</sup> Institute of Aerospace Systems, Technical University of Braunschweig, Braunschweig, Germany

<sup>3</sup> University of Tübingen, Center for Applied Geophysics, Tübingen, Germany

**Um bodengebundene in-situ Aerosolmessungen zu erweitern und diese an vertikale Fernerkundungsmethoden anzubinden, stellen unbemannte Fluggeräte (< 25 kg) eine vielversprechende Möglichkeit dar. Deshalb wurde in den letzten zwei Jahren am TROPOS eine kleine und leichte Aerosolnutzlast (< 2.5 kg) entwickelt und diese im Rahmen einer Feldkampagne zur Untersuchung des Grenzschichtaerosols in Melpitz das erste Mal geflogen.**

## Introduction

Besides numerous ground-based measurements only limited in situ aerosol data from higher altitudes taken by airborne instrumentation is available. These data showed a number of interesting phenomena, such as new particle formation often induced by clouds or turbulence. One approach to realize airborne measurements with low logistical effort compared to manned aircraft measurements is the application of unmanned aerial vehicles (UAV) for atmospheric studies. The new UAV Carolo-P360 "ALADINA", developed by the Technical University of Braunschweig, equipped with aerosol instrumentation, provides a unique and flexible tool for characterizing the vertical and horizontal variability of the boundary layer aerosol. ALADINA, with a wingspan of 3.6 m, is designed to carry up to 3 kg of payload in the front compartment. With electrical propulsion, it has an endurance of about 40 minutes. The cruising speed is about 25 m/s and the maximum ceiling is about 1 km.

## Instrumentation

For aerosol measurements, ALADINA was equipped by TROPOS with a set of light-weight aerosol instruments. To reach the weight limit of 3 kg for the total payload, commercially available instruments were chosen and modified with respect to space, weight, power consumption, and detection

properties. Two Condensation Particle Counters, CPCs, (model 3007, TSI Inc.) with different lower threshold diameters are used to measure the total particle number concentration. The difference between the readings of both CPCs is used as indicator for new particle formation. To reduce weight, the housing, internal batteries, and the display of the CPCs were removed. In order to investigate the connection between the aerosol particle concentration and atmospheric turbulence, the CPCs should be fast. Therefore the aerosol volume flow of the CPCs was increased from originally 0.1 l/min to 0.16 l/min. The response time of the new set-up was checked with a three-way-valve and ambient and filtered air, respectively. Figure 1a shows that the response time of the new set-up is surprisingly fast compared to the original instrument with < 1.3 s for the  $t_{10\%-90\%}$  time.

The larger flow through the CPC, however, leads to a smaller supersaturation in the condenser and thus to larger lower threshold diameters compared to the original instrument (10 nm vs. 18.4 nm, see Fig. 1b). This could be partly compensated by applying higher temperature differences inside one of the CPCs (11.3 nm). Nevertheless, there has to be made a compromise between the lower threshold diameter and the response time.

Particles larger 0.3  $\mu\text{m}$  are measured using an Optical Particle Counter, OPC (GT-526, Met One). This OPC counts particles in 6 size bins from 0.3 to 10.0  $\mu\text{m}$ . Again, housing, battery, and display were

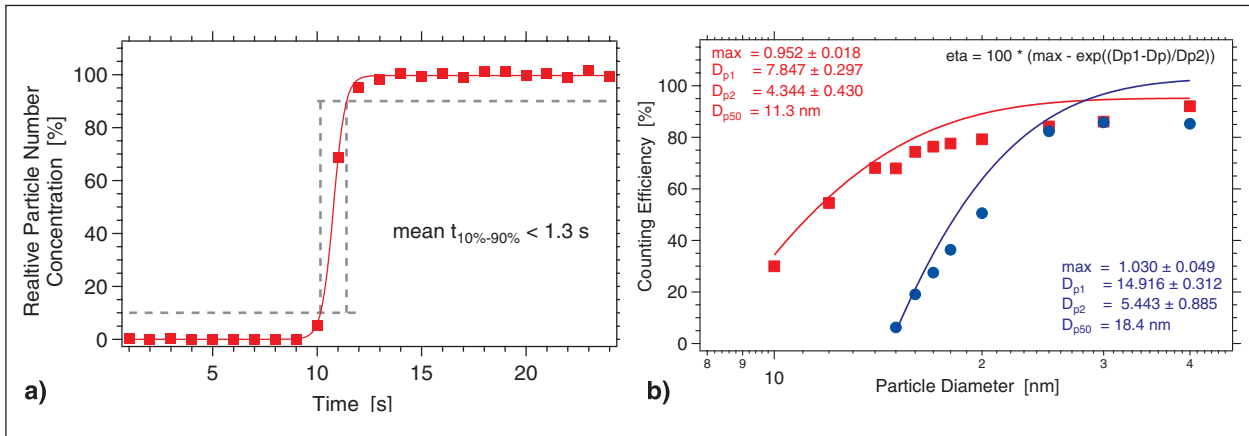


Fig. 1: Characteristics of the miniaturized CPCs (a) response time (b) counting efficiencies.

removed. As inlet system a 3/16" stainless steel tube is used with rounded inlet lips, but no shroud, in order to minimize weight.

The central data acquisition and meteorological payload for ALADINA was developed by the University of Tübingen. The meteorological sensor package includes a five-hole probe, IMU/ GPS, two temperature sensors (LTK001 thermocouple cold junction compensator and matched amplifier; fine wire platinum resistance thermometer), and a humidity sensor (P14 Rapid). The data acquisition system offers the possibility of real-time data transfer by a telemetry downlink. Due to this, it is possible to identify layers of enhanced aerosol concentration and temperature inversions during the flight and modify the flight mission accordingly. Electrical power for all measurement instruments are provided by a common rechargeable battery (7.4 V). Figure 2 shows the

aerosol and meteorological sensors mounted in the sensor compartment of ALADINA.

### First Application

ALADINA was flight tested for proper instrument operation while airborne in fall 2013. A measurement campaign took place at the Melpitz observatory on 8 and 9 October 2013. In total three measurement flights of ALADINA were performed accompanied by parallel flights of the UAV "MASC", which is equipped with turbulence measurement instrumentation.

Figure 3 shows vertical profiles of selected parameters measured with ALADINA on October 9: number concentrations from both CPCs (CPC1, CPC2), number concentrations from two OPC channels (OPC1: 390 - 590 nm, OPC2: 590 – 840 nm), potential temperature ( $\Theta$ ), and water vapour mixing

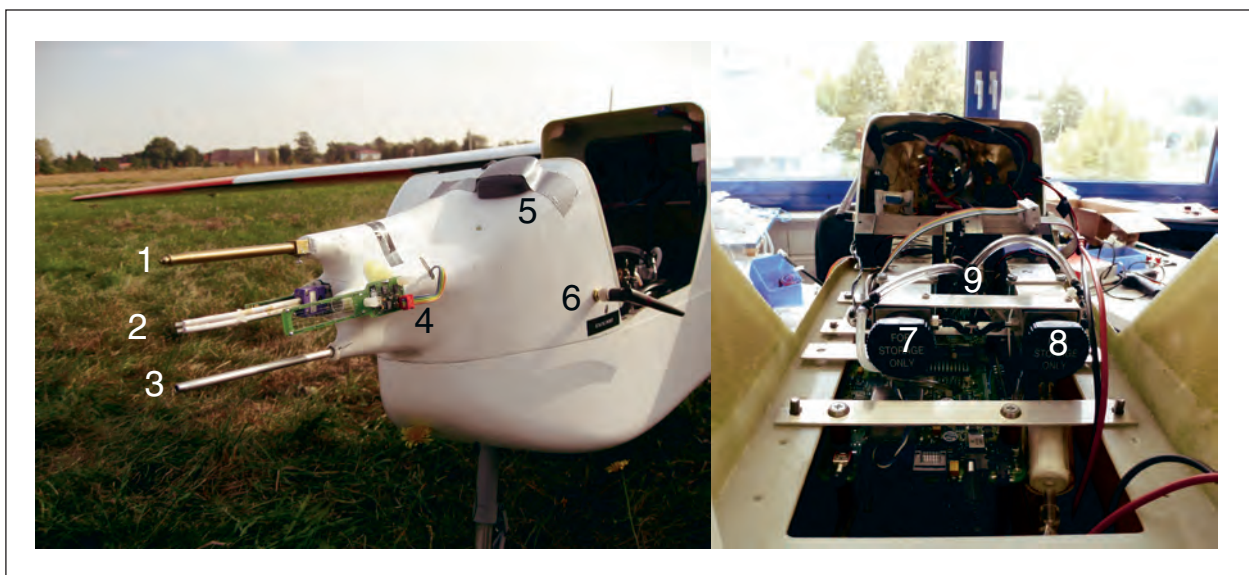
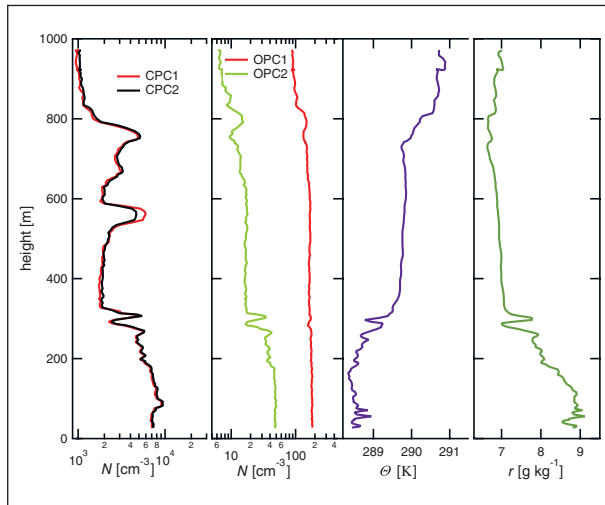


Fig. 2: ALADINA payload: (left - Photo: TU Braunschweig) 1 five-hole probe, 2 temperature and humidity sensor, 3 aerosol inlet, 4 fast temperature sensor, 5 GPS antenna, 6 telemetry antenna (right - Photo: TROPOS) 7 CPC1 , 8 CPC2, and 9 OPC.



*Fig. 3:* Vertical profiles of selected parameters measured on October 9, 2013 during a measurement flight between 8:30 and 9:00 UTC. Presented parameters: Number concentrations of the two CPCs (CPC1 and CPC2), two channels from the OPC (OPC1 and OPC2), potential temperature ( $\Theta$ ), and water vapour mixing ratio ( $r$ ).

ratio ( $r$ ). Both CPCs show a similar behaviour, thus the number concentration between 11 and 18 nm ( $N_{11-18}$ ) is negligible and no new particle formation occurs. A well-mixed layer has been developed up to a height of about 300 m topped by an inversion.

Between 350 and 700 m a neutrally stratified layer follows with constant  $\Theta$  and OPC number concentrations. Only number concentrations measured by both CPCs show an isolated maximum at 550 m, i.e. this is caused by particles < 390 nm with also a significant fraction in  $N_{11-18}$ .

## Conclusions and Outlook

The new UAV ALADINA equipped with aerosol instrumentation is suitable to measure particle number concentrations and meteorological parameters in the boundary layer with low logistical effort compared to other airborne platforms. Due to the different lower cut-offs of the CPCs, layers with increased concentrations of freshly formed particles can be detected. Thus, following campaigns will be conducted to probe the boundary layer frequently to detect isolated aerosol layers and regions where new particle formation occurs.

---

### Funding

German Research Foundation (DFG), Bonn, Germany

---

### Cooperation

Technical University of Braunschweig, Germany

University of Tübingen, Germany

# On the effectiveness of Low Emission Zones: Decrease in ambient black carbon and particle number concentrations in Leipzig

Wolfram Birmili<sup>1</sup>, Fabian Rasch<sup>1</sup>, Kay Weinhold<sup>1</sup>, Stephan Nordmann<sup>1</sup>, André Sonntag<sup>1</sup>, Gerald Spindler<sup>1</sup>, Hartmut Herrmann<sup>1</sup>, Gunter Löschau<sup>2</sup>, Alfred Wiedensohler<sup>1</sup>,

<sup>1</sup> Leibniz Institute for Tropospheric Research, Leipzig, Germany

<sup>2</sup> Saxon State Office for Environment, Agriculture and Geology (LfULG), Dresden, Germany

In Leipzig trat am 1.3.2011 erstmals in Deutschland eine Umweltzone direkt mit der höchsten Regulierungsstufe 3 (grüne Plakette) in Kraft. TROPOS Leipzig und das LfULG Sachsen begleiten mit spezialisierten Aerosolmessungen die Auswirkungen dieser Umweltzone. Trendanalysen von 2009-2013 legen nahe, dass die Einführung der Umweltzone zu einer signifikanten Abnahme der Rußmassenkonzentration (*black carbon*) und der Zahl ultrafeiner Partikel (Durchmesserbereich 50-100 nm) in der Außenluft an Straßen geführt hat. Nach dem derzeitigen Stand der Auswertung ist dies in erster Linie eine Auswirkung abnehmender Verkehrsichten im Gebiet der Umweltzone. Bei der PM<sub>10</sub>-Massenkonzentration konnte hingegen keine signifikante Abnahme registriert werden. Ursache hierfür ist, dass die PM<sub>10</sub>-Konzentration nur gering durch die Maßnahmen der Umweltzone beeinflusst werden kann, und eher von den klimatischen Bedingungen während eines bestimmten Jahres abhängt. Diese Studie kommt zum Schluss, dass die Umweltzone für die Reduzierung der gesundheitlich als hochrelevant eingestuften Teilmengen des Aerosols (Ruß, ultrafeine Partikel) einen deutlichen Nutzen bringen kann, selbst wenn dies bei der Betrachtung der gesetzlich relevanten Metrik PM<sub>10</sub> nicht erkennbar ist.

The city of Leipzig established a low emission zone (LEZ) on March 1, 2011, being the first LEZ in Germany where the highest regulation level 3 was introduced immediately. TROPOS Leipzig and the Saxon State Office for Environment, Agriculture and Geology implemented measurements of ambient black carbon (BC) mass concentrations and particle number size distributions at five monitoring sites (Fig. 1). First trend analyses suggest a decrease in BC and particle number concentration (diameter 50-100 nm) in the vicinity of roads as a result of the LEZ. This decrease seems to be first, an effect of decreasing traffic volumes in the area of the LEZ and only second, an effect of reductions in the vehicles' exhaust emission factors. For PM<sub>10</sub> mass concentrations, however, no decrease could be observed. The prime reason is that the measures undertaken in the LEZ affect total particle mass concentrations only to a minor relative extent. This study concludes that the LEZ can be very effective in reducing the ambient



Fig. 1: Map of the limits of the Leipzig Low Emission Zone, indicating the approximate location of atmospheric monitoring stations for black carbon and particle number size distributions. (Illustration: Stadt Leipzig)

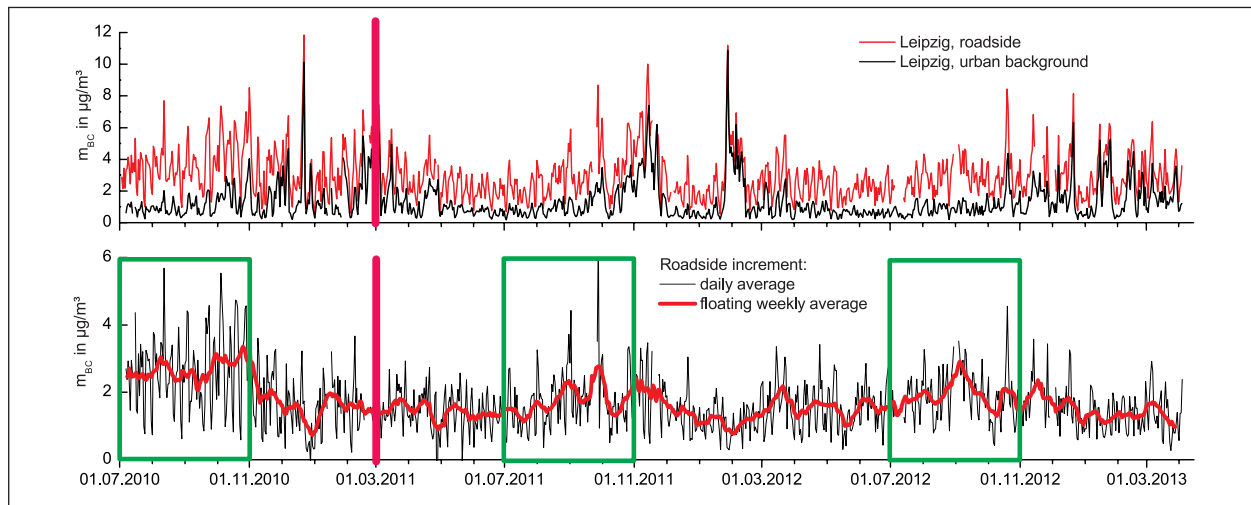


Fig. 2: Black carbon mass concentrations  $m_{BC}$  in Leipzig, 2010-2013. "Roadside" refers to the measurement station Leipzig-Mitte, "urban background" to measurements at Leipzig-West and Leipzig-TROPOS. The upper graph shows measured concentrations, the lower graph the roadside increment. The red line marks the commencement of the Leipzig Low Emission Zone. Green rectangles indicate the periods used for trend analysis in Tab. 1.

concentrations of health-related particulate matter parameters BC and particle number, even if the beneficial effects are not evident from the legal parameter  $PM_{10}$  mass concentration.

## Methods

Ambient black carbon (BC) mass concentrations are measured using Multi Angle Absorption Photometry (MAAP). Particle number size distributions are measured using Twin Differential Mobility Particle Sizers (TDMPS) or Twin Scanning Mobility Particle Sizers (TSMPS). All instruments are nominally identical, and warrant a high degree of inter-comparability [Wiedensohler et al., 2012].

These parameters have been recorded continuously at five observation sites in and around the city of Leipzig: Leipzig-Mitte (roadside, ca. 48 000 veh/day), Leipzig-Eisenbahnstrasse (roadside, ca. 12 000 veh/day), Leipzig-West (urban background), Leipzig-TROPOS (urban background), and Melpitz (regional background), which cover a wide range of exposure situations. For details of these measurement sites, see the first technical report on the Leipzig Low Emission Zone [Löschau et al., 2012], or the web site of the German Ultrafine Aerosol network [TROPOS, 2013].

## Results

Figure 2 illustrates the change of BC mass concentrations in Leipzig during 2010-2013. The upper graph shows the daily average values, which represent a rather noisy signal. Several particulate matter

episodes can be seen, during which concentrations are high both, at roadside and in the background. The lower graph focuses on the roadside increment (roadside measurement – urban background measurement). It is an essential result that around the commencement of the Low Emission Zone (red line), a decrease in measured BC can be seen. After the commencement of the LEZ the daily BC values will only rarely reach  $3 \mu\text{g}/\text{m}^3$  again. A similar trend could also be observed for the roadside measurement site Leipzig-Eisenbahnstrasse (not shown). Table 1 compiles the most relevant observation trends, with annual averages calculated for the time window July–October in each year. At Leipzig-Mitte, the decrease in BC from 2010 to 2011 is about  $0.9 \mu\text{g}/\text{m}^3$ , i.e. roughly a third of the absolute value. Particle number concentration (50-100 nm) dropped by a similar value. Traffic counts in the vicinity of Leipzig-Mitte suggest a decrease in heavy duty traffic as a result of the regulations induced by the LEZ. In stark contrast, no decrease could be seen in  $PM_{10}$  mass concentrations. The main reason is that  $PM_{10}$  is influenced by many particle sources, and local traffic exhaust particles makes only a minor contribution to its absolute value. Roadside black carbon, in contrast, has a much higher concentration gradient between roadside and urban background. Generally, there is struggle to verify the effectiveness of Low Emission Zones in Germany on the basis of  $PM_{10}$  measurements alone [Morfeld et al., 2013]. This study illustrates, however, that the effectiveness of the LEZ can be verified with much greater confidence if traffic-specific PM parameters, such as black carbon and particle number concentration are monitored.

Tab. 1: Geometric mean values and standard error of Black Carbon, particle number ( $N_{[50;100]}$ ) and particle mass ( $PM_{10}$ ), 2009-2012, for the period July-October. Für Leipzig-Mitte and Leipzig-Eisenbahnstrasse, we also indicate the traffic increment separately.

<b>Black carbon</b>											
	Leipzig-Mitte		Leipzig-Eiba		Leipzig-West		Leipzig-Tropos		Melpitz	Leipzig-Mitte Incr.	Leipzig-Eiba Incr.
period	$\mu_{geo}$	$\sigma_\mu$	$\mu_{geo}$	$\sigma_\mu$	$\mu_{geo}$	$\sigma_\mu$	$\mu_{geo}$	$\sigma_\mu$	$\mu_{geo}$	$\sigma_\mu$	$\mu_{geo}$
1.7-31.10.2009	-	-	2.47	(0.16)	-	-	1.04	(0.07)	0.56	(0.05)	-
1.7-31.10.2010	3.48	(0.13)	2.12	(0.08)	0.97	(0.06)	-	-	0.57	(0.04)	2.41
1.7-31.10.2011	2.56	(0.13)	1.77	(0.10)	0.91	(0.07)	0.93	(0.07)	0.48	(0.05)	1.55
1.7-31.10.2012	2.70	(0.11)	1.70	(0.08)	0.81	(0.06)	0.83	(0.05)	0.49	(0.03)	1.75
<b><math>N_{[50;100 \text{ nm}]}</math></b>											
	Leipzig-Mitte		Leipzig-Eiba		Leipzig-West		Leipzig-Tropos		Melpitz	Leipzig-Mitte Incr.	Leipzig-Eiba Incr.
period	$\mu_{geo}$	$\sigma_\mu$	$\mu_{geo}$	$\sigma_\mu$	$\mu_{geo}$	$\sigma_\mu$	$\mu_{geo}$	$\sigma_\mu$	$\mu_{geo}$	$\sigma_\mu$	$\mu_{geo}$
1.7-31.10.2009	-	-	3140	(130)	-	-	1730	(80)	1290	(60)	-
1.7-31.10.2010	3630	(130)	2790	(90)	1520	(60)	-	-	1240	(70)	1580
1.7-31.10.2011	2870	(130)	2180	(110)	1480	(80)	1500	(90)	1050	(70)	1270
1.7-31.10.2012	2970	(100)	2700	(120)	1430	(70)	1550	(80)	1300	(60)	1350
<b><math>PM_{10}</math></b>											
	Leipzig-Mitte				Leipzig-West				Melpitz	Leipzig-Mitte Incr.	Leipzig-Eiba Incr.
period	$\mu_{geo}$	$\sigma_\mu$			$\mu_{geo}$	$\sigma_\mu$			$\mu_{geo}$	$\sigma_\mu$	$\mu_{geo}$
1.7-31.10.2009	27.0	(1.3)			19.2	(1.1)			16.8	(0.8)	7.77
1.7-31.10.2010	26.2	(1.4)			14.6	(0.7)			17.8	(0.6)	11.60
1.7-31.10.2011	28.1	(1.4)			13.8	(0.7)			18.2	(0.6)	14.33
1.7-31.10.2012	26.6	(1.2)			13.5	(0.6)			18.5	(0.6)	13.12

<sup>a</sup> using Leipzig-West as a background

<sup>b</sup> using Melpitz as a background

## References

- Löschau, G., A. Wiedensohler, W. Birmili, et al. (2012), The Leipzig Low Emission Zone, part 1: initial state (Umweltzone Leipzig, Teil 1: Ausgangsbeurteilung), Landesamt für Umwelt, Landwirtschaft und Geologie, 83 pp., download: <https://publikationen.sachsen.de/bdb/artikel/14411>.
- Morfeld, P., R. Stern, P. Builtjes et al. (2013), Einrichtung einer Umweltzone und ihre Wirksamkeit auf die PM10-Feinstaubkonzentration – eine Pilotanalyse am Beispiel München, *Zbl. Arbeitsmed.*, 63, 104–115.
- Rasch, F., W. Birmili, K. Weinhold et al. (2013), Significant reduction of ambient black carbon and particle number in Leipzig as a result of the low emission zone (Signifikante Minderung von Ruß und Anzahl ultrafeiner Partikel in Außenluft als Folge der Umweltzone in Leipzig), *Gefahrst. Reinh. Luft*, 73(11/12), 483-489.
- TROPOS (2013), Description of the German Ultrafine Aerosol Network (GUAN) <http://wiki.tropos.de/index.php/GUAN>
- Wiedensohler, A., W. Birmili, A. Nowak et al. (2012), Mobility particle size spectrometers: harmonization of technical standards and data structure to facilitate high quality long-term observations of atmospheric particle number size distributions, *Atmos. Meas. Tech.*, 5, 2012.

## Funding

The Saxon State Office for Environment, Agriculture and Geology (LfULG), Dresden, Germany  
The Mayor of Leipzig, Environmental Office

## Cooperation

German Federal Environment Ministry (BMU) grants F&E 370343200 and F&E 371143232

# Influence of the traffic on the particle mass concentration of equivalent black carbon and the particle number size distribution in La Paz, Bolivia

Alfred Wiedensohler<sup>1</sup>, Kay Weinhold, M. Andrade<sup>2</sup>, F. Velarde<sup>2</sup>, I. Moreno<sup>2</sup>, and F. Avila<sup>2</sup>

<sup>1</sup> Leibniz Institute for Tropospheric Research, Leipzig, Germany

<sup>2</sup> Laboratory for Atmospheric Physics, Department of Physics, University Mayor de San Andres, La Paz, Bolivia

**Das Leibniz Institut für Troposphärenforschung und die Universität „Mayor de San Andres“; La Paz, Bolivien, haben gemeinsam eine Intensiv-Messkampagne im Zentrum von La Paz (16°30'13.83"S; 68° 7'45.56"W; 3580 m a.s.l.) durchgeführt. Ziel war es den Einfluss der verkehrsbedingten Emissionen auf Eigenschaften des urbanen Aerosols zu untersuchen. Partikelanzahl-Größenverteilungen wurden mit einem Mobilitäts-Partikelgrößenspektrometer gemessen während Partikel-Massenkonzentrationen von äquivalentem schwarzen Kohlenstoff mittels eines Mehrwinkel-Absorptionsphotometers (MAAP) bestimmt wurden. Meteorologische Parameter sowie Kohlenmonoxid-Konzentrationen wurden zusätzlich ermittelt. Die Instrumente wurden am Planetarium der Universität „Mayor de San Andres“ betrieben. Das Gebäude befindet sich in der Nähe einer Straße mit Personenwagen- und Lastkraftwagen-Verkehr. Da La Paz sich in einem Tal befindet, das sich von ca. 3200 bis 4000 a.s.l. erstreckt, fahren Personenwagen und Lastkraftwagen bergauf unter erhöhter Last. Während der Messperiode gab uns der Tag der nationalen Volkszählung einen einmaligen Datensatz Tage mit Verkehr mit einem Tag ohne Verkehr zu vergleichen. Am Tag der Volkszählung mussten Einwohner zu Hause bleiben.**

## Introduction

The Leibniz Institute for Tropospheric Research and the University Mayor de San Andres, La Paz, Bolivia, carried out an intensive measurement campaign in centre of La Paz (16°30'13.83"S; 68° 7'45.56"W; 3580 m a.s.l.). The goal was to investigate the influence of traffic emissions on properties of the urban aerosol. Particle number size distributions have been measured using a Mobility Particle Size Spectrometer, whereas the particle mass concentration of equivalent black carbon (eBC) was determined using a Multi Angle Absorption Photometer (MAAP). Meteorological parameters as well as carbon monoxide concentration were collected. The instruments were set up at the Planetarium of University Mayor de San Andres. The building is located beside a road with light and heavy traffic. Since La Paz is located in a valley reaching from approximately 3200 to 4000 m a.s.l., cars and trucks are operated on a high load when driving uphill.

During the intensive measuring time period, the national day of census provided a unique data set, comparing days with traffic and one day without traffic. At the national day of census, all people have to stay home.

## Results

La Paz and El Alto (located at approximately 4000 m a.s.l.) are two of the major cities in the region. There are no other larger settlements in the surrounding. During November 21, 2012, the whole traffic was banned because of a national day of census in both cities, giving us the opportunity to study the influence of the traffic on the black carbon particle mass concentration, the particle number size distribution as well as the carbon monoxide gas concentration.

As seen from Fig. 1, on November 21, 2012, the carbon monoxide gas concentration dropped to a value near Zero ppm from around 2 ppm, during

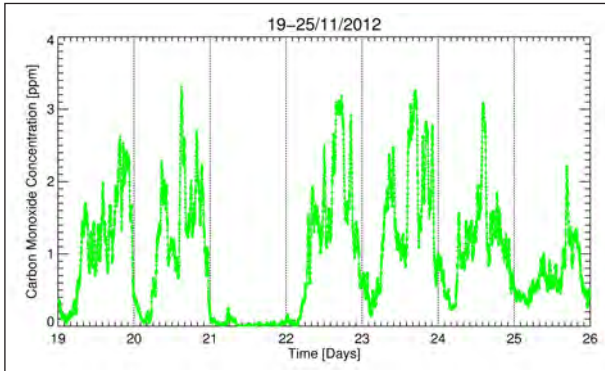


Fig. 1: Time series of carbon monoxide during the week November 19 to 25, 2012.

workdays November 19-20 and 22-23, 2012. This indicates that due to the traffic ban, almost all sources of incomplete combustion have been switched-off.

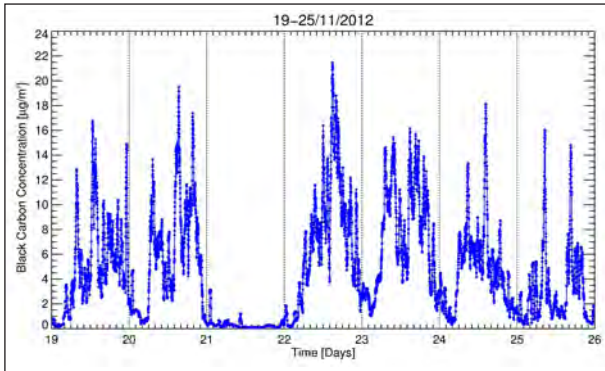


Fig. 2: Time series of equivalent black carbon concentration during the week November 19 to 25, 2012.

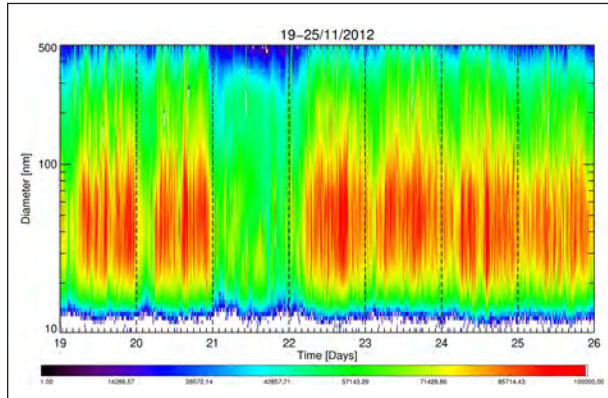


Fig. 3: Time series of the particle number size distribution during week November 19 to 25, 2012.

Figure 2 illustrates the same behaviour for the BC particle mass concentration, meaning that BC was almost exclusively produced by the traffic. During regular working days, peaks of BC particle mass concentration have been around  $15 \mu\text{g}/\text{m}^3$ , whereas on November 21, 2012, the values were clearly below  $1 \mu\text{g}/\text{m}^3$ .

In Fig. 3, a contour plot of the particle number size distribution of the week November 19 to 25, 2012 is shown. The red colour illustrates high, whereas green and blues describe low particle number concentrations. Again, on November 21, the concentrations dropped drastically, demonstrating that the major fraction of aerosol particles in the city of La Paz is produced by traffic.

# Investigation of nucleation, dynamic growth and surface properties of single ice crystals

Jens Voigtländer<sup>1</sup>, Henner Bielick<sup>1</sup>, Tina Clauss<sup>1</sup>, Paul Herenz<sup>1</sup>, Dennis Niedermeier<sup>1</sup>, Cédric Chou<sup>2</sup>, Zbigniew J. Ulanowski<sup>2</sup>, Frank Stratmann<sup>1</sup>

<sup>1</sup> Leibniz Institute for Tropospheric Research, Leipzig, Germany

<sup>2</sup> Science & Technology Research Institute, University of Hertfordshire, UK

Zur Untersuchung der Einflüsse thermodynamischer Zustandsänderungen auf die optischen (Streu-)Eigenschaften von Eiskristalloberflächen werden am TROPOS in Kooperation mit der Universität Hertfordshire an einem laminaren Strömungsrohr experimentelle Untersuchungen zum Eiskristallwachstums an stationären Einzelkristallen durchgeführt. Ein optischer Eispartikelzählers [SID-3 Instrument, Kaye et al., 2008] und ein optisches Mikroskop liefern zeitaufgelöste Informationen über die Größe, Form und Oberflächeneigenschaften des Eiskristalls. Die Untersuchungen haben gezeigt, dass sowohl Eiskristallform als auch Oberflächeneigenschaften vom verwendeten Eiskeim abhängig sind, und dass sich die optischen Streueigenschaften des Eiskristalls (Oberflächenrauhigkeit) in Abhängigkeit seiner Wachstumsrate verändern.

## Introduction

Nucleation and growth of atmospheric ice particles are of importance for both, weather and climate. However, knowledge is still sparse, e.g. when considering the influences of ice particle surface properties on the radiative properties of clouds. Therefore, in collaboration with the University of Hertfordshire (UK), and supported by the European Union (EU) research project EUROCHAMP-2 (funded within the 7<sup>th</sup> Framework Program, Section “Support for Research Infrastructures – Integrated Infrastructure Initiative”), we developed a new device to characterize nucleation, dynamic growth and optical light scattering properties of a fixed single ice crystal in dependence on both, the type of the ice nucleus (IN) and the prevailing, precisely controlled thermodynamic conditions.

## Experiments

A schematic diagram of the experimental set up is shown in Fig. 1. The instrument is based on our experiences with the laminar flow tube chamber LACIS [Leipzig Aerosol Cloud Interaction Simulator, Stratmann et al., 2004; Hartmann et al., 2011]. Connected to the flow tube is a Small Ice Detector

[SID-3-type, Kaye et al., 2008]. This instrument, called LISA (Leipzig Ice Scattering Apparatus), has been additionally equipped with an optical microscope. A single IN with a dry size of 2-10 micrometer is attached to a thin glass fibre and positioned within the optical measuring volume of LISA. The fixed particle is exposed to the thermodynamically precisely controlled air flow, exiting the flow tube. Two mass flow controllers adjusting a dry and a humidified gas

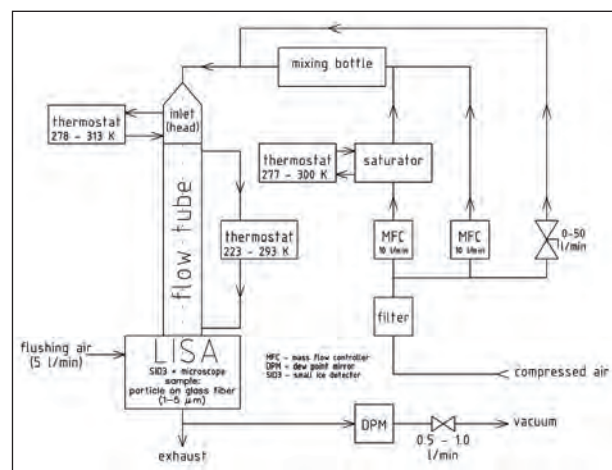


Fig. 1: Schematic diagram of the experimental set up.

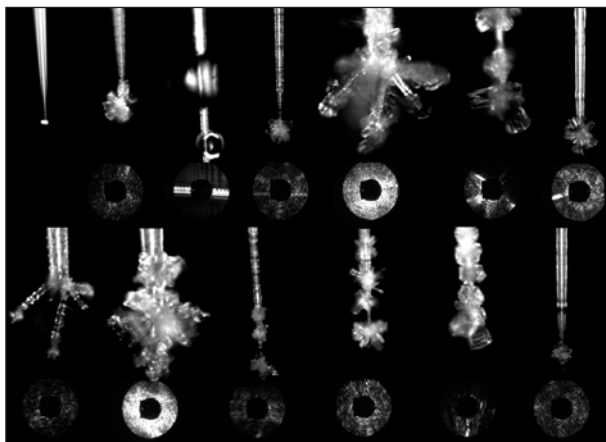


Fig. 2: Randomly selected 2D light scattering patterns and microscope images of different experiments.

flow are applied to control both, the temperature and the saturation ratio on a short time scale (<5 s). Dependent on both properties, ice nucleation and ice particle growth/shrinkage occur and can be studied. Thereby, the LISA instrument is applied to obtain 2D light scattering patterns, and the additional optical microscope allows a time dependent visualization of the particle/droplet/ice crystal (Fig. 2). Both devices together allow to investigate the influence of thermodynamic conditions on ice particle growth, the particle shape and its surface properties [Ulanowski et al., 2012; Ulanowski et al., 2013].

## Results

**Thermodynamical characterization of the experimental set up.** The thermodynamic conditions in the experiments are characterized using a) computational fluid dynamics (CFD) calculations, b)

temperature and dew-point measurements, and c) evaluation of droplet and ice particle growth data. Computational fluid dynamics simulations have been done with the commercial available CFD code Fluent (Ansys Inc., Canonsburg, PA, USA) to design the experiments and to define possible boundary conditions. The simulation results were compared to the results of the temperature and dew point measurements. Both data sets were in good agreement and show that the thermodynamic conditions in the measuring volume can be controlled over a wide range and varied on a short time scale (<5 s). However, for low wall temperatures below about -20°C the conditions are changing with time because of ice formation at the tube wall. Therefore, the optical microscope, which allows a continuous time dependent observation of the droplet/ice particle growth, is additionally used to characterize the thermodynamics during the experiments.

**Ice crystal growth experiments.** In first measurement campaigns we could show the feasibility of the set up to investigate droplet activation, as well as ice particle nucleation and growth. We successfully performed condensation freezing and deposition nucleation experiments considering ATD (Arizona Test Dust), kaolinite, illite and Snomax™ (Johnson Controls Snow, Colorado, USA) particles as IN. In the experiments we could prove that different temperatures and saturation ratios result in different growth rates and ice crystal shapes, but also in different surface properties (Fig. 2). Exemplarily, Fig. 3 shows the time dependent evolution of ice particle size and relative surface roughness (0 – smooth, 1 – rough) determined from the LISA data. In general, comparing simple ice particles (like single columns) with complex crystals (such as dendrites), the surface roughness is larger for the latter ones. Furthermore we found that, regarding one single ice crystal, the surface roughness can be modified by varying the prevailing saturation ratio. Thereby, the surface roughness tends to increase for growing, and to decrease for shrinking ice particles. We could also prove that these findings are independent of the absolute particle size (Fig. 3).

## Conclusions

A device to investigate nucleation, dynamic growth and light scattering properties of a fixed ice crystal in dependence on the prevailing thermodynamic conditions was developed and successfully applied in first measurements. The optical surface properties of an ice crystal were found to be dependent on both, the type of the IN and the growth rate of the ice particle.

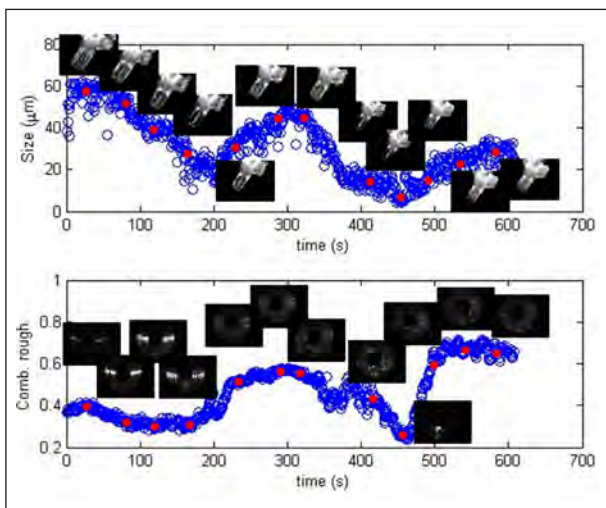


Fig. 3: Example of the time dependent evolution of ice particle size and surface roughness (0 – smooth, 1 – rough).

---

## References

- Hartmann, S., D. Niedermeier, J. Voigtlander, T. Clauss, R. A. Shaw, H. Wex, A. Kiselev, and F. Stratmann (2011), Homogeneous and heterogeneous ice nucleation at LACIS: Operating principle and theoretical studies, *Atmos. Chem. Phys.*, 11, 1753-1767, doi:10.5194/acp-11-1753-2011.
- Kaye, P., E. Hierst, R. S. Greenaway, Z. Ulanowski, E. Hesse, P. J. DeMott, C. Saunders, and P. Conolly (2008), Classifying atmospheric ice crystals by spatial light scattering, *Opt. Lett.*, 33(13), 1545-1547, doi:10.1364/OL.33.001545.
- Stratmann, F., A. Kiselev, S. Wurzler, M. Wendisch, J. Heintzenberg, R. J. Charlson, K. Diehl, H. Wex, and S. Schmidt (2004), Laboratory studies and numerical simulations of cloud droplet formation under realistic super-saturation conditions, *J. Atmos. Ocean. Tech.*, 21(6), 876 - 887.
- Ulanowski, Z., E. Hirst, P. H. Kaye, and R. S. Greenaway (2012), Retrieving the size of particles with rough surfaces from 2D scattering patterns, *J. Quant. Spectr. Rad. Trans.*, 113(18), 2457-2464, doi:10.1016/j.jqsrt.2012.06.019.
- Ulanowski, Z., P. H. Kaye, E. Hirst, R. S. Greenaway, R. J. Cotton, E. Hesse, and C. T. Collier (2013), Incidence of rough and irregular atmospheric ice particles from Small Ice Detector 3 measurements, *Atmos. Chem. Phys. Discuss.*, 13, 24975-25012, doi:10.5194/acpd-13-24975-2013.

---

## Funding

The project is financially supported by the European Union (EU) research project EUROCHAMP-2, funded within the 7<sup>th</sup> Framework Program, Section “Support for Research Infrastructures – Integrated Infrastructure Initiative”

---

## Cooperation

Science & Technology Research Institute, University of Hertfordshire, UK

# Variability of CCN number concentration and particle activation properties at the central European regional background site Melpitz, Germany

Silvia Henning, Verena Brock, Wolfram Birmili, Laurent Poulain, Achim Grüner, Alfred Wiedensohler, Frank Stratmann

An der TROPOS Forschungsstation in Melpitz wurde an Hand des ersten kontinuierlichen CCN Datensatzes über ein Jahr das Aktivierungsverhalten atmosphärischer Aerosolpartikel untersucht. Insbesondere betrachtet wurden dabei die Hygroskopizität der Partikel, die CCN-Gesamtanzahlkonzentration und der Mischungszustand der Partikel. Der Hygroskopizitätsparameter  $\kappa$  wies einen Jahressgang mit höchsten Werten in den Wintermonaten ( $0.37 \pm 0.05$  im März 2013 bei 0.3% Übersättigung) und den niedrigsten Werten in den Sommer- bzw. Frühjahrsmonaten ( $0.22 \pm 0.04$  im Juni 2013 bei 0.3% Übersättigung) auf. Zusätzlich wurde ein Tagesgang von  $\kappa$  festgestellt - mit höchsten Werte gegen Mittag - der im Sommer stärker als im Winter ausgeprägt ist und durch den Tagesgang der einzelnen chemischen Verbindungen erklärt werden kann.

One of the important factors influencing cloud properties and thereby the earth's radiation budget is the availability of Cloud Condensation Nuclei (CCN). However, long-term data sets are rare, which are taken at regionally representative sites. The European Aerosols, Clouds, and Trace gases Research InfraStructure Network (ACTRIS) aims at integrating European ground-based stations equipped with advanced atmospheric probing instrumentation for aerosols, clouds, and short-lived gas-phase species. Within this network, standardised long-term observations of CCN number concentrations [Gysel *et al.*, 2013] and particle activation properties were launched in August 2012 at the TROPOS field station Melpitz, Germany. Aerosol and CCN properties measured at this site are regionally representative for central Europe.

CCN size spectra are measured between 25 and 300 nm at 5 different supersaturation (SS) levels (0.1, 0.2, 0.3, 0.5, 0.7%). Therefore, the CCN counter (DMT-100, Boulder, USA) was operated downstream of a Vienna-Type Differential Mobility Analyzer (DMA). The calibration and also the setup

of the monodisperse CCN measurements follow the recommendations of the ACTRIS Standard Operation Procedure (SOP) for CCN measurements. In addition to the CCN data, particle number size distribution measurements, a wide variety of chemical gas and particle measurements as well as standard meteorological parameters are available on a continuous basis at the Melpitz station.

Presently, we analysed CCN data for the first year of continuous measurements in the time period August 2012 to August 2013. The CN and CCN spectra were corrected for multiple charges and the size-dependent activation fraction (AF) was calculated dividing CCN by particle number concentration. This was done for all SS levels. By fitting the resulting AF at certain SS with the sigmoid error function, the 50% activation diameter could be derived ( $D_{p50}$ ). For given SS and  $D_{p50}$ , the corresponding  $\kappa$ -value (hygroscopicity parameter) was calculated as given by Petters and Kreidenweis [2007]. The annual mean value of  $\kappa$  was found to be  $0.29 \pm 0.08$  for 0.2% SS and  $0.27 \pm 0.08$  for 0.3% SS, which compares well to the  $\kappa$ -value recommended by others for continental

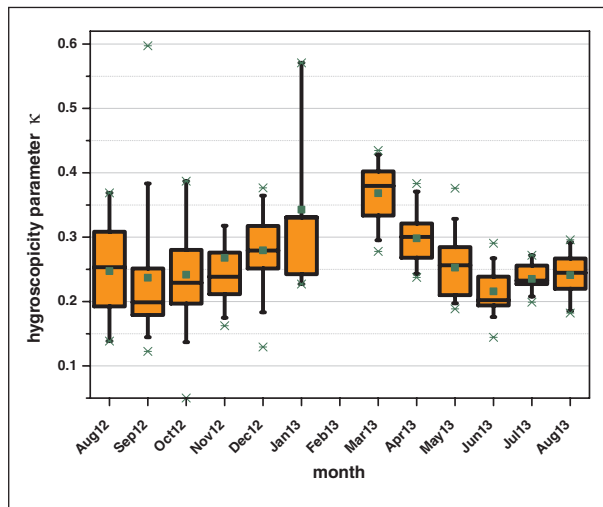


*Fig. 1:* Boxplot of the hygroscopicity parameter  $\kappa$ ; box gives median, 25 and 75% percentile, whiskers stand for 5% and 95% percentile. Stars give 1 and 99% percentile and the filled squares give the mean value of  $\kappa$ . The presented statistic analysis is done for monthly  $\kappa$ -values measured at a supersaturation of 0.3%.

aerosol [Pringle et al., 2010; Wex et al., 2010]. In this first year of data,  $\kappa$  exhibited an annual cycle (Fig. 1), with lowest values in summer ( $\kappa(0.3\%) = 0.22 \pm 0.04$ ) and highest values in winter ( $\kappa(0.3\%) = 0.37 \pm 0.05$ ). A daily cycle was observed for the summer data, with low  $\kappa$ -values (around 0.2) during the night hours and a maximum around noon and seems to follow thereby the daily cycle of solar radiation. In winter, this daily cycle in the  $\kappa$ -value was less pronounced (Fig. 2).

The total particle number concentration ranged between almost  $10000 \text{ cm}^{-3}$  (Aug '12) and

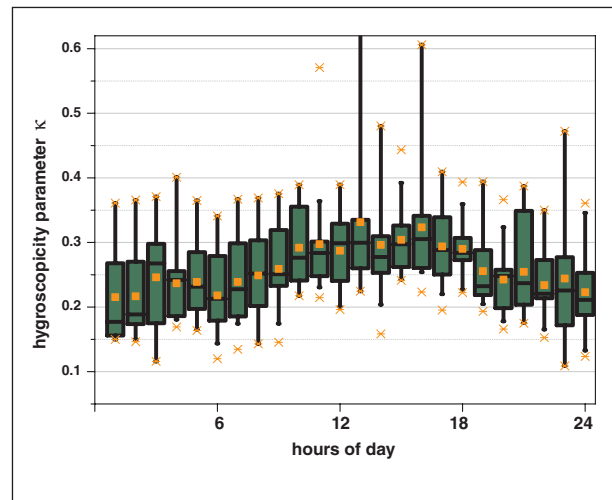


*Fig. 2:* Diurnal variation of the hygroscopicity parameter  $\kappa$ . Presented are hourly averages at a supersaturation of 0.3% from August '12 to August '13; box gives median, 25 and 75% percentile, whiskers stand for 5% and 95% percentile. Stars give 1 and 99% percentile and the filled squares give the mean value of  $\kappa$ .

$4000 \text{ cm}^{-3}$  (Jan '13). The total CCN number concentration was found to peak in March with about  $3000 \text{ cm}^{-3}$  (SS = 0.3 %) and thereby correlating well with the maximum in the accumulation mode particle number concentration ( $D_p > 100 \text{ nm}$ ). A cluster analysis concerning the dominating air masses showed that in the period with highest values in CCN number concentrations, the site was mainly influenced by air masses from central continental regions. As during this period also very low temperatures were observed it is likely that this is connected to the heating period.

## References

- Gysel, M., and F. Stratmann (2013), WP3 -- NA3: In-situ chemical, physical and optical properties of aerosols, Deliverable D3.11: Standardized protocol for CCN measurements. <http://www.actris.net/Publications/ACTRISQualityStandards/tabcid/11271/language/en-GB/Default.aspx>
- Petters, M.D. and S.M. Kreidenweis (2007), A single parameter representation of hygroscopic growth and cloud condensation nucleus activity, *Atmos. Chem. Phys.*, 7, 1961-1971.
- Pringle, K.J., H. Tost, A. Pozzer, U. Pöschl, and J. Lelieveld (2010), Global distribution of the effective aerosol hygroscopicity parameter for CCN activation, *Atmos. Chem. Phys.*, 10, 5241–5255, doi:10.5194/acp-9-4131-2009.
- Wex, H., McFiggans, G., Henning, S., and F. Stratmann (2010): Influence of the external mixing state of atmospheric aerosol on derived CCN number concentrations, *Geophys. Res. Lett.*, 37, L10805, doi:10.1029/2010GL043 337.

## Cooperation

ACTRIS - Consortium

# Dual-field-of-view Raman lidar measurements: Investigation of aerosol-cloud interactions

Jörg Schmidt, Johannes Bühl, Albert Ansmann, Ulla Wandinger

Eine neue Lidartechnik wurde am TROPOS entwickelt. Mit Hilfe von Ramanlidar-Messungen unter Nutzung zweier Gesichtsfelder können Profile von Wolkeneigenschaften (z.B. Tröpfchengröße, Tröpfchenanzahlkonzentration) bestimmt werden. Diese Methode wurde gemeinsam mit konventionellen Lidartechniken genutzt, um Aerosol-Wolken-Wechselwirkungen zu untersuchen. Dabei korrelierten Aerosol- und Wolkeneigenschaften bei kleinen Wolkeneindringtiefen sowie während Aufwinden am stärksten.

## Introduction

From the various interactions between aerosol particles and clouds, the Twomey effect is one of the most important interactions, due to its high significance for Earth's radiative budget and thus climate science [Forster *et al.*, 2007]. This effect describes that aerosol particles act as cloud condensation nuclei (CCN) and thereby increase the cloud droplet number concentration (CDNC), which leads to a brightening of the cloud and a cooling of the Earth [Twomey, 1977]. Despite of its importance, the Twomey effect is not well understood [Forster *et al.*, 2007, Stocker *et al.*, 2013]. At TROPOS, the new, unique dual-field-of-view (dual-FOV) Raman lidar technique was developed, which is described and presented here. It permits detailed ground-based remote-sensing measurements of cloud properties and thus investigations of aerosol-cloud interactions. Here, the most recent results of these studies are presented.

## Instrumentation

**Raman lidar MARTHA – aerosol measurements.** The Multiwavelength Atmospheric Raman lidar for Temperature, Humidity, and Aerosol profiling (MARTHA) has been used for ground-based remote sensing of aerosol properties at TROPOS since 1997. From the lidar measurements, high-quality profile

information of numerous aerosol properties, e.g., aerosol particle extinction coefficient, can be derived.

**Raman lidar MARTHA – cloud measurements.** The dual-FOV Raman lidar technique was implemented in the Raman lidar MARTHA [Schmidt *et al.*, 2013]. This upgrade allows the determination of profiles of cloud microphysical properties. From the measurements the cloud extinction coefficient and cloud droplet effective radius are derived, which are used to calculate the liquid-water content and the CDNC. An important feature of this technique is the detection of Raman-scattered light, which makes this technique more simple and robust compared to similar lidar approaches.

Through this upgrade, MARTHA is capable of measuring profiles of aerosol and cloud properties simultaneously, which provides optimum conditions for investigations of aerosol-cloud interactions.

**Doppler lidar WiLi – vertical wind velocity measurements.** The vertical wind velocity has a strong influence on aerosol-cloud interactions [Schmidt *et al.*, 2014] and thus should be considered for investigations of aerosol-cloud interactions. TROPOS runs the Doppler wind lidar WiLi, which is capable of deriving the vertical wind velocity at the base of probed clouds. WiLi was located within a distance of 10 m of MARTHA. Hence, both instruments probed the same volume.

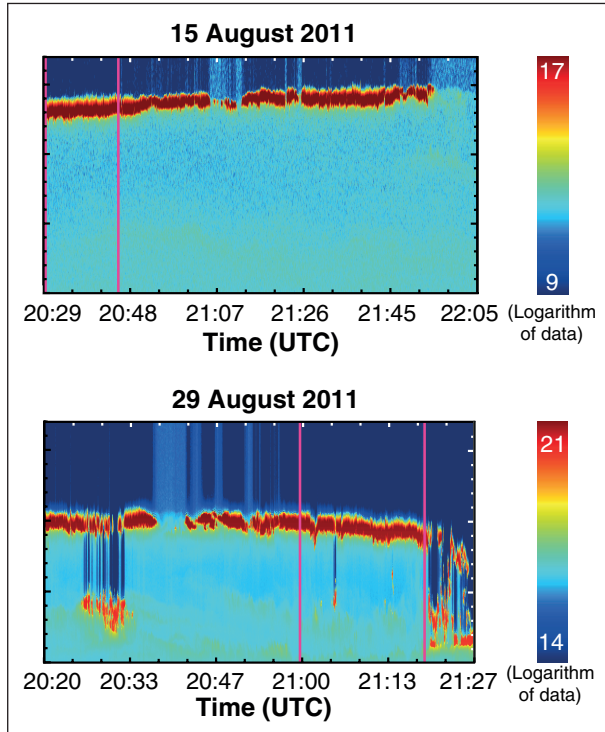


Fig. 1: Time-height cross section for measurements on 15 and 29 August 2011. Clouds are shown in red color. The time periods used for the cloud analyses are indicated by pink lines.

## Results

**Case study.** Figure 1 shows the time-height cross sections of two dual-FOV Raman lidar measurements from 15 and 29 August 2011. The measurements were supported with Doppler wind lidar probings. The cloud analyses were done for homogeneous cloud regions, which are highlighted with pink lines in Fig. 1, as well as for updraft time periods within these regions. The derived aerosol particle extinction coefficients as well as CDNCs are presented in Fig. 2.

The correlation between the aerosol extinction and CDNC is quantified with  $ACI_N$  values, introduced by McComiskey [2009]. Generally,  $ACI_N$  values are in the range between 0 and 1, with larger values indicating stronger aerosol-cloud interactions. For the corresponding calculation, the aerosol extinction coefficient was averaged in the height range from

Tab. 1:  $ACI_N$  values for the case study using the measurements on 15 and 29 August 2011.

	Updraft	Complete Cloud
Cloud Base	0.55	0.71
Vertical Mean	0.32	-0.07

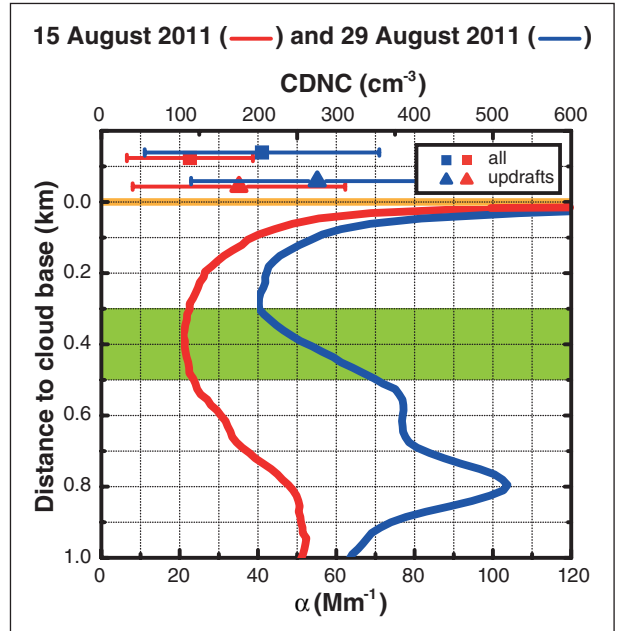


Fig. 2: Aerosol particle extinction coefficient below the clouds measured on 15 and 29 August 2011 and the corresponding CDNCs derived at cloud base for updraft regions as well as the complete cloud probing. The cloud base height is shown in orange color. The measurement in which a higher aerosol load is measured yields higher CDNC in accordance with predictions of the Twomey effect.

300 to 500 m below cloud base, which is highlighted in Fig. 2.  $ACI_N$  values were calculated for CDNCs obtained directly at cloud base as well as their vertical averages, during updraft time periods as well as during the complete highlighted cloud probing period.

Table 1 presents the derived results. For a quantitative analysis, a comprehensive dataset of measurements has to be used, because there are numerous other influencing factors for cloud properties besides the aerosol (e.g., turbulence and entrainment). As this study comprises only two measurements it merely suits as a demonstration of the capabilities of dual-FOV Raman lidar measurements. However, reasonable results are obtained as, e.g., the stronger correlation between aerosol load and cloud properties at cloud base, where aerosol particles are mixed into the cloud. The  $ACI_N$  derived at cloud base match the results of corresponding ground-based remote-sensing studies as well as airborne in-situ measurements [Painemal and Zuidema, 2013, McComiskey et al., 2009, Lu et al., 2008].

**Statistical analysis.** The  $ACI_N$  approach, followed in the previous section, was applied to a dataset of 29 dual-FOV Raman lidar measurements. Figure 3 shows the CDNCs derived 30 – 70 m above cloud base (without consideration of the vertical wind velocity) versus the aerosol particle extinction coefficient below the cloud. Despite the multitude of

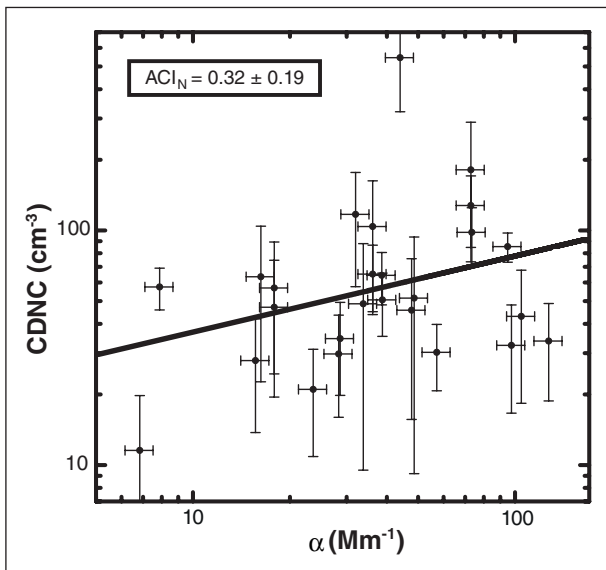


Fig. 3: CDNC (30 to 70 m above cloud base) versus aerosol particle coefficient below cloud base without consideration of the vertical wind velocity. The scattered dataset shows a tendency for the CDNC to increase with increasing aerosol load. This effect is quantified with  $ACI_N = 0.32 \pm 0.19$ .

cloud-influencing processes, which lead to a relatively scattered plot, the trend that CDNC increases with aerosol load below the cloud becomes clear.

Figure 4 summarizes  $ACI_N$  values obtained for several cloud penetration depths with and without consideration of the vertical wind velocity. Stronger aerosol-cloud relationships are found in updraft regions where cloud properties are stronger influenced from the intake of aerosol. Furthermore,

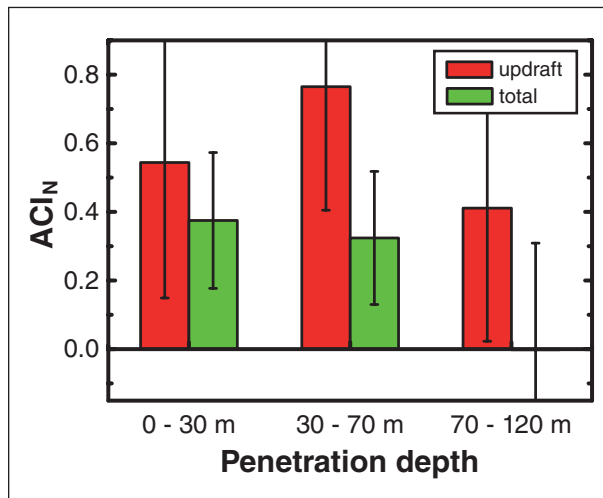


Fig. 4: Magnitude of aerosol-cloud interactions, quantified with  $ACI_N$  values for different height levels within the clouds. Analyses of updraft regions are shown in green color, whereas results of studies ignoring the vertical wind information are shown in red. Aerosol and cloud properties show the strongest correlation for low penetration depths and in updraft regions.

stronger aerosol-cloud correlations are found for lower penetration depths.

### Conclusions.

The new and unique dual-FOV Raman lidar technique, developed at TROPOS, proved to be an appropriate and valuable approach for the investigation of aerosol-cloud interactions. A clear effect of aerosol particles on cloud particles was derived.

## References

- Forster, P. et al. (2007), Changes in atmospheric constituents and in radiative forcing, in *Climate Change 2007 - The Physical Science Basis. Contribution of Working Group I to the Fourth Assessment Report of the Intergovernmental Panel on Climate Change*, pp. 129 – 234.
- Lu, M.-L., G. Feingold, H. H. Jonsson, P. Y. Chuang, H. Gates, R. C. Flagan, and J. H. Seinfeld (2008), Aerosol-cloud relationships in continental shallow cumulus, *J. Geophys. Res.*, 113, D15, doi:10.1029/2007JD009354.
- McComiskey et al. (2009), An assessment of aerosol-cloud interactions in marine stratus clouds based on surface remote sensing, *J. Geophys. Res.*, 114, D9, doi:10.1029/2008JD011006.
- Painemal, D., and P. Zuidema (2013), The first aerosol indirect effect quantified through airborne remote sensing during vocals-rex, *Atmos. Chem. Phys.*, 13, doi:10.5194/acp-13-917-2013.
- Schmidt, J., U. Wandinger, and A. Malinka (2013), Dual-field-of-view raman lidar measurements for the retrieval of cloud microphysical properties, *Appl. Opt.*, 52, 2235 – 2247.
- Schmidt, J., A. Ansmann, J. Bühl, H. Baars, U. Wandinger, and A. Malinka (2014), Dual-field-of-view raman lidar measurements of aerosol-cloud-dynamics interaction: case studies, submitted to *J. Geophys. Res.*
- Stocker, T.F., (2013), Summary for Policymakers. in *Climate Change 2013: The Physical Science Basis. Contribution of Working Group I to the Fifth Assessment Report of the Intergovernmental Panel on Climate Change*.
- Twomey, S. (1977), Influence of pollution on shortwave albedo of clouds, *J. Atmos. Sc.*, 34, pp. 1149 – 1152.

## Cooperation

B. I. Stepanov Institute of Physics, National Academy of Sciences of Belarus, Minsk

# SÆMS: Long-term monitoring of relative-humidity dependence of ambient particle extinction coefficient in the urban atmosphere

Annett Skupin, Albert Ansmann

Seit 2009 werden am TROPOS in Leipzig kontinuierliche Messungen des spektralen Partikelextinktionskoeffizienten der unbeeinflussten atmosphärischen Partikel mit dem SÆMS (Spectral Aerosol Extinction Monitoring System) durchgeführt. Diese Messungen werden genutzt, um die Änderung der optischen Eigenschaften der Partikel in Abhängigkeit der relativen Luftfeuchte zu untersuchen. Es werden Wachstumsfaktoren des Partikelextinktionskoeffizienten berechnet, die das Verhältnis der Partikelextinktionskoeffizienten bei einer relativen Feuchte von 95% zu 40% beschreiben. Diese werden hinsichtlich der Luftmassenanströmrichtung ausgewertet. Aus den feuchteabhängigen Partikelextinktionskoeffizienten wird eine Parametrisierung erarbeitet, die Berechnungen des Wachstumsfaktors ermöglicht.

## Introduction

Optical and microphysical properties of atmospheric particles show a strong dependency on relative humidity. We have performed continuous observations of the spectral extinction coefficient at ambient humidity conditions since 2009. We have characterized the optical properties at very high relative humidities and have developed a parameterization of the relationship between relative humidity and optical properties for the range from about 30% to nearly 100% relative humidity.

## Instrumentation and Methodology

The principle of the SÆMS is presented in *Skupin et al. [2013]*. Particle extinction coefficients  $b_e(\lambda)$  in the wavelength range of  $\lambda = 300\text{--}1000\text{ nm}$  were measured on a horizontal light path (5.68 km length) 30–50 m above ground at TROPOS. The reference path has a length of 600 m. Retroreflector arrays are mounted at towers at the end of each measurement path. Relative-humidity and temperature sensors are installed at the towers. Since the start of the continuous measurements we obtained a large data set of particle extinction coefficients and related relative-humidity values .

## Results

In Fig. 1 we present the particle extinction coefficient for the period 2009–2012 at a wavelength of 550 nm as a function of relative humidity. On top of the approximately 15000 data points the mean extinction coefficient for 10%-ranges of relative humidity and the standard deviation are shown. There is a tendency for larger particle extinction coefficients at higher

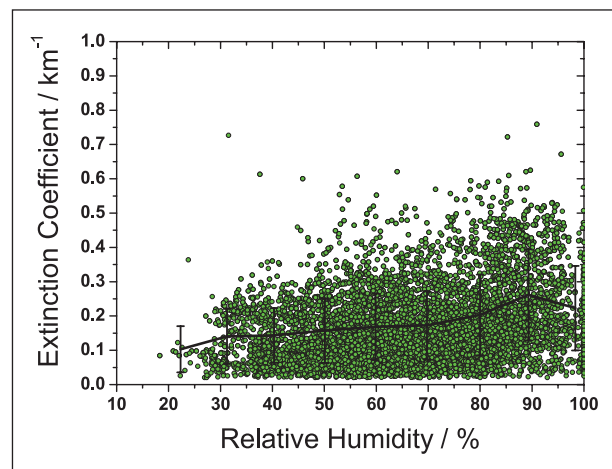


*Fig. 1: Particle extinction coefficient at 550 nm measured with SÆMS as a function of relative humidity. Summary of the measurement period from 2009 to 2012.*

humidity up to 90%. Furthermore, we have calculated the enhancement factor:

$$b_{f_1, f_2} = \frac{b_e(f_2)}{b_e(f_1)},$$

which describes the increase of the particle extinction coefficient for a defined humidity  $f_2$  with respect to the value for nearly dry conditions ( $f_1 \geq 40\%$ ). We calculate the enhancement factor for 95%/40% relative humidity. By means of a HYSPLIT analysis [Draxler and Rolph, 2011] all results are evaluated in accordance to their air mass origin and classified in 8 sectors. The result is shown in Fig. 2 for the period of 2009–2012. With values of  $3.81 \pm 0.88$  enhancement factors are largest for aerosols originating from sector 1, which may contain maritime and Arctic aerosol. Relatively large enhancement factors are also observed for sectors 5, 7, and 8, which may contain maritime aerosol components.

The parameterization of the enhancement factor [Hänel, 1984; Hänel and Mieghem, 1976] with

$$b_{f_1, f_2} = (1 - f)^{-\gamma}$$

could be performed for suitable measurements for which a rapid change of the ambient relative humidity occurred during a period of 1–2 h. For all air-mass

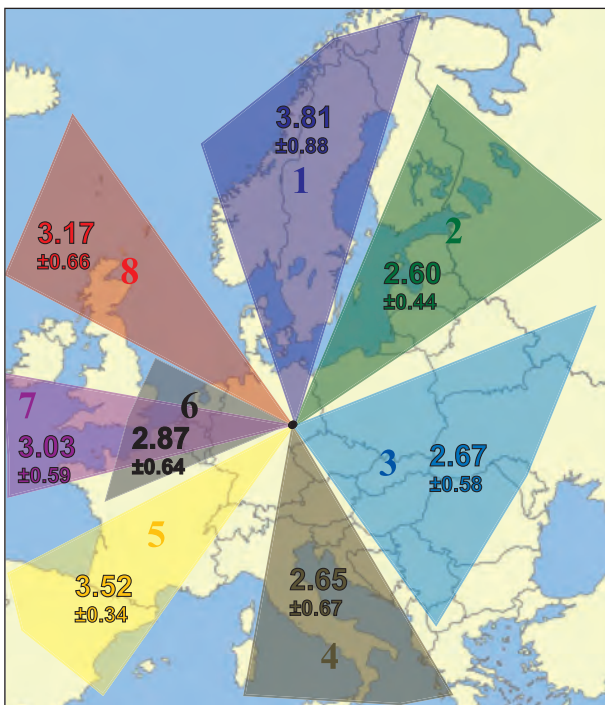


Fig. 2: Calculated extinction enhancement factor for 40%–95% relative humidity as a function of the air mass origin of 2009–2012.

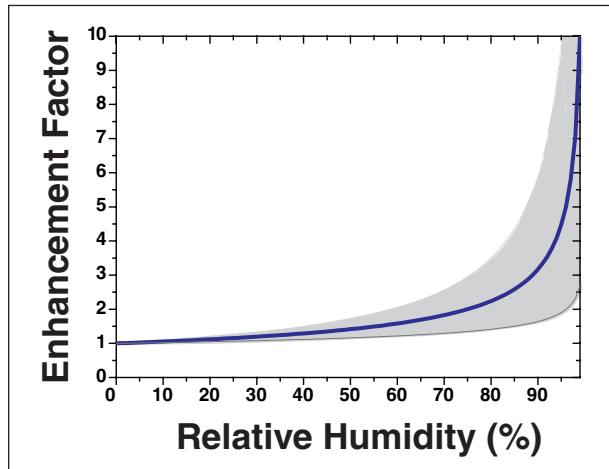


Fig. 3: Parameterization of the extinction enhancement factor on the basis of measurements between 2009 and 2012.

origins (all aerosol types) a mean parameter of  $\gamma = 0.46 \pm 0.21$  was determined. This result is schematically shown in Fig. 3. These parameterizations have been provided for all 8 sectors with the result of larger  $\gamma$  for sector 1 in comparison to the other sectors.

## Conclusions

The calculation of the extinction enhancement factors on the basis of long-term measurements can be performed with the SÆMS under ambient conditions and with direct optical measurements for the first time. Larger enhancement factors for air masses which contain maritime or Arctic aerosol were found. With the help of our measurements we are now able to parameterize the particle extinction coefficient as a function of ambient relative humidity for the aerosol at the TROPOS site, to give a prognosis on visibility, and also to complete our lidar measurements with surface optical data (in order to apportion the total aerosol optical depth to the entire tropospheric profile).

---

## References

- Draxler, R. R., and G. D. Rolph (2011), HYSPLIT (HYbrid Single-Particle Lagrangian Integrated Trajectory) Model access via NOAA ARL READY Website (<http://ready.arl.noaa.gov/HYSPLIT.php>) edited, NOAA Air Resources Laboratory, Silver Spring, MD.
- Hänel, G. (1984), Parametrization of the Influence of Relative Humidity on Optical Aerosol Properties *A. Deepak, Hampton, Virginia* 117-122.
- Hänel, G., and H. E. L. a. J. V. Mieghem (1976), The Properties of Atmospheric Aerosol Particles as Functions of the Relative Humidity at Thermodynamic Equilibrium with the Surrounding Moist Air, in *Adv. Geophys.*, edited, pp. 73-188, Elsevier.
- Skupin, A., A. Ansmann, R. Engelmann, and H. Baars (2013), Spectral Aerosol Extinction Monitoring System (SÆMS): setup, observational products, and comparisons, *Atmos. Meas. Tech. Discuss.*, 6(5), 8647-8677, doi: 10.5194/amtd-6-8647-2013.

---

## Cooperation

German Research Foundation (DFG), Bonn, Germany

# ACTRIS: Aerosols, Clouds, and Trace Gases Research Infrastructure Network

Ulla Wandinger, Alfred Wiedensohler, Gerald Spindler, Patric Seifert, Holger Baars, Thomas Kanitz, Albert Ansmann, Anja Schwarz, Ronny Engelmann, Jörg Schmidt, Johannes Bühl, Dietrich Althausen, Birgit Heese, Kay Weinhold, André Sonntag, Maik Merkel, Wolfram Birmili, Thomas Müller, Thomas Tuch, Laurent Poulain, Hartmut Herrmann

**ACTRIS ist ein europäisches Forschungsinfrastrukturprojekt, dessen Ziel die Integration hochentwickelter, bodengebundener Messnetze für die In-situ- und Fernmessung von Aerosolen, Wolken und reaktiven Gasen ist. Mit ACTRIS soll eine nachhaltige, langfristige europäische Forschungsinfrastruktur aufgebaut werden, mit der qualitätsgesicherte Langzeitdaten zu Klimaänderungen, Luftqualität und Transport von Schadstoffen auf regionaler und kontinentaler Skala gewonnen werden können. ACTRIS entwickelt dafür Standards für die Qualitätssicherung, fördert die Entwicklung und Anwendung neuer Methoden, realisiert den freien Zugang zu den gewonnenen Daten und unterstützt internationale Kooperationen durch transnationalen Zugang zu modernsten Beobachtungsstationen. Dieser Beitrag gibt einen Überblick über die Aktivitäten von TROPOS in ACTRIS.**

## Goals and Structure

ACTRIS aims at the development of a sustainable European research infrastructure for providing long-term quality-assured observational data relevant to climate and air-quality research. It integrates sophisticated ground-based networks equipped with in-situ and remote-sensing instrumentation for the observation of aerosols, clouds, and short-lived trace gases. ACTRIS develops quality-assurance standards, promotes the development and application of new methods and technologies, supports transnational access to large infrastructures, and provides open access to high-quality information and services. ACTRIS builds on three previously developed research infrastructures: the European Supersites for Atmospheric Aerosol Research EUSAAR, the European Aerosol Research Lidar Network EARLINET, and the cloud-observing network CLOUDNET. A new trace-gas network component is implemented into the single coordinated framework as well. The work is organized in 22 work packages covering coordination, network, service, and joint research activities as well as transnational access (Fig. 1). A brief overview on the TROPOS contributions to ACTRIS is presented in the following.

## Aerosol and Trace-Gas In-Situ Observations

ACTRIS Network Activity WP3 is co-ordinated by TROPOS and deals with in-situ chemical, physical,

and optical properties of aerosol particles. The network comprises about 30 measurement stations distributed over Europe. Observables are the particle number size distribution, particle light scattering and absorption coefficients, organic and elemental carbon, organic tracers, as well as concentrations of cloud condensation nuclei. Activities include the implementation of existing standards at new stations and the development of new measurement protocols. A major

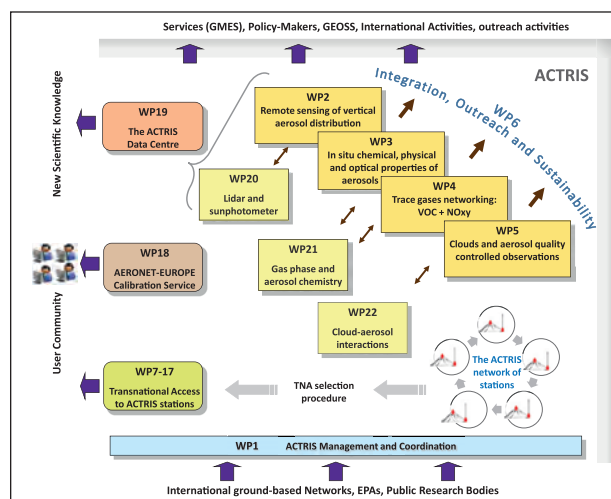


Fig. 1: Structure of ACTRIS in the currently funded project of the 7th Framework Programme. Work packages 2-6 comprise Networking Activities. Work packages 20-21 represent Joint Research Activities. Work packages 7-19 are dedicated to Transnational Access and Service Activities (source: <http://www.actris.net>).

task of TROPOS within WP3 is the intercomparison and calibration of the ACTRIS mobility particle size spectrometers, including their condensation particle counters, for which the facilities of the World Calibration Center for Aerosol Physics (WCCAP) are used. TROPOS is also responsible for the intercomparison of ACTRIS integrating nephelometers and absorption photometers and the development of a standardized reference method for multi-wavelength particle light absorption measurements. Figure 2 shows an example of the intercomparison workshop in March 2013. Here, the particle light absorption coefficient determined by a PSAP (Particle Soot Absorption Photometer) is compared to values measured with the reference method (extinction minus scattering).

Network Activity WP4 is dedicated to the development of a new trace-gas network with focus on volatile organic carbon and nitrogen oxides. In 2012, TROPOS has started measurements of  $\text{NO}_2$  with a monitor based on a blue light converter at the research station Melpitz. The Joint Research Activity WP21 is focused on the implementation of comprehensive gas-phase and aerosol chemistry. In this context, thermal-optical analysis of OC/EC was initiated at TROPOS.

### Ground-Based Remote Sensing of Aerosols and Clouds

ACTRIS WP2 is dedicated to remote sensing of the vertical aerosol distribution and covers all activities of EARLINET with its 27 European stations. Tasks

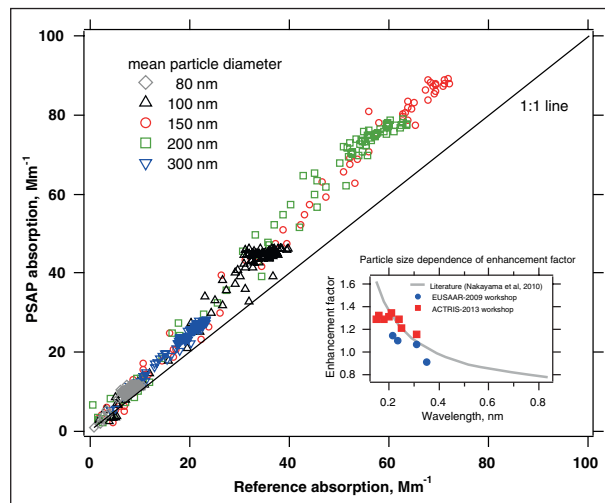


Fig. 2: Particle light absorption coefficient determined by a PSAP compared to values measured with the reference method (extinction minus scattering). The small box indicates the size dependency of the particle light absorption coefficient determined by a PSAP, which could explain the difference compared to the reference method.

include the development and application of quality-assurance tools, exchange of expertise, and the improvement of lidar techniques and algorithms. One of the activities in which TROPOS is involved is the

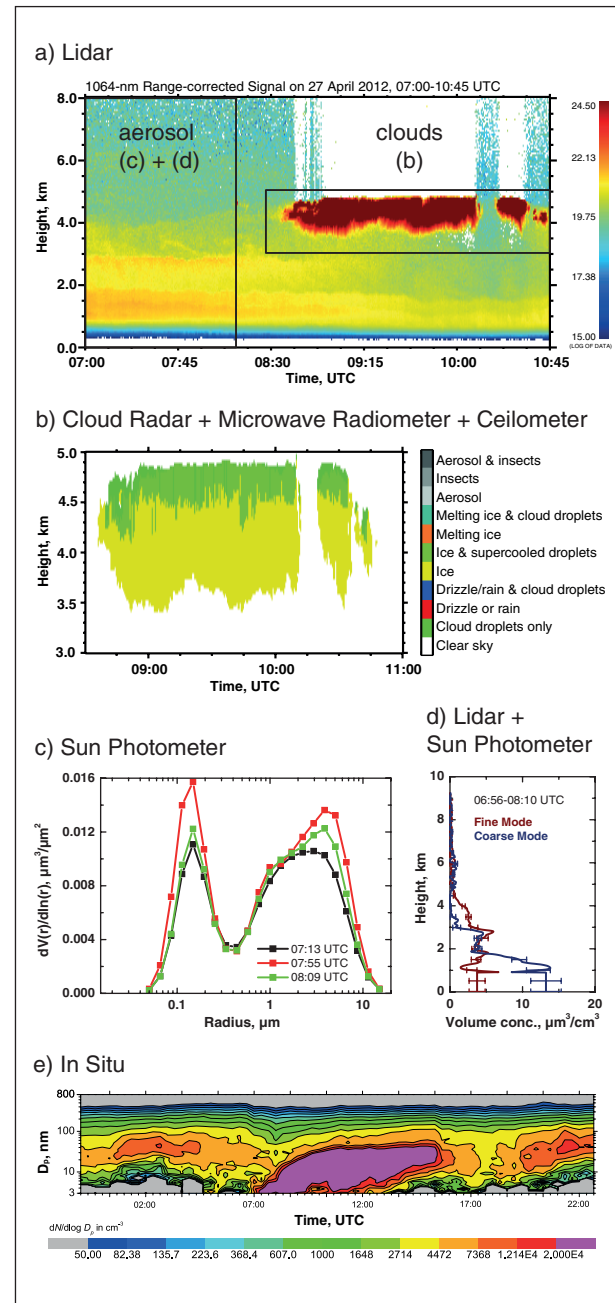


Fig. 3: Example of an integrated ACTRIS observation performed on 27 April 2012. a) The lidar time-height cross section of the 1064-nm attenuated backscatter signal shows the development of a cloud layer in the presence of aerosol. b) The CLOUDNET target classification indicates that ice is formed in the cloud and falls out of a layer with super-cooled water droplets. c) The AERONET volume size distribution shows the presence of fine (pollution) and coarse (dust) particle in the atmospheric column. d) LIRIC makes use of lidar (a) and sun photometer (c) information to retrieve vertical profiles of the volume concentration for the fine and coarse mode particles. e) In-situ observations of the dry fine particle size distribution (diameter < 800 nm) at ground level show a strong event of new particle formation.

deployment of a common lidar data analysis algorithm. This work aims at the development of a target classification mask and new modules for the calculation of optical and microphysical particle parameters from multi-wavelength Raman and polarization lidar measurements. Another key aspect of the remote-sensing activities within the past two years was the integration of the new TROPOS cloud observing instruments in the CLOUDNET measurement and data evaluation routines as contribution to ACTRIS WP5 and WP22 (see Fig. 1).

The topic of ACTRIS Joint Research Activity WP20, which is coordinated by TROPOS as well, is the integration of lidar and sun photometer observations. The activity focuses on the improvement of daytime capabilities of lidar instruments, the generation of combined lidar and sun photometer data sets, and the development of combined retrieval algorithms for improved vertically resolved aerosol characterization. TROPOS contributes with combined observations and with extended tests of the newly developed algorithms [Wagner et al., 2013]. An example of integrated observations of aerosols and clouds with TROPOS ground-based in-situ and remote-sensing instrumentation is presented in Fig. 3.

## Outreach and future planning

A large number of ACTRIS activities are related to scientific cooperation, training of young researchers, communication with end users, and public relations. TROPOS is actively involved in diverse efforts regarding, e.g., coordination among European research infrastructures, cooperation between European projects and the US Atmospheric Radiation Measurement (ARM) program, and collaboration with the WMO Global Atmosphere Watch (GAW) program.

ACTRIS is planning to strengthen its efforts within a new Integrated Activity of the European Framework Programme HORIZON 2020. To ensure long-term prospects, ACTRIS aims at becoming listed on the ESFRI (European Strategy Forum on Research Infrastructures) roadmap. A national consortium ACTRIS-D has been initiated to promote ACTRIS in Germany and coordinate German interests at the European level.

---

## References

- Wagner, J., A. Ansmann, U. Wandinger, P. Seifert, A. Schwarz, M. Tesche, A. Chaikovsky, and O. Dubovik (2013), Evaluation of the Lidar/Radiometer Inversion Code (LIRIC) to determine microphysical properties of volcanic and desert dust, *Atmos. Meas. Tech.*, 6, 1707-1724, doi:10.5194/amt-6-1707-2013.

---

## Funding

ACTRIS receives funding from the European Union Seventh Framework Programme (FP7/2007-2013) under grant agreement n° 262254

---

## Cooperation

The ACTRIS consortium consists of 29 full partners and more than 60 associated partners from 30 countries

# Combining the perspective of satellite- and ground-based observations to analyze cloud frontal systems

Anja Hünerbein<sup>1</sup>, Ulrich Görsdorf<sup>2</sup>, Hartwig Deneke<sup>1</sup>, Andreas Macke<sup>1</sup>

<sup>1</sup> Leibniz Institute for Tropospheric Research, Leipzig, Germany

<sup>2</sup> Lindenberg Meteorological Observatory, Deutscher Wetterdienst (DWD), Germany

Zur Untersuchung von Wolkensystemen an Fronten wurden boden- und satellitengebundene Messungen verknüpft. Die Kombination ermöglicht eine verbesserten Beschreibung der Struktur der Wolken sowie ihren Lebenszyklus mit Hilfe der Euler- Betrachtungsweise. Hierbei wurde mit Hilfe von synthetischen Satellitendaten, basierend auf den vertikal Profilen der bodengebundenen Messungen und einem Vorwärtsmodell, Metriken zur Quantifizierung der Qualität der Verknüpfung bestimmt. Nach der Konsistenzüberprüfung werden disjunkte Größen kombiniert, um das Wolkensystem zu analysieren. Im Folgenden wird anhand eines Fallbeispiels eines Kaltfront-Durchzuges über dem Messstandort Lindenberg die Methodik skizziert.

## Introduction

In Europe, a number of supersites have been established under the umbrella of the CloudNET project [Illingworth et al., 2007], which will be consolidated within the ACTRIS project (Aerosols, Clouds, and Trace gases Research InfraStructure Network). At these stations, the synergy of cloud radar, lidar and microwave radiometer is exploited to continuously provide data products of cloud properties among others. The number of these high-quality measurement sites will however always remain insufficient to fully capture the spatial variation and the different states of a cloud system due to the point nature of the observations. In this study, we propose a method to combine ground-based measurements with geostationary satellite observations from SEVIRI (Spinning Enhanced Visible and Infrared Imager) over Europe for a comprehensive view on frontal cloud systems. The surface sites provide Euler time series of parameters of the passing cloud systems with high vertical resolution, while the passive remotely sensed products from the geostationary satellite offer temporally and also horizontally resolved views on the cloud fields (Fig. 1). An example, the passage of a cloud frontal system at the supersite Lindenberg, is analyzed to demonstrate the approach.

## Methods

A method is presented to combine the information on the vertical profiles of cloud properties from ground-based observations with information on the spatial variability of clouds from satellite. By using the forward model RTTOV [Saunders, 2009] and the ground-based CloudNET products we simulate synthetic satellite observations at Lindenberg, which are subsequently compared to the actual

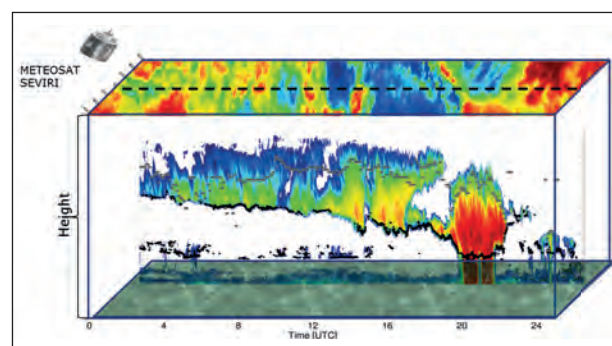


Fig. 1: Cloudradar reflectivity at 30 s resolution from CloudNET on 12 May 2011, Lindenberg with SEVIRI cloud top height (grey dots) and the ceilometer cloud base (black dots). At the top of the cuboid the SEVIRI BT at 10.8  $\mu$ m are plotted over the time with a N-S distance of  $\pm$  60km from Lindenberg station (dashed line).

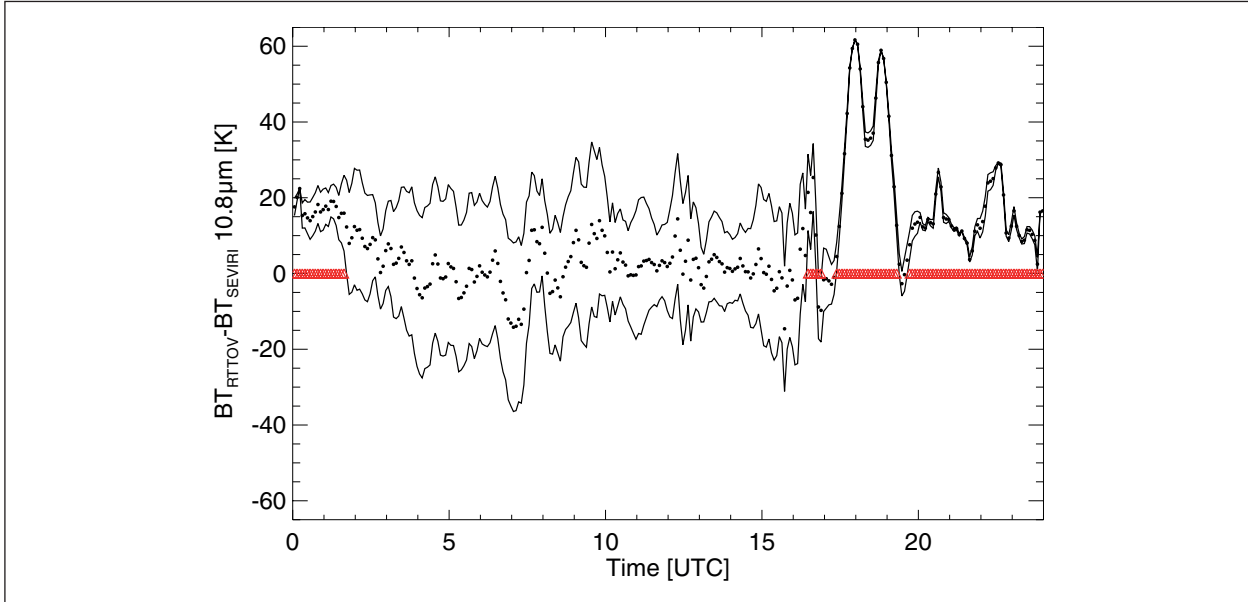


Fig. 2: Difference of the observed and synthetic brightness temperature at  $10.8\text{ }\mu\text{m}$  on 12 May 2011, Lindenberg. The errors are calculated with the uncertainties of the CloudNET products. The red dots indicate the periods which did not pass the consistency tests.

observations of the Meteosat SEVIRI instrument. We considered different metrics to quantify and interpret the consistency of the synthetic and the observed satellite data: brightness temperatures (BT) at the thermal IR channels, the split window channels and tri-spectral combinations of channels, as well as the outgoing longwave radiation (OLR). Error bars were computed for the simulated BTs based on the uncertainty estimates of the CloudNET products, and turned out to be very helpful as a consistency check. In this way, the uncertainties of the individual data sets and their scale differences are investigated. Figure 2 shows exemplary the difference of the observed and synthetic BT at  $10.8\text{ }\mu\text{m}$  with their calculated uncertainties. The red dots indicate the periods, which did not pass the consistency test. Between 1740-1910 UTC a precipitation event took place, which invalidated the ground-based retrieval of liquid water path. The disagreement between 0000 UTC and 0145 UTC as well as 2000 UTC and 24 UTC has been analysed in detail in sensitivity studies. During the first period the synthetic BTs and the OLR were overestimated relative to the observations. The analysis suggests an underestimation of the CloudNET IWC by as much as a factor of 10. The discrepancy observed during the second period likely results from multiple physical reasons, including errors in the forecast humidity profile and inhomogeneity of the cloud field. This knowledge provides the motivation to combine the cloud products from the satellite for the periods, which have passed the consistency test with ground measurement to characterize the passing cloud systems over the sites.

## Results

Figure 1 presents the time series of the vertical profile of the radar reflectivity at the Lindenberg site together with the cloud top height retrieved from SEVIRI measurements and the cloud base height provided by the ground-based ceilometer. The passing cold front is preceded by cirrostratus with intermittent altocumulus below. By 1600 UTC, the surface front passed Lindenberg which can be identified by a minimum in the surface pressure and a drop in the surface temperature (not shown). Heavy rain with rain rates up to 9 mm/h occurred between 1740 UTC and 1910 UTC after the passage of the surface front. Afterwards it cleared up with 1-7 octal cumulus cloud coverage. Note that the SEVIRI cloud microphysical cloud products are only available during daytime. In the morning, the cloud was semi-transparent having an optical thickness of 1.8 and increased to 15 at 1625 UTC (Fig. 3). The retrieved ice effective radius had an average size of  $22\text{ }\mu\text{m}$ . The REF decreased from  $22\text{ }\mu\text{m}$  at 0530 UTC to  $12\text{ }\mu\text{m}$  at 1050 UTC, and increased again to  $32\text{ }\mu\text{m}$  at 1205 UTC. During the latter time period (1050 UTC - 1205 UTC), the variance of the Doppler velocities measured by the cloud radar increased in the upper layer of the cloud, which is an indication for higher atmospheric instability and a pronounced turbulent flux. This can lead to the growth of ice particles as reflected by the increase of REF. The effective radius reached a maximum value of  $36\text{ }\mu\text{m}$  at 1500 UTC. When broken multi-layer clouds passed Lindenberg from 1500 UTC to 1600 UTC the effective radius decreased.

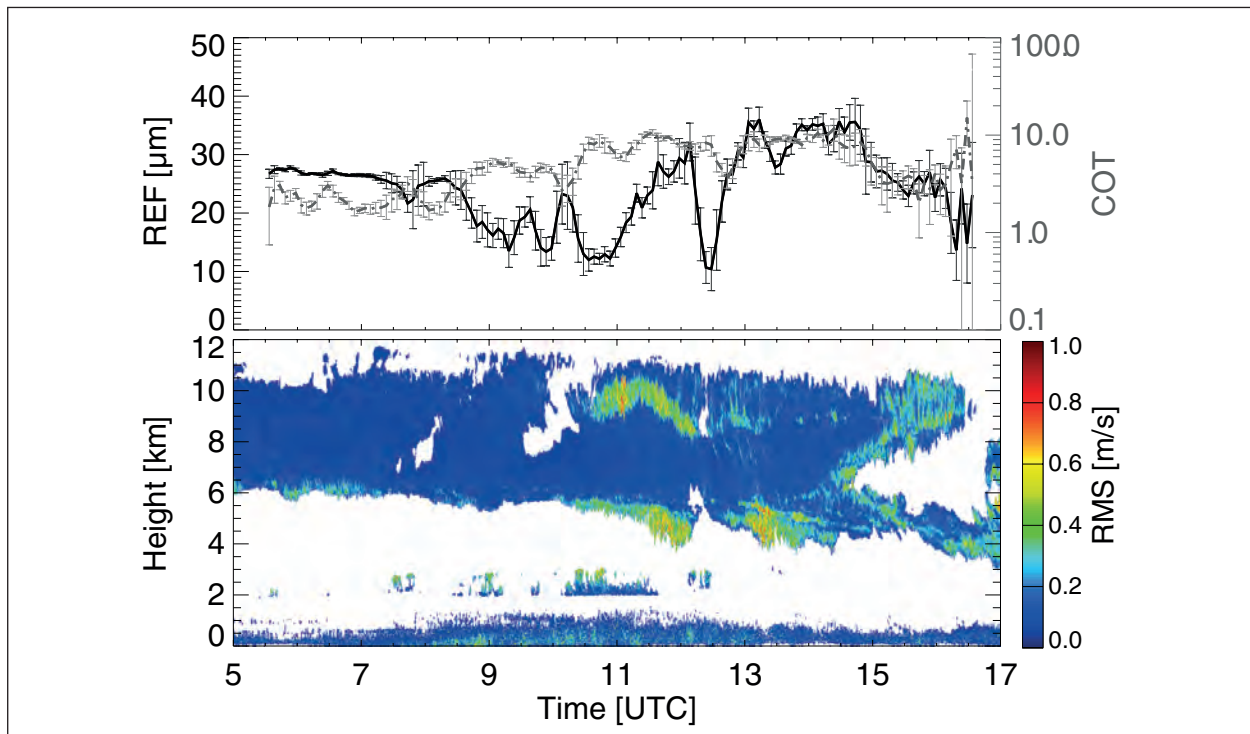


Fig. 3: The diurnal cycle of the SEVIRI cloud effective radius (black) and cloud optical thickness (grey) with the standard deviation of the  $5 \times 3$  surrounded satellite pixels (error bars) at the top as well as the Doppler spectral width at the bottom on 12 May 2011, Lindenberg.

## Conclusions

The combination of the ground-based and the satellite observation gives us the possibility to study the microphysical process of the clouds. In the next

step, we will conduct a statistical analysis of a one year dataset of cloud frontal systems. Together with the modelling groups at TROPOS the observed vertical structure will be related to the larger scale dynamical and microphysical processes.

## References

- Illingworth, A. J. and Coauthors, 2007: Cloudnet: Continuous evaluation of cloud profiles in seven operational models using ground-based observations. *Bull. Amer. Meteor. Soc.*, 88, 883-898.  
 Saunders, R. W., M. Matricardi, and A. Geer (2009): Rttov9.1 user guide, eumetsat, nwpasf- mo-ud-016. *Tech. rep.*.

## Funding

German Research Foundation within the project ICOS - Integrating Cloud Observations from Ground and Space under grant CR111/8-1

## Cooperation

Deutscher Wetterdienst (DWD), Meteorological Observatory Lindenberg (Richard Aßmann Observatory), Germany

# Investigation of the first indirect aerosol effect: Comparison of the satellite and ground perspective

Daniel Merk<sup>1</sup>, Hartwig Deneke<sup>1</sup>, Bernhard Pospichal<sup>2</sup>, Patric Seifert<sup>1</sup>, Albert Ansmann<sup>1</sup>

<sup>1</sup> Leibniz Institute for Tropospheric Research (TROPOS), Leipzig, Germany

<sup>2</sup> Leipzig University, , Faculty of Physics and Earth Sciences, Leipzig Institute for Meteorology (LIM), Germany

**Unter Verwendung bestehender Algorithmen für boden- und satellitengestützte Fernerkundung, wurden die Schlüsselparameter für den ersten indirekten Aerosoleffekt genauer untersucht. Dazu wurde für die Ableitung der Tropfenanzahlkonzentration aus Bodenfernerkundungsdaten eine Radar-Radiometer Methode einer Optimal Estimation Methode gegenübergestellt und zusätzlich mit einem einfachen adiabatischen Ansatz für das Satellitenretrieval verglichen.**

## Introduction

The magnitude of the first indirect effect [Twomey, 1977] remains one of the major uncertainty factors of anthropogenic climate change. Geostationary satellites offer the opportunity to investigate cloud properties globally with high temporal and spatial resolution. Two key properties relevant for the first indirect effect are the cloud droplet number concentration (CDNC) and the geometrical cloud extent [Pawlowska and Brenguier, 2000]. Missing information about the vertical cloud structure requires assumptions about the liquid water content distribution within the cloud. A common choice is to assume a linearly increasing liquid water content profile above cloud base, the so-called adiabatic model [e.g. Bennartz et al., 2007]. Satellite retrieved geometrical extent can be compared directly to ground site remote sensing applied at TROPOS, Leipzig. The verification of CDNC is not as straightforward due to a lack of direct measurements of this quantity. We apply two approaches for this comparison: (1) a retrieval based on radar-radiometer observations [Remillard et al., 2013], and (2) an optimal estimation technique.

## Data

At the measurement site at TROPOS a number of remote sensing instruments is operationally observing clouds. Here we apply the HATPRO

microwave radiometer, the 35 GHz MIRA cloud radar and the CHM15X ceilometer. The observed data are processed with the Cloudnet algorithm [Illingworth and Hogan, 2007]. The final dataset includes the radar reflectivity, the liquid water path, cloud base and top height, and are provided at a vertical resolution of 60 m and a temporal resolution of 30 s.

Satellite observations from MSG SEVIRI at 5 min temporal resolution are processed with the NWC SAF ([www.nwcsaf.org](http://www.nwcsaf.org)) and KNMI-CPP ([msgcpp.knmi.nl](http://msgcpp.knmi.nl)) packages. This provides the cloud top height, the optical depth and the effective radius. The latter two are only available during daytime.

## Method

The radar-radiometer-retrieval assumes a Gamma shaped droplet size distribution and a constant CDNC with height. Profiles affected by drizzle or rain are excluded. Since microphysical properties are directly linked to the different moments of the droplet size distribution [Frisch et al., 2002], it is possible to derive the CDNC (zeroth moment) from the liquid water path (third moment) and radar reflectivity factor (sixth moment). Following the relationship between these quantities as derived from Fox and Illingworth [1997], we are able to retrieve the CDNC from observed quantities.

The optimal estimation approach tries to find the optimal state of a vector by combining an a priori

state with the observations and considering their error covariances. We minimize the cost function [Rodgers, 2000] of a state vector containing the liquid water content profile and the vertically constant cloud droplet number concentration. Our observation vector contains the radar reflectivity profile as well as the liquid water content. The required forward model consists of a radar simulator, that uses the theoretical relationship as described in Fox and Illingworth [1997], and of a numerical integration of the liquid water content. Thereby our forward model remains simple and cheap compared to a full radiative transfer model. Within the error covariance matrices, only the diagonal elements are nonzero, assuming that there is no correlation between the different vertical levels and the different quantities in our vectors. The observation error covariances are determined from the standard deviations given from the Cloudnet algorithm. For the background state we set the CDNC to  $300 \text{ cm}^{-3}$  with a standard deviation of  $300 \text{ cm}^{-3}$ , and the LWC to the adiabatic profile, scaled by the measured LWP. To avoid unphysical, negative results within the optimal estimation we use the natural logarithm of the liquid water content. The standard deviation for  $\ln(\text{lwc})$  is set to  $2.5 \ln(\text{g cm}^{-3})$ .

For the satellite retrieval we assume pure adiabatic clouds with a factor  $\alpha = 1.37 \times 10^{-5} \text{ m}^{0.5}$  relating the optical depth and effective radius [Quaas et al., 2006].

## Results

The 27th of September 2012 provides good conditions to test the described methods. A rather homogeneous low-level liquid water cloud layer is present between 9 and 15 UTC as can be seen by the Cloudnet classification in Fig. 1a. The cloud top height determined from the satellite and ground perspective show good agreement (correlation of 85%) while the cloud layer is unbroken, considering the differences in the field of view and the spatial resolution of the satellite and the ground based instruments.

A comparison of the retrieved CDNC is shown in Fig. 1b. The CDNC obtained with the radar-radiometer method shows outliers, including unrealistically high physical values of more than  $1000 \text{ cm}^{-3}$  (not shown). This might be attributed to invalid assumptions. The optimal estimation of the CDNC shows values in a similar range as the radar-radiometer-retrieval but without outliers. Both methods rely on the same observational data and therefore the optimal estimation method seems to be more stable against outliers. The satellite-retrieved values have a much coarser temporal resolution and are therefore not able to reproduce variations within short time-periods. A

good agreement of the CDNC can be seen especially between 9 and 10 UTC where the cloud is rather thick and without gaps. Broken cloud layers observed from satellite lead to contamination of radiances from the surface and therefore results in deviations of the retrieved cloud properties.

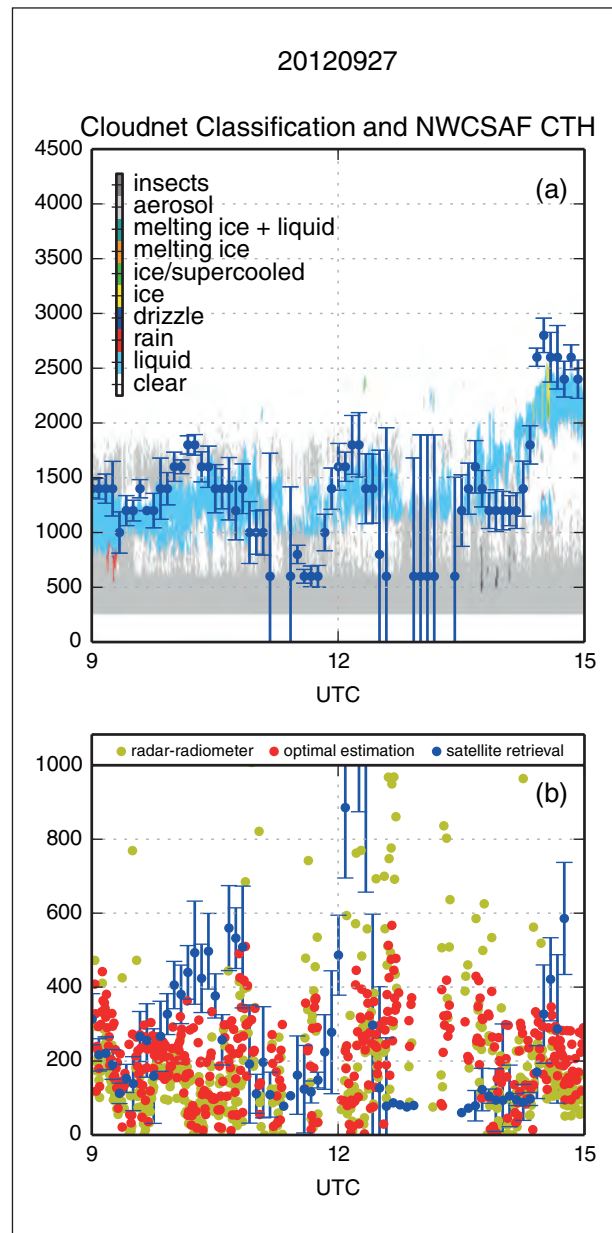


Fig. 1: (a) Cloudnet target classification (shaded areas) and cloud top height from the NWC SAF algorithm (blue dots). The error bars for the NWC SAF cloud top height represent the standard deviation of the surrounding  $\pm 1$  satellite pixel. (b) Cloud droplet number concentration retrieved with the different methods. Yellow dots represent the ground-site radar-radiometer retrieved values, red dots the values resulting from the ground-site optimal estimation and the blue dots from the adiabatic retrieval from the satellite perspective. Error bars for the latter again represent the standard deviation in the surrounding  $\pm 1$  pixels.

## Conclusion

To investigate the possibilities of geostationary satellites to quantify the first indirect aerosol effect we have taken a closer look at two key quantities: geometrical cloud extent and cloud droplet number concentration. Assumptions about the vertical cloud structure are necessary in order to retrieve these

quantities from satellite or ground remote sensing. We compared two retrieval methods from ground and one from satellite for a time-period where homogeneous liquid water clouds were observed. A systematic application of the described methods to more case studies should allow an assessment of the validity of assumptions made within the described retrievals.

---

## References

- Bennartz, R., (2007), Global assessment of marine boundary layer cloud droplet number concentration from satellite, *J. Geophys. Res.*, 112, D02201, doi:10.1029/2006JD007547.
- Brenguier, J.-L., H. Pawlowska, L. Schüller, R. Preusker, J. Fischer, and Y. Fouquart (2000), Radiative properties of boundary layer clouds: Droplet effective radius versus number concentration, *J. Atmos. Sci.*, 57, 6, 803–821.
- Fox, N. I., and A. J. Illingworth (1997), The retrieval of stratocumulus cloud properties by ground-based cloud RADAR, *J. Appl. Meteorol.*, 36, 5, 485–492.
- Illingworth, A. J., R. J. Hogan, E. J. O'Connor, D. Bouniol, M. E. Brooks, J. Delanoe, D. P. Donovan, N. Gaussiat, J. W. F. Goddard, M. Haeffelin, H. Klein Baltink, O. A. Krasnov, J. Pelon, J. M. Piriou, and G. J. van Zadelhoff (2007), Cloudnet – continuous evaluation of cloud profiles in seven operational models using ground-based observations, *Bull. Amer. Meteor. Soc.*, 88, 6, 883–898.
- Quaas, J., O. Boucher, U. Lohmann (2006), Constraining the total aerosol indirect effect in the LMDZ and ECHAM4 GCMs using MODIS satellite data, *Atmos. Chem. Phys.*, 6, 4, 947-955.
- Twomey, S. (1977). The influence of pollution on the shortwave albedo of clouds. *J. Atmos. Sci.*, 34, 7, 1149–1152.
- Rémillard, J., P. Kollias, and W. Szyrmer (2013), Radar-radiometer retrievals of cloud number concentration and dispersion parameter in nondrizzling marine stratocumulus, *Atmos. Meas. Tech.*, 6, 7, 1817-1828.
- Rodgers, C. D. (2000), Inverse Methods for Atmospheric Sounding: Theory and Practice, *World Sci.*, River Edge, N. J..

---

## Funding

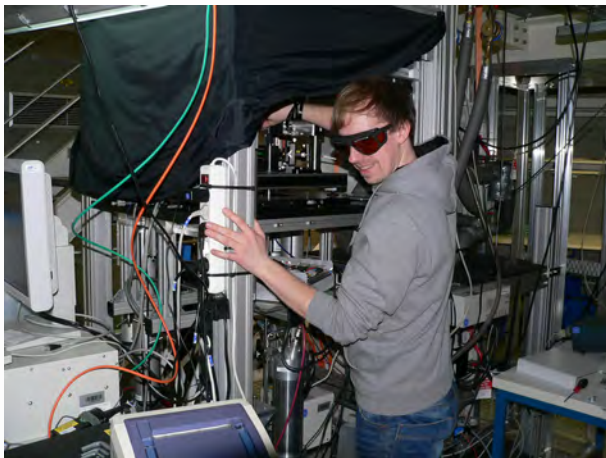
Leipzig Graduate School on “Aerosol, Clouds and Radiation: Mineral dust” (LGS-CAR)

---

## Cooperation

Leipzig University, Faculty of Physics and Earth Sciences, Leipzig Institute for Meteorology (LIM)

## Appendices





## Publications

### Publication statistics

	2012	2013
Total number of publications	336	310
Books (author, editor)	1	1
Book sections	2	6
Conference proceedings	36 <sup>a</sup> )	7
Publications, peer-reviewed	81	85
Publications, other	3	22
Lectures, invited	21	20
Conference contributions / Lectures, other	192	169

<sup>a</sup> due to 28 contributions to the 26th International Laser Radar Conference (ILRC) in 2012

## Publications

### 2012

- Aas, W., Tsyro, S., Bieber, E., Bergström, R., Ceburnis, D., Ellermann, T., Fagerli, H., Frölich, M., Gehrig, R., Makkonen, U., Nemitz, E., Otjes, R., Perez, N., Perrino, C., Prévôt, A. S. H., Putaud, J. P., Simpson, D., **Spindler, G.**, Vana, M. and Yttri, K. E. 2012. Lessons learnt from the first EMEP intensive measurement periods. *Atmos. Chem. Phys.*, **12**, 8073-8094. doi:10.5194/acp-12-8073-2012.
- Alves, C., Vicente, A., Pio, C., Kiss, G., Hoffer, A., Decesari, S., Prévôt, A. S. H., Minguillón, M. C., Querol, X., Hillamo, R., **Spindler, G.** and Swietlicki, E. 2012. Organic compounds in aerosols from selected European sites - Biogenic versus anthropogenic sources. *Atmos. Environ.*, **59**, 243-255. doi:10.1016/j.atmosenv.2012.06.013.
- Ansmann, A., Seifert, P., Tesche, M. and Wandinger, U.** 2012. Profiling of fine and coarse particle mass: Case studies of Saharan dust and Eyjafjallajökull/Grimsvötn volcanic plumes. *Atmos. Chem. Phys.*, **12**, 9399-9415. doi:10.5194/acp-12-9399-2012.
- Baars, H., Ansmann, A., Althausen, D., Engelmann, R., Heese, B., Müller, D., Artaxo, P., Paixao, M.**, Pauliquevis, T. and Souza, R. 2012. Aerosol profiling with lidar in the Amazon Basin during the wet and dry season. *J. Geophys. Res. - Atmos.*, **117**, D21201. doi:10.1029/2012JD018338.
- Baumgardner, D., Avallone, L., Bansemer, A., Borrmann, S., Brown, P., Bundke, U., Chuang, P. Y., Cziczo, D., Field, P., Gallagher, M., Gayet, J.-F., Heymsfield, A., Korolev, A., Krämer, M., McFarquhar, G., **Mertes, S.**, Möhler, O., Lance, S., Lawson, P., Petters, M., Pratt, K., Roberts, G., Rogers, D., Stetzer, O., Stith, J., Strapp, W., Twohy, C. and Wendisch, M. 2012. In situ, airborne instrumentation: Addressing and solving measurement problems in ice clouds. *Bull. Amer. Meteor. Soc.*, **93**, ES29-ES34. doi:10.1175/BAMS-D-11-00123.1.
- Baumgardner, D., Popovicheva, O., Allan, J., Bernadoni, V., Cao, J., Cavalli, F., Cozic, J., Diapouli, E., Eleftheriadis, K., Genberg, P. J., Gonzalez, C., Gysel, M., John, A., Kirchstetter, T. W., Kuhlbusch, T. A. J., Laborde, M., Lack, D., **Müller, T.**, Niessner, R., Petzold, A., Piazzalunga, A., Putaud, J. P., Schwarz, J., Sheridan, P., Subramanian, R., Swietlicki, E., Valli, G., Vecchi, R. and Viana, M. 2012. Soot reference materials for instrument calibration and intercomparisons: A workshop summary with recommendations. *Atmos. Meas. Tech. (AMT)*, **5**, 1869-1887.
- Bengtsson, L., Koumoutsaris, S., Bonnet, R.-M., Allan, R. P., Fröhlich, C., **Heintzenberg, J.**, Ingmann, P., Kandel, R., Loeb, N., Soden, B. and Trenberth, K. E. (Eds.) (2012), Observing and modeling earth's energy flows, 484 pp., Springer, Dordrecht. (Space Sciences Series of ISSI)
- Berndt, T.** 2012. Formation of carbonyls and hydroperoxyenals (HPALDs) from the OH radical reaction of isoprene for low-NO<sub>x</sub> conditions: Influence of temperature and water vapour content. *J. Atmos. Chem.*, **69**, 253-272.

## Appendices: Publications

- Berndt, T.**, Jokinen, T., Mauldin III, R. L., Petäjä, T., Herrmann, H., Junninen, H., Paasonen, P., Worsnop, D. R. and Sipilä, M. 2012. Gas-phase ozonolysis of selected olefins: The yield of stabilized criegee intermediate and the reactivity toward SO<sub>2</sub>. *J. Phys. Chem. Lett.*, **3**, 2892-2896. doi:10.1021/jz301158u.
- Berndt, T.** and **Richters, S.** 2012. Products of the reaction of OH radicals with dimethyl sulphide in the absence of NO<sub>x</sub>: Experiment and simulation. *Atmos. Environ.*, **47**, 316-322.
- Bühl, J.**, **Engelmann, R.** and **Ansmann, A.** 2012. Removing the laser-chirp influence from coherent doppler lidar datasets by two-dimensional deconvolution. *J. Atmos. Ocean. Tech.*, **29**, 1042–1051.
- Chen, J., **Zhao, C. S.**, Ma, N., Liu, P. F., **Göbel, T.**, **Hallbauer, E.**, Deng, Z. Z., Ran, L., Xu, W. Y., Liang, Z., Liu, H. J., Yan, P., Zhou, X. J. and **Wiedensohler, A.** 2012. A parameterization of low visibilities for hazy days in the North China Plain. *Atmos. Chem. Phys.*, **12**, 4935-4950. doi:10.5194/acp-12-4935-2012.
- Cheng, Y. F.**, Su, H., Rose, D., Gunthe, S. S., **Berghof, M.**, **Wehner, B.**, **Achert, P.**, **Nowak, A.**, Takegawa, N., Kondo, Y., Shiraiwa, M., Gong, Y. G., Shao, M., Hu, M., Zhu, T., Zhang, Y. H., Carmichael, G. R., **Wiedensohler, A.**, Andreae, M. O. and Poschl, U. 2012. Size-resolved measurement of the mixing state of soot in the megacity Beijing, China: diurnal cycle, aging and parameterization. *Atmos. Chem. Phys.*, **12**, 4477-4491. doi:10.5194/acp-12-4477-2012.
- Ditas, F.**, **Shaw, R. A.**, **Siebert, H.**, **Simmel, M.**, **Wehner, B.** and **Wiedensohler, A.** 2012. Aerosols-cloud microphysics-thermodynamics-turbulence: Evaluating supersaturation in a marine stratocumulus cloud. *Atmos. Chem. Phys.*, **12**, 2459-2468. doi:10.5194/acp-12-2459-2012.
- Dolgorouky, C., Gros, V., Sarda-Estève, R., Sinha, V., Williams, J., Marchand, N., Sauvage, S., **Poulain, L.**, Sciare, J. and Bonsang, B. 2012. Total OH reactivity measurements in Paris during the 2010 MEGAPOLI winter campaign. *Atmos. Chem. Phys.*, **12**, 9593-9612. doi:10.5194/acp-12-9593-2012.
- Dupart, Y., King, S. M., **Nekat, B.**, **Nowak, A.**, **Wiedensohler, A.**, **Herrmann, H.**, David, G., Thomas, B., Miffre, A., Rairoux, P., D'Anna, B. and George, C. 2012. Mineral dust photochemistry induces nucleation events in the presence of SO<sub>2</sub>. *Proc. Nat. Acad. Sci. (PNAS)*, **109**, 20842-20847. doi:10.1073/pnas.1212297109
- Ekman, A. M. L., **Hermann, M.**, Groß, P., **Heintzenberg, J.**, Kim, D.-C. and Wang, C. 2012. Sub-micrometer aerosol particles in the upper troposphere/lowermost stratosphere as measured by CARIBIC and modeled using the MIT-CAM3 global climate model. *J. Geophys. Res. - Atmos.*, **117**, D11202. doi:10.1029/2011JD016777.
- Engler, C.**, **Birmili, W.**, **Spindler, G.** and **Wiedensohler, A.** 2012. Analysis of exceedances in the daily PM10 mass concentration (50 µg m<sup>-3</sup>) at a roadside station in Leipzig, Germany. *Atmos. Chem. Phys.*, **12**, 10107-10123. doi:10.5194/acp-12-10107-2012.
- Fountoukis, C., Riipinen, I., van der Gon, H., Charalampidis, P. E., Pilinis, C., **Wiedensohler, A.**, O'Dowd, C., Putaud, J. P., Moerman, M. and Pandis, S. N. 2012. Simulating ultrafine particle formation in Europe using a regional CTM: contribution of primary emissions versus secondary formation to aerosol number concentrations. *Atmos. Chem. Phys.*, **12**, 8663-8677. doi:10.5194/acp-12-8663-2012.
- George, C., D'Anna, B., **Herrmann, H.**, **Weller, C.**, Vaida, V., Donaldson, D. J., Bartels-Rausch, T. and Ammann, M. 2012. Emerging areas in atmospheric photochemistry. *Top. Curr. Chem.*, online. doi:10.1007/128\_2012\_393.
- Gnauk, T.**, Müller, K., **Brüggemann, E.**, **Birmili, W.**, **Weinhold, K.**, **van Pinxteren, D.**, Löschnau, G., **Spindler, G.** and **Herrmann, H.** 2012 (2011). A study to discriminate local, urban and regional source contributions to the particulate matter concentrations in the city of Dresden, Germany. *J. Atmos. Chem.*, **68**, 199-231. doi:10.1007/s10874-012-9216-7
- Gu, J., Pitz, M., Breitner, S., **Birmili, W.**, von Klot, S., Schneider, A., Soentgen, J., Reller, A., Peters, A. and Cyrys, J. 2012. Selection of key ambient particulate variables for epidemiological studies — Applying cluster and heatmap analyses as tools for data reduction. *Sci. Total Environ.*, **435-436**, 541-550.
- Hänel, A.**, **Baars, H.**, **Althausen, D.**, **Ansmann, A.**, **Engelmann, R.** and Sun, J. Y. 2012. One-year aerosol profiling with EUCAARI Raman lidar at Shangdianzi GAW station: Beijing plume and seasonal variations. *J. Geophys. Res. - Atmos.*, **117**, D13201 (11 p.). doi:10.1029/2012JD017577.
- Hanschmann, T.**, **Deneke, H.**, Roebeling, R. and **Macke, A.** 2012. Evaluation of the shortwave cloud radiative effect over the ocean by use of ship and satellite observations. *Atmos. Chem. Phys.*, **12**, 12243-12253. doi:10.5194/acp-12-12243-2012.
- Haustein, K., Pérez, C., Baldasano, J. M., Jorba, O., Basart, S., Miller, R. L., Janjic, Z., Black, T., Nickovic, S., Todd, M. C., Washington, R., **Müller, D.**, **Tesche, M.**, Weinzierl, B., Esselborn, M. and Schladitz, A. 2012. Atmospheric dust modeling from meso to global scales with the online NMMB/BSC-Dust model – Part 2: Experimental campaigns in Northern Africa. *Atmos. Chem. Phys.*, **12**, 2933-2958. doi:10.5194/acp-12-2933-2012.

## Appendices: Publications

- Healy, R. M., Sciare, J., **Poulain, L.**, Kamilli, K., Merkel, M., Müller, T., Wiedensohler, A., Eckhardt, S., Stohl, A., Sarda-Estève, R., McGillicuddy, E., O'Connor, I. P., Sodeau, J. R. and Wenger, J. C. 2012. Source and mixing state of size-resolved elemental carbon particles in a European megacity: Paris. *Atmos. Chem. Phys.*, **12**, 1681-1700. doi:10.5194/acp-12-1681-2012.
- Heinold, B., Tegen, I., Wolke, R., Ansmann, A., Mattis, I., Minikin, A., Schumann, U. and Weinzierl, B. 2012. Simulations of the 2010 Eyjafjallajökull volcanic ash dispersal over Europe using COSMO–MUSCAT. *Atmos. Environ.*, **48**, 195-204. doi:10.1016/j.atmosenv.2011.05.021.
- Heintzenberg, J. 2012. The aerosol-cloud-climate conundrum. *Int. J. Global Warming*, **4**, 219-241.
- Heintzenberg, J. and Leck, C. 2012. The summer aerosol in the central Arctic 1991 - 2008: Did it change or not? *Atmos. Chem. Phys.*, **12**, 3969-3983. doi:10.5194/acp-12-3969-2012.
- Henning, S., Ziese, M., Kiselev, A., Saathoff, H., Möhler, O., Mentel, T. F., Buchholz, A., Spindler, C., Michaud, V., Monier, M., Sellegrí, K. and Stratmann, F. 2012. Hygroscopic growth and droplet activation of soot particles: Uncoated, succinic or sulfuric acid coated. *Atmos. Chem. Phys.*, **12**, 4525-4537. doi:10.5194/acp-12-4525-2012.
- Herold, C., Althausen, D., Müller, D., Tesche, M., Seifert, P., Engelmann, R., Flamant, C., Bhawar, R. and Di Girolamo, P. 2012. Comparison of Raman lidar observations of water vapor with COSMO-DE forecasts during COPS 2007. *Weather Forecast*, **26**, 1056-1066.
- Hesse, E., Macke, A., Havemann, S., Baranc, A. J., Ulanowskia, Z. and Kayea, P. H. 2012. Modelling diffraction by faceted particles. *J. Quant. Spectrosc. Radiat. Transfer*, **113**, 342–347.
- Hieronymi, M. and Macke, A. 2012. On the influence of wind and waves on underwater irradiance fluctuations. *Ocean Sci.*, **8**, 455-471. doi:10.5194/os-8-455-2012.
- Hieronymi, M., Macke, A. and Zielinski, O. 2012. Modeling of wave-induced irradiance variability in the upper ocean mixed layer. *Ocean Sci.*, **8**, 103-120. doi:10.5194/os-8-103-2012.
- Horn, S. 2012. ASAMgpu V1.0 – a moist fully compressible atmospheric model using graphics processing units (GPUs). *Geosci. Model Dev.*, **5**, 345-353. doi:10.5194/gmd-5-345-2012.
- Horn, S., Raabe, A., Will, H. and Tackenberg, O. 2012. TurbSeed - A model for wind dispersal of seeds in turbulent currents based on publicly available climate data. *Ecol. Model.*, **237**, 1-10. doi: 10.1016/j.ecolmodel.2012.04.009.
- Jebens, S., Knoth, O. and Weiner, R. 2012. Linearly implicit peer methods for the compressible Euler equations. *Appl. Numer. Math.*, **62**, 1380-1392. doi:10.1016/j.apnum.2012.06.013.
- Kalisch, J. and Macke, A. 2012. Radiative budget and cloud radiative effect over the Atlantic from ship-based observations. *Atmos. Meas. Tech. (AMT)*, **5**, 2391-2401. doi:10.5194/amt-5-2391-2012.
- Katzwinkel, J., Siebert, H. and Shaw, R. A. 2012. Observation of a self-limiting, shear-induced turbulent inversion layer above marine stratocumulus. *Bound.-Lay. Meteorol.*, **145**, 131-143. doi:10.1007/s10546-011-9683-4.
- König, M., Wolke, R., Knoth, O. and Renner, E. 2012. *Modelling of atmospheric processes*. K. Binder, G. Münster, and M. Kremer (Ed.), In: . John von Neumann Institute for Computing, Jülich, **NIC Series 45**, p. 313-320.
- Komppula, M., Mielonen, T., Arola, A., Korhonen, K., Lihavainen, H., Hyvärinen, A.-P., Baars, H., Engelmann, R., Althausen, D., Ansmann, A., Müller, D., Panwar, T. S., Hooda, R. K., Sharma, V. P., Kerminen, V.-M., Lehtinen, K. E. J. and Viisanen, Y. 2012. Technical note: One year of Raman-lidar measurements in Gual Pahari EUCAARI site close to New Delhi in India – Seasonal characteristics of the aerosol vertical structure. *Atmos. Chem. Phys.*, **12**, 4513-4524. doi:10.5194/acp-12—4513-2012.
- Kristensen, T. B., Wex, H., Nekat, B., Nørgaard, J. K., van Pinxteren, D., Lowenthal, D. H., Mazzoleni, L. R., Dieckmann, K., Bender Koch, C., Mentel, T. F., Herrmann, H., Hallar, A. G., Stratmann, F. and Bilde, M. 2012. Hygroscopic growth and CCN activity of HULIS from different environments. *J. Geophys. Res. - Atmos.*, **117**, D22203. doi:10.1029/2012JD018249.
- Laakso, L., Vakkari, V., Virkkula, A., Laakso, H., Backman, J., Kulmala, M., Beukes, J. P., van Zyl, P. G., Tiitta, P., Josipovic, M., Pienaar, J. J., Chiloane, K., Gilardoni, S., Vignati, E., Wiedensohler, A., Tuch, T., Birmili, W., Piketh, S., Collett, K., Fourie, G. D., Komppula, M., Lihavainen, H., de Leeuw, G. and Kerminen, V.-M. 2012. South African EUCAARI measurements: Seasonal variation of trace gases and aerosol optical properties. *Atmos. Chem. Phys.*, **12**, 1847-1864. doi:10.5194/acp-12-1847-2012.

## Appendices: Publications

- Li, X., Brauers, T., Häseler, R., Bohn, B., Fuchs, H., Hofzumahaus, A., Holland, F., Lou, S., Lu, K. D., Rohrer, F., Hu, M., Zeng, L. M., Zhang, Y. H., Garland, R. M., Su, H., **Nowak, A.**, **Wiedensohler, A.**, Takegawa, N., Shao, M. and Wahner, A. 2012. Exploring the atmospheric chemistry of nitrous acid (HONO) at a rural site in Southern China. *Atmos. Chem. Phys.*, **12**, 1497-1513. doi:10.5194/acp-12-1497-2012.
- Lieber, M., Grützun, V., **Wolke, R.**, Müller, M. S. and Nagel, W. E. 2012. . K. Jónasson (Ed.), In: . Springer, Heidelberg et al., p. 131-141. (Lecture Notes in Computer Science (LNCS) ; 7133)
- Ma, N., Zhao, C. S., **Müller, T.**, **Cheng, Y. F.**, Liu, P. F., Deng, Z. Z., Xu, W. Y., Ran, L., **Nekat, B.**, **van Pinxteren, D.**, **Gnauk, T.**, **Müller, K.**, **Herrmann, H.**, Yan, P., Zhou, X. J. and **Wiedensohler, A.** 2012. A new method to determine the mixing state of light absorbing carbonaceous using the measured aerosol optical properties and number size distributions. *Atmos. Chem. Phys.*, **12**, 2381-2397. doi:10.5194/acp-12-2381-2012.
- Mamouri, R. E., Papayannis, A., Amiridis, V., **Müller, D.**, Kokkalis, P., Rapsomanikis, S., Karageorgos, E. T., Tsaknakis, G., Nenes, A., Kazadzis, S. and Remoundaki, E. 2012. Multi-wavelength Raman lidar, sunphotometric and aircraft measurements in combination with inversion models for the estimation of the aerosol optical and physico-chemical properties over Athens, Greece. *Atmos. Meas. Tech. (AMT)*, **5**, 1793-1808.
- Matthias, V., Aulinger, A., Bieser, J., Cuesta, J., Geyer, B., Langmann, B., Serikov, I., **Mattis, I.**, Minikin, A., Mona, L., Quante, M., Schumann, U. and Weinzierl, B. 2012. The ash dispersion over Europe during the Eyjafjallajökull eruption – Comparison of CMAQ simulations to remote sensing and air-borne in-situ observations. *Atmos. Environ.*, **48**, 184-194. doi:10.1016/j.atmosenv.2011.06.077.
- Mauldin III, R. L., **Berndt, T.**, Sipilä, M., Paasonen, P., Petäjä, T., Kim, S., Kurtén, T., **Stratmann, F.**, Kerminen, V. M. and Kulmala, M. 2012. A new atmospherically relevant oxidant of sulphur dioxide. *Nature*, **488**, 193-197. doi:10.1038/nature11278.
- Meier, J.**, **Tegen, I.**, Heinold, B. and **Wolke, R.** 2012. Direct and semi-direct radiative effects of absorbing aerosols in Europe: Results from a regional model. *Geophys. Res. Lett.*, **39**, L09802. doi:10.1029/2012GL050994.
- Meier, J.**, **Tegen, I.**, **Mattis, I.**, **Wolke, R.**, Alados Arboledas, L., Apituley, A., Balis, D., Barnaba, F., Chaikovsky, A., Sicard, M., Pappalardo, G., Pietruczuk, A., Stoyanov, D., Ravetta, F. and Rizi, V. 2012. A regional model of European aerosol transport: Evaluation with sun photometer, lidar and air quality data. *Atmos. Environ.*, **47**, 519-532. doi:10.1016/j.atmosenv.2011.09.029.
- Mona, L., Liu, Z., **Müller, D.**, Omar, A., Papayannis, A., Pappalardo, G., Sugimoto, N. and Vaughan, M. 2012. Lidar measurements for desert dust characterization: A review. *Adv. Meteo.*, **2012**, ID 356265 (36 p.). doi:10.1155/2012/356265.
- Monge, M. E., Rosenørn, T., Favez, O., Müller, M., Adler, G., Riziq, A. A., Rudich, Y., **Herrmann, H.**, George, C. and D'Anna, B. 2012. Alternative pathway for atmospheric particles growth. *Proc. Nat. Acad. Sci.*, **109**, 6840-6844. doi:10.1073/pnas.1120593109.
- Müller, D.**, Lee, K.-H., Gasteiger, J., **Tesche, M.**, Weinzierl, B., Kandler, K., **Müller, T.**, Toledano, C., Otto, S., **Althausen, D.** and **Ansmann, A.** 2012. Comparison of optical and microphysical properties of pure Saharan mineral dust observed with AERONET Sun photometer, Raman lidar, and in situ instruments during SAMUM 2006. *J. Geophys. Res. - Atmos.*, **117**, D07211, 1-25. doi:10.1029/2011JD016825.
- Müller, K.**, **Spindler, G.**, **van Pinxteren, D.**, **Gnauk, T.**, **Iinuma, Y.**, **Brüggemann, E.** and **Herrmann, H.** 2012. Ultrafine and fine particles in the atmosphere - Sampling, chemical characterization and sources. *Chem.-Ing.-Tech.*, **84**, 1-8. doi:10.1002/cite.201100208.
- Nielsen, C. J., **Herrmann, H.** and **Weller, C.** 2012. Atmospheric chemistry and environmental impact of the use of amines in carbon capture and storage (CCS). *Chem. Soc. Rev.*, **41**, 6684-6704. doi:10.1039/c2cs35059a.
- Noh, Y. M., **Müller, D.**, Lee, H., Lee, K. H., Kim, K., Shin, S. and Kim, Y. J. 2012. Estimation of radiative forcing by the dust and non-dust content in mixed East Asian pollution plumes on the basis of depolarization ratios measured with lidar. *Atmos. Environ.*, **61**, 221-231.
- Paasonen, P., Olenius, T., Kupiainen, O., Kurtén, T., Petäjä, T., **Birmili, W.**, Hamed, A., Hu, M., Huey, L. G., Plass-Duelmer, C., Smith, J. N., **Wiedensohler, A.**, Loukonen, V., McGrath, M. J., Ortega, I. K., Laaksonen, A., Vehkamäki, H., Kerminen, V.-M. and Kulmala, M. 2012. On the formation of sulphuric acid - amine clusters in varying atmospheric conditions and its influence on atmospheric new particle formation. *Atmos. Chem. Phys.*, **12**, 9113-9133. doi:10.5194/acp-12-9113-2012.
- Pietikäinen, J.-P., O'Donnell, D., Teichmann, C., Karstens, U., **Pfeifer, S.**, Kazil, J., Podzun, R., Fiedler, S., Kokkola, H., **Birmili, W.**, O'Dowd, C., Baltensperger, U., Weingartner, E., Gehrig, R., **Spindler, G.**, Kulmala, M., Feichter, J., Jacob, D. and Laaksonen, A. 2012. The regional aerosol-climate model REMO-HAM. *Geosci. Model Dev.*, **5**, 1323-1339.

## Appendices: Publications

- Rauthe-Schöch, A., Weigelt, A., **Hermann, M.**, Martinsson, B. G., Baker, A. K., Heue, K.-P., Brenninkmeijer, C. A. M., Zahn, A., Scharffe, D., Eckhardt, S., Stohl, A. and Velthoven, P. F. J. 2012. CARIBIC aircraft measurements of Eyjafjallajökull volcanic clouds in April/May 2010. *Atmos. Chem. Phys.*, **12**, 879–902. doi:10.5194/acp-12-879-2012.
- Reichardt, J., **Wandinger, U.**, Klein, V., **Mattis, I.**, Hilber, B. and Begbie, R. 2012. RAMSES: German Meteorological Service autonomous Raman lidar for water vapor, temperature, aerosol, and cloud measurements. *Appl. Optics*, **51**, 8111-8130.
- Romakkaniemi, S., Arola, A., Kokkola, H., **Birmili, W.**, **Tuch, T.**, Kerminen, V.-M., Räisänen, P., Smith, J. N., Korhonen, H. and Laaksonen, A. 2012. Effect of aerosol size distribution changes on AOD, CCN and cloud droplet concentration: Case studies from Erfurt and Melpitz, Germany. *J. Geophys. Res. - Atmos.*, **117**, D07202. doi:10.1029/2011JD017091.
- Schaefer, T.**, **Schindelka, J.**, **Hoffmann, D.** and **Herrmann, H.** 2012. Laboratory kinetic and mechanistic studies on the OH-initiated oxidation of acetone in aqueous solution. *J. Phys. Chem. A*, **116**, 6317-6326. doi:10.1021/jp2120753.
- Schepanski, K., **Tegen, I.** and **Macke, A.** 2012. Comparison of satellite based observations of Saharan dust source areas. *Remote Sens. Environ.*, **123**, 90-97. doi:10.1016/j.rse.2012.03.019.
- Schlegel, M.**, **Knoth, O.**, Arnold, M. and **Wolke, R.** 2012. Numerical solution of multiscale problems in atmospheric modeling. *Appl. Numer. Math.*, **62**, 1531-1543. doi:10.1016/j.apnum.2012.06.023.
- Schlegel, M.**, **Knoth, O.**, Arnold, M. and **Wolke, R.** 2012. Implementation of splitting methods for air pollution modeling. *Geosci. Model Dev.*, **5**, 1395-1405.
- Schulz, M., Prospero, J. M., Baker, A. R., Dentener, F., Ickes, L., Liss, P. S., Mahowald, N. M., Nickovic, S., Pérez, C. G.-P., Rodríguez, S., Sarin, M., **Tegen, I.** and Duce, R. A. 2012. The atmospheric transport and deposition of mineral dust to the ocean - Implications for research needs. *Environ. Sci. Technol.*, **46**, 10390–10404. doi:10.1021/es300073u.
- Setyan, A., Zhang, Q., **Merkel, M.**, Knighton, W. B., Sun, Y., Song, C., Shilling, J. E., Onasch, T. B., Herndon, S. C., Worsnop, D. R., Fast, J. D., Zaveri, R. A., Berg, L. K., **Wiedensohler, A.**, Flowers, B. A., Dubey, M. K. and Subramanian, R. 2012. Characterization of submicron particles influenced by mixed biogenic and anthropogenic emissions using high-resolution aerosol mass spectrometry: Results from CARES. *Atmos. Chem. Phys.*, **12**, 8131-8156. doi:10.5194/acp-12-8131-2012.
- Smirnov, A., Sayer, A. M., Holben, B. N., Hsu, N. C., Sakerin, S. M., **Macke, A.**, Nelson, N. B., Courcoux, Y., Smyth, T. J., Croot, P., Quinn, P. K., Sciare, J., Gulev, S. K., Piketh, S., Losno, R., Kinne, S. and Radionov, V. F. 2012. Effect of wind speed on aerosol optical depth over remote oceans, based on data from the Maritime Aerosol Network. *Atmos. Meas. Tech. (AMT)*, **5**, 377–388. doi:10.5194/amt-5-377-2012.
- Solazzo, E., Bianconi, R., Pirovano, G., Matthias, V., Vautard, R., Appel, W., Bessagnet, B., Brandt, J., Christensen, J., Chemel, C., Coll, I., Ferreira, J., Forkel, R., Francis, X., Chemel, G., Grossi, P., Hansen, A., Miranda, A., Moran, M., Nopmongcol, U., Prank, M., Sartelet, K., Schaap, M., Silver, J., Sokhi, R., Vira, J., Werhahn, J., **Wolke, R.**, Yarwood, G., Zhang, J., Rao, S. T. and Galmarini, S. 2012. Operational model evaluation for particulate matter in Europe and North America in the context of the AQMEII project. *Atmos. Environ.*, **53**, 75-92. doi:10.1016/j.atmosenv.2012.02.045.
- Solazzo, E., Bianconi, R., Vautard, R., Appel, K. W., Bessagnet, B., Brandt, J., Christensen, J. H., Chemel, C., Coll, I., van der Gon, H. D., Ferreira, J., Forkel, R., Francis, X. V., Grell, G., Grossi, P., Hansen, A. B., Jerićević, A., Kraljević, L., Miranda, A. I., Moran, M. D., Nopmongcol, U., Pirovano, G., Prank, M., Riccio, A., Sartelet, K. N., Schaap, M., Silver, J. D., Sokhi, R. S., Vira, J., Werhahn, J., **Wolke, R.**, Yarwood, G., Zhang, J., Rao, S. T. and Galmarini, S. 2012. Model evaluation and ensemble modelling of surface-level ozone in Europe and North America in the context of AQMEII. *Atmos. Environ.*, **53**, 60-74. doi:10.1016/j.atmosenv.2012.01.003.
- Spiegel, J. K., Aemisegger, F., Scholl, M., Wienhold, F. G., Collett Jr., J. L., Lee, T., **van Pinxteren, D.**, **Mertes, S.**, **Tilgner, A.**, **Herrmann, H.**, Werner, R. A., Buchmann, N. and Eugster, W. 2012. Temporal evolution of stable water isotopologues in cloud droplets in a hill cap cloud in central Europe (HCCT-2010). *Atmos. Chem. Phys.*, **12**, 11679-11694. doi:10.5194/acp-12-11679-2012.
- Spiegel, J. K., Aemisegger, F., Scholl, M., Wienhold, F. G., Collett Jr., J. L., Lee, T., **van Pinxteren, D.**, **Mertes, S.**, **Tilgner, A.**, **Herrmann, H.**, Werner, R. A., Buchmann, N. and Eugster, W. 2012. Stable water isotopologue ratios in fog and cloud droplets of liquid clouds are not size-dependent. *Atmos. Chem. Phys.*, **12**, 9855-9863. doi:10.5194/acp-12-9855-2012.

## Appendices: Publications

- Spindler, G., Gnauk, T., Grüner, A., Iinuma, Y., Müller, K., Scheinhardt, S. and Herrmann, H.** 2012. Size-segregated characterization of PM10 at the EMEP site Melpitz (Germany) using a five-stage impactor: A six year study. *J. Atmos. Chem.*, **69**, 127-157. doi:10.1007/s10874-012-9233-6.
- Tatarov, B., Müller, D., Noh, Y.-M., Lee, K.-H., Shin, D.-H., Shin, S.-K., Sugimoto, N., Seifert, P. and Kim, Y.-J. 2012. Record heavy mineral dust outbreaks over Korea in 2010: Two cases observed with multiwavelength aerosol/depolarization/Raman-quartz lidar. *Geophys. Res. Lett.*, **39**, 1-5. doi:10.1029/2012GL051972.
- Tesche, M., Glantz, P., Johansson, C., Norman, M., Hiebsch, A., Ansmann, A., Althausen, D., Engelmann, R. and Seifert, P. 2012. Volcanic ash over Scandinavia originating from the Grímsvötn eruptions in May 2011. *J. Geophys. Res. - Atmos.*, **117**, D09201. doi:10.1029/2011JD017090.
- Tobo, Y., DeMott, P. J., Raddatz, M., Niedermeier, D., Hartmann, S., Kreidenweis, S. M., Stratmann, F. and Wex, H. 2012. Impacts of chemical reactivity on ice nucleation of kaolinite particles: A case study of levoglucosan and sulfuric acid. *Geophys. Res. Lett.*, **39**, L19803. doi:10.1029/2012GL053007.
- van Pinxteren, D., Teich, M. and Herrmann, H. 2012. Hollow fibre liquid-phase microextraction of functionalised carboxylic acids from atmospheric particles combined with capillary electrophoresis/mass spectrometric analysis. *J. Chromatogr. A*, **1267**, 178-188 doi:10.1016/j.chroma.2012.06.097.
- van Pinxteren, M., Müller, C., Iinuma, Y., Stolle, C. and Herrmann, H. 2012. Chemical characterization of dissolved organic compounds from coastal sea surface microlayers (Baltic Sea, Germany) *Environ. Sci. Technol.*, **46**, 10455–10462. doi:10.1021/es204492b.
- Vautard, R., Moran, M. D., Solazzo, E., Gilliam, R. C., Matthias, V., Bianconi, R., Chemel, C., Ferreira, J., Geyer, B., Hansen, A. B., Jericevic, A., Prank, M., Segers, A., Silver, J. D., Werhahn, J., Wolke, R., Rao, S. T. and Galmarini, S. 2012. Evaluation of the meteorological forcing used for the Air Quality Model Evaluation International Initiative (AQMEII) air quality simulation. *Atmos. Environ.*, **53**, 15-37. doi:10.1016/j.atmosenv.2011.10.065.
- Voigtlander, J., Duplissy, J., Rondo, L., Kürten, A. and Stratmann, F. 2012. Numerical simulations of mixing conditions and aerosol dynamics in the CERN CLOUD chamber. *Atmos. Chem. Phys.*, **12**, 2205-2214. doi:10.5194/acp-12-2205-2012.
- Wagner, R., Ajtai, T., Kandler, K., Lieke, K., Linke, C., Müller, T., Schnaiter, M. and Vragel, M. 2012. Complex refractive indices of Saharan dust samples at visible and near UV wavelengths: A laboratory study. *Atmos. Chem. Phys.*, **12**, 2491-2512. doi:10.5194/acp-12-2491-2012.
- Weinzierl, B., Sauer, D., Dahlkötter, F., Minikin, A., Reitebuch, O., Tegen, I., Mayer, B., Emde, C., Gasteiger, J., Petzold, A., Veira, A. and Schuhmann, U. 2012. On the visibility of airborne volcanic ash and mineral dust from the pilot's perspective in flight. *Phys. Chem. Earth*, **45-46**, 87-102. doi:10.1016/j.pce.2012.04.003.
- Wolke, R., Schröder, W., Schrödner, R. and Renner, E. 2012. Influence of grid resolution and meteorological forcing on simulated European air quality: A sensitivity study with the modeling system COSMO-MUSCAT. *Atmos. Environ.*, **53**, 110-130. doi:10.1016/j.atmosenv.2012.02.085.

### 2013

- Almeida, J., Schobesberger, S., Kürten, A., Ortega, I. K., Kupiainen-Määttä, O., Praplan, A. P., Adamov, A., Amorim, A., Bianchi, F., Breitenlechner, M., David, A., Dommen, J., Donahue, N. M., Downard, A., Dunne, E., Duplissy, J., Ehrhart, S., Flagan, R. C., Franchin, A., Guida, R., Hakala, J., Hansel, A., Heinritzi, M., Henschel, H., Jokinen, T., Junninen, H., Kajos, M., Kangasluoma, J., Keskinen, H., Kupc, A., Kurtén, T., Kvashin, A. N., Laaksonen, A., Lehtipalo, K., Leiminger, M., Leppä, J., Loukonen, V., Makhmutov, V., Mathot, S., McGrath, M. J., Nieminen, T., Olenius, T., Onnela, A., Petäjä, T., Riccobono, F., Riipinen, I., Rissanen, M., Rondo, L., Ruuskanen, T., Santos, F. D., Sarnela, N., Schallhart, S., Schnitzhofer, R., Seinfeld, J. H., Simon, M., Sipilä, M., Stozhkov, Y., Stratmann, F., Tomé, A., Tröstl, J., Tsagkogeorgas, G., Vaattovaara, P., Viisanen, Y., Virtanen, A., Vrtala, A., Wagner, P. E., Weingartner, E., Wex, H., Williamson, C., Wimmer, D., Ye, P., Yli-Juuti, T., Carslaw, K. S., Kulmala, M., Curtius, J., Baltensperger, U., Worsnop, D. R., Vehkämäki, H. and Kirkby, J. 2013. Molecular understanding of sulphuric acid–amine particle nucleation in the atmosphere. *Nature*, **502**, 359–363. doi:10.1038/nature12663.
- Amiridis, V., Wandinger, U., Marinou, E., Giannakaki, E., Tsekeli, A., Basart, S., Kazadzis, S., Gkikas, A., Taylor, M., Baldasano, J. and Ansmann, A. 2013. Optimizing CALIPSO Saharan dust retrievals. *Atmos. Chem. Phys.*, **13**, 12089-1210. doi:10.5194/acp-13-12089-2013.

## Appendices: Publications

- Andersson, S., Martinsson, B. G., Friberg, J., Brenninkmeijer, C. A. M., Rauthe-Schöch, A., **Hermann, M.**, van Velthoven, P. F. J. and Zahn, A. 2013. Composition and evolution of volcanic aerosol from eruptions of Kasatochi, Sarychev and Eyjafjallajökull in 2008 – 2010 based on CARIBIC observations. *Atmos. Chem. Phys.*, **13**, 1781-1796. doi:10.5194/acp-13-1781-2013.
- Asmi, A., Coen, M. C., Ogren, J. A., Andrews, E., Sheridan, P., Jefferson, A., Weingartner, E., Baltensperger, U., Bukowiecki, N., Lihavainen, H., Kivekas, N., Asmi, E., Aalto, P. P., Kulmala, M., **Wiedensohler, A.**, **Birmili, W.**, **Hamed, A.**, O'Dowd, C., Jennings, S. G., Weller, R., Flentje, H., Fjaeraa, A. M., Fiebig, M., Myhre, C. L., Hallar, A. G., Swietlicki, E., Kristensson, A. and Laj, P. 2013. Aerosol decadal trends - Part 2: In-situ aerosol particle number concentrations at GAW and ACTRIS stations. *Atmos. Chem. Phys.*, **13**, 895-916. doi:10.5194/acp-13-895-2013.
- Augustin, S.**, **Hartmann, S.**, Pummer, B., Grothe, H., **Niedermeier, D.**, **Clauss, T.**, **Voigtlander, J.**, **Tomsche, L.**, **Wex, H.** and **Stratmann, F.** 2013. Immersion freezing of birch pollen washing water. *Atmos. Chem. Phys.*, **13**, 10989-11003. doi:10.5194/acp-13-10989-2013.
- Bange, J., Esposito, M., Lenschow, D. H., Brown, P. R. A., Dreiling, V., Giez, A., Mahrt, L., Malinowski, S., Rodi, A. R., Shaw, R. A., **Siebert, H.**, Smit, H. and Zöger, M. 2013. . M. Wendisch and J.-L. Brenguier (Ed.), In: . Wiley-VCH, Weinheim, Germany, p. 7-76 (Chapter 2).
- Brückner, M.**, **Macke, A.**, Wendisch, M., **Kanitz, T.** and Pospichal, B. 2013. . R. F. Cahalan and J. Fischer (Ed.), In: . 1531, p. 264-267. (AIP Conference Proceedings)
- Birmili, W.**, **Rehn, J.**, Vogel, A., Boehlke, C., Weber, K. and **Rasch, F.** 2013. Micro-scale variability of urban particle number and mass concentrations in Leipzig, Germany. *Meteorol. Z.*, **22**, 155-165. doi:10.1127/0941-2948/2013/0394.
- Birmili, W.**, **Tomsche, L.**, **Sonntag, A.**, Opelt, C., **Weinhold, K.**, **Nordmann, S.** and Schmidt, W. 2013. Variability of aerosol particles in the urban atmosphere of Dresden (Germany): Effects of spatial scale and particle size. *Meteorol. Z.*, **22**, 195-211. doi:10.1127/0941-2948/2013/0395.
- Bley, S.** and **Deneke, H.** 2013. A threshold-based cloud mask for the high-resolution visible channel of Meteosat Second Generation SEVIRI. *Atmos. Meas. Tech. (AMT)*, **6**, 2713-2723. doi:10.5194/amt-6-2713-2013.
- Böge, O.**, **Mutzel, A.**, **Iinuma, Y.**, Yli-Pirilä, P., **Kahnt, A.**, Joutsensaari, J. and **Herrmann, H.** 2013. Gas-phase products and secondary organic aerosol formation from the ozonolysis and photooxidation of myrcene. *Atmos. Environ.*, **79**, 553-560. doi:10.1016/j.atmosenv.2013.07.034.
- Bräuer, P.**, **Tilgner, A.**, **Wolke, R.** and **Herrmann, H.** 2013. Mechanism development and modelling of tropospheric multiphase halogen chemistry: The CAPRAM Halogen Module 2.0 (HM2). *J. Atmos. Chem.*, **70**, 19-52. doi:10.1007/s10874-013-9249-6.
- Bühl, J.**, **Ansmann, A.**, **Seifert, P.**, **Baars, H.** and **Engelmann, R.** 2013. Toward a quantitative characterization of heterogeneous ice formation with lidar/radar: Comparison of CALIPSO/CloudSat with ground-based observations. *Geophys. Res. Lett.*, **40**, 4404–4408. doi:10.1002/grl.50792.
- Chi, X., Winderlich, J., Mayer, J.-C., Panov, A. V., Heimann, M., **Birmili, W.**, **Heintzenberg, J.**, Cheng, Y. and Andreae, M. O. 2013. Long-term measurements of aerosol and carbon monoxide at the ZOTTO tall tower to characterize polluted and pristine air in the Siberian taiga. *Atmos. Chem. Phys.*, **13**, 12271-12298. doi:10.5194/acp-13-12271-2013.
- Clauss, T.**, **Kiselev, A.**, **Hartmann, S.**, **Augustin, S.**, **Pfeifer, S.**, **Niedermeier, D.**, **Wex, H.** and **Stratmann, F.** 2013. Application of linear polarized light for the discrimination of frozen and liquid droplets in ice nucleation experiments. *Atmos. Meas. Tech. (AMT)*, **6**, 1041-1052. doi:10.5194/amt-6-1041-2013.
- Crippa, M., Canonaco, F., Slowik, J. G., El Haddad, I., DeCarlo, P. F., Mohr, C., Heringa, M. F., Chirico, R., Marchand, N., Temime-Roussel, B., Abidi, E., **Poulain, L.**, **Wiedensohler, A.**, Baltensperger, U. and Prevot, A. S. H. 2013. Primary and secondary organic aerosol origin by combined gas-particle phase source apportionment. *Atmos. Chem. Phys.*, **13**, 8411-8426. doi:10.5194/acp-13-8411-2013.
- Crippa, M., DeCarlo, P. F., Slowik, J. G., Mohr, C., Heringa, M. F., Chirico, R., **Poulain, L.**, Freutel, F., Sciare, J., Cozic, J., Di Marco, C. F., Elsasser, M., Nicolas, J. B., Marchand, N., Abidi, E., **Wiedensohler, A.**, Drewnick, F., Schneider, J., Borrmann, S., Nemitz, E., Zimmermann, R., Jaffrezo, J. L., Prevot, A. S. H. and Baltensperger, U. 2013. Wintertime aerosol chemical composition and source apportionment of the organic fraction in the metropolitan area of Paris. *Atmos. Chem. Phys.*, **13**, 961-981. doi:10.5194/acp-13-961-2013.
- Cusack, M., Perez, N., Pey, J., **Wiedensohler, A.**, Alastuey, A. and Querol, X. 2013. Variability of sub-micrometer particle number size distributions and concentrations in the Western Mediterranean regional background. *Tellus Series B*, **65**, doi:10.3402/tellusb.v65i0.19243.

## Appendices: Publications

- Cziczo, D. J., Garimella, S., **Raddatz, M.**, Hoehler, K., Schnaiter, M., Saathoff, H., Moehler, O., Abbatt, J. P. D. and Ladino, L. A. 2013. Ice nucleation by surrogates of Martian mineral dust: What can we learn about Mars without leaving Earth? *J. Geophys. Res. - Planets*, **118**, 1-10. doi:10.1002/jgre.20155.
- Ebell, K., Orlandi, E., **Hünerbein, A.**, Löhnert, U. and Crewell, S. 2013. Combining ground-based with satellite-based measurements in the atmospheric state retrieval: Assessment of the information content. *J. Geophys. Res. - Atmos.*, **118**, 6940-6956. doi:10.1002/jgrd.50548.
- Fiedler, S., **Schepanski, K.**, **Heinold, B.**, Knippertz, P. and **Tegen, I.** 2013. Climatology of nocturnal low-level jets over North Africa and implications for modeling mineral dust emission. *J. Geophys. Res. - Atmos.*, **118**, 6100-6121. doi:10.1002/jgrd.50394.
- Fomba, K. W.**, **Müller, K.**, **van Pinxteren, D.** and **Herrmann, H.** 2013. Aerosol size-resolved trace metal composition in remote northern tropical Atlantic marine environment: Case study Cape Verde Islands. *Atmos. Chem. Phys.*, **13**, 4801-4814. doi:10.5194/acp-13-4801-2013.
- Freutel, F., Schneider, J., Drewnick, F., von der Weiden-Reinmüller, S. L., Crippa, M., Prévôt, A. S. H., Baltensperger, U., **Poulain, L.**, **Wiedensohler, A.**, Sciare, J., Sarda-Estève, R., Burkhardt, J. F., Eckhardt, S., Stohl, A., Gros, V., Colomb, A., Michoud, V., Doussin, J. F., Borbon, A., Haeffelin, M., Morille, Y., Beekmann, M. and Borrmann, S. 2013. Aerosol particle measurements at three stationary sites in the megacity of Paris during summer 2009: Meteorology and air mass origin dominate aerosol particle composition and size distribution. *Atmos. Chem. Phys.*, **13**, 933-959. doi:10.5194/acp-13-933-2013.
- Genberg, J., van der Gon, H., Simpson, D., Swietlicki, E., Areskoug, H., Beddows, D., Ceburnis, D., Fiebig, M., Hansson, H. C., Harrison, R. M., Jennings, S. G., Saarikoski, S., **Spindler, G.**, Visschedijk, A. J. H., **Wiedensohler, A.**, Yttri, K. E. and Bergstrom, R. 2013. Light-absorbing carbon in Europe - Measurement and modelling, with a focus on residential wood combustion emissions. *Atmos. Chem. Phys.*, **13**, 8719-8738. doi:10.5194/acp-13-8719-2013.
- Guo, J., **Tilgner, A.**, Yeung, C. P., Wang, Z., Louie, P., Luk, C., Xu, Z., Yuan, C., Gao, Y., Poon, S., **Herrmann, H.**, Lee, S., Lam, K. S. and Wang, T. 2013. Atmospheric peroxides in a polluted subtropical environment: Seasonal variation, sources and sinks, and importance of heterogeneous processes. *Environ. Sci. Technol.*, online. doi:10.1021/es403229x.
- Hamburger, T., Matisāns, M., Tunved, P., Ström, J., Calderon, S., Hoffmann, P., Hochschild, G., Gross, J., **Schmeissner, T.**, **Wiedensohler, A.** and Krejci, R. 2013. Long-term in situ observations of biomass burning aerosol at a high altitude station in Venezuela – sources, impacts and interannual variability. *Atmos. Chem. Phys.*, **13**, 9837–9853. doi:10.5194/acp-13-9837-2013.
- Harris, E., Sinha, B., **van Pinxteren, D.**, **Tilgner, A.**, **Fomba, W.**, Schneider, J., Roth, A., **Gnauk, T.**, **Fahlbusch, B.**, **Mertes, S.**, Lee, T., Collett, J., Foley, S., Borrmann, S., Hoppe, P. and **Herrmann, H.** 2013. Enhanced role of transition metal ion catalysis during in-cloud oxidation of  $\text{SO}_2$ . *Science*, **340**, 727-730. doi:10.1126/science.1230911.
- Hartmann, S.**, **Augustin, S.**, **Clauss, T.**, **Wex, H.**, Šantl-Temkiv, T., **Voigtlander, J.**, **Niedermeier, D.** and **Stratmann, F.** 2013. Immersion freezing of ice nucleation active protein complexes. *Atmos. Chem. Phys.*, **13**, 5751-5766. doi:10.5194/acp-13-5751-2013.
- Healy, R. M., Sciare, J., **Poulain, L.**, Crippa, M., **Wiedensohler, A.**, Prévôt, A. S. H., Baltensperger, U., Sarda-Estève, R., McGuire, M. L., Jeong, C.-H., McGillicuddy, E., O'Connor, I. P., Sodeau, J. R., Evans, G. J. and Wenger, J. C. 2013. Quantitative determination of carbonaceous particle mixing state in Paris using single-particle mass spectrometer and aerosol mass spectrometer measurements. *Atmos. Chem. Phys.*, **13**, 9479-9496. doi:10.5194/acp-13-9479-2013.
- Heinold, B., Knippertz, P., Marsham, J. H., Fiedler, S., Dixon, N. S., Schepanski, K., Laurent, B. and **Tegen, I.** 2013. The role of deep convection and nocturnal low-level jets for dust emission in summertime West Africa: Estimates from convection-permitting simulations. *J. Geophys. Res. - Atmos.*, **118**, 4385–4400. doi:10.1002/jgrd.50402.
- Heintzenberg, J.**, **Birmili, W.**, **Seifert, P.**, Panov, A., Chi, X. and Andreae, M. O. 2013. Mapping the aerosol over Eurasia from the Zotino Tall Tower (ZOTTO). *Tellus B*, **65**, UNSP 20062. doi:10.3402/tellusb.v65i0.20062.
- Hellmuth, O.**, Khvorostyanov, V. I., Curry, J. A., Shchekin, A. K., Schmelzer, J. W. P., Feistel, R., Djikaev, Y. S. and Baidakov, V. G. (Eds.) (2013), Review series on selected topics of atmospheric sol formation: Volume 1 : Selected aspects of atmospheric ice and salt crystallisation, ix, 513 pp., Joint Institute for Nuclear Research (JINR), Dubna. (Nucleation theory and applications : Special issues)

## Appendices: Publications

- Hellmuth, O.**, Khvorostyanov, V. I., Curry, J. A., Shchekin, A. K., Schmelzer, J. W. P., Feistel, R., Djikaev, Y. S. and Baidakov, V. G. 2013. . J. W. P. Schmelzer and **O. Hellmuth** (Ed.), In: . Joint Institute for Nuclear Research (JINR), Dubna, **Vol. 1: Selected aspects of atmospheric ice and salt crystallisation**, p. 349-484. (Nucleation theory and applications : Special issues)
- Hellmuth, O.**, Khvorostyanov, V. I., Curry, J. A., Shchekin, A. K., Schmelzer, J. W. P., Feistel, R., Djikaev, Y. S. and Baidakov, V. G. 2013. . J. W. P. Schmelzer and **O. Hellmuth** (Ed.), In: . Joint Institute for Nuclear Research (JINR), Dubna, **Vol. 1: Selected aspects of atmospheric ice and salt crystallisation**, p. 69-347. (Nucleation theory and applications : Special issues)
- Hellmuth, O.**, Khvorostyanov, V. I., Curry, J. A., Shchekin, A. K., Schmelzer, J. W. P. and Baidakov, V. G. 2013. . J. W. P. Schmelzer and **O. Hellmuth** (Ed.), In: . Joint Institute for Nuclear Research (JINR), Dubna, **Vol. 1: Selected aspects of atmospheric ice and salt crystallisation**, p. 1-67. (Nucleation theory and applications : Special issues)
- Hieronymi, M.** and **Macke, A.** 2013. . R. F. Cahalan and J. Fischer (Ed.), In: . **1531**, p. 915-918. (AIP Conference Proceedings)
- Hillemann, L., Zschoppe, A., Caldow, R., Sem, G. J. and **Wiedensohler, A.** 2013. An ultrafine particle monitor for size-resolved number concentration measurements in atmospheric aerosols. *J. Aerosol Sci.*, online first. doi:10.1016/j.jaerosci.2013.10.007.
- Horváth, Á.** 2013. Horváth, Á. (2013), Improvements to MISR stereo motion vectors. *J. Geophys. Res. - Atmos.*, **118**, 5600-5620. doi:10.1002/jgrd.50466.
- Iinuma, Y.**, Kahnt, A., **Mutzel, A.**, **Böge, O.** and **Herrmann, H.** 2013. Ozone-driven secondary organic aerosol production chain. *Environ. Sci. Technol.*, **47**, 3639-3647. doi:10.1021/es305156z.
- Jähn, M.**, **Wolke, R.** and **Sändig, B.** 2013. Detection of odor sources and high concentrations of pollutants in the Ore Mountains by modeling of air mass paths. *Meteorol. Z.*, **22**, 213-220. doi:10.1127/0941-2948/2013/0389
- Kanitz, T.**, **Ansmann, A.**, **Engelmann, R.** and **Althausen, D.** 2013. North-south cross sections of the vertical aerosol distribution over the Atlantic Ocean from multiwavelength Raman/polarization lidar during Polarstern cruises. *J. Geophys. Res. - Atmos.*, **118**, 2643-2655. doi:10.1002/jgrd.50273.
- Kanitz, T.**, **Ansmann, A.**, **Seifert, P.**, **Engelmann, R.**, **Kalisch, J.** and **Althausen, D.** 2013. Radiative effect of aerosols above the northern and southern Atlantic Ocean as determined from shipborne lidar observations. *J. Geophys. Res. - Atmos.*, **118**, First published online. doi:10.1002/2013JD019750.
- Karl, M., Leck, C., Coz, E. and **Heintzenberg, J.** 2013. Marine nanogels as a source of atmospheric nanoparticles in the high Arctic. *Geophys. Res. Lett.*, **40**, 3738-3743. doi:10.1002/grl.50661.
- Keskinen, H., Virtanen, A., Joutsensaari, J., **Tsagkogeorgas, G.**, Duplissy, J., Schobesberger, S., Gysel, M., Riccobono, F., Slowik, J. G., Bianchi, F., Yli-Juuti, T., Lehtipalo, K., Rondo, L., Breitenlechner, M., Kupc, A., Almeida, J., Amorim, A., Dunne, E. M., Downard, A. J., Ehrhart, S., Franchin, A., Kajos, M. K., Kirkby, J., Kürten, A., Nieminen, T., Makhmutov, V., Mathot, S., Miettinen, P., Onnela, A., Petäjä, T., Praplan, A., Santos, F. D., Schallhart, S., Sipilä, M., Stozhkov, Y., Tomé, A., Vaattovaara, P., Wimmer, D., Prevot, A., Dommen, J., Donahue, N. M., Flagan, R. C., Weingartner, E., Viisanen, Y., Riipinen, I., Hansel, A., Curtius, J., Kulmala, M., Worsnop, D. R., Baltensperger, U., **Wex, H.**, **Stratmann, F.** and Laaksonen, A. 2013. Evolution of particle composition in CLOUD nucleation experiments. *Atmos. Chem. Phys.*, **13**, 5587-5600. doi:10.5194/acp-13-5587-2013.
- Knoth, O.** and Wensch, J. 2013. Generalized split-explicit Runge-Kutta methods for the compressible Euler equations. *Mon. Wea. Rev.*, First published online. doi:10.1175/MWR-D-13-00068.1.
- Kristensen, T. B.**, Prisle, N. L. and Bilde, M. 2013. Cloud droplet activation of mixed model HULIS and NaCl particles: Experimental results and kappa-Köhler theory. *Atmos. Res.*, online. doi:10.1016/j.atmosres.2013.09.017.
- Liu, C., Panetta, R. L., Yang, P., **Macke, A.** and Baran, A. J. 2013. Modeling the scattering properties of mineral aerosols using concave fractal polyhedra. *Appl. Optics*, **52**, 640-652.
- Liu, L., Breitner, S., Schneider, A., Cyrys, J., Brüske, I., Franck, U., Schlink, U., Leitte, A. M., Herbarth, O., **Wiedensohler, A.**, **Wehner, B.**, Pan, X. C., Wichmann, H.-E. and Peters, A. 2013. Size-fractionated particulate air pollution and cardiovascular emergency room visits in Beijing, China. *Environ. Res.*, **121**, 52-63. doi:10.1016/j.envres.2012.10.009.
- Merk, D.** and Zinner, T. 2013. Detection of convective initiation using Meteosat SEVIRI: Implementation in and verification with the tracking and nowcasting algorithm Cb-TRAM. *Atmos. Meas. Tech. (AMT)*, **6**, 1903-1918. doi:10.5194/amt-6-1903-2013.

## Appendices: Publications

- Mouchel-Vallon, C., **Bräuer, P.**, Camredon, M., Valorso, R., Madronich, S., **Herrmann, H.** and Aumont, B. 2013. Explicit modeling of volatile organic compounds partitioning in the atmospheric aqueous phase. *Atmos. Chem. Phys.*, **13**, 1023-1037. doi:10.5194/acp-13-1023-2013.
- Müller, D.**, Veselovskii, I., Kolgotin, A., **Tesche, M.**, **Ansmann, A.** and Dubovik, O. 2013. Vertical profiles of pure dust and mixed-smoke-dust plumes inferred from inversion of multiwavelength Raman/Polarization lidar data and comparison to AERONET retrievals and in situ observations. *Appl. Optics*, **52**, 3178-3202. doi:10.1364/AO.52.003178.
- Mutzel, A.**, **Rodigast, M.**, **Iinuma, Y.**, **Böge, O.** and **Herrmann, H.** 2013. An improved method for the quantification of SOA bound peroxides (Technical note). *Atmos. Environ.*, **67**, 365-369. doi:10.1016/j.atmosenv.2012.11.012.
- Navas-Guzmán, F., **Müller, D.**, Bravo-Aranda, J. A., Guerrero-Rascado, J. L., Granados-Muñoz, M. J., Pérez-Ramírez, D., Olmo, F. J. and Alados-Arboledas, L. 2013. Eruption of the Eyjafjallajökull volcano in spring 2010: Multiwavelength Raman lidar measurements of sulphate particles in the lower troposphere. *J. Geophys. Res. - Atmos.*, **118**, 1804-1813. doi:10.1002/jgrd.50116.
- Nicolae , D., Nemuc, A., Talianu, C., Vasilescu, J., Belegante, L. and **Müller, D.** 2013. Characterization of fresh and aged biomass burning events using multiwavelength Raman lidar and mass spectrometry. *J. Geophys. Res. - Atmos.*, **118**, 2956-2965. doi:10.1002/jgrd.50324.
- Niedermeier, D., Ervens, B., **Clauss, T.**, **Voigtlander, J.**, **Wex, H.**, **Hartmann, S.** and **Stratmann, F.** 2013. A computationally-efficient description of heterogeneous freezing: A simplified version of the Soccer ball model. *Geophys. Res. Lett.*, online first. doi:10.1002/2013GL058684.
- Noh, Y. M., **Müller, D.**, Lee, H. and Choi, T. J. 2013. Influence of biogenic pollen on optical properties of atmospheric aerosols observed by lidar over Gwangju, South Korea. *Atmos. Environ.*, **69**, 139-147. doi:10.1016/j.atmosenv.2012.12.018.
- Nordmann, S.**, **Birmili, W.**, **Weinhold, K.**, **Müller, K.**, **Spindler, G.** and **Wiedensohler, A.** 2013. Measurements of the mass absorption cross section of atmospheric soot particles using Raman spectroscopy. *J. Geophys. Res. - Atmos.*, **118**, 12075-12085. doi:10.1002/2013JD020021.
- Paasonen, P., Asmi, A., Petäjä, T., Kajos, M. K., Aijala, M., Junninen, H., Holst, T., Abbatt, J. P. D., Arneth, A., **Birmili, W.**, van der Gon, H. G., Hamed, A., Hoffer, A., Laakso, L., Laaksonen, A., Leaitch, W. R., Plass-Dülmer, C., Pryor, S. C., Raisanen, P., Swietlicki, E., **Wiedensohler, A.**, Worsnop, D. R., Kerminen, V.-M. and Kulmala, M. 2013. Warming-induced increase in aerosol number concentration likely to moderate climate change. *Nat. Geosci.*, **6**, 438-442. doi:10.1038/ngeo1800.
- Pappalardo, G., Mona, L., D'Amico, G., **Wandinger, U.**, Adam, M., Amodeo, A., **Ansmann, A.**, Apituley, A., Arboledas, L. A., Balis, D., Boselli, A., Bravo-Aranda, J. A., Chaikovsky, A., Comeron, A., Cuesta, J., De Tomasi, F., Freudenthaler, V., Gausa, M., Giannakaki, E., Giehl, H., Giunta, A., Grigorov, I., Gross, S., Haefelin, M., **Hebsch, A.**, Iarlori, M., Lange, D., Linne, H., Madonna, F., Mattis, I., Mamouri, R. E., McAuliffe, M. A. P., Mitev, V., Molero, F., Navas-Guzman, F., Nicolae, D., Papayannis, A., Perrone, M. R., Pietras, C., Pietruczuk, A., Pisani, G., Preissler, J., Pujadas, M., Rizi, V., Ruth, A. A., Schmidt, J., Schnell, F., **Seifert, P.**, Serikov, I., Sicard, M., Simeonov, V., Spinelli, N., Stebel, K., **Tesche, M.**, Trickl, T., Wang, X., Wagner, F., Wiegner, M. and Wilson, K. M. 2013. Four-dimensional distribution of the 2010 Eyjafjallajökull volcanic cloud over Europe observed by EARLINET. *Atmos. Chem. Phys.*, **13**, 4429-4450. doi:10.5194/acp-13-4429-2013.
- Petzold, A., Ogren, J. A., Fiebig, M., Laj, P., Li, S. M., Baltensperger, U., Holzer-Popp, T., Kinne, S., Pappalardo, G., Sugimoto, N., Wehrli, C., **Wiedensohler, A.** and Zhang, X. Y. 2013. Recommendations for reporting „black carbon“ measurements. *Atmos. Chem. Phys.*, **13**, 8365-8379. doi:10.5194/acp-13-8365-2013.
- Reiche, N., **Mothes, F.**, Fiedler, P. and Borsdorf, H. 2013. A solid-phase microextraction method for the in vivo sampling of MTBE in common reed (*Phragmites australis*). *Environmental Monitoring and Assessment*, **185**, 7133-7144. doi:10.1007/s10661-013-3089-3.
- Richters, S.** and **Berndt, T.** 2013. Gas-phase reaction of monomethylhydrazine with ozone: Kinetics and OH radical formation. *Int. J. Chem. Kinet.*, online. doi:10.1002/kin.20816.
- Rizzo, L. V., Artaxo, P., **Müller, T.**, **Wiedensohler, A.**, Paixao, M., Cirino, G. G., Arana, A., Swietlicki, E., Roldin, P., Fors, E. O., Wiedemann, K. T., Leal, L. S. M. and Kulmala, M. 2013. Long term measurements of aerosol optical properties at a primary forest site in Amazonia. *Atmos. Chem. Phys.*, **13**, 2391-2413. doi:10.5194/acp-13-2391-2013.

## Appendices: Publications

- Scheinhardt, S., Müller, K., Spindler, G. and Herrmann, H.** 2013. Complexation of trace metals in size-segregated aerosol particles at nine sites in Germany. *Atmos. Environ.*, **74**, 102-109. doi:10.1016/j.atmosenv.2013.03.023.
- Scheinhardt, S., Spindler, G., Leise, S., Müller, K., Iinuma, Y., Zimmermann, F., Matschullat, J. and Herrmann, H.** 2013. Comprehensive chemical characterisation of size-segregated PM<sub>10</sub> in Dresden and estimation of changes due to global warming. *Atmos. Environ.*, **75**, 365-373. doi:10.1016/j.atmosenv.2013.04.059.
- Schepanski, K., Flamant, C., Chaboureau, J.-P., Kocha, C., Banks, J. R., Brindley, H. E., Lavaysse, C., Marnas, F., Pelon, J. and Tulet, P.** 2013. Characterization of dust emission from alluvial sources using aircraft observations and high-resolution modeling. *J. Geophys. Res. - Atmos.*, **118**, 1-23. doi:10.1002/jgrd.50538.
- Schindelka, J., Iinuma, Y., Hoffmann, D. and Herrmann, H.** 2013. Sulfate radical-initiated formation of isoprene-derived organosulfates in atmospheric aerosols. *Faraday Discuss.*, **165**, 237-259. doi:10.1039/C3FD00042G.
- Schmidt, J., Wandinger, U. and Malinka, A.** 2013. Dual-field-of-view Raman lidar measurements for the retrieval of cloud microphysical properties. *Appl. Optics*, **52**, 2235-2247.
- Shchekin, A., Shabaev, I. and Hellmuth, O.** 2013. Thermodynamic and kinetic theory of nucleation, deliquescence and efflorescence transitions in the ensemble of droplets on soluble particles. *J. Chem. Phys.*, **138**, 054704. doi:10.1063/1.4789309.
- Shin, S., Müller, D., Kim, Y. J., Tatarov, B., Shin, D., Seifert, P. and Noh, Y. M.** 2013. The retrieval of the Asian dust depolarization ratio in Korea with the correction of the polarization-dependent transmission. *Asia-Pac. J. Atmos. Sci.*, **49**, 19-25. doi:10.1007/s13143-013-0003-4.
- Siebert, H., Bethke, J., Bierwirth, E., Conrath, T., Dieckmann, K., Ditas, F., Ehrlich, A., Farrell, D., Hartmann, S., Izaguirre, M. A., Katzwinkel, J., Nuijens, L., Roberts, G., Schäfer, M., Shaw, R. A., Schmeissner, T., Serikov, I., Stevens, B., Stratmann, F., Wehner, B., Wendisch, M., Werner, F. and Wex, H.** 2013. The fine-scale structure of the trade wind cumuli over Barbados – an introduction to the CARRIBA project. *Atmos. Chem. Phys.*, **13**, 10061-10077. doi:10.5194/acp-13-10061-2013.
- Spindler, G., Grüner, A., Müller, K., Schlimper, S. and Herrmann, H.** 2013. Long-time size-segregated particle (PM<sub>10</sub>, PM<sub>2.5</sub>, PM<sub>1</sub>) characterization study at Melpitz - Influence of air mass inflow, weather conditions and season. *J. Atmos. Chem.*, **70**, 165-195. doi:10.1007/s10874-013-9263-8.
- Tegen, I., Schepanski, K. and Heinold, B.** 2013. Comparing two years of Saharan dust source activation obtained by regional modelling and satellite observations. *Atmos. Chem. Phys.*, **13**, 2381-2390. doi:10.5194/acp-13-2381-2013.
- Teich, M., van Pinxteren, D. and Herrmann, H.** 2013. Determination of nitrophenolic compounds from atmospheric particles using hollow fibre liquid-phase micro extraction and capillary electrophoresis/mass spectrometry analysis. *Electrophoresis*, online. doi:10.1002/elps.201300448.
- Tesche, M., Wandinger, U., Ansmann, A., Althausen, D., Müller, D., Omar, A. H. and Vaughan, M. A.** 2013. Ground-based validation of CALIPSO observations of dust and smoke in the Cape Verde region. *J. Geophys. Res. - Atmos.*, **118**, 2889-2902. doi:10.1002/jgrd.50248.
- Tilgner, A., Bräuer, P., Wolke, R. and Herrmann, H.** 2013. Modelling multiphase chemistry in deliquescent aerosols and clouds using CAPRAM3.0i. *J. Atmos. Chem.*, **70**, 221-256. doi:10.1007/s10874-013-9267-4.
- van Pinxteren, M. and Herrmann, H.** 2013. Glyoxal and methylglyoxal in Atlantic seawater and marine aerosol particles: Method development and first application during the Polarstern cruise ANT XXVII/4. *Atmos. Chem. Phys.*, **13**, 11791-11802. doi:10.5194/acp-13-11791-2013.
- von Bismarck-Osten, C., Birmili, W., Ketzel, M., Massling, A., Petäjä, T. and Weber, S.** 2013. Characterization of parameters influencing the spatio-temporal variability of urban particle number size distributions in four European cities. *Atmos. Environ.*, **77**, 415-429.
- Wagner, J., Ansmann, A., Wandinger, U., Seifert, P., Schwarz, A., Tesche, M., Chaikovsky, A. and Dubovik, O.** 2013. Evaluation of the Lidar/Radiometer Inversion Code (LIRIC) to determine microphysical properties of volcanic and desert dust. *Atmos. Meas. Tech. (AMT)*, **6**, 1707-1724. doi:10.5194/amt-6-1707-2013.
- Wang, W., Iinuma, Y., Kahnt, A., Ryabtsova, O., Mutzel, A., Vermeylen, R., van der Veken, P., Maenhaut, W., Herrmann, H. and Claeys, M.** 2013. Formation of secondary organic aerosol tracers from the photooxidation of isoprene and isoprene-derived alkene diols under low-NOx conditions. *Faraday Discuss.*, **165**, 261-272. doi:10.1039/C3FD00092C.

## Appendices: Publications

- Wang, Z. B.**, Hu, M., Mogensen, D., Yue, D. L., Zheng, J., Zhang, R. Y., Liu, Y., Yuan, B., Li, X., Shao, M., Zhou, L., **Wiedensohler, A.** and Boy, M. 2013. The simulations of sulfuric acid concentration and new particle formation in an urban atmosphere in China. *Atmos. Chem. Phys.*, **13**, 11157–11167. doi:10.5194/acp-13-11157-2013.
- Wang, Z. B.**, Hu, M., Sun, J. Y., **Wu, Z. J.**, Yue, D. L., Shen, X. J., Zhang, Y. M., Pei, X. Y., Cheng, Y. F. and **Wiedensohler, A.** 2013. Characteristics of regional new particle formation in urban and regional background environments in the North China Plain. *Atmos. Chem. Phys.*, **13**, 12495–12506. doi:10.5194/acp-13-12495-2013.
- Wang, Z. B.**, Hu, M., **Wu, Z. J.**, Yue, D. L., He, L. Y., Huang, X. F., Liu, X. G. and **Wiedensohler, A.** 2013. Long-term measurements of particle number size distributions and the relationships with air mass history and source apportionment in the summer of Beijing. *Atmos. Chem. Phys.*, **13**, 10159–10170. doi:10.5194/acp-13-10159-2013.
- Weller, C.**, **Horn, S.** and **Herrmann, H.** 2013. Effects of Fe(III)-concentration, speciation, excitation-wavelength and light intensity on the quantum yield of iron(III)-oxalato complex photolysis. *J. Photoch. Photobio. A*, **255**, 41–49. doi:10.1016/j.jphotochem.2013.01.014.
- Weller, C.**, **Horn, S.** and **Herrmann, H.** 2013. Photolysis of Fe(III) carboxylato complexes: Fe(II) quantum yields and reaction mechanisms. *J. Photoch. Photobio. A*, **268**, 24–36. doi:10.1016/j.jphotochem.2013.06.022.
- Werner, F., **Ditas, F.**, **Siebert, H.**, **Simmel, M.**, **Wehner, B.**, Pilewski, P., **Schmeissner, T.**, Shaw, R. A., **Hartmann, S.**, **Wex, H.**, Roberts, G. C. and Wendisch, M. 2013. Twomey effect observed from collocated microphysical and remote sensing measurements over shallow cumulus. *J. Geophys. Res. - Atmos.*, online first. doi:10.1002/2013JD020131.
- Werner, F., **Siebert, H.**, Pilewskie, P., **Schmeissner, T.**, Shaw, R. A. and Wendisch, M. 2013. New airborne retrieval approach for trade wind cumulus properties under overlying cirrus. *J. Geophys. Res. - Atmos.*, **118**, 3634–3649. doi:10.1002/jgrd.50334.
- Westervelt, D. M., Pierce, J. R., Riipinen, I., Trivitayanurak, W., **Hamed, A.**, Kulmala, M., Laaksonen, A., Decesari, S. and Adams, P. J. 2013. Formation and growth of nucleated particles into cloud condensation nuclei: Model-measurement comparison. *Atmos. Chem. Phys.*, **13**, 7645–7663. doi:10.5194/acp-13-7645-2013.
- Wu, Z.**, **Birmili, W.**, **Poulain, L.**, **Merkel, M.**, **Fahlbusch, B.**, **van Pinxteren, D.**, **Herrmann, H.** and **Wiedensohler, A.** 2013. Particle hygroscopicity during atmospheric new particle formation events: Implications for the chemical species contributing to particle growth. *Atmos. Chem. Phys.*, **13**, 6637–6646. doi:10.5194/acp-13-6637-2013.
- Wu, Z. J.**, **Poulain, L.**, **Henning, S.**, **Dieckmann, K.**, **Birmili, W.**, **Merkel, M.**, **van Pinxteren, D.**, **Spindler, G.**, Müller, K., **Stratmann, F.**, **Herrmann, H.** and **Wiedensohler, A.** 2013. Relating particle hygroscopicity and CCN activity to chemical composition during the HCCT-2010 field campaign. *Atmos. Chem. Phys.*, **13**, 7983–7996. doi:10.5194/acp-13-7983-2013.
- Yue, D. L., Hu, M., Wang, Z. B., Wen, M. T., Guo, S., Zhong, L. J., **Wiedensohler, A.** and Zhang, Y. H. 2013. Comparison of particle number size distributions and new particle formation between the urban and rural sites in the PRD region, China. *Atmos. Environ.*, **76**, 181–188. doi:10.1016/j.atmosenv.2012.11.018.
- Zhang, Q. J., Beekmann, M., Drewnick, F., Freutel, F., Schneider, J., Crippa, M., Prevot, A. S. H., Baltensperger, U., **Poulain, L.**, **Wiedensohler, A.**, Sciare, J., Gros, V., Borbon, A., Colomb, A., Michoud, V., Doussin, J. F., van der Gon, H., Haefelin, M., Dupont, J. C., Siour, G., Petetin, H., Bessagnet, B., Pandis, S. N., Hodzic, A., Sanchez, O., Honore, C. and Perrussel, O. 2013. Formation of organic aerosol in the Paris region during the MEGAPOLI summer campaign: Evaluation of the volatility-basis-set approach within the CHIMERE model. *Atmos. Chem. Phys.*, **13**, 5767–5790. doi:10.5194/acp-13-5767-2013.

## Appendices: Overview of Appendices / Überblick der Anhänge

### Overview of Appendices

#### Knowledge transfer and public visibility

**TROPOS research for the expert public.** On account of the application oriented fundamental research of the institute its scientific knowledge is mainly transferred through scientific publications and conference contributions (see list, p. 115).

During the reporting period two significant conferences were hosted and co-organized by TROPOS. TROPOS hosted the 16<sup>th</sup> "International Conference on Clouds and Precipitation" (ICCP 2012) in Leipzig with about 500 participants from 37 countries and with 650 contributions. Conducted only the second time in Germany after 1988 this meeting of the worlds leading cloud experts was the most extensive ever. The "International Radiation Symposium" (IRS 2012) in Berlin with 533 participants from 33 countries and with nearly 600 contributions to the field of solar and thermal radiation transport in the Earth's atmosphere was an event of a similar magnitude and co-organised by TROPOS. The IRS meeting was only conducted in Germany for the second time after 1976. ICCP and IRS represent the largest and most important conferences for researchers in the field of cloud physics and radiation (see list, p. 144).

Technologies developed at TROPOS are commercially used via the membership in the Saxon Agency for Patent Exploitation. The institute supports the founding of spin-off companies (only one so far).

Results of the TROPOS research contribute to environmental policy advice. For example for the Land of Saxony and the Federal Environmental Agency (UBA) practise oriented investigations regarding the behaviour and the future development of air pollutants are conducted. In the framework of projects in collaboration with the Environmental Agency and the Saxon State Office for the Environment, Agriculture and Geology (LfULG) measurement data of fine and ultrafine particles are collected, evaluated and provided for further interpretation of the concentration and chemical composition of this particles.

In the field of clean air policy advice TROPOS also contributes with its own studies, which are used for air directive discussions and the implementation of clean air strategies. In addition the institute uses regional and national parliamentary evenings as well as national forums for the presentation of research results. For example the conversation series "Leibniz im Bundestag" emerged as an effective measure for policy advice. In total 130 individual meetings were organized by the Leibniz Society. In 2012 and 2013 TROPOS covered the topics air quality, particulate matter, and low emission zones.

### Überblick der Anhänge

#### Wissenstransfer und Außenwirkung

**TROPOS-Forschung für Fachpublikum.** Auf Grund der Ausrichtung des Institutes als anwendungsorientiertes Grundlagenforschungsinstitut erfolgt die Verwertung hauptsächlich in Fachpublikationen und Konferenzbeiträgen (siehe Liste, S. 115). Von den wissenschaftlichen Tagungen, an deren Organisation TROPOS beteiligt war, stachen im Berichtszeitraum zwei heraus: TROPOS organisierte die „16<sup>th</sup> International Conference on Clouds and Precipitation“ (ICCP 2012) in Leipzig und hat das „International Radiation Symposium“ (IRS 2012) in Berlin mitorganisiert.

An der ICCP hatten rund 500 Teilnehmer aus 37 Ländern mit fast 650 verschiedenen Beiträgen teilgenommen. Dieses alle vier Jahre organisierte Treffen der Wolkenexperten aus aller Welt wurde nach 1988 erst zum zweiten Male in Deutschland ausgerichtet und war in diesem Umfang bisher einmalig. In gleicher Größenordnung bewegte sich ebenfalls das „International Radiation Symposium“ (IRS 2012) in Berlin mit 533 Teilnehmern aus 33 Ländern und fast 600 Beiträgen zum solaren und thermischen Strahlungstransport in der Erdatmosphäre. Auch dieses alle vier Jahre organisierte Treffen der Strahlungsexperten aus aller Welt wurde nach 1976 erst zum zweiten Male in Deutschland ausgerichtet. ICCP und IRS sind die größten und bedeutendsten Fachtagungen für die Forschungsgemeinschaft im Bereich Wolkenphysik und Strahlung (siehe Liste, S. 144).

Weiterhin werden Technologien entwickelt, deren kommerzielle Verwertung über die Mitgliedschaft des Instituts in der Sächsischen Patent-Verwertungs-Agentur organisiert wird. Zusätzlich zu den anderen Verwertungswegen werden Ausgründungen von TROPOS-Mitarbeitern unterstützt (bisher eine).

Die Forschungsergebnisse des TROPOS dienen auch als ein Beitrag zur Politikberatung im Umweltbereich. So werden für das Land Sachsen und das Umweltbundesamt (UBA) praxisrelevante Untersuchungen zum Verhalten und zur künftigen Entwicklung von Schadstoffen in der Atmosphäre durchgeführt. Außerdem werden im Rahmen von Auftragsprojekten für das UBA und das Sächsische Landesamt für Umwelt und Geologie (LfULG) über längere Zeiträume Messdaten zu den Konzentrationen feiner und ultrafeiner Aerosolpartikel sowie zur chemischen Partikelzusammensetzung in der Atmosphäre erhoben, ausgewertet und diesen Institutionen zur weiteren Interpretation zur Verfügung gestellt.

Im Bereich der Luftreinhaltung trägt TROPOS zur Politikberatung auch durch eigene

## Appendices: Overview of Appendices / Überblick der Anhänge



Fig. / Abb. 1: Panel discussion "Frontline Research for Improved Air Quality and Climate Action", 14.05.2013 in Brussels. / Panel-Diskussion „Spitzenforschung zur Verbesserung der Luftqualität und zum Klimaschutz“, 14.05.2013 in Brüssel.

**TROPOS research results for the public at large.** TROPOS seeks dialogue with the public using print media, radio and TV. The disseminations of press releases have been significantly increased and shall be maintained at this level. Both in 2012 and 2013 15 press releases have been published. Subsequently 118 publications in 2012 and 128 publications in 2013 were registered.

TROPOS is part of the public relations work of the German Climate Consortium (DKK), the "Klimanavigator" and the Leibniz Association.

To renew the appearance in public TROPOS created a new corporate design and developed an expanded website. The detailed web pages help scientists and partners to easily find relevant information, to learn about research projects and results, the existing technologies at TROPOS, and to find contacts for collaborations. At the same time the websites address the public at large. The menu item "Discover" explains the goals of tropospheric research in a generally comprehensible form.

Together with 40 other institutions TROPOS was part of the "Science Night" on 29 June, 2012. 200 events with a length of 900 hours gave an insight into laboratories, lecture halls, institutes, clinics, repositories and archives.

**Selected topics and activities during the reporting period.** Especially the competence of TROPOS in the area of air quality (particulate matter and low emission zones) in urban regions as well as in cloud formation and volcanic ash characterize the external presentation.

In 2012 media activities and public relations on the issue of low emission zones resulted in three press releases followed by 22 publications in print and other media. Several events like "Umweltstammtisch" on 10 October 2012, "Leipzig Low Emission Zone

Forschungsergebnisse bei, die in der Richtliniendiskussion und bei der Erstellung von Luftreinhalteplänen verwendet werden.

Das Institut nutzt zusätzlich regionale und gesamtstaatliche parlamentarische Abende sowie nationale Innovations- und Forschungsforen für die Präsentation und Darstellung seiner Forschung. Als ein effektives Element der Politikberatung hat sich in den letzten Jahren die Gesprächsreihe „Leibniz im Bundestag“ entwickelt, bei der Wissenschaftler in Einzelgesprächen Bundestagsabgeordneten Rede und Antwort stehen. Rund 130 Termine hatte die Leibniz-Gemeinschaft dazu im Juni 2013 insgesamt organisiert. Auch hier war wie bereits 2012 das Wissen des TROPOS zu Luftqualität, Feinstaub und Umweltzonen gefragt.

**TROPOS Forschung für die breite Öffentlichkeit.** TROPOS sucht den Dialog mit der Öffentlichkeit auch über Printmedien sowie Hör- und Fernsehfunk. Die Veröffentlichung von Pressemitteilungen ist erheblich intensiviert worden und soll auf dem aktuellen Niveau gehalten werden. Es wurden im Berichtszeitraum in beiden Jahren je 15 Pressemitteilungen verfasst.

Hierauf erfolgten im Jahr 2012 118 Medienveröffentlichungen. Im Jahr 2013 waren es 128 Veröffentlichungen. TROPOS ist an den Öffentlichkeitsaktionen des Deutschen Klimakonsortiums (DKK), des Klimanavigators und der Leibniz-Gemeinschaft aktiv beteiligt. Das Institut hat weiterhin 2012 und 2013 den öffentlichen Auftritt durch ein zeitgemäßes Design und einen erweiterten Internetauftritt erneuert. Die umfangreicheren Internetseiten sollen relevante Informationen für WissenschaftlerInnen und Kooperationspartner einfacher zugänglich machen, die mehr über Forschungsprojekte und Forschungsergebnisse oder vorhandene Technologien am TROPOS erfahren möchten und Kontaktpersonen für Kooperationen suchen. Das Internetangebot richtet sich zugleich an die breite Öffentlichkeit. Die neu geschaffene Rubrik „Entdecken“ hat zum Ziel, die Forschung für alle Interessierten zu erläutern.

Zusammen mit 40 anderen Institutionen beteiligte sich TROPOS an der alle zwei Jahre stattfindenden „Langen Nacht der Wissenschaften“ am 29. Juni 2012, die insgesamt 200 Veranstaltungen mit 900 Stunden Programm und Einblicken in Labore, Hörsäle, Institute, Kliniken, Magazine und Archive bot.

**Ausgewählte Themen und Aktivitäten im Berichtszeitraum.** Insbesondere die Kompetenz des TROPOS im Bereich Luftqualität (Feinstaub und Umweltzonen) in urbanen Regionen sowie

## Appendices: Overview of Appendices / Überblick der Anhänge

press conference" on 6th March 2013 (both in co-operation with the city of Leipzig) and "How useful are low emission zones - Leipzig and Beijing, City versus Megacity - a comparison" on 23 March 2013 (in cooperation with DKK and Research Center Jülich) showed the decrease of the soot pollution by nearly one third as a result of the implementation of the low emission zone in Leipzig. This study and the accompanying activities help to objectify this overheated public debate (see article, p. 88).

In 2013 the European Commission launched the "Year of Air" which became manifest in the "Clean Air Policy Package" adopted on 18 December 2013. TROPOS actively contributed to the review process of the EU air policy with participation in the public consultation and with events during the "Year of Air".

TROPOS presented activities and projects on an exhibition booth at the GREEN WEEK 2013 from 4-7 June in Brussels. Under the title "Frontline Research for Improved Air Quality and Climate Action", representatives from science, politics and industry have discussed in Brussels upon invitation of TROPOS on 14 May 2013. This panel discussion was an official satellite event of the GREEN WEEK 2013.

On account of the political dimension of the air quality review in Europe in 2013 the editors of the Leibniz Journal could be convinced to dedicate one issue of the journal to this topic. The issue 4/2012 ("Stop breathing. How smallest particles provide huge problems") was published with a circulation of 24.000 copies and was distributed among stakeholders within Germany.

### **Equal opportunities and promotion of young researchers**

Already during recruiting processes measures for the absolutely non-discriminatory collaboration are



Fig. / Abb. 2: GREEN WEEK 2013 "Cleaner Air for All" within the "Year of the Air", Brussels, 04.06. - 07.06.2013. / GREEN WEEK 2013 „Cleaner Air for All“ im Rahmen des „Jahres der Luft“, Brüssel, 04.06. - 07.06.2013.

Wolkenbildung und Vulkanasche prägte die Außen-darstellung des Instituts.

So wurde im Jahr 2012 aktive Medien- und Öffentlichkeitsarbeit zum Thema Umweltzone mit drei Pressemitteilungen und folgend 22 Mediener-scheinungen (Print, Funk und Fernsehen) betrieben. In den Veranstaltungen „Umweltstammtisch“ am 10.10.2012, „Pressekonferenz zur Leipziger Umwelt-zone“ am 06.03.2013 (beide zusammen mit der Stadt Leipzig) und „Sind Umweltzonen nutzlos? - Leipzig und Peking, Stadt vs. Megacity - ein Vergleich“ am 23.04.2013 (zusammen mit dem DKK und FZ Jülich) wurde gezeigt, dass in Leipzig als Folge der Umwelt-zone eine Abnahme der Rußbelastung im Feinstaub an der Straße um ca. ein Drittel nachgewiesen werden konnte (siehe Artikel, S. 88). Diese europaweit einmalige Leipziger Studie und die dazugehörigen Aktivitäten tragen auch dazu bei, mit neuen fachlichen Argumenten die überhitzte Diskussion zum Für und Wider der Umweltzonen zu versachlichen.

Die Europäische Kommission hat 2013 zum „Jahr der Luft“ erklärt und ihren überarbeiteten Maßnahmenkatalog für die Luftreinheit in dem am 20. Dezember 2013 herausgegebenen Aktionsplan mani-festiert. TROPOS hat sich mit der wissenschaftlichen Zuarbeit bei der öffentlichen europäischen Konsulta-tion an diesem Prozess beteiligt und Veranstaltungen im europäischen Jahr der Luft 2013 begleitet. So zeigte TROPOS seine Aktivitäten mit einem Stand auf der GREEN WEEK 2013, die vom 4. bis 7. Juni in Brüssel stattfand. Zum offiziellen GREEN WEEK Satellite Event „Spitzenforschung zur Verbesserung der Luftqualität und für den Klimaschutz“ hatten am 14. Mai auf Einladung des TROPOS Vertreter aus Wissenschaft, Politik und Industrie in Brüssel diskutiert.

Durch die politische Dimension, die das Thema Luftqualität 2013 in Europa genossen hat, gelang es, die Redaktion des Leibniz-Journals zu über-zeugen, eine Ausgabe diesem Schwerpunktthema zu widmen. Die Ausgabe 4/2014 („Luft anhalten. Wie kleinste Partikel größte Probleme bereiten“) erschien mit zwei Beiträgen zur Forschung des TROPOS im November in einer Auflage von 24.000 Exemplaren und wurde deutschlandweit unter Entscheidungsträ-gern verbreitet.

### **Chancengleichheit und Nachwuchsförderung**

Am TROPOS werden Maßnahmen zur absolut diskriminierungsfreien Zusammenarbeit am Institut bereits im Einstellungsverfahren angewendet und fortlaufend verbessert.

## Appendices: Overview of Appendices / Überblick der Anhänge

applied at the institute and are improved constantly. TROPOS intends to further increase the proportion of international researchers.

Following the so-called Leibniz cascade model TROPOS also intends to increase the proportion of women, especially in post-doc and leading positions. Therefore, a stage-model was implemented in 2012, which was defined according to the current structure of employees at the institute. Particularly worth mentioning here is the appointment of Prof. Ina Tegen as head of the department "Modelling of atmospheric processes" in 2012 and the participation of Dr. Kerstin Schepanski in the Leibniz Mentoring program for women in 2013.

**Audit „berufundfamilie“** An important prerequisite for equal opportunities and career orientation is the reconciliation of career and family, especially for the promotion of young researchers.

In 2011 the TROPOS efforts in this direction were internal and external manifested in the certificate for the "career and family audit." The preparations for the re-audit 2014 were started in 2013.

**Promotion of young researchers.** TROPOS actively promotes young researchers in the Bachelor- and Master education at the Leipzig University as well as during and after doctoral research projects. The institute is involved in the development and implementation of the new Bachelor and Master programs and is exclusively responsible for four modules and partially responsible for further two modules.

Highly qualified scientists of the institute contribute to teaching activities in cooperation with the Leipzig University as joint appointments. In addition to Meteorology students also Chemistry and Physics students are trained at TROPOS (see list, p. 135).

The institute offers young researchers an individualized realization of their dissertation projects supported by the supervision committee in the framework of the structured doctoral training programme.

TROPOS scientists give lectures at the Universities of Jena, Beijing, Jinan and Shanghai, Helsinki and Stockholm, in international summer and winter schools and training courses and networks (see list, p. 133).

In 2012 the Leipzig Graduate School on "Aerosol, Clouds and Radiation: Mineral dust" was formed on the subject of characteristics and effects of mineral dust aerosol particles. This structured doctoral training program in collaboration with the Leipzig University is member of the Research Academy Leipzig (RAL).

**Create future.** TROPOS is a partner within the MINT-Individual network to inspire and generate

Das Institut ist weiterhin bestrebt, den Anteil an internationalen Wissenschaftlerinnen und Wissenschaftlern zu erhöhen.

TROPOS will den Anteil von Frauen vor allem in wissenschaftlichen Führungspositionen weiter erhöhen und verfolgt dabei das so genannte Kaskadenmodell nach den Empfehlungen der Leibniz-Gemeinschaft, wobei ein an die institutsspezifische momentane Stellensituation angepasstes Stufenmodell im Jahr 2012 definiert wurde. Speziell erwähnt sei hier die Berufung von Frau Prof. Ina Tegen auf die Leitung der Abteilung Modellierung atmosphärischer Prozesse in 2012 und die Aufnahme von Frau Dr. Kerstin Schepanski in das Leibniz Mentoring Programm für Frauen in 2013.

**Audit „berufundfamilie“** Eine Voraussetzung für die Chancengleichheit ist die Vereinbarkeit von Beruf und Familie für den wissenschaftlichen Nachwuchs und somit eine bessere Karriereplanung. Mit der Zertifizierung zum Audit „berufundfamilie“ am 25. Mai 2011 wird das Engagement des TROPOS für die Vereinbarkeit von Beruf und Familie nach innen und außen dokumentiert und seit dem angewendet. Die Vorbereitungen für die Reauditierung wurden Ende des Jahres 2013 begonnen.

**Nachwuchsförderung.** TROPOS fördert aktiv den wissenschaftlichen Nachwuchs in der Bachelor- und Masterausbildung, während der Promotionsvorhaben und darüber hinaus.

Das Institut ist eng in die Entwicklung und in die Durchführung der neuen Bachelor- und Masterstudiengänge an der Universität Leipzig eingebunden und ist für vier Module exklusiv und für zwei weitere Module teilweise verantwortlich.

Hochqualifizierte Mitarbeiterinnen und Mitarbeiter beteiligen sich als gemeinsame Berufungen an der Lehre der Universität Leipzig. Neben Studierenden der Meteorologie werden am TROPOS auch Chemie- und Physikstudenten und -studentinnen ausgebildet. (siehe Liste, S. 135)

Das Institut bietet jungen Wissenschaftlerinnen und Wissenschaftlern individuell abgestimmte und von einem Betreuungsteam begleitete Realisierung ihrer Promotionen im Rahmen der strukturierten Doktorandenausbildung. Mitarbeiter des TROPOS halten Kurse an den Universitäten von Jena, Peking, Jinan und Shanghai, Helsinki und Stockholm und in internationalen Sommerschulen, Ausbildungskursen und -netzwerken (siehe Liste, S. 133).

Die im Juli 2012 gegründete Leibniz-Graduiertenschule „Wolken, Aerosole und Strahlung am Beispiel des Mineralstaubs“ hat die DoktorandInnenausbildung

## Appendices: Overview of Appendices / Überblick der Anhänge



Fig. / Abb. 3: Members of the Leipzig Graduate School „Aerosol, Clouds and Radiation: Mineral dust“. / Mitglieder der Leipzig-Graduiertenschule „Wolken, Aerosole und Strahlung am Beispiel des Mineralstaubes“.

interest in technical and scientific studies, and especially shows career perspectives in tropospheric research. Students get to know research work in a playful manner and have the possibility to directly talk to scientists from the MINT field. In the framework of this initiative the institute regularly participates in the Girls' Day (girls future day). In 2012 and 2013 interested students could gain insight into laboratories and career opportunities as scientists and other professions at TROPOS.

As in the last years TROPOS will continue to finance an apprentice position.

### Cooperations and networking

Numerous grown networks within the Leibniz Association, with Universities, with Max Planck Institutes, with institutes of the Helmholtz Society, and collaborations at the international level demonstrate the actual level of TROPOS networking in the field of interdisciplinary aerosol and cloud research. Similar alike TROPOS is networked on the European and global level and actively develops research programmes (see list, p. 151).

Technological developments at TROPOS lead to international standards in the experimental direct and indirect acquisition of aerosols and hydrometeors from ground up to the high atmosphere as well as in model-based descriptions of the complex multiphase system.

TROPOS uses its national cooperation through several pathways (see list, p. 156). Examples are e.g.:

1. the CARIBIC project in cooperation with Lufthansa that was ensured for another 10 years after running already for 10 years,

am TROPOS gemeinsam mit der Universität Leipzig auf eine solide Grundlage gestellt und ist in der „Research Academy Leipzig“ (RAL) verortet.

**Zukunft schaffen.** TROPOS ist Partner im Netzwerk MINT-Individual und unterstützt den Weg zum naturwissenschaftlichen Studium und zeigt berufliche Perspektiven im Bereich der Atmosphärenforschung. SchülerInnen lernen die Forschungsarbeit auf spielerische Art kennen und kommen mit Forscherinnen und Forschern aus dem MINT-Bereich ins Gespräch. Im Rahmen der MINT-Initiative, die zum Ziel hat, Jugendliche für einen Beruf in den Fächern Mathematik, Informatik, Naturwissenschaften und Technik zu begeistern, beteiligt sich TROPOS auch am Girls' Day, dem Mädchen-Zukunftstag. In den Jahren 2012 und 2013 konnten sich an diesem Tag interessierte Schülerinnen in den Laboren über Ausbildungsmöglichkeiten informieren.

TROPOS wird auch in den nächsten Jahren mindestens einen Lehrlingsausbildungsplatz aus Haushaltssmitteln finanzieren.

### Bedeutende Kooperationen und Vernetzung in der Forschung

Zahlreiche bisher gewachsene Vernetzungen innerhalb der Leibniz-Gemeinschaft, mit Universitäten, mit Max-Planck-Instituten, mit Instituten der Helmholtz-Gemeinschaft sowie auf internationaler Ebene zeigen den derzeitigen Stand der Vernetzung des TROPOS in der interdisziplinären Aerosol- und Wolkenforschung. Ähnlich ist TROPOS auf der europäischen und weltweiten Ebene vernetzt und entwickelt hier aktiv Forschungsprogramme (siehe Liste, S. 151).

Technologische Entwicklungen am TROPOS führen zu internationalen Standards in der experimentellen direkten und indirekten Erfassung von Aerosolen und Hydrometeoren vom Boden bis zur hohen Atmosphäre sowie in der modellmäßigen Beschreibung des komplexen Multiphasensystems.

Die inländischen Kooperationen (siehe Liste, S. 156) des Institutes werden über mehrere Pfade intensiv genutzt, so z.B.:

1. durch das seit über 10 Jahren laufende und durch einen Kooperationsvertrag mit der Lufthansa für weitere 10 Jahre gesicherte CARIBIC-Projekt,
2. durch die Beteiligung an der DFG-Forschergruppe INUIT zum Thema der atmosphärischen Eisnukleation, in dem TROPOS mit acht nationalen Partnern zusammenarbeitet,

## Appendices: Overview of Appendices / Überblick der Anhänge

2. the TROPOS participation in the DFG research group INUIT investigating the atmospheric ice nucleation together with eight partners,
3. the DFG priority programmes, and the implementation and use of the new HALO aircraft platform,
4. the cooperation with the Federal Environmental Agency for the characterization of aerosol particles,
5. the DWD projects (Deutscher Wetterdienst) for the development of LIDAR measurement devices and ceilometer measurement networks,
6. the contribution to the DWD Hans Ertel Centre for weather research, subject 1 "Atmospheric dynamics and predictability";
7. the coordination and active participation in the BMBF project "Clouds and precipitations for advancing climate prediction" with permanent measurements at the "supersites" Leipzig/Lindenberg and the evaluation of results of an intensive measurement campaign 2013 in Jülich and Melpitz,
8. the national cooperation for the chemical analysis within the maritime context (MPI Jena, GEOMAR),
9. the cooperation with the Leibniz Institute for Baltic Sea Research Warnemünde (IOW) and the Centre for Tropical Marine Ecology in Bremen (ZMT) for the investigation of exchange processes between the polluted ocean and the polluted atmosphere,
10. the cooperation within the newly established Leibniz research networks, currently these networks are "Crises in a Globalised World" and "Infectious Diseases".
3. über die laufenden DFG-Schwerpunktprogramme und über den Aufbau und die Nutzung der neuen Flugzeugplattform HALO,
4. über das Umweltbundesamt zur deutschlandweiten Aerosolcharakterisierung,
5. über Projekte des DWD (Deutscher Wetterdienst) zur Lidarentwicklung und Ceilometer-Messnetzen,
6. über einen Beitrag zum Hans-Ertel-Zentrum für Wetterforschung des Deutschen Wetterdienstes im Themenbereich 1 „Atmosphärendynamik und Vorhersagbarkeit“;
7. über die Koordination und aktive Beteiligung an der nationalen BMBF-Förderung „Wolken und Niederschlag im Kontext der Klimaforschung“ mit kontinuierlichen Messungen an den „Supersites“ Leipzig/Lindenberg und der Auswertung einer Intensivmesskampagne in 2013 in Jülich und Melpitz,
8. über Kooperationen auf nationaler Ebene bezüglich chemischer Untersuchungen mit maritimem Bezug (MPI Jena, IFM-GEOMAR),
9. über Kooperationen mit dem Leibniz-Institut für Ostseeforschung Warnemünde (IOW) und dem Leibniz-Zentrum für Maritime Tropenökologie (ZMT) zur Untersuchung von Austauschprozessen zwischen dem belasteten Ozean und der belasteten Atmosphäre,
10. über Kooperationen in den neu gegründeten Leibniz-Forschungsverbünden, zur Zeit in den Verbünden „Krisen einer Globalisierten Welt“ und „Infektionskrankheiten“.

In the framework of the Leibniz competition funds TROPOS establishes collaborations within the Leibniz Association or with university institutes. TROPOS has built cooperation for example with the Peking University, the Korean Meteorological Information Service Institute, and the Bulgarian Academy of Sciences. The ground-based remote sensing and in-situ measurement activities of the institute are integrated into the long-term orientated Infrastructure ACTRIS and into ESA policy advice. The in-situ measurements of aerosol particles are part of the EMEP and WMO GAW networks. The collaboration with partners from eastern Europe is being established (see list, p. 151).

Im Rahmen des Wettbewerbsfonds der Leibniz-Gemeinschaft werden die Kooperationsmöglichkeiten innerhalb der WGL und mit Universitätsinstituten ausgebaut. Durch Kooperationsvereinbarungen ist das Institut beispielsweise mit der Peking University, dem Forschungsinstitut des Koreanischen Wetterdienstes und der Bulgarischen Akademie der Wissenschaften verbunden. Die bodengebundenen Fernerkundungs- und in-situ-Messungen sind international eingebunden in die langfristigen ACTRIS-Arbeiten und in Beratungstätigkeiten für die ESA. Die in-situ-Aerosolaktivitäten sind international in den EMEP- und WMO-GAW-Netzwerken eingebunden. Die Zusammenarbeit mit Osteuropäischen Partnern zur Umweltbelastung und Aerosolferntransporten im europäischen Raum wird angebahnt (siehe Liste, S. 151).

## Appendices: University courses

### University courses

Lecturer	Course	WS 2011/ 2012	SS 2012	WS 2012/ 2013	SS 2013	WS 2013/ 2014
Althausen, D.	Optical Measurement Techniques	x				
Ansmann, A. Althausen, D. Seifert, P. Engelmann, R.	Active Remote Measurement in Atmospheric Research Seminar Active Remote Sensing			x x		x x
Ansmann, A.	Active remote sensing (LIDAR) in environmental and atmospheric research and passive aerosol remote sensing (Photometer, Satellite)	x				
Hellmuth, O.	Guest lecture: Numerical Weather Prediction, Technical University Dresden, one-day course		x		x	
Hermann, M. Wendisch, M.	Airborne Physical Measurements + Exercise	x		x		x
Herrmann, H.	Atmospheric Chemistry I + Exercises Atmospheric Chemistry II + Exercises Atmospheric Chemistry Seminar Atmospheric Chemistry Lab experiences	x x x	x x x	x x x	x x x	x x
	Guest lecture: The First Sino-European School on Atmospheric Chemistry, Shanghai, May 18 - 26, 2013				x	
	Guest Lecture: Tropospheric multiphase chemistry, Shandong University (SDU), Jinan, October 22 - 24, 2013					x
Macke, A.	Atmospheric Radiation	x		x		x
Macke, A. Deneke, H.	Satellite Remote Sensing		x		x	
Macke, A. Stratmann, F.	Cloud Physics + Exercises		x		x	
Schepanski, K.	Guest lecture: EUMETSAT/WMO Training course, Dust Variability and Dust-Climate Interactions, Sultan Qaboos University, Sultanate of Oman, December 08 - 12, 2013, one lecture			x		
Siebert, H.	Modern Meteorological Instruments		x			

## Appendices: University courses

Lecturer	Course	WS 2011/ 2012	SS 2012	WS 2012/ 2013	SS 2013	WS 2013/ 2014
Stratmann, F.	Co-organization and guest lecture: INUIT Summer School, Braunfels, Different Approaches to Classical Nucleation Theory, September 15 - 20, 2013, 1 lecture			x		
	Organization and guest lectures: CLOUD Summer School, Cloud Microphysical Processes, Braunfels, September 08 - 15, 2013, 2 lectures			x		
Tegen, I.	Modeling of Atmospheric Trace Substances Seminar Modeling of Atmospheric Trace Substances, Energy and Environment			x x		x x
	Basics of Mesoscale Model Simulations				x	
Wandinger, U.	Scattering and Atmospheric Optics Seminar Applied Scattering Theory		x x		x x	
Wiedensohler, A. Stratmann, F. Birmili, W. Müller, T.	Atmospheric Aerosols I incl. Lab Experiences	x		x		x
Wiedensohler, A.	Guest lecture: 8 <sup>th</sup> Summer School on Atmospheric Aerosol Physics, Measurement, and Sampling Hytylä, Finland, May 5 - 11, 2012		x			
	Guest lecture: PKU Summer School Atmospheric Aerosol Physics, Beijing, June 25 - 29, 2012		x			
	ITTM Winter School on aerosol physics, instrumentation, and sampling, Pune, January 7 - 11, 2013			x		
	Guest lecture: International School on Atmospheric Aerosol Physics, Measurement, and Sampling La Paz, Bolivia, June 26 - July 3, 2013					
van Pinxteren, M.	Guest lecture: Analysis and Spectroscopy: Gas Chromatography, Lecture in an one week course			x		x

## **Academical degrees**

### **Completed academic qualifications 2012/2013**

<b>Academic degree<sup>a)</sup></b>	<b>Name</b>	<b>Title</b>	<b>Faculty</b>	<b>Year</b>
Ph. D.	Baars, H.	Aerosol profiling with lidar in the Amazon Basin during the wet and dry season 2008	Leipzig University, Faculty of Physics and Earth Science	2012
	Dieckmann, K.	Hygroscopic growth and activation measurements of aerosol particles in lab and field	Leipzig University, Faculty of Physics and Earth Science	2012
	Kahnt, A.	Semivolatile compounds from atmospheric monoterpene oxidation	Leipzig University, Faculty of Chemistry and Mineralogy	2012
	Kanitz, T.	Vertical distribution of aerosols above the Atlantic Ocean, Punta Arenas (Chile), and Stellenbosch (South Africa)	Technical University Berlin, Faculty Process Sciences	2012
	Meier, J.	Regional aerosol modeling in Europe: Evaluation with focus on vertical profiles and radiative effects	Leipzig University, Faculty of Physics and Earth Science	2013
	Niedermeier, D.	Heterogeneous ice nucleation in droplets containing mineral dust particles: An experimental and theoretical study	Leipzig University, Faculty of Physics and Earth Science	2012
	Nordmann, S.	Light absorption of atmospheric soot particles over Central Europe	Leipzig University, Faculty of Physics and Earth Sciences	2013
	Rusumdar, A. J.	Treatment of non-ideality in the multiphase model SPACCIM and investigation of its influence on tropospheric aqueous phase chemistry	Brandenburg University of Technology Cottbus, Faculty of Environmental Sciences and Process Engineering	2013
	Schaefer, T.	Kinetische und mechanistische Untersuchungen der radikalischen Oxidation organischer kurzkettiger Carbonylverbindungen in wässriger Lösung	Leipzig University, Faculty of Chemistry and Mineralogy	2012
	Scheinhardt, S.	Größenaufgelöste Charakterisierung von Aerosolpartikeln in Deutschland: Einfluss klimatischer Änderungen und Bildung von Metallkomplexen	Leipzig University, Fakultät für Chemie und Mineralogie	2013
	Schlegel, M.	A class of general splitting methods for air pollution models: Theory and practical aspects	Martin Luther University Halle-Wittenberg, Faculty of Natural Sciences II	2012

## Appendices: Academical degrees

Academic degree <sup>a)</sup>	Name	Title	Faculty	Year
Ph. D.	Skupin, A.	Optische und mikrophysikalische Charakterisierung von urbanem Aerosol bei (hoher) Umgebungsfeuchte	Leipzig University, Faculty of Physics and Earth Sciences	2013
Dipl.	Elsen, K.	Numerische Lösung der Advektionsgleichung mittels logarithmischer Rekonstruktion	University of Greifswald, Institute of Mathematics and Computer Sciences	2012
	Klepel, A.	Experimental study on the correlation between depolarization ratios and lidar ratios of cirrus clouds over Leipzig, Germany, with the lidar systems BERTHA and Polly <sup>XT</sup>	Leipzig University, Faculty of Physics and Earth Sciences	2013
	Wölbing, D.	Erweiterung des Mehrwellenlängenlidars MARTHA um zwei Rotations-Ramakanäle für Temperatur- und Extinktionsmessungen	Leipzig University, Faculty of Physics and Earth Sciences	2013
M.Sc.	Assmann, D.	Optische Eigenschaften des Aerosols in der atlantischen marinen Grenzschicht - ein Querschnitt von Punta Arenas bis Bremerhaven	Leipzig University, Faculty of Physics and Earth Sciences	2013
	Augustin, S.	Immersionsgefrierverhalten biologischer Partikel am Leipzig Aerosol Cloud Interaction Simulator (LACIS)	Leipzig University, Faculty of Physics and Earth Science	2012
	Bauditz, M.	Charakterisierung des Aerosols mit einem Dual-Polar Sonnenphotometer in Guangzhou/China 2011/12	Leipzig University, Faculty of Physics and Earth Sciences	2013
	Bethke, J.	Liquid water content measurements in trade wind cumuli	Leipzig University, Faculty of Physics and Earth Science	2012
	Däumlich, V.	Kinetische und spektroskopische Untersuchungen des Peroxomonosulfat-Radikalanions SO <sub>5</sub> <sup>-</sup>	Leipzig University, Faculty of Chemistry and Mineralogy	2012
	Dietzsch, F.	Validierung satellitenbasierter Früherkennung konvektiver Gewitter mittels Rückwärtstrajektorien	Leipzig University, Faculty of Physics and Earth Science	2013
	Fischer, S.	WRF-Simulation zur Quantifizierung der Invarianzeigenschaften der Ertelschen Potentiellen Vortizität während der Entwicklung einer Zyklone	Leipzig University, Faculty of Physics and Earth Science	2012
	Foth, A.	Bestimmung der vertikalen Aerosolverteilung über Punta Arenas, Chile (53.2°S, 70.9°W)	Leipzig University, Faculty of Physics and Earth Science	2012
	Hirte, K.	Charakterisierung zweier „Particle-into-liquid sampler“ zur Bestimmung der sekundären ionischen Verbindungen Sulfat, Nitrat und Oxalat in atmosphärischen Partikeln	Leipzig University, Faculty of Chemistry and Mineralogy	2012

## Appendices: Academical degrees

Academic degree <sup>a)</sup>	Name	Title	Faculty	Year
M.Sc.	Höpner, F.	Messung des hygroskopischen Wachstums von submikronen Aerosolpartikeln in der marinen Grenzschicht des Atlantischen Ozeans	Leipzig University, Faculty of Physics and Earth Science	2012
	Horn, S.	Speziation und Photolyse von Fe(III)-Carboxylat Komplexen in wässriger Lösung	Leipzig University, Faculty of Chemistry and Mineralogy	2012
	Leistert, M.	Hygroskopisches Wachstum des submikronen Aerosols in der atlantischen marinen Grenzschicht - ein Querschnitt von Punta Arenas bis Bremerhaven	Leipzig University, Faculty of Physics and Earth Sciences	2013
	Oelsner, P.	Aufbau eines High-Spectral-Resolution-Kanals und Vergleich mit dem Raman-Kanal eines Aerosol-Lidars	Leipzig University, Faculty of Physics and Earth Science	2012
	Pfitzenmaier, L.	Determination of microphysical properties of cloud and drizzle droplets based on observations with radar, microwave radiometer, and lidar	Leipzig University, Faculty of Physics and Earth Science	2012
	Pröhl, T.	Experimentelle Bestimmung der bipolaren Ladungsverteilung eines neuartigen Soft X-Ray Diffusionsaufladers für Aerosole	Hochschule Merseburg	2013
	Puschmann, D.	Partitionierte Rosenbrock-Verfahren für nicht-hydrostatische Atmopshärenmodelle	HTWK Leipzig, Faculty for Informatics, Mathematics and Natural Sciences	2013
	Putian, Z.	Large-Eddy Simulation of the turbulent flow within and above a forest canopy with the LES-model ASAM	University of Helsinki, Department of Physics	2013
	Richters, S.	Gas-phase reaction of monomethylhydrazine with ozone: Product formation, kinetics and OH-radical formation	Leipzig University, Faculty of Chemistry and Mineralogy	2013
	Rodigast, M.	Untersuchung und Optimierung von Quantifizierungsmethoden zur Peroxidanalyse	Leipzig University, Faculty of Chemistry and Mineralogy	2012
	Tomsche, L.	Der Einfluss chemischer Alterungsprozesse auf das Immersionsgefrierverhalten von Mineralstaub	Leipzig University, Faculty of Physics and Earth Science	2013
	Wagner, J.	Microphysical aerosol properties retrieved from combined lidar and sun photometer measurements	Leipzig University, Faculty of Physics and Earth Science	2012

## Appendices: Academical degrees

Academic degree <sup>*)</sup>	Name	Title	Faculty	Year
M.Sc.	Wenzel, J.	Optische Eigenschaften des Aerosols in der atlantischen marinen Grenzschicht: Ein Querschnitt von Kapstadt bis Bremerhaven	Leipzig University, Faculty of Physics and Earth Science	2012
	Wiesner, A.	Optical properties of tropical rainforest aerosol during a field campaign in Danum Valley, Malaysia	Leipzig University, Faculty of Physics and Earth Sciences	2013
	Zenker, K.	Physikalische Eigenschaften des tropischen Regenwaldaerosols	Leipzig University, Faculty of Physics and Earth Sciences	2013
B.Sc.	Ander, K.	Estimation of statistical measurement errors in the determination of ice fractions at the Leipzig Aerosol Cloud Interaction Simulator (LACIS)	Leipzig University, Faculty of Physics and Earth Science	2012
	Hoffmann, E.	Troposphärische Multiphasen-Halogenchemie in Küstengebieten	Leipzig University, Faculty of Chemistry and Mineralogy	2012
	Luttkus, M.	Parametrisierung von biogenen Emissionen in atmosphärischen Chemie-Transport-Modellen	Leipzig University, Faculty of Physics and Earth Science	2012
	Osterloh, V.	Reasons for Seasonality of the Meteorological Parameters on the Bolivian High Plateau "Altiplano"	Leipzig University, Faculty of Physics and Earth Science	2013
	Rau, A.	Größenaufgelöste Bestimmung von Dicarbonsäuren in atmosphärischen Partikeln an drei Messstationen in Sachsen	Leipzig University, Faculty of Chemistry and Mineralogy	2012
	Rempel, M.	Gewittervorhersage auf dem Prüfstand - Möglichkeiten der objekt-basierten COSMO-DE Validierung mittels Satellitenprodukt RDT	Leipzig University, Faculty of Physics and Earth Science	2013
	Schuldt, A.	Nichtflüchtiger Kohlenstoff im atmosphärischen Aerosol: Zeitliche und geographische Charakteristika und Korrelation mit optischen Messgrößen	Leipzig University, Faculty of Physics and Earth Science	2012
	Völker, G. S.	Theoretical investigations into the optimisation of an optical particle spectrometer for the detection of ice particles at LACIS	Leipzig University, Faculty of Physics and Earth Science	2012
	Zedler, P.	Charakterisierung von Wolkenkondensationskernen	Leipzig University, Faculty of Physics and Earth Science	2012

<sup>\*)</sup> Habil.: Habilitation, Ph. D.: Doctoral theses, Dipl.: Diploma, M.Sc.: Master of Science, B.Sc.: Bachelor of Science

## Appendices: Academical degrees / Awards / Reviews

### Summary of completed academic qualifications

Academical degrees	Number		Total
	2012	2013	
Doctoral theses	7	5	12
Diploma	1	2	3
Master of Science	13	11	24
Bachelor of science	7	2	9

### Awards

Name	Title	Prize	Awarding institution	Year
Schmidt, J.	Determination of cloud microphysical properties with dual-field-of-view Raman lidar measurements	Best Oral Presentation at the 26 <sup>th</sup> International Laser Radar Conference, Porto Heli, Greece, 25 - 29 June 2012	Organizing committee 26th ILRC	2012
Niedermeier, D.	Heterogeneous ice nucleation: exploring the transition from stochastic to singular freezing behavior	Publication award of the Leibniz Institute of Tropospheric Research 2011	TROPOS	2012
Heinold, B.	Simulations of the 2010 Eyjafjallajökull volcanic ash dispersal over Europe using COSMO-MUSCAT	Publication award of the Leibniz Institute of Tropospheric Research 2012	TROPOS	2013
Mertes, S.	For outstanding service to the authors and readers of Geophysical Research Letters	2012 Editor's Citation for Excellence in Refereeing	American Geophysical Union	2013

### Reviews

Reviews	Number	
	2012	2013
Journals	103	147
Projects	23	21
Others	21	11
Total	147	179

## Appendices: Guest scientists

### Guest scientists

Name	Period of stay	Institution
Jokinen, T.	04.01.- 28.02.12	University of Helsinki, Finland
Kienast-Sjögren, E.	09.01. - 13.01.12	Swiss Federal Institute of Technology Zürich, Switzerland
Rolf, C.	09.01. - 13.01.12	Jülich Research Centre, Germany
Morozov, I.	15.01.- 14.03.12	Russian Academy of Science, Moscow, Russia
Pummer, B.	29.01. - 10.02.12	Vienna University of Technology, Austria
Hamed, A.	06.02. - 20.02.12	University of Kuopio, Finland
de Mott, P.	05.03. - 21.03.12	Colorado State University, Fort Collins, USA
Tobo, Y.	05.03. - 28.03.12	Colorado State University, Fort Collins, USA
Mykhalchuk, B.	18.03. - 24.03.12	Medved's Institute of Ecohygiene and Toxicology, Kiev, Ukraine
Bastian, S.	19.03. - 20.03.12	Saxon State Office for the Environment, Agriculture and Geology, Dresden, Germany
Malinka, A.	15.04. - 20.04.12	B.I. Stepanov Institute of Physics, Minsk, Belarus
Cheng, Y.	16.04. - 20.04.12	Peking University, China
Schüttauf, S.	04.05. - 11.05.12	TU Bergakademie Freiberg, Germany
Wiedemann, K.	04.05. - 19.05.12	University of Arizona, USA
Zhou, P.	22.05. - 08.06.12	University of Helsinki, Finland
Charlesworth, E.	14.06. - 31.08.12	Seattle University, USA
Barbosa, H.	18.06. - 20.06.12	University of Sao Paulo, Brazil
Ervens, B.	02.07. - 15.07.12	National Oceanic and Atmospheric Administration (NOAA), Boulder, USA
Morozov, I.	12.07. - 28.07.12	Russian Academy of Science, Russia
Wiedemann, K.	23.07. - 01.08.12	University of Arizona, Tucson, USA
Kahnt, A.	30.07. - 10.08.12	University of Antwerp, Belgium
Shchekin, A. K.	30.07. - 03.08.12	St. Petersburg State University, Moscow, Russia
Wu, W.	30.07. - 10.08.12	University of Antwerp, Belgium

## Appendices: Guest scientists

Name	Period of stay	Institution
Reisen, F.	09.09. - 21.09.12	CSIRO, Clayton, Australia
Chou, C.	10.09. - 21.09.12	University of Hertfordshire, UK
Ulanowski, J.	10.09. - 14.09.12	University of Hertfordshire, UK
Granados Munoz, M.	18.09. - 14.12.12	University of Granada, Spain
Titos, G.	30.09. - 01.12.12	University of Granada, Spain
Chen, J.	04.10. - 30.11.12	Peking University, China
Liu, H.	04.10. - 30.11.12	Peking University, China
Kalapow, I.	14.10. - 20.10.12	Institute for Nuclear Research and Nuclear Energy, Sofia, Bulgaria
Ogren, J.	14.10. - 22.10.12	National Oceanic and Atmospheric Administration (NOAA), Boulder, USA
Bundke, U.	12.11. - 23.11.12	Johann Wolfgang Goethe University Frankfurt am Main, Germany
Klimach, T.	12.11. - 16.11.12	Max Planck Institute for Chemistry, Mainz, Germany
Nilius, B.	12.11. - 23.11.12	Johann Wolfgang Goethe University Frankfurt am Main, Germany
Schmidt, S.	12.11. - 16.11.12	Max Planck Institute for Chemistry, Mainz, Germany
Schneider, J.	12.11. - 16.11.12	Max Planck Institute for Chemistry, Mainz, Germany
Velarde, F.	17.11. - 02.12.12	University of the Mayor de San Andrés University, La Paz, Bolivia
Chou, C.	27.11. - 06.12.12	University of Hertfordshire, UK
Stachlewska, I.	27.11. - 21.12.12	University of Warsaw, Poland
Kolgotin, A.	15.12. - 31.12.12	Physics Instrumentation Center, Troitsk, Moscow Region, Russia
Chemysakin, E.	16.12. - 31.12.12	NASA Langley Research Center, Hampton, USA
Hamed, A.	08.01. - 28.03.13	University of Kuopio, Finland
Knobel, L.	28.01. - 08.02.13	University of Paderborn, Germany
Alves Couveia, D.	11.02. - 16.02.13	Universidade de Sao Paulo, Brazil
Murugavel, P.	18.02. - 16.03.13	Indian Institute of Tropical Meteorology, Pune, India

## Appendices: Guest scientists

Name	Period of stay	Institution
Godson, A.	20.02. - 01.03.13	University of Ibadan, Nigeria
Chou, C.	26.02. - 08.03.13	University of Hertfordshire, UK
Stachlewska, I.	08.04. - 19.04.13	University of Warsaw, Poland
Argyrouli, A.	22.04. - 26.04.13	National Technical University of Athens, Greece
Andrade, M.	13.05. - 17.05.13	University of the Mayor de San Andrés University, La Paz, Bolivia
Zhou, P.	20.05. - 07.06.13	University of Helsinki, Finnland
Boose, Y.	27.05. - 19.06.13	Swiss Federal Institute of Technology, Zurich, Switzerland
Nilius, B.	27.05. - 19.06.13	Johann Wolfgang Goethe University Frankfurt am Main, Germany
Bingemer, H.	27.05. - 19.06.13	Johann Wolfgang Goethe University Frankfurt am Main, Germany
Schmidt, S.	27.05. - 19.06.13	Max Planck Institute for Chemistry, Mainz, Germany
Izaguirre, M.	03.06. - 07.06.13	University of Miami, USA
Wang, X.	10.06. - 14.06.13	Max Planck Institute for Chemistry, Mainz, Germany
Fiedler, S.	01.07. - 01.08.13	University of Leeds, UK
Yao, S. Q.	01.07. - 24.08.13	Mount Holyoke College, USA
Morozov, I.	08.07. - 06.08.13	Institute for Chemical Physics, Russian Academy of Sciences, Moscow, Russia
Syromyatnikov, A.	08.07. - 06.08.13	Institute for Chemical Physics, Russian Academy of Sciences, Moscow, Russia
Kecorius, S.	01.09. - 30.09.13	Resaerch Council of Lithuania, Vilnius, Lithuania
Flagan, R.	08.09. - 15.09.13	California Institute of Technology, Pasadena, USA
Quaas, J.	09.09. - 15.09.13	Institute for Meteorology, Leipzig University, Germany
Ewald, F.	09.09. - 30.09.13	Ludwig Maximilians University Munich, Germany
Zhang, Y.	12.09. - 30.11.13	Tsinghua University, Beijing, China
Zhang, S.	12.09. - 31.12.13	Chinese Academy of Science, Beijing, China
de Mott, P.	15.09. - 24.09.13	Colorado State University, Fort Collins, USA
Fugal, J.	15.09. - 24.09.13	Max Planck Institute for Chemistry, Mainz, Germany
Lohmann, U.	15.09. - 24.09.13	Swiss Federal Institute of Technology (ETHZ), Zürich, Switzerland

## Appendices: Guest scientists / Visits of TROPOS scientists

Name	Period of stay	Institution
Murray, B.	15.09. - 24.09.13	University of Leeds, UK
Girimella, S.	20.09. - 28.09.13	Massachusetts Institute of Technology, Cambridge, USA
Knobel, L.	25.10. - 31.10.13	University of Paderborn, Germany
Gonzalez, R.	02.11. - 18.11.13	Universidad de Valladolid, Spain
Preißler, J.	20.11. - 24.11.13	University of Galway, Ireland
Elsen, K.	25.11. - 29.11.13	University of Bologna, Italy

## Visits of TROPOS scientists

Name	Period of stay	Institution
Tegen, I.	20.02. - 26.02.12	University of Leeds, UK
Schindelka, J.	05.03. - 23.03.12	IRCELYON Institut de recherches sur la catalyse et l'environnement de Lyon, France
Wiedensohler, A.	31.03. - 05.04.12	Universidad Mayor de San Andrés, La Paz, Bolivia
Siebert, H.	01.07. - 30.09.12	Max Planck Institut for Meteorology, Hamburg, Germany
Hellmuth, O.	19.11. - 23.11.12	St. Petersburg State University, Russia
Wiedensohler, A.	07.01. - 11.01.13	Indian Institute for Tropospheric Meteorology, Pune, India
Wiedensohler, A.	05.04. - 13.04.13	Malaysian Meteorological Service, Kuala Lumpur, Malaysia; Clean Air Asia, Beijing, China
Ansmann, A.	16.04. - 13.04.13	University of Technology, Limassol, Cyprus
Schepanski, K.	25.06. - 03.07.13	LATMOS Laboratoire Atmosphères, Milieux, Observations Spatiales, Paris, France
Wiedensohler, A.	07.09. - 13.09.13	Universidad Mayor de San Andrés, La Paz, Bolivia
Wiedensohler, A.	15.09. - 20.09.13	Peking University, China
Wiedensohler, A.	20.10. - 24.10.13	Chinese Ministry of Environmental Pollution, Beijing, China
Herrmann, H.	21.10. - 30.10.13	Shandong University, Jinan, China
Stratmann, F.	29.10. - 16.11.13	CERN, Genf, Switzerland
Wiedensohler, A.	10.12. - 19.12.13	Peking University, China

## Appendices: Meetings

### Meetings

Meetings	Date	National / international	Number of participants
GUAN-Workshop (German Ultrafine Aerosol Network), Leipzig	28.03.2012	national	24
16 <sup>th</sup> International Conference on Clouds and Precipitation (ICCP), Leipzig	30.07. - 03.08.12	international	569
International Radiation Symposium (IRS), Berlin	05.08. - 10.08.12	international	554
2 <sup>nd</sup> ACTRIS WP3 Workshop (Aerosols, Clouds, and Trace gases Research InfraStructure Network), Leipzig	15.10. - 19.10.12	international	57
SALTRACE Kick-off Meeting (Saharan Aerosol Long-range Transport and Aerosol-Cloud-Interaction Experiment), Leipzig	28.01.2013	international	25
ACTRIS intercomparison workshop, Nephelometer and Absorption Photometer (Aerosols, Clouds, and Trace gases Research InfraStructure Network)	18.02. - 08.03.13	international	23
Final Workshop "SOPRAN-II" - Kickoff-Meeting "SOPRAN-III" Faculty of Chemistry at Leipzig University	19.03. - 20.03.13	national	53
INUIT Meeting (Ice Nuclei Research Unit), project workshop, Leipzig	06.- 07.06.13	international	20
Graduate School "Mineral Dust", Intersection Workshop, Leipzig	19.06.2013	national	25
Summer School on Remote Sensing of Clouds and Precipitation, Hans Ertel Centre on Weather Research, Bonn	15.07. - 19.07.13	international	35
CLOUD-TRAIN Summer school (Cosmics Leaving OUtdoor Droplets), Training Network EU Marie Curie Project, Braunfels	08.09. - 14.09.13	International	25
WORKSHOP "Belasteter Ozean - belastete Troposphäre", Berlin	16.09. - 17.09.13	national	25
ACTRIS intercomparison workshop (Aerosols, Clouds, and Trace gases Research InfraStructure Network), CPCs and Mobility Particle Size Spectrometers, Leipzig	16.09. - 04.10.13	international	21
ICPWS 2013, London, Workshop on Humidity Metrology, Greenwich	03.09.13	international	25
Graduate School "Mineral Dust", Advanced Training Module, "Absorbing aerosol and its impact of clouds and dynamics", Leipzig	15.10. - 16.10.13	international	25
HOPE Workshop (HD(CP)2 Observational Prototype Experiment), Leipzig	03.12. - 04.12.13	international	30

## Appendices: International and national field campaigns

### International and national field campaigns

Campaign	Project partner
<b>ACRIDICON-Zugspitze</b> Schneefernerhaus, Zugspitze TROPOS: EACMph. Dept. <sup>1)</sup>	Max Planck Institute for Chemistry, Mainz, Germany; University of Frankfurt, Germany Leipzig University, Germany; Forschungszentrum Jülich, Germany KIT Karlsruhe, Germany; DLR Oberpfaffenhofen, Germany
<b>Aerosol Measurements</b> on the research vessel Polarstern TROPOS: EACMph. Dept.	no partners
<b>CAREBeijing-North China Plain</b> Campaigns of Air Quality Research in Beijing TROPOS: Chemistry + EACMph. Dept.	China, France, UK, USA, Germany
<b>IGOS-CARIBIC</b> 36 intercontinental measurement flights 2012 TROPOS: EACMph. Dept.	CARIBIC Consortium
<b>CLOUD7</b> (Cosmics Leaving Outdoor Droplets) CERN, Geneva, Switzerland TROPOS: EACMph. Dept.	Switzerland, Austria, Finland, Germany, Portugal, Russia, UK, USA, Sweden
<b>CLOUD8</b> (Cosmics Leaving Outdoor Droplets) CERN, Geneva, Switzerland TROPOS: EACMph. Dept.	Switzerland, Austria, Finland, Germany, Portugal, Russia, UK, USA, Sweden
<b>CLOUDNET</b> (permanent experiment) Cloud Measurement Network Leipzig, Germany TROPOS: Remote Sensing Dept.	CLOUDNET Consortium
<b>EARLINET</b> (permanent experiment) European Aerosol Research Lidar Network Leipzig, Germany TROPOS: Remote Sensing Dept.	EARLINET Consortium
<b>EMEP<sup>1)</sup>/ACTRIS</b> Summer Campaign Melpitz, Germany TROPOS: Chemistry and EACMph. Dept.	Switzerland, Czech Republic, Denmark, Spain, Ireland, Italy, The Netherlands, Norway, UK (EMEP-Consortium)
<b>EMEP<sup>1)</sup>/ACTRIS</b> Winter Campaign Melpitz, Germany TROPOS: Chemistry and EACMph. Dept.	Switzerland, Czech Republic, Denmark, Spain, Ireland, Italy, The Netherlands, Norway, UK (EMEP-Consortium)

## Appendices: International and national field campaigns

Campaign	Project partner
<b>GUAN</b> German Ultrafine Aerosol Network TROPOS: EACMph. + Chemistry Dept.	German Federal Environmental Agency Langen, Germany; German Research Center for Environmental Health, Munich, Germany; Saxon State Ministry of the Environment and Agriculture, Dresden, Germany; Institute of Energy and Environmental Technology e.V. (IUTA), Duisburg, Germany; Deutscher Wetterdienst (DWD) Hohenpeißenberg, Germany; ISSEP, Liège, Belgium
<b>HCCT 2010</b> Hill Cap Cloud Thuringia 2010, Schmücke Thüringen TROPOS: EACMph., Modeling, and Chemistry Dept.	Germany, UK, France, USA
<b>IAGOS-CARIBIC 46 intercontinental measurement flights</b> Civil Aircraft for Remote Sensing and In situ measurement in Tropospheric and Lower Stratosphere based on the Instrumentation Container Concept TROPOS: EACMph. Dept.	CARIBIC Consortium
<b>Intensive Campaign La Paz</b> La Paz, Bolivia TROPOS: EACMph. Dept.	Universidad Mayor de San Andrés, La Paz, Bolivia
<b>INUIT-TO</b> Ice Nuclei Research Unit - Taunus Observatory Kleiner Feldberg, Taunus, Germany TROPOS: EACMph. Dept.	Max Planck Institute for Chemistry, Mainz, Germany; University of Frankfurt, Germany; Technical University Darmstadt, Germany; University Mainz, Germany
<b>INUIT-JFJ 2013</b> Jungfraujoch, Switzerland TROPOS: EACMph. Dept.	Max Planck Institute for Chemistry, Mainz, Germany; University of Frankfurt, Germany; KIT Karlsruhe, Germany; Technical University of Darmstadt, Germany; Paul Scherrer Institute, Villigen, Switzerland; University of Manchester, UK; ETH Zurich, Zurich, Switzerland
<b>INUIT-LACIS-Campaign</b> Ice Nuclei Research Unit - LACIS Leipzig, Germany TROPOS: EACMph. Dept.	Max Planck Institute for Chemistry, Mainz, Germany; University of Frankfurt, Germany; Technical University Darmstadt, Germany; ETH, Zürich, Switzerland
<b>LACIS Campaign Examination of coated and uncoated Kaolinite-Particles</b> LACIS, TROPOS, Leipzig, Germany TROPOS: EACMph. Dept.	Colorado State University, USA
<b>LACIS Campaign Pollen-washing-water</b> LACIS, TROPOS, Leipzig, Germany TROPOS: EACMph. Dept.	Technical University Vienna, Austria
<b>LACIS Campaign examination of surface roughness</b> LACIS, TROPOS, Leipzig, Deutschland TROPOS: EACMph. Dept.	University of Hertfordshire, UK

## Appendices: International and national field campaigns

Campaign	Project partner
<b>Lagrangian Turbulence of Cloud Droplets</b> Environmental Research Station Zugspitze, Germany TROPOS: EACMph. Dept.	Michigan Technology University, Houghton, Michigan, USA; Max Planck Institute for Dynamics and Self-Organization, Göttingen, Germany; University of Warsaw, Poland
<b>LEAK Campaign BMU Feinstaub 2</b> LEAK TROPOS Leipzig, Germany TROPOS: Chemistry and EACMph. Dept.	Deutsches BiomasseForschungsZentrum, Leipzig, Germany; TU Hamburg-Harburg, Germany; University Konstanz, Germany
<b>LfULG Aerosol 2013</b> Leipzig, Germany TROPOS: Chemistry Dept. + EACMph. Dept.	Saxon State Ministry of the Environment and Agriculture, Dresden, Germany
<b>MEGACITIES-3 2011</b> Guangzhou, China TROPOS: Remote Sensing Dept.	Leipzig University, Germany; University of Bielefeld, Germany; Sun Yat-sen University, Guangzhou, China; Taiwan National Tsing Hua University, Taiwan; Montana University, USA
<b>Mobile Research Station on Polarstern Research Vessel</b> Route ANTXXVIII-5 and ANTXXIX-1GEOMAR: Polarstern TROPOS: EACMph. Dept.	GEOMAR, Kiel, Germany; Alfred Wegener Institute für Polar and Marine Research (AWI), Bremerhaven, Germany; Institute for Meteorology, Leipzig University (LIM), Germany; Max Planck Institut for Meteorology, Hamburg, Germany; University of Hamburg, Germany
<b>Mobile Research Station on Meteor Research Vessel</b> Atlantic transect M96 TROPOS: Physics Dept.	University of Hamburg, Germany; GEOMAR, Kiel, Germany; Max Planck Institut for Meteorology, Hamburg, Germany; Institute for Meteorology, Leipzig University (LIM), Germany; Institute for Space Sciences, Free University of Berlin, Germany
<b>PEGASOS Field Campaign</b> Bologna, Italien TROPOS: Chemistry Dept.	PEGASOS Consortium
<b>PHOTOPAQ</b> Bergamo Italia TROPOS: Chemistry Dept.	PHOTOPAQ Consortium
<b>PollyNet</b> (permanent experiment) Network of institutions with a PollyXT TROPOS: Remote Sensing Dept.	PollyNet Consortium
<b>RICE1+2</b> Roughness of ICE (optical surface properties of single ice crystals) Leipzig, Germany TROPOS: EACMph. Dept.	University of Hertfordshire, Science & Technology Research Institute, Hertfordshire, UK
<b>RICE3</b> Roughness of ICE (optical surface properties of single ice crystals) Leipzig, Germany TROPOS: EACMph. Dept.	University of Hertfordshire, Science & Technology Research Institute, Hertfordshire, UK

## Appendices: International and national field campaigns / Memberships

Campaign	Project partner
<b>SALTRACE</b> Saharan Aerosol Long-range Transport and Aerosol-Cloud-Interaction Experiment Barbados TROPOS: all departments	Germany, Barbados, Spain, France, USA
<b>SOPRAN</b> Surface Ocean Processes in the Anthropocene Cape Verde TROPOS: EACMph., Chemistry and Modeling Dept.	Germany, UK, Cape Verde
<b>SPIN-OPC-comparison</b> Leipzig, Germany TROPOS: EACMph. Dept.	Massachusetts Institute of Technology (MIT), Cambridge, USA
<b>Strömungsfeldmessungen</b> Flow field measurements at the AIDA experimental chamber Karlsruhe, Germany TROPOS: EACMph. Dept.	Institute of Technology, Karlsruhe, Germany
<b>Low Emission Zone Leipzig</b> Leipzig, Germany TROPOS: EACMph. Dept.	Saxon State Ministry of the Environment and Agriculture, Dresden, Germany
<b>HOPE-Jülich</b> HD(CP)2 Observations Prototype Experiment Jülich, Germany TROPOS: Remote Sensing Dept.	HD(CP)2 Consortium
<b>HOPE-Melpitz</b> HD(CP)2 Observations Prototype Experiment Melpitz, Germany TROPOS: all departments	Ludwig Maximilian University, Munich, Germany; Leipzig Institute for Meteorology, Leipzig University, Germany, Free University of Berlin, Germany

<sup>1)</sup> Experimental Aerosol and Cloud Microphysics Department

<sup>1)</sup> EMEP: Co-operative Programme for Monitoring and Evaluation of the Long-Range Transmission of Air Pollutants in Europe

## Memberships

Name	Board	Year
Althausen, D.	Kommission Reinhaltung der Luft im VDI und DIN - Normenausschuss KRdL, NA 134-02-01-22 UA "Bodengebundene Fernmessung meteorologischer Größen" im Fachbereich II Umweltmeteorologie	2012/2013
Birmili, W.	Editorial Board Member "Atmospheric Chemistry and Physics"	2012/2013
Hellmuth, O.	Membership in the International Association for the Properties of Water and Steam (IAPWS), Working Group Thermophysical Properties of Water and Steam (TPWS)	2012/2013
Hermann, M.	Wissenschaftlicher Lenkungsausschuss (WLA) HALO	2012/2013

## Appendices: Memberships

Name	Board	Year
Hermann, M.	Member of the “Stratospheric Sulfur and its Role in Climate” (SSIRC) SPARC initiative planning committee	2012/2013
Herrmann, H.	Vorsitz des Arbeitskreises “Atmosphärenchemie” in der GDCh-Fachgruppe “Umweltchemie und Ökotoxikologie (AKAC)”	2012/2013
	DECHEMA/GDCh/Bunsengesellschaft; Gemeinschaftsausschuss “Chemie der Atmosphäre”	2012/2013
	“DECHEMA/GDCh/KRdL Expertengruppe Feinstaub” - Mitglied der Lenkungsgruppe, Co-Vorsitz seit 2013	2012/2013
	Mitglied des wissenschaftlichen Beirats der “Kommission zur Reinhaltung der Luft” (KRdL) des Vereins Deutscher Ingenieure (VDI)	2012/2013
	Fellow of International Union of Pure and Applied Chemistry	2012/2013
	Editorial Board Member “Atmospheric Measurement Techniques”	2012/2013
	Editorial Board Member “Atmospheric Pollution Research”	2012/2013
Inuma, Y.	Chair der Working Group “Aerosol Chemistry within the EAA (European Aerosol Assembly)”	2012/2013
	Editorial Board Member “Atmospheric Measurement Techniques”	2012/2013
Macke, A.	Mitglied des Beirates der “Meteorologische Zeitschrift”	2012/2013
	Mitglied des “Wissenschaftlichen Beirats des Deutschen Wetterdienstes”	2012/2013
	Editorial Board Member “Atmospheric Measurement Techniques”	2012/2013
	Mitglied des “Redaktionsausschuss promet”	2012/2013
	Member of the International Radiation Comission	2012/2013
	Mitglied des “Wissenschaftlichen Beirats des Forschungsprogrammes KLIWAS”	2012/2013
	Member of the HALO Science Steering Comitee	2012/2013
	Mitglied des “HALO Kuratoriums”	2012/2013
	Mitglied der “EU-Lenkungsgruppe” der Wissenschaftsgemeinschaft Leibniz	2012/2013
	Member of the DFG Topical Board 313 “Atmosphere and Ocean Research”	2012/2013
	Stellvertretender Vorsitzender der Sektion E der Leibniz-Gesellschaft	2012/2013

## Appendices: Memberships

Name	Board	Year
Schepanski, K.	Co-Convener of AGU 2013 Session on “Mineral Dust Aerosols: From Small-Scale Insights to Large-Scale Understanding”	2013
	Guest Editor AGU 2013 Aeolian Research Special Issue (preliminary title of the Special Issue: “Mineral dust aerosols: from small-scale insights to large-scale understanding”)	2013
Siebert, H.	WG4 leader and Management Comity in “COST ACTION MP0806-Particles in Turbulence”	2012/2013
Stratmann, F.	Work Package (WP) Leader EU-Projekt EUROCHAMP 2	2012/2013
	Member of the EUROCHAMP 2 User Selection Panel (USP)	2012/2013
	Board-Member of the International Comission on Clouds and Precipitation (ICCP)	2012/2013
	Member of the International Conference on Clouds and Precipitation (ICCP) 2012 local organizing committee	2012
Tegen, I.	GESAMP (Group of Experts on the Scientific Aspects of Marine Environmental Protection), Member of Working Group 38, The Atmospheric Input of Chemicals to the Ocean	2012/2013
	“SDS-WAS” (WMO Sand and Dust Storm Warning Advisory and Assessment System), Member of Steering Committee	2012/2013
	ADOM (Atmospheric Dynamics during the last glacial cycle: Observation and Modeling) Co-Chair Eolian Records – Atmospheric Dynamics Working Group of PAGES (Past Global Changes, IGBP)	2012/2013
	Associate Editor, Journal of Geophysical Research, Atmospheres	2012/2013
	HAMMOZ Steering committee member	2013
Wandinger, U.	Member of the ESA-JAXA EarthCARE Joint Mission Advisory Group	2012/2013
	Member of the EARLINET Council	2012/2013
	Member Scientific Steering Committee and Work Package Leader EU Project ACTRIS	2012/2013
	Editorial Board Member Atmospheric Chemistry and Physics	2013
Wehner, B.	Mitglied des GAeF-Vorstands (Gesellschaft für Aerosolforschung)	2012
	Vorsitzende des Zweigvereins Leipzig der DMG (Deutsche Meteorologische Gesellschaft)	2012/2013
	Co-Chair of the Working Group “Atmospheric Aerosols” within the EAA (European Aerosol Assembly)	2012/2013

## Appendices: Memberships / Cooperations

Name	Board	Year
Wehner, B.	Chair of the Working Group "Atmospheric Aerosols" within the EAA (European Aerosol Assembly)	2013
Wex, H.	Head of the local organizing committee for the International Conference on Clouds and Precipitation (ICCP)	2012
Wiedensohler, A.	"Scientific Advisory Group" for aerosols within the "Global Atmosphere Watch"- program of the Meteorological Organization"	2012/2013
	VDI-Ausschuss "Partikelzählung in der Atmosphäre"	2012/2013
	Member Scientific Steering Committee (SSC) and Work Package (WP) Leader EU Project ACTRIS	2012/2013
	Member SSC EU-Projekt ACTRIS	2012/2013
	Guest Professor "Peking University", Department of Environmental Science, China	2012/2013
	Head of the World Calibration Center WMO-GAW	2012/2013
	Editorial Board Member "Atmospheric Chemistry and Physics"	2012/2013
	Editorial Board Member "Atmospheric Measurement Techniques"	2012/2013
	Chief editor Atmospheric Environment	2013
	Vorsitzender der Arbeitsgruppe "Afrika" im Deutschen Klima-Konsortium (DKK)	2012/2013

## Cooperations

### International Cooperations

Research project	Cooperation partners
<b>ACTOS</b> Airborne Cloud Turbulence Observation System - Interaction between turbulent mixing processes and cloud micro-physical characteristics in stratiform boundary layer clouds	Michigan Technological University, Department of Physics, Houghton, USA
<b>ACTRIS</b> Aerosols, Clouds, and Trace gases Research InfraStructure Network	>50 partners
<b>AERONET</b> Aerosol Robotic Network	National Aeronautics and Space Administration (NASA), USA

## Appendices: Cooperations

Research project	Cooperation partners
<b>AIE</b> Atmospheric Environmental Impacts of Aerosol in East Asia	30 partners
Anthropogenic influence of Asian aerosol on tropical cirrus clouds	National Center for Atmospheric Research (NCAR), Boulder, Colorado, USA
<b>AQMEII</b> Air Quality Model Evaluation International Initiative	Austria, Australia, Belgium, Canada, Switzerland, Cyprus, Germany, Denmark, Finland, France, Greece, Italy, Luxembourg, Malta, The Netherlands, Norway, Poland, Portugal, Sweden, UK, USA
<b>ATMOCHEM</b> Modeling the multiphase evolution of organic carbon in the troposphere: Development of an expert system based on a self generating approach	LISA - Laboratoire Interuniversitaire des Systèmes Atmosphériques, Université Paris, France
<b>Atmospheric Nucleation</b>	Universities of Helsinki and Kuopio, Finland
<b>BACCHUS</b> Impact of Biogenic versus Anthropogenic emissions on Clouds and Climate: towards a Holistic UnderStanding	20 Partners from Switzerland, Finland, Germany, UK, Norway, Greece, Italy, Ireland, Bulgaria, Israel, France, Cyprus
<b>BIOSOA</b> Biogenic Influences on Oxidants and Secondary Organic Aerosol: theoretical, laboratory and modelling investigations	Institut d'Aéronomie Spatiale de Belgique, Katholieke Universiteit Leuven, University of Antwerp, Belgium
<b>Central European particulate matter (PM) studies</b>	Poland, Czech Republic, Germany
<b>CAREBeijing-North China Plain</b> Air Quality Research in Beijing	China, France, UK, USA, Germany
<b>CARIBIC/AGOS</b> Civil Aircraft for Remote Sensing and In situ measurement in Tropospheric and Lower Stratosphere based on the Instrumentation Container Concept	Germany, UK, France, The Netherlands, Switzerland, Sweden
<b>CARRIBA</b> Cloud, Aerosol, Radiation, and turbulence in the trade wind regime over Barbados	Caribbean Institute for Meteorology and Hydrology, Barbados; Meteo France, France; Max Planck Institute for Meteorology, Germany; Leipzig Institute for Meteorology (LIM), Leipzig University
<b>Central European Air Quality Cooperation</b> Harmonization of aerosol sampling and measurement; exchange of measurement data; comparison of PM transport models	Poland, Czech Republic
<b>ChArMEx/ADRIMED</b> Chemistry-Aerosol Mediterranean Experiment / Aerosol Direct Radiative Impact on the regional climate in the Mediterranean region	France, Italy, Germany

## Appendices: Cooperations

Research project	Cooperation partners
<b>CLOUD-ITN</b> Cosmics leaving Outdoor Droplets - International Training Network	Germany, Switzerland, Finland, Austria, UK
<b>CLOUD-train</b> Cosmics leaving Outdoor Droplets - International Training Network	Germany, Switzerland, Finland, Austria, UK
<b>CLOUD</b> Cosmics Leaving Outdoor Droplets	Germany, Switzerland, Finland, Austria, Portugal, Russia, UK, USA
Cooperation partners involved in research projects at the TROPOS Research Station Melpitz	Norway, UK, Italy, Switzerland, Czech Republic, Hungary, Ireland, Finland, Austria, Sweden, Bulgaria, Belgium, France, Greece, The Netherlands, Spain, Denmark, Latvia, Poland, Portugal
<b>COST</b> Chemistry transport model intercomparison	Germany, Denmark, Finland, France, Bulgaria, Estonia, Italy, Malta, Spain, The Netherlands, Norway, Poland, Switzerland, UK, Greece, Israel
Development and evaluation of methods for the quantification of trace compounds produced by biomass burning	Academy of Science of Taipei, Taiwan
<b>EARLINET</b> European Aerosol Research Network	Germany, Italy, Spain, Greece, Switzerland, Sweden, Portugal, Poland, Belarus, France, Bulgaria, Romania, Norway, The Netherlands, Finland, Ireland, Cyprus
<b>EMEP</b> Summer/winter Campaign Melpitz TROPOS: Chemistry and Physics Dept.	>20 partners
<b>ESA-ADM</b> European Space Agency, Atmospheric Dynamics Mission	European Space Research and Technology Center (ESTEC), The Netherlands
<b>ESA-EarthCARE</b> European Space Agency, Earth Clouds, Aerosol and Radiation Explorer	European Space Research and Technology Center (ESTEC), The Netherlands; Japan Aerospace Exploration Agency
<b>EUFAR</b> European Fleet for Airborne Research in the Field of Environment and Geo Science	Germany, UK, France, Ireland, Sweden
<b>EUROCHAMP-II</b> Integration of European Simulation Chambers for Investigating Atmospheric Processes	Denmark, Germany, Italy, Spain, UK, Ireland, France, Switzerland, Sweden
<b>HCCT 2010</b> Hill Cap Cloud Thuringia 2010	Germany, UK, France, USA, Switzerland

## Appendices: Cooperations

Research project	Cooperation partners
Heterogeneous ice and salt crystallisation in aqueous electrolyte and polymeric solutions	State University St. Petersburg, Russia; University Rostock, Germany; IOW Warnemünde, Germany; Institute of Thermomechanics AS, Czech Republic; University of Odessa, Ukraine; Kharkov Institute of Technology, Ukraine
<b>IAGOS</b> Integration of routine Aircraft measurements into a Global Observing System	Germany, UK, France
Intercomparison of Satellite Derived Wind Observations	EUMETSAT, Darmstadt, Germany
<b>ITARS-ITN</b> Initial Training for Atmospheric Remote Sensing - Marie Curie Initial Training Network	Germany, Spain, Italy, UK, The Netherlands, Romania, France
<b>ICON-HAMMOZ development</b> Model development	Max Planck Institute for Meteorologie, Hamburg, Germany; ETH Zurich, Institute for Atmospheric and Climate Science, Zurich, Switzerland
<b>IRMA</b> Imager Retrieval Methods and ATLID synergy	European Space Research and Technology Center (ESTEC), The Netherlands; BMT ARGOSS, The Netherlands; University of Bremen, Germany; Deutscher Wetterdienst, Richard Aßmann Observatory Lindenberg, Germany
Laboratory investigations in the field of liquid phase chemistry	National Institute of Chemistry Ljubljana, Slovenia; Université de Lyon, France; Université de Marseilles, France; Semenov Institute of Chemical Physics, Moscow, Russia
<b>LACCT</b> Leipzig Aerosol Cloud Turbulence Tunnel	University of Ilmenau, Deutschland, Michigan Technological University, Houghton, USA
<b>LACIS</b> Leipzig Aerosol Cloud Interaction Simulator	USA, UK, Denmark, Germany, Finland, Austria, Schweiz
Lagrangian turbulence in clouds	Max Planck Institute for Dynamics and Self-Organization, Göttingen, Germany; Ilmenau University of Technology, Germany; Michigan Technological University, USA; University of Warsaw, Poland
<b>LEAK</b> Leipziger Aerosolkammer	Denmark, Germany, Italy, Spain, UK, Ireland, France, Switzerland, Sweden
<b>LIVAS</b> Lidar Climatology of Vertical Aerosol Structure for Space-Based Lidar Simulation Studies	Institute for Space Applications and Remote Sensing, National Observatory of Athens, Greece; Institute of Methodologies for Environmental Analysis of the National Research Council of Italy (IMAA-CNR), Potenza, Italy

## Appendices: Cooperations

<b>Research project</b>	<b>Cooperation partners</b>
<b>MEGACITIES</b> Satellite-Based Aerosol Mapping over Megacities: Development of Methodology and Application in Health and Climate Related Studies	Leipzig University, Germany; University of Bielefeld, Germany; Peking University, China; Anhui Institute of Optics and Fine Mechanics, Chinese Academy of Sciences, Hefei, China; Sun Yat-sen University, Guangzhou, China; Taiwan National Tsing Hua University, Taiwan; Montana University, USA
Multiple scattering in Raman lidar signals	National Academy of Science of Belarus, Institute of Physics, Minsk, Republic of Belarus
<b>PAREST</b> PArtikel-REduktions-STRategien	Germany, The Netherlands
<b>PEGASOS</b> Pan-European Gas-AeroSOLs-climate interaction Study	>20 partners
<b>PhotoPaq</b> Demonstration of Photocatalytic Remediation Processes on Air Quality	CNRS-IRCELYON, France; CNRS-ICARE, France; BUW, Germany; CTG, Italy; AUTH- LHTEE, Greece; BRRC, Belgium; Paris12-LISA, France
<b>PollyNet</b> Collaboration in the development and application of Polly systems	Finnish Meteorological Institute (FMI), Kuopio, Finland; Department of Applied Environmental Science (ITM), Stockholm University, Sweden; Institute of Geophysics, University of Warsaw, Poland; Universidade de Évora, Centro de Geofísica de Évora, Portugal; National Institute of Environmental Research, Air Quality Research Division, Korea
<b>PRADACS</b> Puerto Rico African Dust And Cloud Study	Germany, Puerto Rico, USA, Switzerland, Mexico, Brazil
Regional Scale Amine Chemistry Dispersion Modelling	TCM - Technology Center Mongstad, Norway; University of Oslo, Norway
Relations between directly emitted wood burning emissions and ambient particle concentration in the Melbourne region	Commonwealth Scientific and Industrial Research Organization (CSIRO), Melbourne, Australia
<b>RICE</b> Roughness of ICE (optical surface properties of single ice crystals)	University of Hertfordshire, Science & Technology Research Institute, Hertfordshire, UK
Saharan Dust Emission Processes	Leeds University, UK
Submicrometer particle size distribution processes across the European continent	National Centre for Atmospheric Science, University of Birmingham, UK; Institut de Ciències del Mar, Barcelona, Spain; Department of Physics, University of Helsinki, Finland

## Appendices: Cooperations

Research project	Cooperation partners
Theory of Ice and Salt Crystallization in Aqueous Electrolyte and Polymeric Solutions	Georgia Institute of Technology, Atlanta, Georgia, USA; IAWPS International Association for the Properties of Water and Steam; Institute for Thermal Physics, Ekaterinburg, Russia; Joint Institute for Nuclear Research Dubna, Russia; St. Petersburg State University, Saint Petersburg, Russia; SUNY at Buffalo, Buffalo, NY, USA
Twinning Partnership with GAW-Stations	Korean Meteorological Service; Global Atmosphere Watch (GAW), Anmyeon, Republic of Korea; Malaysian Meteorological Service, Danum Valley, Malaysia; Bulgarian Academy of Sciences, BEO-Moussala, Bulgaria
<b>UFIREG</b> - ultrafine particles & health	Germany, Czech Republic, Slovenia, Ukraine
<b>Ultraschwarz</b> - ultrafine particle exposure	Germany, Czech Republic
<b>ZOTTO</b> Zotino Tall Tower Facility (sources and budgets of tropospheric aerosols over Siberia)	Max Planck Institute for Biogeochemistry, Jena, Germany; Max Planck Institute for Chemistry, Mainz, Germany; IFOR-RASS, Krasnojarsk, Russia
Ocean Science Center Mindelo (OSCM)	Instituto Nacional de Desenvolvimento das Pescas (INDP), Mindelo, S. Vicente, Republic of Cape Verde; Helmholtz Centre for Ozean Research Kiel (GEOMAR), Germany

## National Cooperations

Research project	Cooperation partners
<b>ACRIDICON</b> Aerosol, Cloud, Precipitation, and Radiation Interactions and Dynamics of Convective Cloud System	16 partners
Absorption efficiency of Black Carbon: determining representative atmospheric values and implications for radiative transfer	Max Planck Institute for Chemistry, Mainz
<b>AirShield (BMBF-Verbundprojekt)</b> Airborne remote sensing for hazard inspection by network enabled lightweight drones	8 partners
<b>ALADINA</b> Investigating the Small-Scale Vertical and Horizontal Variability of the Atmospheric Boundary Layer Aerosol using Unmanned Aerial Vehicles	Technical University Baunschweig; Technical University Tübingen

## Appendices: Cooperations

<b>Research project</b>	<b>Cooperation partners</b>
Analyse der grenzüberschreitenden Beiträge der Feinstaubbelastung in Deutschland	Federal Environmental Agency, Dessau-Roßlau
<b>BMU Particulate matter-II</b> Heat from wood-particulate matter emissions: influence of fuel, user, secondary measures, characterization, toxicity	German Biomass Research Centre (DBFZ) Leipzig; Technical University Hamburg-Harburg; University Konstanz; The Technology and Support Centre (TFZ), Straubing
<b>CLOUD-12 (BMBF-Projekt)</b>	Goethe University Frankfurt am Main
<b>DFG-Forschergruppe INUIT</b> Ice Nuclei Research Unit	Max Planck Institute for Chemistry, Mainz; Goethe University Frankfurt am Main, Technical University Darmstadt; University Mainz; University Bielefeld; KIT Karlsruhe
<b>DFG-SPP HALO</b> Konzeption der HALO-Datenbank und eines HALO-Missionsplanungswerkzeugs	World Data Center for Climate; Max Planck Institute for Meteorology, Hamburg; German Aerospace Center (DLR), Oberpfaffenhofen
<b>DFG-Forschergruppe SAMUM</b> Saharan Mineral Dust Experiment	9 partners
<b>DWD-Raman-Lidar</b>	Kayser-Threde GmbH, Munich; Deutscher Wetterdienst (DWD), Offenbach; Meteorological Observatory, Lindenberg; inqbus it-consulting, Leipzig; Loritus GmbH, Munich
Ultrafine particle pollution in large urban areas on the example of Dresden and Leipzig	Technical University Dresden, Dresden (Transport); Technical University Freiberg, Interdisciplinary Environmental Center; Federal Environmental Agency Berlin
Experimentelle Verifizierung der Aufladung von Aerosolpartikel durch Röntgenstrahlung	Institute for Polymer Materials and Processes (PMP), University of Paderborn
<b>GERUCH</b> Ermittlung der Quellen von Gerüchen und hohen Schadstoffkonzentrationen im Erzgebirge über die Modellierung der Luftmassenbahnen	Saxon State Ministry of the Environment and Agriculture, Dresden
<b>GUAN</b> German Ultrafine Aerosol Network	Federal Environmental Agency, Dessau-Roßlau, Langen, Garmisch-Partenkirchen, Hofsgrund; Deutscher Wetterdienst (DWD), Hohenpeißenberg; IUTA Duisburg e. V.; Helmholtz Zentrum München - German Research Center for Environmental Health; University Augsburg
<b>Hans Ertel Zentrum für Wetterforschung</b>	Deutscher Wetterdienst (DWD), Offenbach; University Bonn
<b>HD(CP)2 (BMBF)</b> High definition clouds and precipitation for advancing climate prediction	16 partners

## Appendices: Cooperations

Research project	Cooperation partners
Highly resolved modeling of clouds and gravity wavelenghts: scale analyses, numerics, validation (Leibniz-Pakt-Verfahren)	Leibniz Institute of Atmospheric Physics, Rostock; Potsdam Institute for Climate Impact Research (PIK), Potsdam
<b>ICOS</b> (Integrating Cloud Observations from Ground and Space – a Way to Combine Time and Space Information)	University of Cologne; Free University Berlin
Ion particle interactions during particle formation and growth in coniferous forest in central Europe	University of Bayreuth, BayCEER, Atmospheric Chemistry
Influence of domestic wood stoves on particulate concentrations in rural areas of Saxony	Saxon State Ministry of the Environment and Agriculture, Dresden
Maps of particulate air pollution for the „Nationalatlas aktuell“	Institute for Regional Geography (IfL), Leipzig
<b>KLENOS</b> Influence of changes in energy policy and climate change on air quality and consequences on the abidance of limit values	Federal Environmental Agency, Dessau-Roßlau; TU Dresden, Institut für Hydrologie und Meteorologie
<b>LfULG Aerosol 2013</b>	Saxon State Ministry of the Environment and Agriculture, Dresden, Germany
<b>MARGA</b> Physikalisch-chemische Charakterisierung des dynamischen Verhaltens von Ammoniumsalzen im Feinstaub-Aerosol – Erprobung eines neuen zeitlich hochauflösenden Messverfahrens an der EMEP-Level 3-Station Melpitz	Federal Environmental Agency, Dessau-Roßlau
Messtechnische Begleitung und vertiefende Analysen zur Umweltzone Leipzig	Saxon State Ministry of the Environment and Agriculture, Dresden
<b>Mobile Seestation</b> Autonome Messplattformen zur Bestimmung des Stoff- und Energieaustauschs zwischen Ozean und Atmosphäre	GEOMAR, Kiel; Alfred Wegener Institute for Polar and Marine research (AWI), Bremerhaven; Institut for Meteorology, Leipzig University (LIM), Max Planck Institute for Meteorology, Hamburg; University Hamburg
<b>ML-CIRRUS</b> Mid-Latitude Cirrus	12 partners
<b>OCEANET</b> Autonome Messplattformen zur Bestimmung des Stoff- und Energieaustauschs zwischen Ozean und Atmosphäre	GEOMAR, Kiel; GKSS Research Centre Geesthacht; Alfred Wegener Institute for Polar and Marine research (AWI), Potsdam; University Bremen
Paralleles Kopplungs-Framework und moderne Zeitintegrationsverfahren für detaillierte Wolkenprozesse in atmosphärischen Modellen	Technical University Dresden, Centre for Information Services and High Performance Computing (ZIH); Martin Luther University Halle-Wittenberg

## Appendices: Cooperations

<b>Research project</b>	<b>Cooperation partners</b>
Photokatalytische Bestandsfassaden-LWB	MFPA Leipzig GmbH Leipzig Institute for Materials Research and Testing, funded by the Leipziger Wohnungs- und Baugesellschaft (LWB)
Qualitätssicherung und Qualitätskontrolle der Messung ultrafeiner Partikel in der Außenluft im Jahr 2010	Saxon State Ministry of the Environment and Agriculture, Dresden
<b>REGKLAM (BMBF-Verbundprojekt)</b> Entwicklung und Erprobung eines integrierten regionalen Klimaanpassungsprogramms für die Modellregion Dresden	6 partners
<b>SALTRACE</b> Saharan Aerosol Long-range Transport and Aerosol-Cloud-Interaction Experiment	DLR Oberpfaffenhofen, University of Munich, TU Darmstadt
Short-term Health Effects of Fine and Ultra-fine Particle Pollution in Beijing, China	GSF Institute for Epidemiology, Neuherberg; Helmholtz Centre for Environmental Research (UFZ), Department Human Exposure Research and Epidemiology, Leipzig
<b>SOPRAN (BMBF)</b> Surface Ocean Processes in the Anthropocene	8 partners
Theory of ice and salt crystallisation in aqueous electrolyte and polymeric solutions	Polymer Physics, University Rostock; Leibnitz Institute for Baltic Sea Research, Warnemünde (IOW)
<b>UFP 2012</b> Aufwandsreduzierung in der Qualitätskontrolle der Messung ultrafeiner Partikel in der Außenluft im Luftgütemessnetz Sachsen	Saxon State Ministry of the Environment and Agriculture, Dresden
<b>UFP 2013</b> Verbesserung der Vergleichbarkeit der Messdaten ultrafeiner Partikel in der Außenluft	Saxon State Ministry of the Environment and Agriculture, Dresden
Comparison of mobility spectrometer type UFP	Saxon State Ministry of the Environment and Agriculture, Dresden; TSI GmbH, Aachen; Topas GmbH, Dresden; Gewerbeaufsichtsamt, Hildesheim; Helmholtz-Zentrum München

## Appendices: Boards

### Boards

#### Boards of trustees

Name	Institution
RORin C. Liebner	Saxon State Ministry for Science and the Arts
RDin Dr. G. Helbig	Federal Ministry of Education and Research
Prof. Dr. S. Borrmann	Max Planck Institute for Chemistry (Otto Hahn Institute); Johannes Gutenberg University Mainz

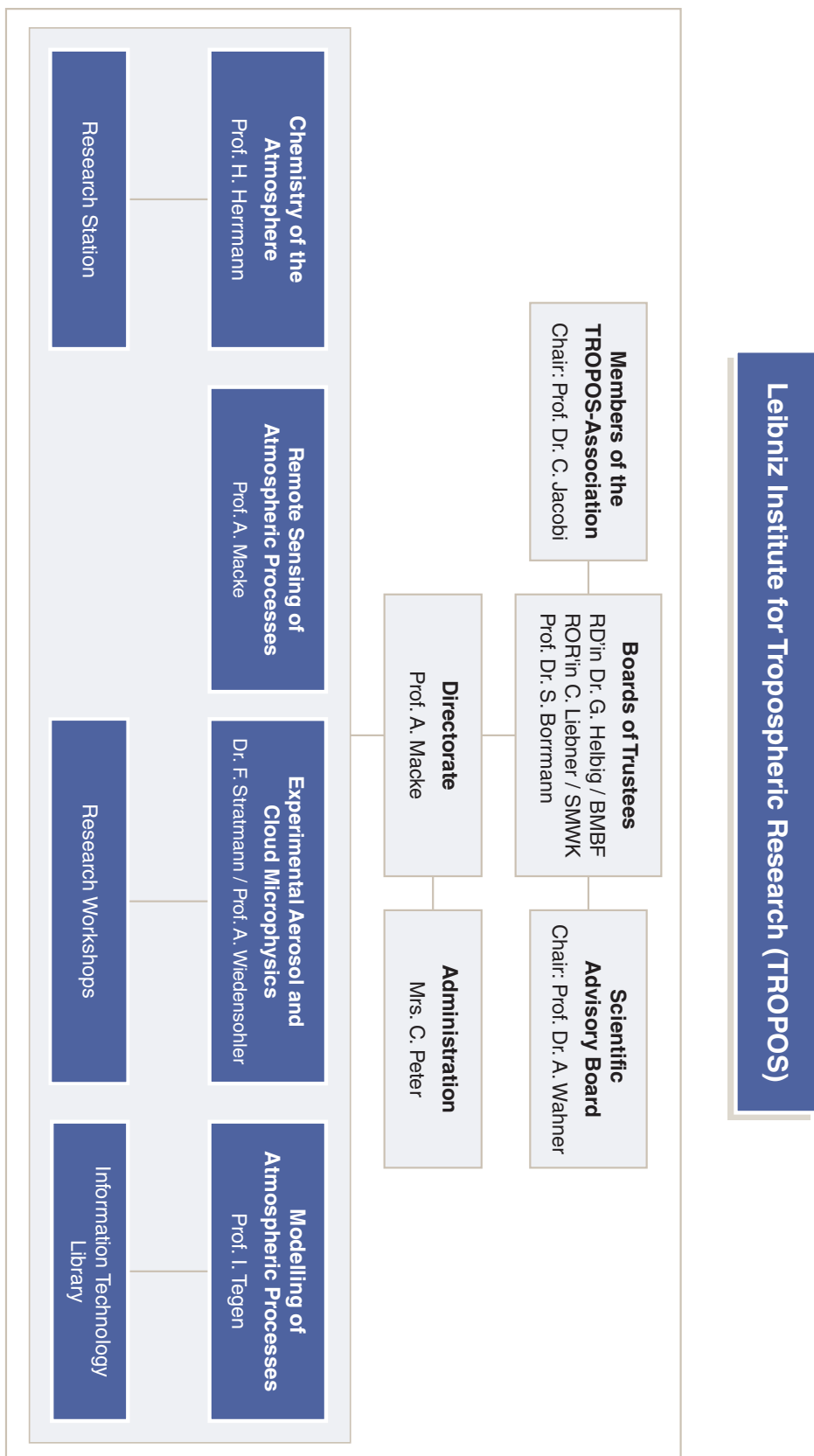
#### Scientific advisory board

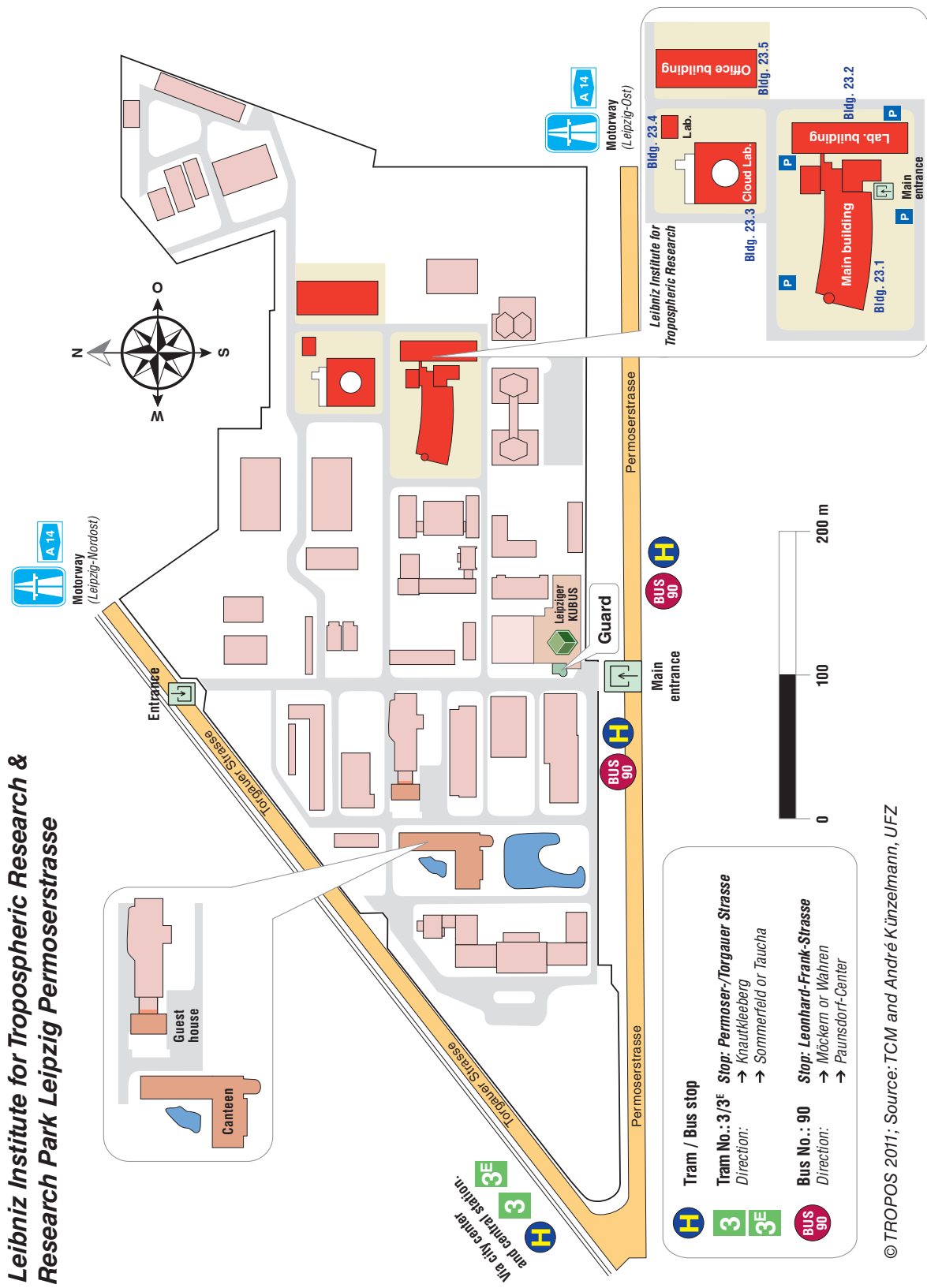
Name	Institution
Prof. Dr. A. Wahner <b>(Chairman)</b>	Forschungszentrum Jülich GmbH; Institute for Energy and Climate Research, IEK-8: Troposphere
PD Mag. Dr. F. H. Berger	Deutscher Wetterdienst (DWD), Lindenberg Meteorological Observatory - Richard Aßmann Observatory
Prof. Dr. A. Bott	University Bonn, Institute for Meteorology
Dr. G. Ehret	German Aeronautics and Space Research Centre (DLR), Institute of Atmospheric Physics, Lidar
Dr. C. George	IRCELYON - Institut de Recherches sur la Catalyse et l'Environnement de Lyon, University Claude Bernard
Prof. Dr. M. Kulmala	University of Helsinki; Department of Physics
Prof. Dr. J. Orphal	Karlsruhe Institute of Technology (KIT), Institute for Meteorology and Climate Research (IMK)
Prof. Dr. K. H. Schlünzen	University of Hamburg, Institute for Meteorology, KlimaCampus
Prof. Dr. R. Shaw	Michigan Technological University, Department of Physics
Prof. Dr. M. Wendisch	Leipzig University, Institute for Meteorology

### **Members of the TROPOS Association**

Name	Institution
Prof. Dr. C. Jacobi <b>(Chairman)</b>	Leipzig University, Leipzig Institute for Meteorology
Frau RORin C. Liebner	Saxon State Ministry for Science and the Arts
Frau RDin Dr. G. Helbig	Federal Ministry of Education and Research
Prof. Dr. P. Warneck	Professor emeritus
Prof. Dr. B. Brümmer	University of Hamburg, Institute for Meteorology
Prof. Dr. J. Quaas	Leipzig University, Leipzig Institute for Meteorology
Dr. H.-H. Richnow	Helmholtz Centre for Environmental Research (UFZ)
Prof. Dr. B. Abel	Leipzig University, Wilhelm Ostwald Institute for Physical and Theoretical Chemistry
Prof. Dr. C. Simmer	Rhineland Friedrich Wilhelm University Bonn, Institute for Meteorology
Prof. Dr. W. Engewald	Leipzig University, Faculty for Chemistry and Mineralogy
Prof. Dr. E. Renner, honorary member	Professor emeritus
Prof. Dr. J. Heintzenberg, honorary member	Professor emeritus

## Appendices: Organigram









## **TROPOS**

Leibniz Institute for Tropospheric Research  
Leibniz-Institut für Troposphärenforschung e.V. Leipzig  
Member of the Leibniz Association ( WGL )

Permoserstraße 15  
04318 Leipzig  
Germany

Phone: ++49 (341) 2717-7060  
Fax: ++49 (341) 2717-99-7060  
Email: [info@tropos.de](mailto:info@tropos.de)  
Internet: <http://www.tropos.de>